USGS
science for a changing world

Prepared in cooperation with the Hampton Roads Planning District Commission

Simulation of Groundwater Flow in the Coastal Plain Aquifer System of Virginia

Scientific Investigations Report 2009–5039

U.S. Department of the Interior
U.S. Geological Survey

Cover. **Landsat image of the Chesapeake Bay and adjacent coastal plain in Virginia and southern Maryland** *(photograph was contributed by the U.S. Geological Survey/National Aeronautics and Space Administration Landsat Program)*.

Simulation of Groundwater Flow in the Coastal Plain Aquifer System of Virginia

By Charles E. Heywood and Jason P. Pope

Prepared in cooperation with the Hampton Roads Planning District Commission

Scientific Investigations Report 2009–5039

U.S. Department of the Interior
U.S. Geological Survey

U.S. Department of the Interior
KEN SALAZAR, Secretary

U.S. Geological Survey
Suzette M. Kimball, Acting Director

U.S. Geological Survey, Reston, Virginia: 2009

Suggested citation:
Heywood, C.E., and Pope, J.P., 2009, Simulation of groundwater flow in the Coastal Plain aquifer system of Virginia: U.S. Geological Survey Scientific Investigations Report 2009–5039, 115 p.

ISBN 978–1–4113–2418–3

Contents

Abstract 1
Introduction 1
Purpose and Scope 3
Previous Studies 4
Description of the Virginia Coastal Plain 6
Hydrogeologic Framework 6
Hydrologic Conditions 10
Precipitation 11
Evapotranspiration 11
Recharge 11
Groundwater Underflow from the Piedmont Province 14
Hydraulic Properties 14
Hydraulic Conductivity 14
Specific Storage 15
Specific Yield 16
Discharge 16
Saltwater Transition Zone 17
Simulation of Transient Groundwater Flow 19
Projection System 19
Numerical Method 19
Spatial Discretization 20
Internal Flow Package 21
Temporal Discretization 22
Boundary Conditions 22
Specified Flux Boundaries 22
Transient Areal Recharge 22
Transient Underflow to Maryland 24
Constant Underflow from Piedmont 24
Transient Groundwater Pumpage 24
Reported Withdrawals 24
Domestic Withdrawals 26
Head-Dependent Flux Boundaries 26
Evapotranspiration 26
Rivers 26
Chesapeake Bay and Ocean Floor Leakage 26
Hydraulic-Property Distribution 27
Horizontal Interpolation of Hydraulic Conductivity 27
Depth-Dependence of Potomac Aquifer Horizontal Hydraulic Conductivity. 27

Model Calibration....29
Calibration Data Set....30
Water-Level Observation Errors....33
Weights....33
Modification of First Stress Period Time-Discretization for Parameter Estimation....34
Hydraulic Property Parameterization....34
Boundary Flux Parameterization....36
Simulated Conditions....36
Water Levels....36
Surficial Aquifer....37
Yorktown-Eastover Aquifer....41
St. Marys Aquifer....45
Piney Point Aquifer....49
Aquia Aquifer....53
Peedee Aquifer....57
Virginia Beach Aquifer....60
Potomac Aquifer....63
Water Budget....73
Steady-State Water Budget....73
Transient Water Budget....74
Calibration Assessment....74
Residual Plots....74
Weighted Residual Maps....77
Parameter Correlation....84
Parameter Sensitivities....85
Estimated Parameters....85
Aquifer and Confining-Unit Spatial Variability....87
Model Limitations....87
Summary....105
Acknowledgments....106
References Cited....106
Appendix....110
Transient Saltwater-Transport Simulation....110
Boundary Condition Modifications....111
Initial Conditions....111
Simulation of Mass Transport....111
Appendix References Cited....115

Figures

1. Map showing locations of counties and independent cities, the Chesapeake Bay impact crater, and other important geographic and physiographic features of the Virginia Coastal Plain....2
2. Graph showing Virginia reported and domestic groundwater withdrawals....3

3. Map showing finite-difference model grid with row and column numbers of cross sections 5
4. Vertical model cross sections showing distribution of hydrogeologic units from east to west along row 80 (A–A´), east to west along row 95 (B–B´), east to west along row 107 (C–C´), east to west along row 120 (D–D´), north to south along column 50 (E–E´), north to south along column 60 (F–F´), north to south along column 70 (G–G´), and north to south along column 87 (H–H´) 7
5. Stratigraphic correlations of hydrogeologic units of the Virginia Coastal Plain 9
6. Diagram showing generalized predevelopment groundwater flow patterns in the Coastal Plain aquifer system 10
7. Map showing locations of precipitation-measurement stations, control points, and rivers simulated with the River package, other streams, and sea-level areas simulated with the General Head Boundary Package 12
8. Graph of historical measured precipitation at the four precipitation-measurement stations in the Virginia Coastal Plain 13
9. Pie chart showing estimated groundwater withdrawal-use categories in 2000 17
10. Map showing location of Coastal Plain reported withdrawal wells, model domain, and self-supplied withdrawal rate per square mile in 2000 18
11. Graph showing simulated recharge in the Virginia Coastal Plain by year 23
12. Vertical sections of finite-difference model grid, showing cells designated for time-varying specified flux to Maryland in row 1 and constant specified flux from the Piedmont Province in column 1 25
13. Map showing pilot-point locations and simulated horizontal hydraulic conductivity at the top of the Potomac aquifer 28
14. Graph showing decrease with depth of the simulated horizontal hydraulic conductivity of the Potomac aquifer 29
15. Map showing locations and screened hydrogeologic unit of water-level observation wells 31
16. Histogram showing time distribution and spatial distribution by State of water-level observations used for model calibration 32
17. Map of estimated vertical hydraulic conductivity of the Calvert confining unit 35
18. Contour maps of the simulated water table in the Virginia Coastal Plain:
    a. before development 38
    b. drawdown in 2001 39
19. Map showing locations of observation wells screened in the surficial, Yorktown-Eastover, St. Marys, Piney Point, Aquia, and Peedee aquifers for hydrographs depicted in figures 20, 22, 24, 26, 28, and 30 40
20. Hydrograph of observed and simulated water levels in the surficial aquifer well 57D 23 41
21. Contour maps of simulated water levels in the Yorktown-Eastover aquifer:
    a. before development 42
    b. in 2003 43
    c. drawdown from predevelopment to 2003 44
22. Hydrograph of observed and simulated water levels in wells 57H 14, 61B 2, 62A 2, 62C 9, and 57B 8 in the Yorktown-Eastover aquifer 45

23. Contour maps of simulated water levels in the St. Marys aquifer:
    - a. before development 46
    - b. in 2003 47
    - c. drawdown from predevelopment to 2003 48
24. Hydrograph of observed and simulated water levels in well 57C 21 in the St. Marys aquifer 49
25. Contour maps of simulated water levels in the Piney Point aquifer:
    - a. before development 50
    - b. in 2003 51
    - c. drawdown from predevelopment to 2003 52
26. Hydrograph of observed and simulated water levels in wells 56H 29, 54Q 73, and 56G 38 in the Piney Point aquifer 53
27. Contour maps of simulated water levels in the Aquia aquifer:
    - a. before development 54
    - b. in 2003 55
    - c. drawdown from predevelopment to 2003 56
28. Hydrograph of observed and simulated water levels in wells 51M 18, 57G 2, and 55B 67 in the Aquia aquifer 57
29. Contour maps of simulated water levels in the Peedee aquifer:
    - a. before development 58
    - b. in 2003 59
30. Hydrograph of observed and simulated water levels in well 61B 6 in the Peedee aquifer 60
31. Contour maps of simulated water levels in the Virginia Beach aquifer:
    - a. before development 61
    - b. in 2003 62
32. Contour maps of simulated water levels in the Potomac aquifer:
    - a. before development 64
    - b. in 2003 65
    - c. drawdown from predevelopment to 2003 66
33. Map showing locations of observation wells screened in the Potomac aquifer for hydrographs depicted in figures 34–39 67
34. Hydrograph of observed and simulated water levels of selected wells screened in the Potomac aquifer in the southwest model area 68
35. Hydrograph of observed and simulated water levels of selected wells screened in the Potomac aquifer in the southeast model area 68
36. Hydrograph of observed and simulated water levels of selected wells screened in the Potomac aquifer in the western model area 69
37. Hydrograph of observed and simulated water levels of selected wells screened in the Potomac aquifer in the eastern model area 70
38. Hydrograph of observed and simulated water levels of selected wells screened in the Potomac aquifer in the central model area 71
39. Hydrograph of observed and simulated water levels of selected wells screened in the Potomac aquifer in the northern model area 72
40. Graphs of:
    - a. Relation between observed and simulated water levels 75
    - b. Relation between weighted observed and weighted simulated water levels 76

41. Graph of relation between weighted residuals and simulated water levels....................77
42. Maps showing maximum residual magnitudes for observation wells screened in the:
    a. surficial aquifer....................78
    b. Yorktown-Eastover aquifer....................79
    c. Piney Point aquifer....................80
    d. Aquia aquifer....................81
    e. Peedee and St. Marys aquifers....................82
    f. Potomac aquifer....................83
43. Graph of composite scaled sensitivities for model parameters....................85
44. Graph of estimated values, confidence intervals, and reasonable ranges for parameters representing horizontal and vertical hydraulic conductivity, specific storage, and other fluxes....................86
45. Map of estimated transmissivity of the:
    a. Yorktown-Eastover aquifer....................88
    b. St. Marys aquifer....................89
    c. Piney Point aquifer....................90
    d. Aquia aquifer....................91
    e. Peedee aquifer....................92
    f. Virginia Beach aquifer....................93
46. Map of estimated leakance of the:
    a. Yorktown confining zone....................94
    b. St. Marys confining unit....................95
    c. Calvert confining unit....................96
    d. Chickahominy confining unit....................97
    e. Exmore matrix confining unit....................98
    f. Exmore clast confining unit....................99
    g. Nanjemoy-Marlboro confining unit....................100
    h. Peedee confining zone....................101
    i. Virginia Beach confining zone....................102
    j. Upper Cenomanian confining unit....................103
    k. Potomac confining zone....................104
A1. Graph of sea levels during the Pleistocene and Holocene epochs....................110
A2. Map showing simulated water density near the saltwater transition zone of the Virginia Coastal Plain....................112
A3. Cross section showing simulated water density near the saltwater transition zone of the Virginia Coastal Plain....................113
A4. Graph of relation between simulated and observed normalized chloride concentrations....................114

Tables

1. Summary of Potomac aquifer-performance test results....................15
2. Magnitudes of 2003 reported and 2000 self-supplied domestic groundwater withdrawals from the Virginia Coastal Plain by hydrogeologic unit....................17
3. Model grid-layer thicknesses....................21

4. Time discretization for 113-year historical transient simulation..22
5. Number of control points for simulated rivers...27
6. Number of observations and wells primarily associated with each hydrogeologic unit simulated in the Virginia Coastal Plain model...32
7. Steady-state water-budget components for model domain 73
8. Steady-state and transient water-budget components for Virginia sub-domain 73
9. Parameter pairs with absolute correlation coefficients greater than 0.8.........................84
A1. Specified Pleistocene-Epoch sea levels. 111
A2. Values used for transport simulation..111

Conversion Factors and Datums

Inch/Pound to SI

Multiply	By	To obtain
	Length	
inch (in.)	2.54	centimeter (cm)
inch (in.)	25.4	millimeter (mm)
foot (ft)	0.3048	meter (m)
mile (mi)	1.609	kilometer (km)
	Area	
square mile (mi^2)	259.0	hectare (ha)
square mile (mi^2)	2.590	square kilometer (km^2)
	Volume	
cubic foot (ft^3)	0.02832	cubic meter (m^3)
gallon (gal)	3.785	liter (L)
gallon (gal)	0.003785	cubic meter (m^3)
	Flow rate	
cubic feet per day (ft^3/d)	0.02832	cubic meter per day (m^3/d)
million gallons per day (Mgal/d)	0.04381	cubic meter per second (m^3/s)
	Flux	
inch per year (in/yr)	2.54	centimeter per year (cm/yr)
	Mass	
pound, avoirdupois (lb)	0.4536	kilogram (kg)
	Density	
pound per cubic foot (lb/ft^3)	16.02	kilogram per cubic meter (kg/m^3)
pound per cubic foot (lb/ft^3)	0.01602	gram per cubic centimeter (g/cm^3)
	Hydraulic conductivity	
foot per day (ft/d)	0.3048	meter per day (m/d)
	Transmissivity*	
foot squared per day (ft^2/d)	0.09290	meter squared per day (m^2/d)

Temperature in degrees Fahrenheit (°F) may be converted to degrees Celsius (°C) as follows:

$$°C = (°F - 32) / 1.8$$

Vertical coordinate information is referenced to the National Geodetic Vertical Datum of 1929 (NGVD 29).

Horizontal coordinate information is referenced to the North American Datum of 1983 (NAD 83).

Altitude, as used in this report, refers to distance above the vertical datum.

*Transmissivity: The standard unit for transmissivity is cubic foot per day per square foot times foot of aquifer thickness [(ft^3/d)/ft^2]ft. In this report, the mathematically reduced form, foot squared per day (ft^2/d), is used for convenience.

Acronyms and Abbreviations:

BCF	Block-Centered Flow package
CSS	Composite scaled sensitivity
DEM	Digital elevation model
DEQ	Department of Environmental Quality
ET	evapotranspiration
EVT	Evapotranspiration package
FHB	Flow and Head Boundary package
GHB	General Head Boundary package
GIS	Geographic information system
GPS	Global Positioning System
GWMA	Ground Water Management Area
GWSI	Groundwater Site Inventory
HRPDC	Hampton Roads Planning District Commission
HUF	Hydrogeologic-Unit Flow package
IMT	Integrated Mass Transport
KDEP	hydraulic-conductivity depth dependence
LPF	Layer-Property Flow package
mg/L	milligram per liter
MNW	Multi-Node Well package
MSL	mean sea level
PET	potential evapotranspiration
RASA	Regional Aquifer System Analysis
RCH	Recharge package
RIV	River package
RMSE	Root mean square error
SSE	sum-of-squares error
TDS	total dissolved solids
USGS	U.S. Geological Survey
VDF	Variable-Density Flow

Parameter Names and Definitions:

et_max_rate	Maximum evapotranspiration flux.
evapotransp	Evapotranspiration extinction depth.
k_aquia	Horizontal hydraulic conductivity of the Aquia aquifer.
k_aquiclud	Horizontal hydraulic conductivity of the Exmore matrix, Exmore clast, and Chickahominy confining units.
k_aquitard	Horizontal hydraulic conductivity of other confining units.
k_charlesci	Horizontal hydraulic conductivity of the Potomac aquifer at the pilot point located in Charles City.
k_chesapeak	Horizontal hydraulic conductivity of the Potomac aquifer at the pilot point located in Chesapeake County.
k_chesterfi	Horizontal hydraulic conductivity of the Potomac aquifer at the pilot point located in Chesterfield County.
k_columbia	Horizontal hydraulic conductivity of the surficial aquifer.
kdepth1	Lambda exponent in equation 8.
k_franklin	Horizontal hydraulic conductivity of the Potomac aquifer at the pilot point located in the city of Franklin.
k_henrico	Horizontal hydraulic conductivity of the Potomac aquifer at the pilot point located in Henrico County.
k_islewight	Horizontal hydraulic conductivity of the Potomac aquifer at the pilot point located in Isle of Wight County.
k_jamescity	Horizontal hydraulic conductivity of the Potomac aquifer at the pilot point located in James City County.
k_kinggeorg	Horizontal hydraulic conductivity of the Potomac aquifer at the pilot point located in King George County.
k_kingwilli	Horizontal hydraulic conductivity of the Potomac aquifer at the pilot point located in King William County.
k_lancaster	Horizontal hydraulic conductivity of the Potomac aquifer at the pilot point located in Lancaster County.
k_maryland	Horizontal hydraulic conductivity of the Potomac aquifer at the pilot point located in southern Maryland.
k_megabloc	Horizontal hydraulic conductivity of the Potomac aquifer within the Chesapeake Bay Impact Crater.
k_newportne	Horizontal hydraulic conductivity of the Potomac aquifer at the pilot point located in the city of Newport News.
k_peedee_a	Horizontal hydraulic conductivity of the Peedee aquifer.
k_pineyp_jc	Horizontal hydraulic conductivity of the Piney Point aquifer.
k_potom_cz	Horizontal hydraulic conductivity of the Potomac confing zone.
k_princegeo	Horizontal hydraulic conductivity of the Potomac aquifer at the pilot point located in Prince George County.
k_s_mary_a	Horizontal hydraulic conductivity of the Saint Marys aquifer.
k_sohampt_n	Horizontal hydraulic conductivity of the Potomac aquifer at the pilot point located in northern Southhampton County.
k_sohampton	Horizontal hydraulic conductivity of the Potomac aquifer at the pilot point located in Southhampton County.
k_sussex	Horizontal hydraulic conductivity of the Potomac aquifer at the pilot point located in Sussex County.
k_virgin_a	Horizontal hydraulic conductivity of the Virginia Beach aquifer.
k_westmore	Horizontal hydraulic conductivity of the Potomac aquifer at the pilot point located in Westmoreland County.
k_westwestm	Horizontal hydraulic conductivity of the Potomac aquifer at the pilot point located in western Westmoreland County.
k_york_e_a	Horizontal hydraulic conductivity of the Yorktown-Eastover aquifer.
mdflow	Specified flux from finite-difference cells in row 1 shown in figure 12a.
piedflow	Specified flux to finite-difference cells in columns 4–20 shown in figure 12b.
recharge	Specified recharge flux.
river_cond	Hydraulic conductance of simulated riverbeds.
rw	Effective well radius in Multi-Node Well (MNW) package.
spec_yield	Specific yield.
ss_aquitard	Specific storage of other confining units.
ss_other	Specific storage of other aquifers.
ss_potomac	Specific storage of the Potomac aquifer.
ss_upper_ce	Specific storage of the Upper Cenomanian confining unit.
vk_aquifer	Vertical hydraulic conductivity of other hydrogeologic units simulated as aquifers.
vk_calve_c	Vertical hydraulic conductivity of the Calvert confining unit at other pilot point locations.
vk_chickah	Vertical hydraulic conductivity of the Exmore matrix, Exmore clast, and Chickahominy confining units.
vk_james_c	Vertical hydraulic conductivity of the Calvert confining unit at the pilot point located in James City county.
vk_nanjemo	Vertical hydraulic conductivity of the Nanjemoy-Marlboro confining unit.
vk_peede_c	Vertical hydraulic conductivity of the Peedee confining unit.
vk_poto_cz	Vertical hydraulic conductivity of the Potomac confining zone.
vk_potomac	Vertical hydraulic conductivity of the Potomac aquifer.
vk_smary_c	Vertical hydraulic conductivity of the Saint Marys confining zone.
vk_surface	Vertical hydraulic conductivity of the surficial aquifer.
vk_upper_c	Vertical hydraulic conductivity of the Upper Cenomanian confining unit.
vk_virgb_c	Vertical hydraulic conductivity of the Virginia Beach confining unit.
vk_york_cz	Vertical hydraulic conductivity of the Yorktown-Eastover confining zone.

Simulation of Groundwater Flow in the Coastal Plain Aquifer System of Virginia

By Charles E. Heywood and Jason P. Pope

Abstract

The groundwater model documented in this report simulates the transient evolution of water levels in the aquifers and confining units of the Virginia Coastal Plain and adjacent portions of Maryland and North Carolina since 1890. Groundwater withdrawals have lowered water levels in Virginia Coastal Plain aquifers and have resulted in drawdown in the Potomac aquifer exceeding 200 feet in some areas. The discovery of the Chesapeake Bay impact crater and a revised conceptualization of the Potomac aquifer are two major changes to the hydrogeologic framework that have been incorporated into the groundwater model. The spatial scale of the model was selected on the basis of the primary function of the model of assessing the regional water-level responses of the confined aquifers beneath the Coastal Plain. The local horizontal groundwater flow through the surficial aquifer is not intended to be accurately simulated. Representation of recharge, evapotranspiration, and interaction with surface-water features, such as major rivers, lakes, the Chesapeake Bay, and the Atlantic Ocean, enable simulation of shallow flow-system details that influence locations of recharge to and discharge from the deeper confined flow system. The increased density of groundwater associated with the transition from fresh to salty groundwater near the Atlantic Ocean affects regional groundwater flow and was simulated with the Variable Density Flow Process of SEAWAT (a U.S. Geological Survey program for simulation of three-dimensional variable-density groundwater flow and transport). The groundwater density distribution was generated by a separate 108,000-year simulation of Pleistocene freshwater flushing around the Chesapeake Bay impact crater during transient sea-level changes. Specified-flux boundaries simulate increasing groundwater underflow out of the model domain into Maryland and minor underflow from the Piedmont Province into the model domain. Reported withdrawals accounted for approximately 75 percent of the total groundwater withdrawn from Coastal Plain aquifers during the year 2000. Unreported self-supplied withdrawals were simulated in the groundwater model by specifying their probable locations, magnitudes, and aquifer assignments on the basis of a separate study of domestic-well characteristics in Virginia.

The groundwater flow model was calibrated to 7,183 historic water-level observations from 497 observation wells with the parameter-estimation codes UCODE–2005 and PEST. Most water-level observations were from the Potomac aquifer system, which permitted a more complex spatial distribution of simulated hydraulic conductivity within the Potomac aquifer than was possible for other aquifers. Zone, function, and pilot-point approaches were used to distribute assigned hydraulic properties within the aquifer system. The good fit (root mean square error = 3.6 feet) of simulated to observed water levels and reasonableness of the estimated parameter values indicate the model is a good representation of the physical groundwater flow system. The magnitudes and temporal and spatial distributions of residuals indicate no appreciable model bias.

The model is intended to be useful for predicting changes in regional groundwater levels in the confined aquifer system in response to future pumping. Because the transient release of water stored in low-permeability confining units is simulated, drawdowns resulting from simulated pumping stresses may change substantially through time before reaching steady state. Consequently, transient simulations of water levels at different future times will be more accurate than a steady-state simulation for evaluating probable future aquifer-system responses to proposed pumping.

Introduction

During the 20th century, groundwater withdrawals increasingly supplied the domestic, municipal, and industrial water demands of the growing population of the Virginia Coastal Plain (fig. 1). Groundwater withdrawals from the Virginia Coastal Plain aquifers increased substantially after the onset of U.S. involvement in World War II (fig. 2), which resulted in regional cones of depression in which drawdown exceeded 200 feet (ft) in places by 2003. By the early 1970s, concern over the availability, quality, and sustainability of groundwater resources resulted in the Virginia Groundwater Act of 1973. During subsequent years, continued concern over the sustainability of fresh groundwater resources and the increased potential for seawater intrusion

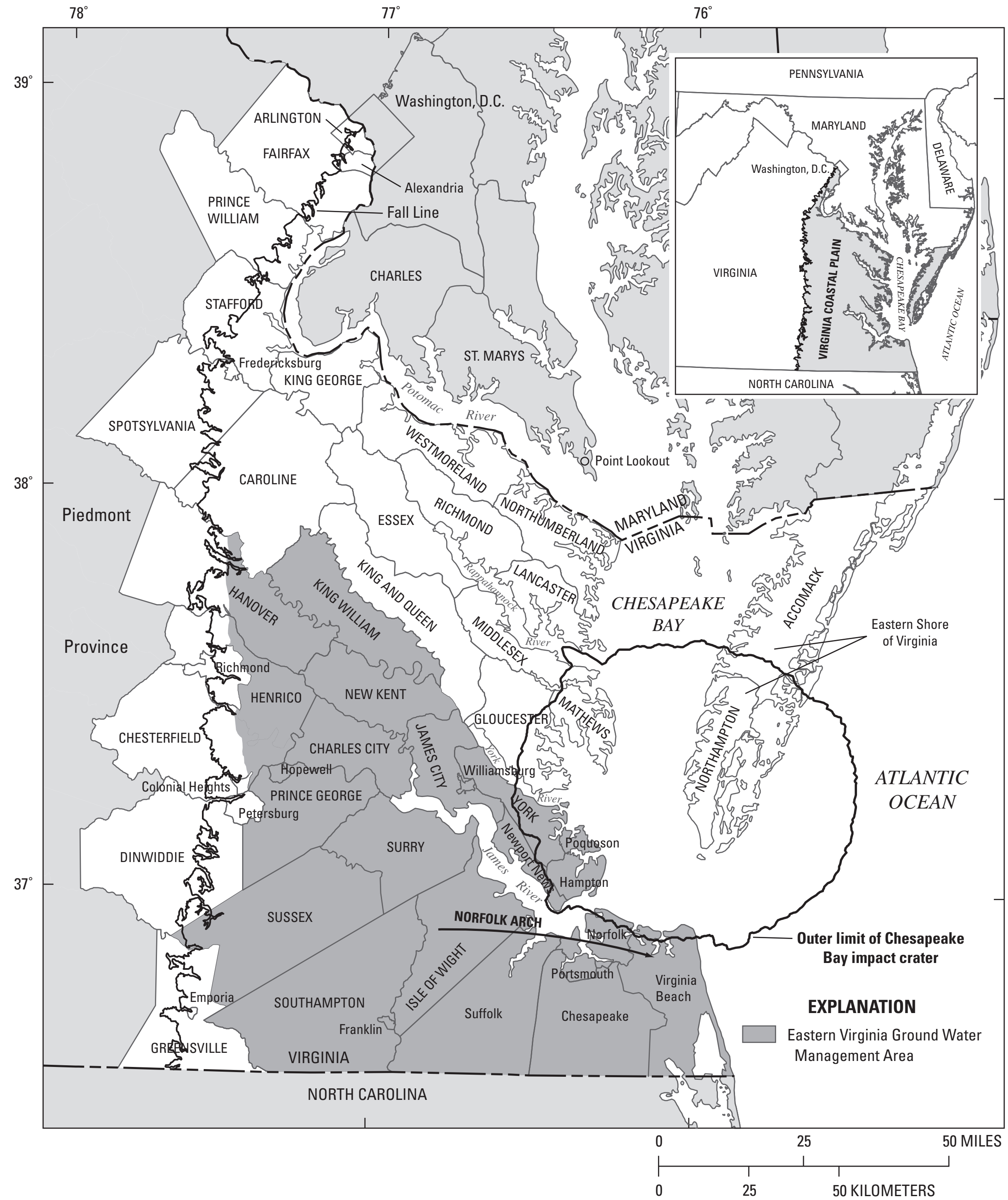

Figure 1. Locations of counties and independent cities, the Chesapeake Bay impact crater, and other important geographic and physiographic features of the Virginia Coastal Plain.

resulted in management of groundwater withdrawals through a State-controlled regulatory process. The Virginia Ground Water Management Act of 1992 empowered a State Water Control Board to create Ground Water Management Areas (GWMA), within which groundwater withdrawals greater than 300,000 gallons (gal) per month must be permitted by the Department of Environmental Quality (DEQ). The southeastern two-thirds of the Virginia Coastal Plain are currently a declared GWMA. Among the criteria for issuing groundwater withdrawal permits are the evaluation of the "area of impact" of a withdrawal and an assessment of the probable additional groundwater drawdown resulting from the proposed withdrawal. A regional groundwater flow model (Harsh and Laczniak, 1990) developed as part of the U.S. Geological Survey (USGS) Regional Aquifer System Analysis (RASA) Program was modified (McFarland, 1998) and used for these

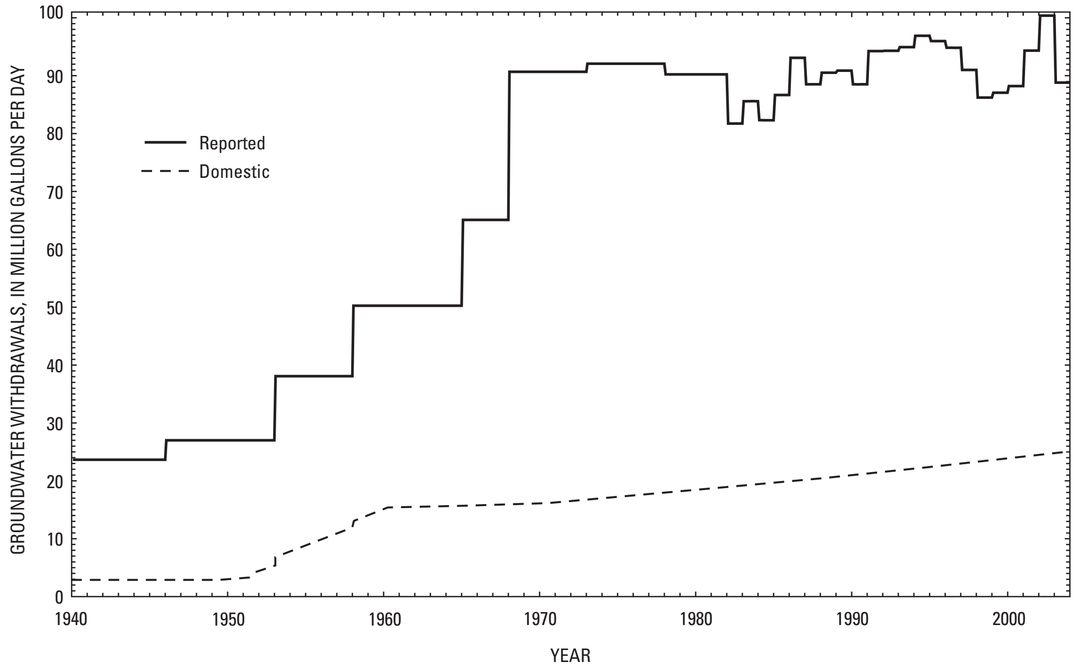

Figure 2. Virginia reported and domestic groundwater withdrawals.

evaluations. Water levels simulated with this modified RASA model differed from corresponding observed water levels by up to 100 ft in some areas of the Coastal Plain (Quinlan, 2004, 2005; Wright, 2006). This magnitude of inaccuracy has decreased the utility of the modified RASA model as a water-resource management tool.

The discovery of a buried impact crater beneath the Chesapeake Bay (Poag and others, 1994; Poag, 1999) revolutionized the conceptualization of the Virginia Coastal Plain hydrogeologic framework (Powars and Bruce, 1999; Powars, 2000). The low permeability of the tsunami-generated Exmore breccia within the Chesapeake Bay impact crater influences regional groundwater flow and the distribution of salty groundwater near the Atlantic Coast. Additional advancements in understanding the Coastal Plain hydrogeologic framework have been made in areas of Virginia outside of the crater.

The changes in conceptualization of the hydrogeologic framework and advances in hydrologic-modeling techniques motivated the development of the new groundwater flow model documented in this report. The DEQ and the Hampton Roads Planning District Commission (HRPDC) intend to use this model in place of the modified RASA model for future predictions of aquifer-system response to proposed groundwater withdrawals. The Virginia Coastal Plain groundwater regulatory scheme currently allocates withdrawals from the Potomac aquifer system as pumpage from either a lower, middle, or upper Potomac aquifer (or some combination) according to the RASA-era hydrogeologic framework. In the latest Virginia Coastal Plain hydrogeologic framework (McFarland and Bruce, 2006), the Potomac aquifer system is considered to be a single aquifer. This new conceptualization of the Potomac aquifer, which is incorporated in this model, may require a re-evaluation of the existing drawdown criteria used for the process of issuing withdrawal permits.

Purpose and Scope

This report describes a new computer simulation of groundwater flow in the aquifer system of the Atlantic Coastal Plain in Virginia. The simulation incorporates the recently revised hydrogeologic framework (McFarland and Bruce, 2006), which includes a redefined Potomac aquifer and representation of the units associated with the Chesapeake Bay impact crater. Development of the model included the identification of pertinent physical properties and processes to be simulated, design of the numerical discretization scheme, specification of initial and boundary conditions, and calibration of simulated to observed water levels by non-linear regression. The primary purpose of the model is to assist in the evaluation of the responses of the confined aquifers to groundwater withdrawals. The changes to aquifer-system water levels since the “predevelopment conditions” prevalent in 1890 are simulated by a 113-year transient simulation consisting of 34 stress periods and 218 time steps. Water-management or planning authorities who wish to assess the possible future regional groundwater drawdown resulting from proposed groundwater withdrawals may modify appropriate model-input files to run predictive simulations.

The scale of the model is appropriate for assessing the regional water-level responses in the confined aquifers of the Coastal Plain. Because groundwater flow in the unconfined surficial aquifer is largely influenced by topographic variations that cannot be represented with the 1-mile (mi) finite-difference cells of the model, local horizontal groundwater flow through the surficial aquifer is not simulated to the degree of accuracy necessary for its assessment as a groundwater resource. However, simulated vertical flow through the surficial aquifer from and to the water table in areas of groundwater recharge and discharge does allow an accurate assessment of groundwater transmission to and from underlying confined aquifers.

The modeled area encompasses all the Virginia Coastal Plain south of Stafford, VA, and the adjacent Coastal Plain areas of North Carolina and Maryland (fig. 3). The small Coastal Plain area in Virginia west of the Potomac River and north of Stafford, VA, is not included in the model domain. Although the Eastern Shore of Virginia (also known as the Delmarva Peninsula) is included in the model domain, accurate simulation of groundwater flow in the shallow unconfined and confined aquifers located there is not within the scope of this study. A more detailed groundwater flow model of the shallow aquifers on the Eastern Shore of Virginia was developed separately by Sanford and others (2009).

The regional scale of the model precludes its use for predicting the fate and transport of anthropogenic contaminants in surficial aquifers. The model does not accurately simulate horizontal flow in the surficial aquifers. However, the model could be used to provide boundary water levels and fluxes for more detailed smaller-scale models assembled to address local groundwater supply or contamination problems.

The increase in groundwater density associated with the transition from fresh to salty groundwater near the Atlantic Ocean affects regional groundwater flow. An approximation of the distribution of modern groundwater density was generated with an ancillary 108,000-year transport simulation of the evolution of the saltwater transition zone during the Pleistocene epoch. The details of this simulation are described in the appendix.

The 113-year transient model described in this report does not simulate saltwater intrusion. Unlike the ancillary 108,000-year transport simulation, the variable-density groundwater flow equation was not coupled to the mass-transport equation for the 113-year transient simulation. Therefore, the three-dimensional distribution of groundwater density does not change with time in the 113-year simulation. Although the numerical dispersion associated with 1-mi-wide finite-difference cells is acceptable for generating the regional groundwater density distribution with the 108,000-year transport simulation, it is not adequate when the simulation of temporal changes in solute concentration require a more accurate solution of the mass-transport equation. Smaller finite-difference cells would be required to accurately simulate solute transport. Appropriate representation of aquifer dispersivity is required for simulation and prediction of solute transport, which requires that numerical dispersion be minimized. However, the more-refined spatial and temporal discretization and computationally intensive solution algorithm required to accomplish this are not compatible with the scale and scope of the 113-year transient model, nor are the long simulation-execution times required by such algorithms compatible with the need for the large number of simulation runs required during parameter estimation.

Previous Studies

An extensive review of previous geologic and hydrologic studies of the Virginia Coastal Plain was recently provided by McFarland and Bruce (2006); a short synopsis from selected studies follows.

Sanford (1913) surveyed the groundwater resources of the Virginia Coastal Plain and provided a preliminary overview of the hydrogeology of the area. During and after the acceleration of groundwater development coinciding with the start of U.S. involvement in World War II, Cederstrom (1943, 1945, 1957, 1969) reported on more detailed studies of Coastal Plain hydrogeology. His groundwater quality analyses recognized the existence of an anomalous “inland saltwater wedge,” now known to coincide with the location of the Chesapeake Bay impact crater.

As a part of the USGS RASA Program, Meng and Harsh (1988) conducted the first comprehensive hydrogeologic analysis of the entire Virginia Coastal Plain aquifer system, in which they defined a hydrogeologic framework consisting of nine aquifers with eight intervening confining units. In this framework, the Potomac aquifer system was subdivided into the upper, middle, and lower Potomac aquifers, which were separated by laterally extensive confining units. Harsh and Laczniak (1990) used this framework to construct the first digital model of Coastal Plain groundwater flow in Virginia and adjacent parts of Maryland and North Carolina. This RASA model was subsequently modified (McFarland, 1998) for use as a management tool by personnel involved in Virginia’s regulatory and groundwater withdrawal permit process. Leahy and Martin (1993) noted the differences in simulated water levels between constant- and variable-density formulations of groundwater flow under the northern Atlantic Coastal Plain, including Virginia. Richardson (1994a) simulated a sharp transition from freshwater to saltwater with a dual-density model of groundwater flow in the shallow aquifers on the Eastern Shore of Virginia.

The discovery of the Chesapeake Bay impact crater enabled a major advancement in understanding the stratigraphy of the eastern part of the Coastal Plain, which was documented by Powars and Bruce (1999) and Powars (2000). McFarland and Bruce (2006) have provided a thorough revision to the earlier RASA hydrogeologic framework, including incorporation of hydrogeologic units associated with the Chesapeake Bay impact crater.

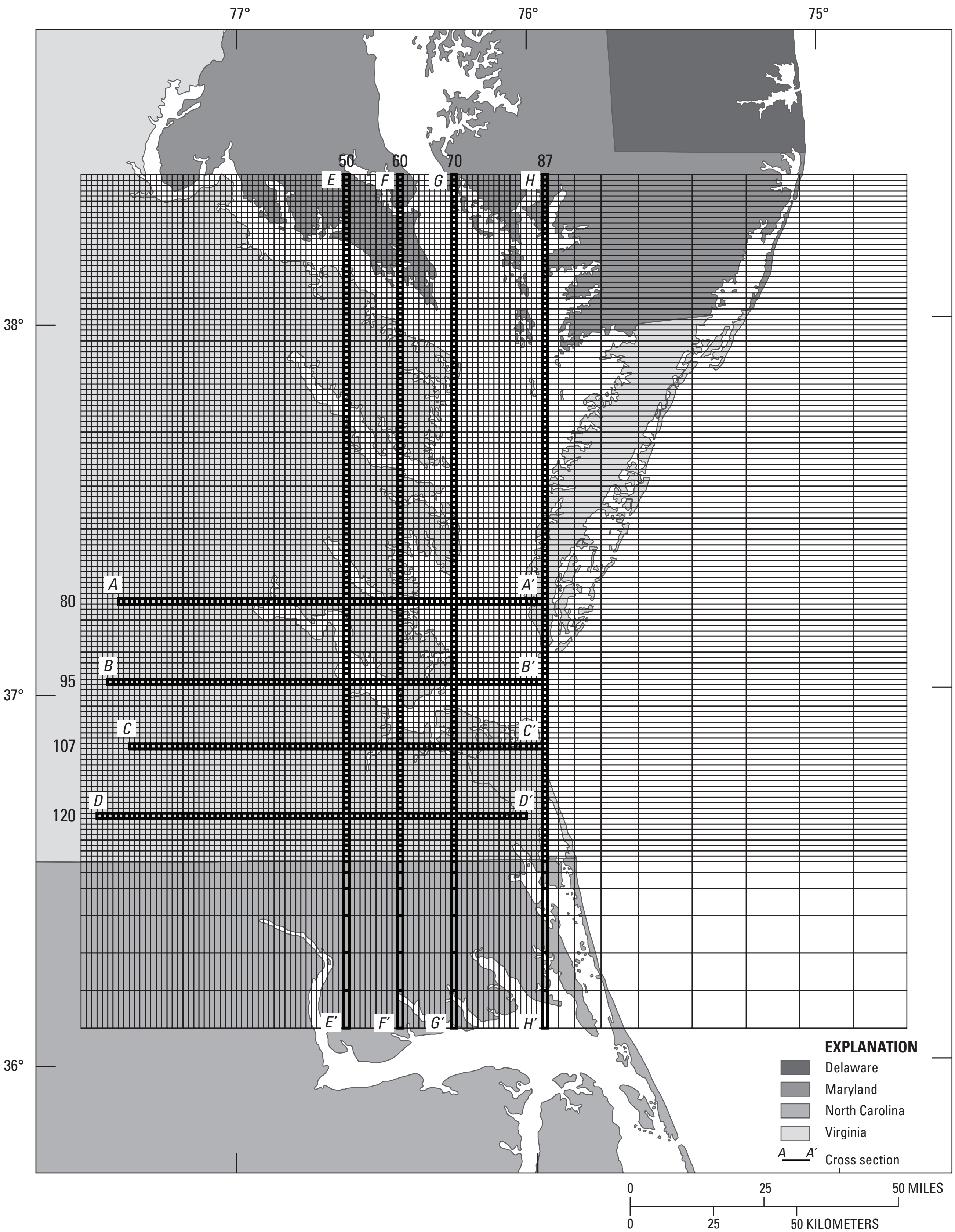

Figure 3. Finite-difference model grid of the Virginia Coastal Plain with row and column numbers of cross sections.

Description of the Virginia Coastal Plain

The Coastal Plain of Virginia is underlain by Early Cretaceous and younger unconsolidated sedimentary deposits that overlie older consolidated sedimentary, igneous, and metamorphic bedrock. The “Fall Line” separates the Coastal Plain from the Piedmont Physiographic Province to the west (fig. 1), which is composed of consolidated lower Mesozoic rift-basin and older crystalline bedrock that also underlie the Coastal Plain sedimentary strata. The “Fall Line” is named for the occurrence of rapids and small waterfalls in rivers that cross the contact from the consolidated rocks of the Piedmont to the more easily eroded Coastal Plain sediments.

Most of the topography of the Virginia Coastal Plain is flat to gently rolling and interspersed with numerous small gaining streams. Some deeply incised stream valleys accentuate the rolling topography in the northwest part of the Coastal Plain. The land-surface altitude ranges from zero to about 350 ft in the northwest part of the Coastal Plain, near the Fall Line in Stafford County. Three large rivers—the Rappahannock, York, and James—separate peninsular regions known as the Northern Neck, Middle, and York-James Peninsulas. The Northern Neck is bounded on the north by the Potomac River. The area south of the James River is known as southeastern Virginia. The Chesapeake Bay separates the mainland Coastal Plain from the Delmarva Peninsula, the Virginia portion of which is also known as the Eastern Shore (fig. 1).

The Coastal Plain climate is temperate; summers are hot and humid, and winters are moderate. The mean annual temperature is about 58 degrees Fahrenheit (°F). Precipitation throughout the year is predominantly rainfall, with occasional light snowfall in winter. The mean annual precipitation for the Coastal Plain is 45.9 inches (in.; Virginia State Climatology Office, 2007).

Hydrogeologic Framework

The sediments that underlie the Virginia Coastal Plain reflect changing depositional conditions during the past 120 million years, resulting in a sedimentary assemblage of gravels, sands, silts, and clays with a complex distribution of hydraulic properties. The Norfolk Arch (fig. 1) is an east-west trending structural high that separated post-Jurassic sedimentation into northern and southern depocenters, termed the Salisbury and Albemarle embayments, respectively. Cretaceous fluvial-deltaic and early Tertiary marine deposition formed a generally eastward-thickening unconsolidated sedimentary assemblage that attains a thickness of over 4,000 ft near the Atlantic coast. A mid-Eocene bolide impact excavated the post-Jurassic sedimentary strata and some older underlying rocks within a 56-mi-diameter area around Cape Charles, on the present-day Eastern Shore of Virginia. At the time of the impact, the sea level was approximately 200 ft higher than the present day, and the shore line was approximately coincident with the Fall Line. Tsunamis generated by this bolide impact on the submerged continental shelf re-deposited a chaotic mix of the excavated strata as clast- and matrix-supported breccias within the excavated crater (Powars and Bruce, 1999). Subsequent late-Eocene through Pliocene low-energy marine deposition buried the impact structure and the surrounding undisrupted Coastal Plain sediments with more clay, silt, and sand. The lower half of the crater contains rotated blocks and submarine-landslide deposits resulting from the impact event but not associated with the tsunami-resurge deposits.

The Coastal Plain strata have been classified into a layered sequence of aquifers and confining units, each of which generally thicken and deepen to the east toward the Atlantic Ocean. McFarland and Bruce (2006) describe the structural configuration of 19 hydrogeologic units within the Virginia Coastal Plain. Borehole electric logs were used along with drill-cutting and undisturbed core samples to define the altitude of the top of each hydrogeologic unit at borehole control points. Cross-borehole correlation enabled generation of two-dimensional surfaces that define the top altitude over the horizontal extent of each unit. Subtraction of the altitudes of adjacent surfaces generated raster representations of the thickness of each hydrogeologic unit. The composite assemblage of the top surfaces and associated thicknesses of all 19 hydrogeologic units comprise a three-dimensional model of the Coastal Plain hydrogeologic framework. This framework provides the primary basis for the distribution of model parameters representing the hydraulic properties that control the simulation of groundwater flow. None of the 19 hydrogeologic units are present throughout the entire domain of the groundwater model; they pinch out at lateral depositional boundaries, some are truncated by the Chesapeake Bay impact crater, and shallow units are discontinuous across incised river drainages. The complex three-dimensional distribution of these hydrogeologic units can be appreciated with computer software for viewing the solid model of the hydrogeologic framework. A series of east-west and north-south two-dimensional cross sections (the locations of which are shown in figure 3) through this solid model that illustrate the vertical relations between the various hydrogeologic units are shown in figure 4. The horizontal extents of each aquifer and confining unit or zone are presented in figures later in the report.

McFarland and Bruce (2006) classified Cretaceous and younger unconsolidated Virginia Coastal Plain sediments into 19 hydrogeologic units, of which 8 are identified as aquifers, 7 are confining units, and 4 are considered “confining zones.” The age, stratigraphic sequence, and relation to geologic formation names in Virginia are summarized in figure 5. The reader is referred to McFarland and Bruce (2006) for an explanation of hydrologic associations that cross stratigraphic boundaries. McFarland and Bruce (2006) distinguish “homogenous aquifers,” which “can have locally gradational changes in texture and(or) composition” from “heterogeneous aquifers,” which “exhibit sharp contrasts in sediment texture

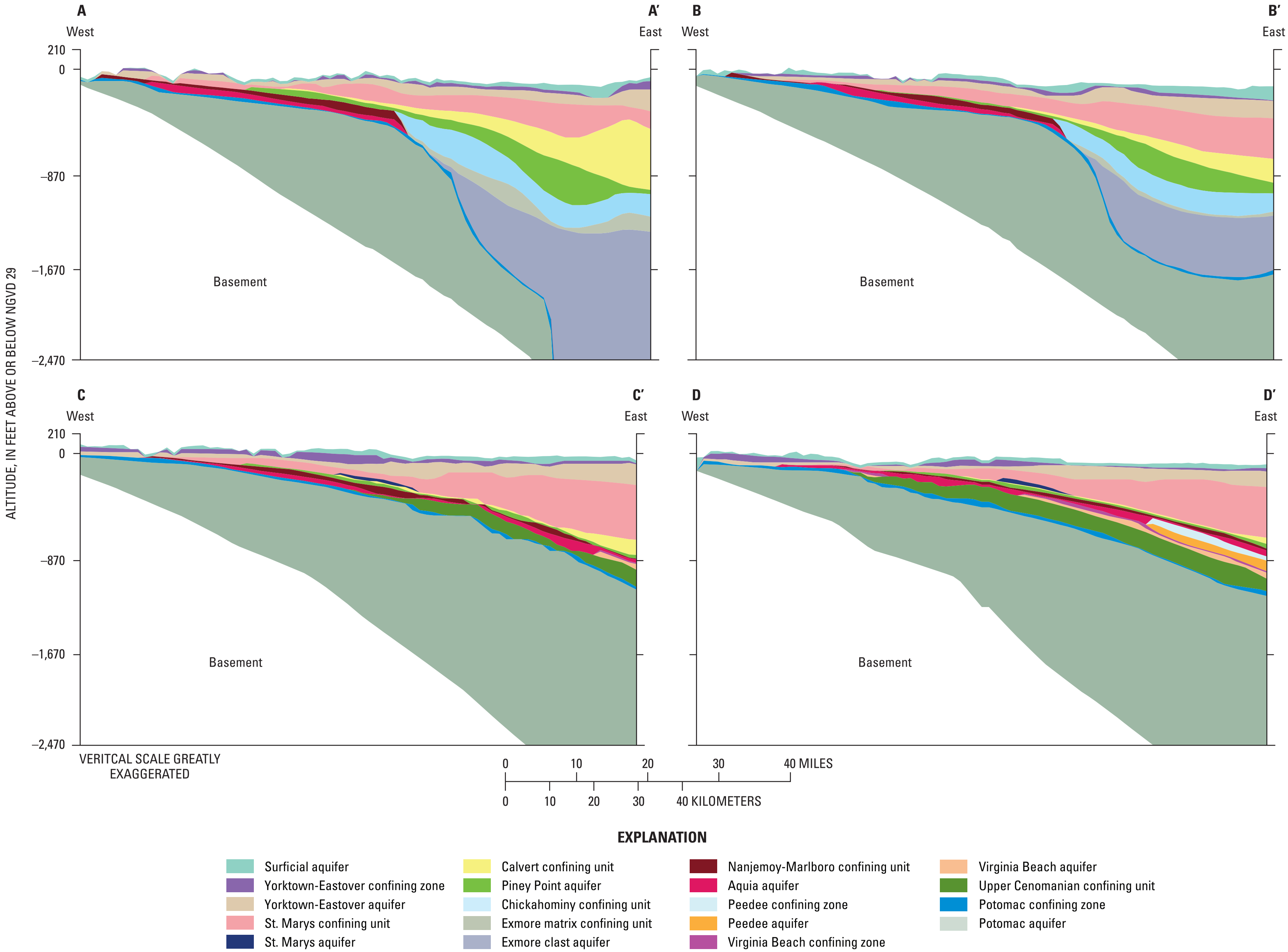

Figure 4. Vertical model cross sections showing distribution of hydrogeologic units from west to east along row 80 (A–A′), west to east along row 95 (B–B′), west to east along row 107 (C–C′), west to east along row 120 (D–D′), north to south along column 50 (E–E′), north to south along column 60 (F–F′), north to south along column 70 (G–G′), and north to south along column 87 (H–H′). (Locations of cross sections are shown in figure 3.)

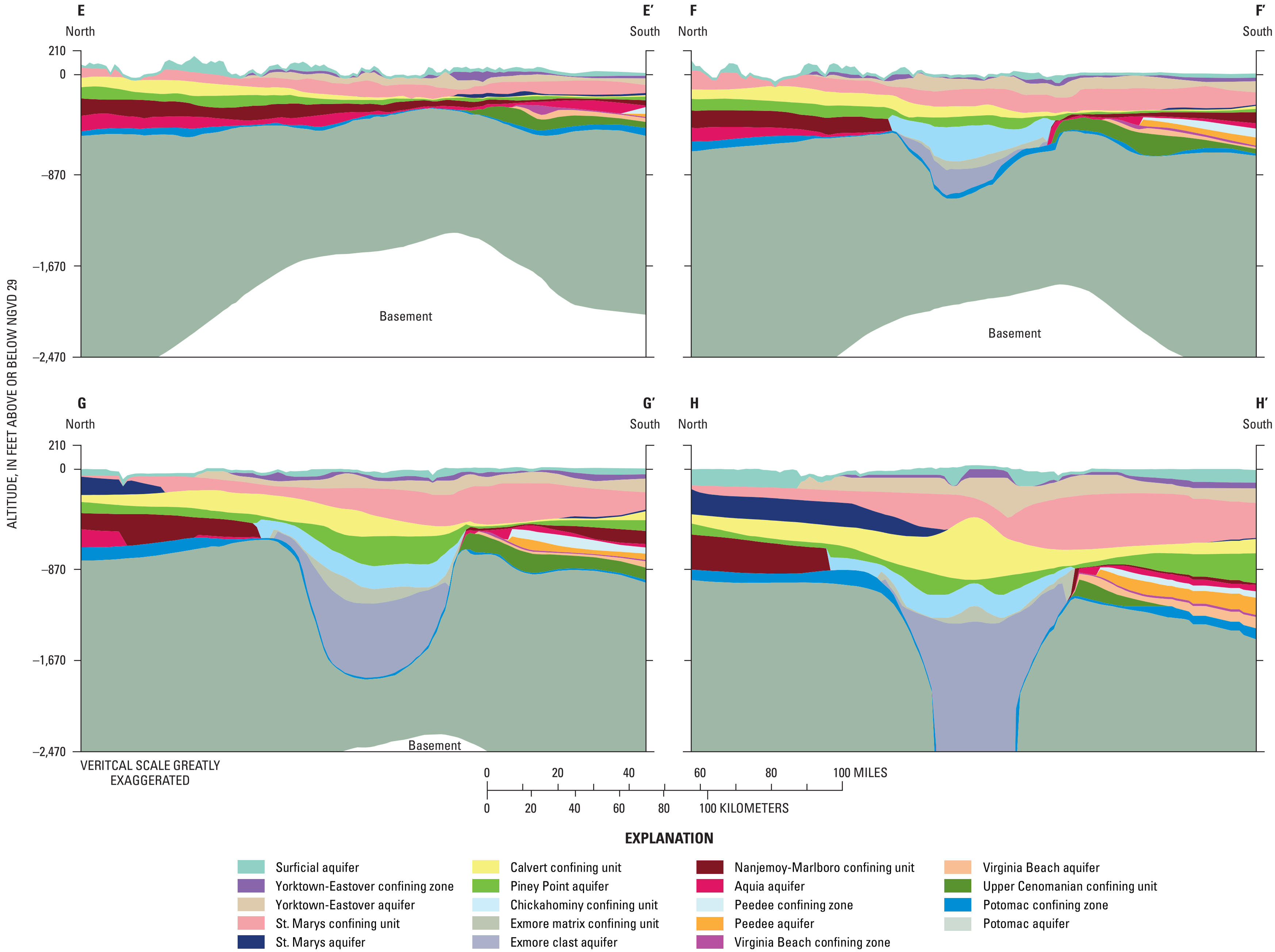

Figure 4. Vertical model cross sections showing distribution of hydrogeologic units from west to east along row 80 (A–A′), west to east along row 95 (B–B′), west to east along row 107 (C–C′), west to east along row 120 (D–D′), north to south along column 50 (E–E′), north to south along column 60 (F–F′), north to south along column 70 (G–G′), and north to south along column 87 (H–H′). (Locations of cross sections are shown in figure 3.)—Continued

ERATHEM/ ERA	PERIOD	SERIES/ EPOCH		GEOLOGIC UNIT Powars and Bruce, 1999; Powars, 2000	HYDROGEOLOGIC UNIT McFarland and Bruce, 2006
Cenozoic	Quaternary	Holocene		undifferentiated	surficial aquifer
		Pleistocene			
	Tertiary	Pliocene	late	Bacons Castle	Yorktown confining zone
				Chowan River	
				Yorktown	Yorktown confining zone
			early		Yorktown-Eastover aquifer
		Miocene	late	Eastover	St. Marys confining unit
				St. Marys	St. Marys aquifer
			middle	Calvert	Calvert confining unit
			early		Piney Point aquifer
		Oligocene	late	Old Church	
			early	Delmarva Beds	
		Eocene	late	Chickahominy	Chickahominy confining unit
				Exmore tsunami-breccia	Exmore matrix confining unit
					Exmore clast confining unit
				megablock beds	Potomac confining zone
					Potomac aquifer
			middle	Piney Point	Piney Point aquifer
			early	Nanjemoy	Nanjemoy-Marlboro confining unit
				Marlboro Clay	
		Paleocene	late	Aquia	Aquia aquifer
			early	Brightseat	Peedee confining zone
Mesozoic	Cretaceous	Late		clayey silty sand	
				organic-rich clay	
				glauconite quartz sand	Peedee
				red beds	aquifer
				glauconitic sand	Virginia Beach confining zone
					Virginia Beach aquifer
				upper Cenomanian beds	Upper Cenomanian confining unit
		Early		Potomac	Potomac confining zone
					Potomac aquifer
	Jurassic	Undifferentiated			Basement
	Triassic				
Paleozoic					
Proterozoic					

Figure 5. Stratigraphic correlations of hydrogeologic units of the Virginia Coastal Plain (modified from McFarland and Bruce, 2006.) Vertical arrows indicate major hydrologic associations that cross stratigraphic boundaries; minor overlaps of hydrogeologic units among adjacent geologic formations are not depicted.

across small distances in the form of discontinuous and locally variable fine-grained sediments that are interbedded with coarse-grained sediments." The surficial, Yorktown-Eastover, Peedee, and Potomac aquifers are considered heterogeneous, and the St. Marys, Piney Point, Aquia, and Virginia Beach aquifers are considered to be homogeneous.

McFarland and Bruce (2006) also identify "…indistinguishable relations that can exist adjacent to heterogeneous aquifers. Confining zones bound major parts of heterogeneous aquifers that extend across distances as great as several tens of miles and that are separated from adjacent aquifers solely by interbeds because no confining unit is present. Moreover, neither an interbed nor a confining unit may be present at many locations across the confining zones, thereby allowing direct contact of the coarse-grained sediments of the adjacent aquifers." Note that areas that are not considered "confining" by common hydrologic meaning may be included in units designated as a "confining zone" according to this stratigraphic usage of this term by McFarland and Bruce (2006).

In contrast to the earlier three-aquifer conceptualization by Meng and Harsh (1988), the Potomac aquifer system is currently considered to be a three-dimensional fluvial-deltaic network of anastomosing sandy river channels and fine-grained overbank deposits composing a single hydrogeologic unit. McFarland and Bruce (2006) determined that the low-resistivity signals identifying individual fine-grained layers within the Potomac Formation generally cannot be correlated between boreholes separated by more than several thousand feet. If more laterally extensive fine-grained layers exist within the Potomac Formation, they have not been mapped or documented as of 2009. The maximum lateral extent of most of the numerous low-permeability clay interbeds within the Potomac Formation is, therefore, probably on the order of several hundred feet.

Hydrologic Conditions

Climatic conditions and surface-water features influence the recharge to and flow through the aquifer system. Before the onset of extensive groundwater extraction in the 20th century, shallow groundwater flowed toward discharge areas at rivers, the Chesapeake Bay, and the Atlantic Ocean and also discharged by evapotranspiration in low-altitude areas. Deeper recharged groundwater flowed east toward a mixing zone with higher-density seawater, where it was deflected upward toward discharge areas near the coast above the deeper higher-density salty groundwater. These generalized patterns of predevelopment groundwater flow are depicted in figure 6. The spatial distributions of the hydraulic properties associated with the various hydrogeologic units, as well as the recharge fluxes and their geometric relation to discharge areas at the land or sea-floor surface, all controlled the directions and

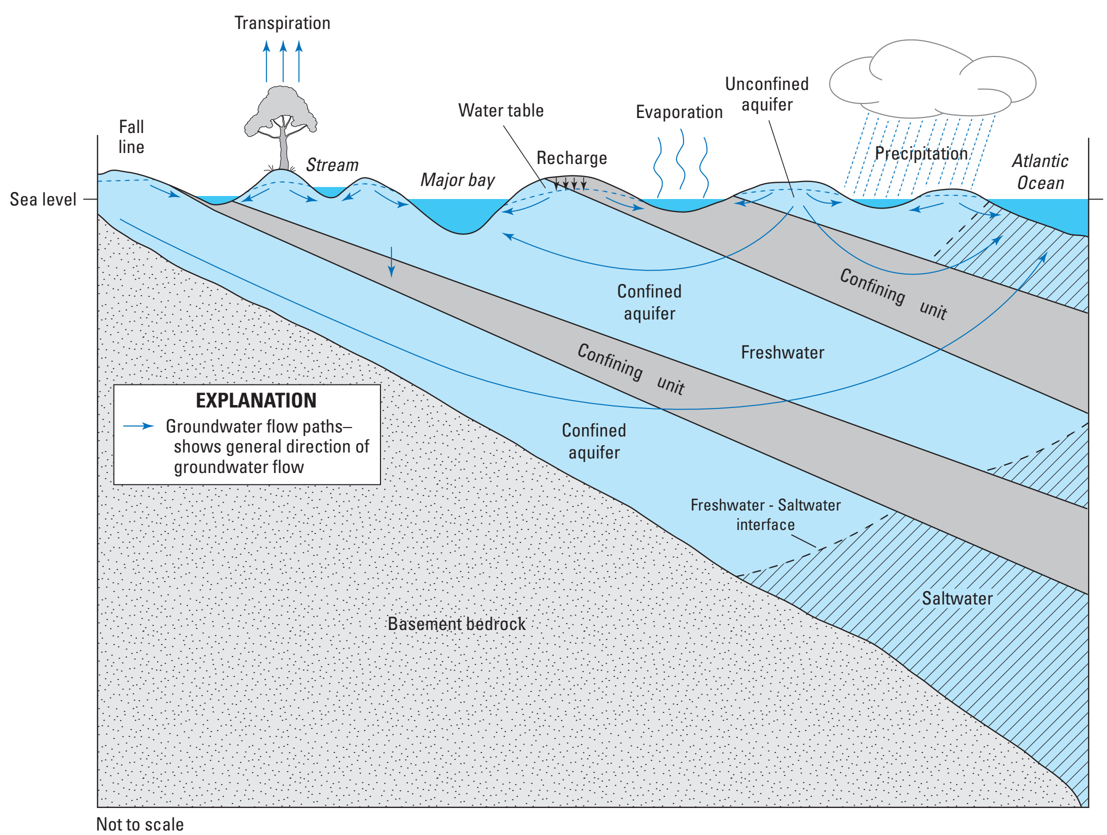

Figure 6. Generalized predevelopment groundwater flow patterns in the Coastal Plain aquifer system (modified from Leahy and Martin, 1993).

rates of predevelopment groundwater flow. After the installation of pumping wells, the commencement of groundwater withdrawals introduced stresses within the aquifer system that modified the groundwater flow rates and directions from their predevelopment conditions.

Precipitation

For the period from 1895 through 2001, the mean annual precipitation for Virginia was 42.5 in. (National Climate Data Center, 2002). The Coastal Plain receives slightly more precipitation than the remainder of Virginia; the average of annual precipitations recorded at Richmond and Norfolk, VA, for the period 1895–1998 was 44.6 in. (Virginia State Climatology Office, 2007). July and August are the wettest months for the Coastal Plain; monthly precipitation for those months averages slightly over 5 in., and other months average between 3 and 4 in. of precipitation.

Precipitation is a large component of groundwater recharge, which is specified as a temporally variable boundary flux in the groundwater model. A simple analysis of the spatial and temporal variations of Coastal Plain precipitation was necessary to quantify groundwater recharge for the model. The locations of precipitation-measurement stations at Williamsburg, Norfolk, Hopewell, and Fredericksburg (Virginia State Climatology Office, 2007) are shown in figure 7, and the annual totals of monthly precipitation measured at these stations over the period from 1891 through 2003 are depicted in figure 8. The mean annual precipitation for these measurement sites for the period from 1895 through 2003 is 45.9 in. The precipitation records illustrate good correlation of total precipitation between these four recording stations. A change of mean annual precipitation measured at Williamsburg is apparent in figure 8. Although precipitation measured at Williamsburg is consistently higher than precipitation measured at Fredericksburg, the difference between these stations becomes less pronounced during the period after 1978. The mean annual precipitation at Williamsburg from 1905 through 1953 was 59.1 in., and from 1958 through 2003 the mean annual precipitation was 48.2 in.

Evapotranspiration

Water evaporates from the surfaces of land and water bodies, the water table, the intervening unsaturated zone, and through the plant stomata (transpiration). It is difficult to separate the amounts of transpiration and evaporation over vegetated land areas, and these two processes commonly are combined and represented by an evapotranspiration (ET) term in hydrologic models. Annual potential ET (PET) is the maximum ET flux that could occur without a shortage of water. The Virginia State Climatology Office (2007) has calculated PET for sites in Virginia by the Thornthwaite (1948) method, which is based on an empirical relation between PET and mean air temperature. The mean annual PET for five sites in the Coastal Plain (Richmond, Williamsburg, Suffolk, Norfolk, and Fredericksburg) is 32 in.

ET from the water table is considered separately from vadose-zone ET because the groundwater model documented in this report only simulates saturated-zone processes. In the absence of plants, evaporative flux decreases with depth to the water table. Gardner and Fireman (1958) studied the evaporation rate as a function of water-table depth for two soil types (sandy loam and clay); evaporation rate decreased to less than 10 percent of the maximum rate for both soil types at depths below about 8 ft. Transpiration losses can occur to the maximum depth to which plant roots are able to penetrate. Canadell and others (1996) reported rooting depths by vegetation and climate types. In temperate climates similar to that of the Virginia Coastal Plain, they reported average maximum-root depths of 9.5 ft (2.9 meters [m]) for deciduous trees and 12.8 ft (3.9 m) for coniferous trees. In the Virginia Coastal Plain, ET losses from the saturated groundwater system are probably negligible when the water table is deeper than about 13 ft below land surface.

Recharge

The fraction of precipitation infiltrating Coastal Plain sediments that is not evaporated or transpired by plants may recharge aquifers and subsequently flow toward areas of groundwater discharge. In areas not covered by a surface-water feature, such as a lake or stream, recharge to the saturated groundwater flow system primarily occurs from deep percolation of precipitation through the unsaturated zone to the water table. Some precipitation that falls on the ground surface (P) runs off to surface streams and rivers without infiltrating the ground (Q_{runoff}). Some of the water that does infiltrate below ground surface is evaporated or transpired from the vadose zone (ET_{vadose}). If the moisture content within the unsaturated zone is sufficiently high, the remaining infiltrated water percolates to the water table and is considered recharge to the saturated groundwater system. Secondary (and volumetrically minor compared to infiltrated precipitation) contributions to recharge are effluent from septic systems, return percolation from irrigation, and leakage from water and septic pipelines (Q_{other}). These components of recharge (R) are summarized by the mass-balance equation:

$$R = P + Q_{other} - Q_{runoff} - ET_{vadose}. \tag{1}$$

The quantity R was required for the simulation and was estimated as a fraction of P; quantification of the components in the remaining fraction ($Q_{other} - Q_{runoff} - ET_{vadose}$) was not necessary. Groundwater at or below the water table may also be lost to evaporation or transpiration by plants or trees with roots that penetrate below the depth of the water table (ET_{sat}). The remaining net recharge to the saturated groundwater flow system is:

$$R - ET_{sat} = P + Q_{other} - Q_{runoff} - ET_{vadose} - ET_{sat}. \tag{2}$$

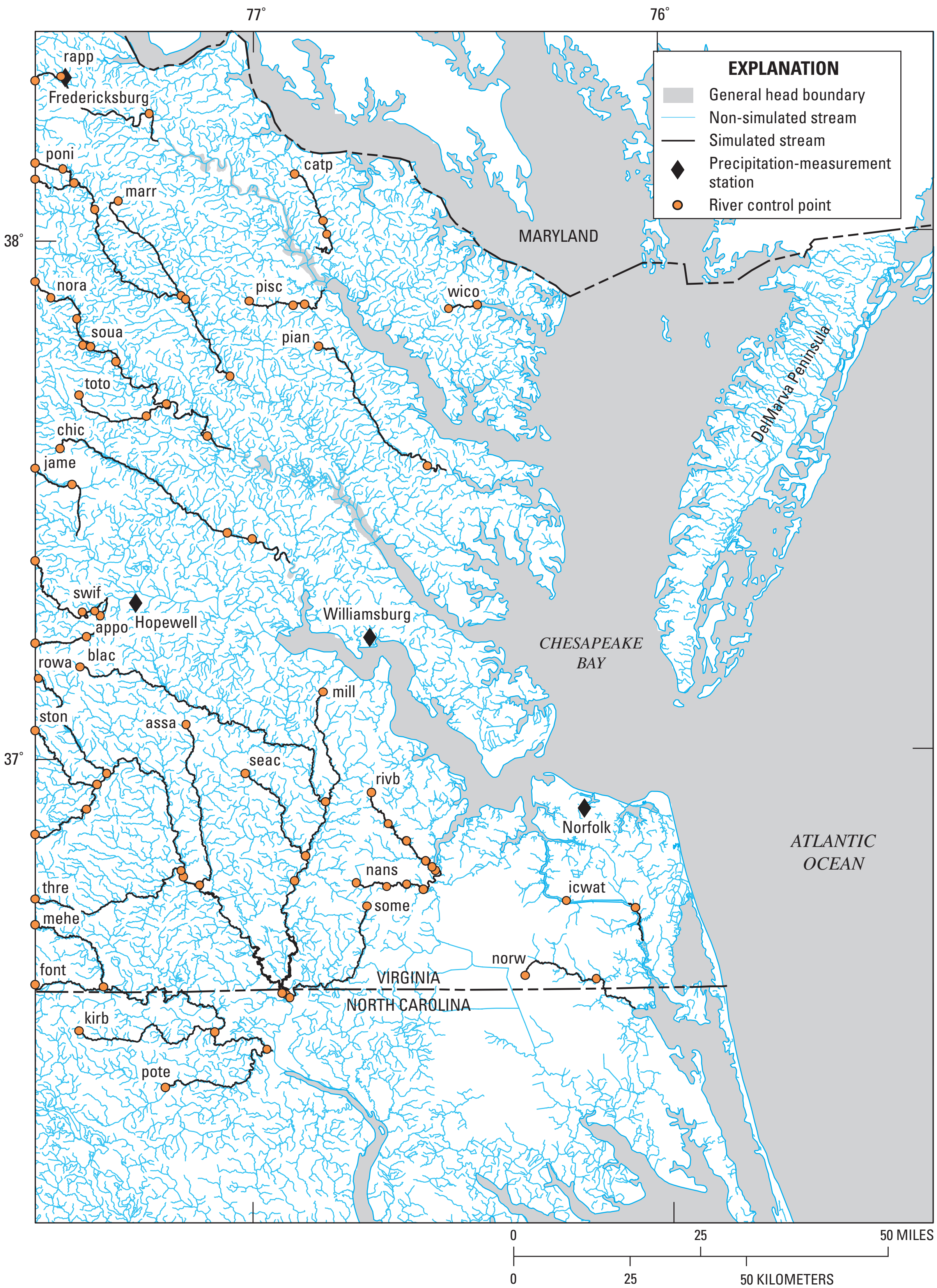

Figure 7. Locations of precipitation-measurement stations, control points, and rivers simulated with the River package, other streams, and sea-level areas simulated with the General Head Boundary Package in the Virginia Coastal Plain. (River-name abbreviations reference table 5.)

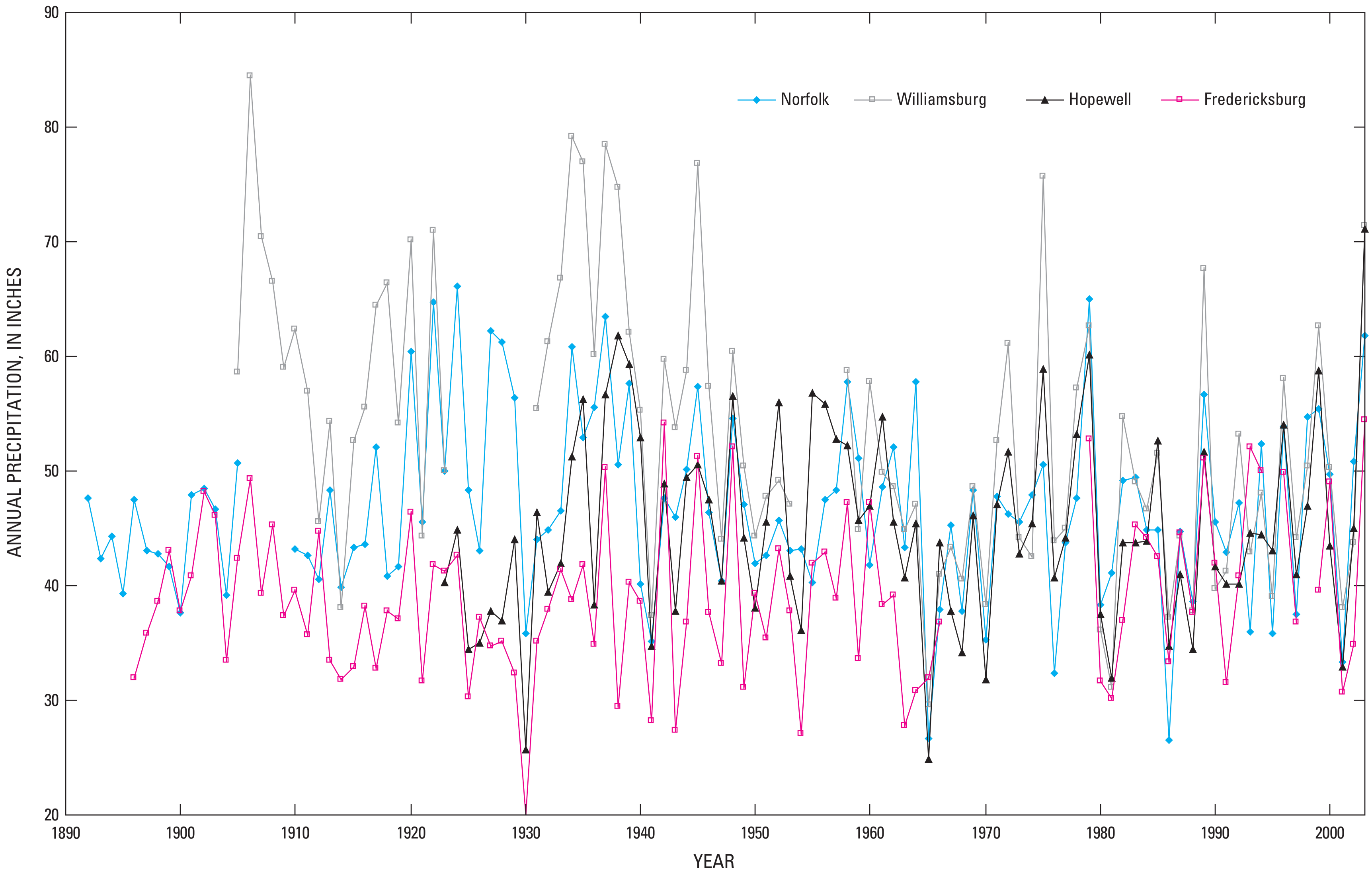

Figure 8. Historical measured precipitation at the four precipitation-measurement stations in the Virginia Coastal Plain. (Site locations are shown in figure 7. Data from Virginia State Climatology Office, 2007.)

Richardson (1994b) used hydrograph-separation (Rutledge, 1993) and hydrogeologic-area approaches to estimate an average discharge flux (base flow) of about 10 in/yr from the Coastal Plain of Virginia. The discharge flux from that study is an estimate of the effective recharge quantified in equation 2.

Groundwater Underflow from the Piedmont Province

Groundwater flow in the Piedmont Province of Virginia generally is thought to be compartmentalized between topographic drainages, and "water is not gained from or lost to deeper regional ground-water flow systems…" (Powell and Abe, 1985). In the Piedmont, recharge over interfluves contributes to storage in the shallow regolith and the flow though the deeper crystalline bedrock fractures that discharges to local rivers and streams. On the basis of this conceptual model, previous Coastal Plain modeling studies have assumed that there is no continuity of groundwater flow across the Fall Line from the Piedmont Province into the Coastal Plain. Harsh and Laczniak (1990) state:

> *The westernmost boundary of the model coincides with the Fall Line and is considered impermeable to flow. This assumption is supported by the large difference in hydraulic conductivity between the rocks of the Piedmont physiographic province and the unconsolidated sediments of the Coastal Plain physiographic province.*

A statistical analysis by Daniel (1989) of North Carolina Piedmont well records indicated that well yields increase with depth to a maximum at 700 to 800 ft below land surface, a greater depth than previously thought. It is possible that some flow through deeper Piedmont bedrock fractures may be regional and discharges through Coastal Plain sediments to the east. The magnitude of this underflow is unknown but is almost certainly a minor component of the Piedmont groundwater budget and a minor source of water to the Coastal Plain groundwater flow system.

Tensional stress in the Norfolk Arch may have fractured Piedmont rocks, thereby enhancing fracture permeability and the flow of groundwater toward the Coastal Plain over the Norfolk Arch (fig. 1). The larger area of the Piedmont Province in southern Virginia may also contribute to more deep groundwater infiltration and underflow to Coastal Plain sediments in southern Virginia than north of the Norfolk Arch. It is speculative if either or both of these effects cause a greater flux of Piedmont groundwater to the Coastal Plain in southern Virginia than further north. In this modeling study, the effect of possible groundwater underflow from the Piedmont to the Coastal Plain over the Norfolk Arch was simulated.

Hydraulic Properties

In steady-state groundwater flow, the water-level distribution and groundwater flux is controlled by hydraulic conductivity (K), which depends on the intrinsic permeability of the porous media and the density and viscosity of the fluid. The variability of these fluid properties (which depend on temperature and solute concentration) in Coastal Plain groundwater is small and has a relatively insignificant effect on changes of hydraulic conductivity. By contrast, the difference in hydraulic conductivity between a gravel and marine clay, which represent end-members on the range of intrinsic permeability expected for the sedimentary deposits comprising Coastal Plain aquifers and confining units, may be 10 orders of magnitude (Domenico and Schwartz, 1990). Within the Coastal Plain aquifer system, changes in hydraulic conductivity associated with the different sedimentary materials occur with different magnitudes at various scales. Hydraulic conductivity contrasts within the fluvial-deltaic Potomac aquifer system may be greater than those in hydrogeologic units formed under more uniform marine depositional environments.

The response of the aquifer or confining unit to a change in hydraulic stress under transient groundwater flow condition is also influenced by a storage property, which is represented in the groundwater flow equation by either specific storage (S_s) or specific yield (S_y).

Hydraulic Conductivity

Hydraulic conductivities determined from laboratory measurements of core-size samples and analyses of aquifer-performance tests may differ greatly because of scale effects, sampling, and testing and analytical methodologies. Review of the range of hydraulic conductivities determined by these methods is useful for comparison to those appropriate at the scale of the regional groundwater flow model, which were estimated during model calibration. These laboratory or field measurements of hydraulic conductivity also help establish the expected "reasonable range" for model parameters representing the horizontal or vertical hydraulic conductivity of various hydrogeologic units.

McFarland and Bruce (2006) reported measured vertical hydraulic conductivities from 33 sediment core samples collected from 3 boreholes within the area of the Chesapeake Bay impact crater; these hydraulic conductivities are considered representative only within an order of magnitude. The largest vertical hydraulic conductivity of 2.8 feet per day (ft/d) was measured from a sand collected from the Potomac aquifer. Permeameter measurements of samples representing the Yorktown-Eastover and Piney Point aquifers ranged from $6x10^{-4}$ to $2x10^{-2}$ ft/d. Permeameter measurements of samples from Potomac sands ranged from $6x10^{-4}$ to 2.8 ft/d. Permeameter measurements of samples from Potomac clay interbeds ranged from $3x10^{-5}$ to $2x10^{-3}$ ft/d. Permeameter measurements of samples representing the St. Marys, Calvert, Chickahominy, and Exmore matrix and clast confining units ranged from $3x10^{-5}$ to $6x10^{-2}$ ft/d. Separate measurements representing the same confining unit differ by up to three orders of magnitude. Measured hydraulic conductivities are not correlated to sample burial depth in any of the sampled hydrogeologic units. McFarland and Bruce (2006) state that non-cohesive coarse-grained sediments could not be collected, and consequently, the higher hydraulic conductivities expected for those sediments may be underrepresented in their sample set.

Transmissivity (T) values from analyses of Potomac aquifer-performance tests are summarized in table 1. These data were provided by the Virginia DEQ (Robin Patton, written commun., 2004). In most cases, either different tests of the same well, different analyses of the same data, or analyses using different observation wells resulted in a range of transmissivity values associated with each pumping well (table 1). The transmissivity values were divided by the screened interval of each well to estimate hydraulic conductivities, which range from 15 to 337 ft/d. Multiple analyses of some wells give a range of transmissivity (and subsequently, hydraulic conductivity) values. For example, hydraulic conductivities from three analyses of aquifer-performance data (by two consulting firms and the Virginia DEQ) from well 161-00371 (located in the City of Suffolk and operated by the Western Tidewater Authority), range from 83 to 337 ft/d. Low hydraulic conductivities from each aquifer performance test range from 15 to 175 ft/d, with a mean of 59 and a standard deviation of 42 ft/d.

Specific Storage

When water levels change under confined conditions, the amount of water stored or released from a representative volume of the porous media is due to the volumetric compressibility of water and the porous medium. These are quantified by the elastic specific storage, which is approximated by the expression:

$$S_{se}=\rho_f g(\alpha+n\beta_w), \tag{3}$$

Table 1. Summary of Potomac aquifer-performance test results.

[-, no analysis; T, transmissivity; ft²/d, feet squared per day; S, storage coefficient; K, hydraulic conductivity; S_s, specific storage; ft/d, feet per day; ft^{-1}, per foot. Data provided by the Virginia Department of Environmental Quality]

Well ID	T low (ft²/d)	T high (ft²/d)	S low	S high	Interval length (ft)	K low (ft/d)	K high (ft/d)	S_s low (ft^{-1})	S_s high (ft^{-1})
161-00380	11,963	-	-	-	202	59	-	-	-
146-00304	5,665	6,564	-	-	76	75	86	-	-
216-00086	6,112	-	0.00022	-	35	175	-	6.3E-06	-
216-00036	3,789	6,234	-	-	66	57	94	-	-
161-00397	8,328	15,774	0.00082	0.0011	150	56	105	5.5E-06	7.3E-06
187-00026	2,693	3,456	0.000052	0.000298	16	168	216	3.3E-06	1.9E-05
147-00262	8,082	8,823	0.000385	-	220	37	40	1.8E-06	-
147-00260	2,874	5,080	0.00054	-	190	15	27	2.8E-06	-
147-00294	12,346	13,700	0.000692	-	305	40	45	2.3E-06	-
147-00232	3,413	3,719	0.0007	0.0012	125	27	30	5.6E-06	9.6E-06
161-00371	31,345	127,395	-	-	378	83	337	-	-
161-00372	14,791	23,323	-	-	380	39	61	-	-
146-00250	10,999	11,782	-	-	220	54	54	-	-
146-00251	17,902	98,160	-	-	310	58	317	-	-
234-00220	2,779	2,779	0.0003	-	188	15	15	1.6E-06	-
234-00221	4,186	7,183	0.000071	0.00044	79	53	91	9.0E-07	5.6E-06
234-00222	6,961	13,334	0.00019	0.00034	94	74	142	2.0E-06	3.6E-06
234-00223	4,805	8,171	0.00016	0.00033	104	46	79	1.5E-06	3.2E-06
216-00041	7,198	-	-	-	455	16	-	-	-
161-00396	12,352	14,611	0.00067	0.001	160	77	91	4.2E-06	6.3E-06
147-00287	10,994	13,700	0.000792	-	440	25	31	1.8E-06	-

where

ρ_f is the density of water,
g is the acceleration of gravity,
α is the uniaxial compressibility of the porous media,
n is porosity, and
β_w is the isothermal compressibility of water.

For porous media with a porosity of 0.3, the component of specific storage resulting from the compressibility of freshwater ($\rho_f g n \beta_w$) at 5 °C is 4.3 x10^{-7} ft^{-1}. Because β_w is essentially constant over the range of pressures and temperatures in groundwater flow systems and *n* varies by less than an order of magnitude, reasonable values of specific storage are constrained by the plausible range of the porous media compressibility (α). For alluvial sediment, the lower limit of α is approximately the same as β_w, so the lower limit of reasonable values of elastic specific storage is about 1x10^{-6} ft^{-1}. Laboratory consolidation tests of the virgin (non-recoverable) compressibility of normally consolidated alluvial materials at effective stress levels substantially higher than the in situ stress are not representative of the elastic compressibility applicable to in situ effective stress changes caused by groundwater level declines that do not exceed the preconsolidation stress in over-consolidated sediments. Widely cited laboratory compressibility measurements (Domenico and Mifflin, 1965) from such tests may be useful for estimating inelastic specific storage (S_{sv}) but are too large and *not* applicable for estimating reasonable values of elastic specific storage (S_{se}). (For a further discussion of this issue see also Riley, 1998.) Extensometric measurements of elastic specific storage in alluvial aquifer systems containing interbedded aquitards from a variety of field sites are consistently in the range from 1.8x10^{-6} to 4x10^{-6} ft^{-1} (Ireland and others, 1984; Heywood, 1995, 1998). Using the one-dimensional vertical compaction model of Helm (1974), Pope and Burbey (2004) determined elastic specific storage values between 1.4x10^{-6} and 1.8x10^{-6} ft^{-1} for Coastal Plain sediments penetrated by vertical extensometers at Franklin and Suffolk, VA. Pope and Burbey (2004) also estimated that the inelastic specific storage values of fine-grained interbeds within the Potomac aquifer system range from 4.6x10^{-6} to 1.6x10^{-5} ft^{-1} and that inelastic specific storage values of post-Cretaceous fine-grained sediments range from 3x10^{-5} to 4.6x10^{-5} ft^{-1} at these sites. Other studies employing compaction modeling have similarly found that, for individual aquitards, elastic specific storage is typically $<$ 2x10^{-5} ft^{-1} for water-level declines resulting in elastic compression, and inelastic specific storage is $<$ 7x10^{-4} ft^{-1} when water-level declines result in inelastic compaction (Ireland and others, 1984; Epstein, 1987).

Some of the Potomac aquifer-performance test analyses summarized in table 1 reported a storage-coefficient value. Estimates of specific storage in table 1 were obtained by dividing these storage-coefficient values by the screened interval of each well; estimates ranged from 9 x10^{-7} to 1.9x10^{-5} ft^{-1}. In the absence of detailed stratigraphic logs, this procedure provides a useful test for reasonableness of aquifer storage-coefficient values. However, it must be recognized that screened intervals are not necessarily truly representative of the aggregate thickness of aquifer material that contributes to the initial transient response to pumping. The cited maximum value of 1.9x10^{-5} ft^{-1} is about an order of magnitude too large for typical sands and may reflect a short screen in a thick aquifer as well as interpretative problems arising from borehole-storage effects, partial penetration, aquitard leakage, or other circumstances.

Specific Yield

At the water table where the aquifer is unconfined, changes in storage occur primarily as drainage or filling of pore space. The fraction of aquifer volume that drains with a unit decline of the water table is quantified by the specific yield, which is a fraction of the total porosity. Johnson (1967) compiled specific yields for various alluvial materials from clays to coarse gravels and determined an average value for fine sands of 0.21 and an average value for coarse sands of 0.27.

Discharge

Before groundwater pumping from the Coastal Plain began, groundwater flowed exclusively to natural discharge areas, some of which continue to be discharge areas today. Much of the recharge discharges to the numerous small streams and rivers (fig. 7) in the Coastal Plain. Water that has infiltrated deeper in the aquifer system may flow toward discharge areas along larger river systems, as well as to the Chesapeake Bay and Atlantic Ocean. Groundwater also discharges by evapotranspiration from the water table in low-altitude areas.

Pumping has increasingly resulted in the capture of groundwater that otherwise would have ultimately flowed to the natural discharge areas under predevelopment conditions. By the year 2003, total groundwater withdrawals from the Coastal Plain study area were about 117 million gallons per day (Mgal/d; fig. 2). Commercial, industrial, and public-supply withdrawals accounted for approximately 74 percent of the total groundwater withdrawals during the year 2000 (fig. 9). The well locations for these reported withdrawals are shown in figure 10. The majority of the groundwater withdrawal flux was concentrated in well fields supplying the industrial centers near West Point and Franklin, VA, where the largest declines in groundwater levels have also occurred.

Domestic groundwater withdrawals accounted for approximately 25 percent of the total groundwater withdrawals during 2000 (fig. 9). Although the individual locations and associated withdrawal magnitudes from wells supplying groundwater for domestic use are unknown, the spatial distribution of self-supplied domestic withdrawals has been estimated by Pope and others (2007). The estimated horizontal distribution of the magnitude of self-supplied withdrawals

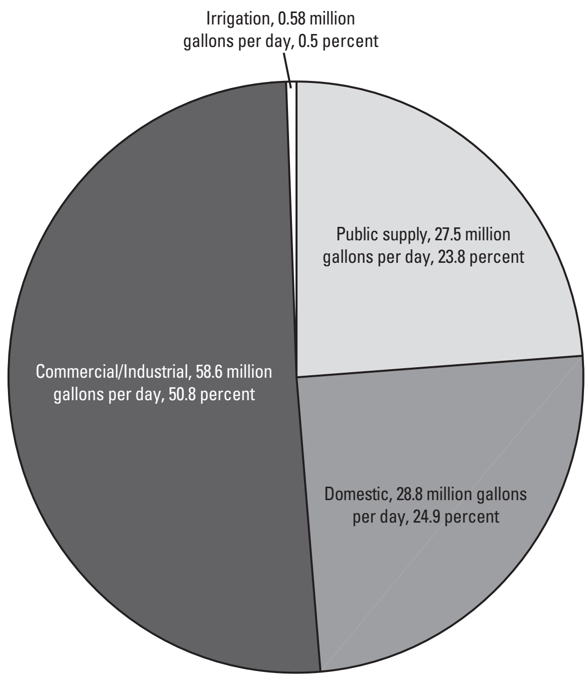

Figure 9. Estimated groundwater withdrawals by category of use in the Virginia Coastal Plain during 2000 (derived from U.S. Geological Survey, 2002).

for the year 2000 is also shown in figure 10. Groundwater withdrawals for municipal, industrial, and commercial uses are sufficiently large to require reporting and are summarized by hydrogeologic unit under the "reported" column in table 2. The estimated total domestic withdrawal from each hydrogeologic unit in the Virginia Coastal Plain, excluding the Eastern Shore, is also summarized in table 2.

Table 2. Magnitudes of 2003 reported and 2000 self-supplied domestic groundwater withdrawals from the Virginia Coastal Plain by hydrogeologic unit.

[Mgal/d, million gallons per day; <, less than; <<, much less than]

Aquifer	Domestic[1] (Mgal/d)	Reported[2] (Mgal/d)	Total (Mgal/d)	Percent of total
Surficial	5.2	0.09	5.3	5
Yorktown-Eastover	10.8	.51	11.3	10
Saint Marys	.05	.0	.05	<<1
Piney Point	1.9	4.6	6.5	5
Aquia	2.8	.48	3.3	3
Peedee	0	0	0	0
Virginia Beach	.09	.08	.17	<1
Potomac	7.5	83	90.5	77
Total	28.3	88	117	100

[1] Estimated from 2000 census data (Pope and others, 2007). Yorktown-Eastover includes Yorktown confining zone. Potomac includes Potomac confining zone.

[2] Groundwater withdrawals greater than 300,000 gallons per month must be permitted. Reported withdrawal magnitudes provided by Virginia Department of Environmental Quality, Groundwater Withdrawal Permit Program.

Saltwater Transition Zone

The increase in groundwater density associated with the transition from fresh to salty groundwater near the Atlantic Ocean has an effect on regional groundwater flow. Mixing of freshwater and saltwater has created a "transition zone," through which salinity generally increases toward the ocean and with depth. This transition zone vertically crosses the layered sequence of Coastal Plain aquifers and confining units of contrasting hydraulic conductivities. Preferential flow and flushing through the relatively conductive aquifer strata has resulted in local vertical salinity inversions (McFarland and Bruce, 2005) within the transition zone.

Cederstrom (1943) mapped the distribution of dissolved solids in groundwater in the Atlantic Coastal Plain of Virginia and noted anomalously high concentrations in an "inland wedge," now known to correspond with the extent of the Chesapeake Bay impact structure (Powers and Bruce, 1999). Geochemical and other geologic and hydrologic evidence suggest a Pliocene or earlier seawater source of the salty groundwater within the impact structure (McFarland and Bruce, 2005). The persistence of saltwater within the crater through the Pleistocene, and possibly since the Eocene, suggests that the low hydraulic conductivity of crater-fill sediments inhibited advective flushing by fresh groundwater. The occurrence of saline groundwater within the Chesapeake Bay impact structure and vertical salinity inversions in other locations indicate that geologic controls, in addition to the hydrodynamic control, affect the salinity distribution near the Atlantic coast.

The transition from fresh groundwater of meteoric origin to seawater occurs across a mixing zone whose horizontal and vertical widths are determined, in part, by the heterogeneity and permeability of the porous media and the periodic tidal or seasonal variations or longer non-periodic variations of both groundwater flux and sea level. Meisler (1989) defined the transition zone beneath the northern Atlantic Coastal Plain as the zone with chloride concentrations between 250 and 18,000 milligrams per liter (mg/L). By this criterion, the horizontal width of the transition zone in Virginia varies from about 25 mi in southeast Virginia to 45 mi across the Chesapeake Bay impact structure.

The equilibrium location of the transition zone is hydrodynamically controlled by the magnitude and distribution of recharge flux, aquifer-system hydraulic conductivities, and sea level. Because climatic conditions and sea level typically are changing through time, the transition zone may not be in equilibrium for the current climate and sea level. The Coastal Plain aquifers were entirely inundated and likely saturated with saltwater most recently during the Pliocene Epoch 2 million years ago, and numerous sea-level changes have occurred since that time. The magnitude of relative sea-level lowering during even the most recent glacial episode, however, is uncertain. The ICE–4G

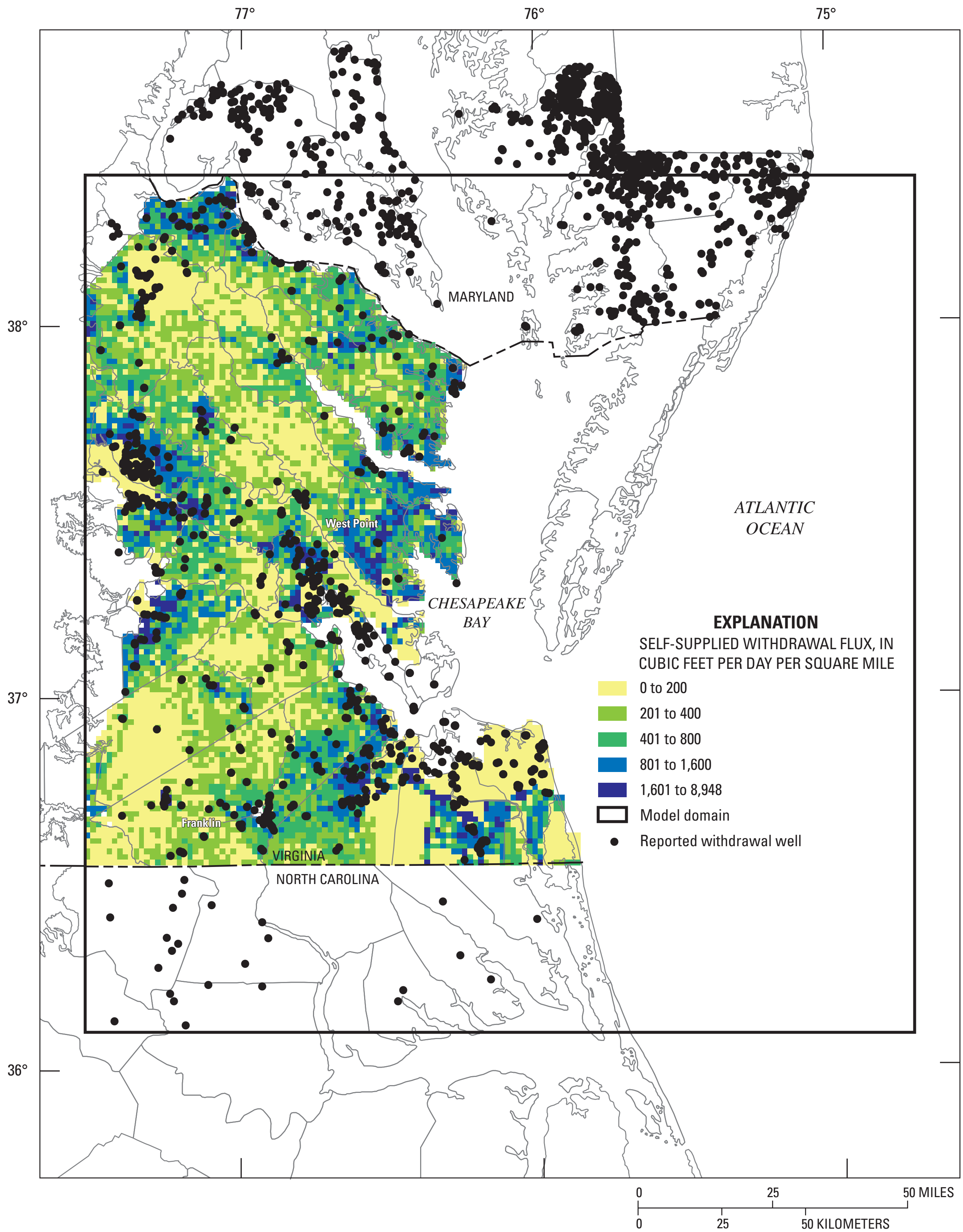

Figure 10. Location of Coastal Plain reported withdrawal wells, model domain, and self-supplied withdrawal rate per square mile in 2000.

model (Peltier, 1994), which incorporates mantle viscosity and lithospheric flexure, computes sea level during the last glacial maximum (21,000 years before present) 470 ft lower than present sea level for the Virginia Coastal Plain. Age dating of basal peat below salt marshes and estuarine sediments in the Chesapeake Bay indicates sea level was 25 ft lower 6,000 years ago (Larsen and Clark, 2003), which is about one-third of the ICE–4G model value for that time. During glacial episodes when the sea receded to the continental-shelf-slope break, the average aquifer-system hydraulic gradient was much greater than present under the current sea-level conditions, especially east of the coastline, causing enhanced flushing of saltwater from aquifers and a seaward migration of the freshwater-saltwater transition zone. Repeated sea-level fluctuations during the late Tertiary and Quaternary have mixed freshwater with seawater, widening the freshwater-saltwater transition zone (Meisler and others, 1984). The general trend of sea-level rise over the past 18,000 years suggests that hydraulic forces affecting the location of the freshwater-saltwater interface may be out of equilibrium, causing landward migration of the transition zone.

The spatial configuration of the transition zone may be represented, either conceptually or from simulated or measured concentrations, by one or more surfaces of equal or iso-concentration (iso-conc). An iso-conc representing 50 percent of the seawater concentration of either chloride or total dissolved solids (TDS) is convenient for approximate depiction of the position of a seawater transition zone with respect to a coastline or other reference. Such a representative iso-conc position can be calculated for simple groundwater systems under static conditions, or simulated for more complex natural systems under conditions of hydrodynamic equilibrium between the groundwater flow and the denser seawater. Because climatic and sea-level conditions change through time, the actual position of the seawater transition zone may differ from the equilibrium condition simulated for the current sea level and climate. The configuration of the simulated transition zone is shown in the appendix (fig. A2).

Simulation of Transient Groundwater Flow

Development of the groundwater model required assembly and organization of a considerable quantity of spatially referenced hydrologic, geologic, and topographic data. A geographic information system (GIS) was used to construct coverages of these diverse data sets, which facilitated preliminary data analysis, construction of model data sets, and visualization and analysis of model output and results. The altitudes of the land surface, tops of the 19 hydrogeologic units, and the pre-Cretaceous basement rocks are represented by raster data structures. Vector GIS coverages describe the location and attributes for water-level and water-quality observation wells, precipitation observations, pumping wells, county and independent city boundaries, state boundaries, surface-water bodies, geologic faults, the impact crater, etc. GIS coverages of the model finite-difference cells and nodes created with the program MODELGRID (Kernodle and Philip, 1988) contain attributes for derived quantities required for model-input definition, such as domestic-withdrawal fluxes and hydrogeologic-unit top altitudes and thicknesses. Specification of MODFLOW (McDonald and Harbaugh, 1988; Harbaugh and others, 2000) River Package input from GIS coverages of rivers and attribute control points was facilitated by use of the program RIVGRID (Leake and Claar, 1999). Construction of coverages of model-simulated water levels was facilitated with the program MODTOOLS (Orzol, 1997).

Projection System

The GIS coverages utilized a Lambert Conformal Conic Projection system, which was chosen to minimize area and angular distortions in the Virginia Coastal Plain. The specific projection parameters include a central longitudinal meridian at –77 °W and standard parallels of latitude at 37 ° and 38 °N. Coordinates in this projection space have units of feet measured positive east of the central meridian and north of latitude 36 °N.

Numerical Method

Spatial variations of dissolved-solid concentrations and consequent groundwater density can affect the patterns and rates of groundwater flow. For many groundwater flow systems, spatial variations of the density and temperature of the groundwater are sufficiently small that the fluid density may be considered constant, in which case the appropriate form of the groundwater flow equation may be conveniently solved with a simulation code such as MODFLOW. In coastal aquifers, the 2.5-percent increase in density across a transition zone from fresh groundwater (62.43 pounds per cubic foot [lb/ft^3]) to seawater (63.99 lb/ft^3) substantially affects groundwater flow. In these cases, more accurate simulations may be obtained with a simulation code that solves a variable-density form of the groundwater flow equation. If groundwater concentrations change with time, it is most appropriate to employ a simulation code that solves a system of coupled equations describing variable-density groundwater flow and mass transport. The major components of seawater are mass-conservative solutes that are not affected by chemical reactions. For the purposes of this model, the effects of groundwater temperature gradients on groundwater flow in the Virginia Coastal Plain are negligible. Accordingly, the governing equations for variable-density flow and mass transport can be simplified to the forms listed in equations 4 and 5:

$$-\nabla \cdot \left(\rho \bar{q}\right) + \bar{\rho} q_S = \rho S_p \frac{\partial P}{\partial t} + \theta \frac{\partial \rho}{\partial C} \frac{\partial C}{\partial t} \qquad (4)$$

$$\frac{\partial C}{\partial t} = \nabla \cdot (D \nabla C) - \nabla \cdot \left(\frac{\bar{q}}{\theta} C \right) - \frac{q_s}{\theta} C_s \quad (5)$$

where

- ∇ is the gradient operator,
- ρ is fluid density [ML^{-3}],
- $\bar{q}$ is specific discharge [LT^{-1}],
- P is fluid pressure [$ML^{-1}T^{-2}$],
- S_p is specific storage in terms of pressure [$M^{-1}LT^{2}$],
- t is time [T],
- θ is effective porosity,
- C is solute concentration [ML^{-3}],
- D is the dispersion coefficient [L^2T^{-1}],
- q_s is flow rate per unit volume representing sources or sinks [T^{-1}],
- $\overline{\rho}$ is source or sink fluid density [ML^{-3}], and
- C_s is source or sink solute concentration [ML^{-3}].

The dependence of fluid density on concentration can be approximated by a linear equation of state:

$$\rho = \rho_f + \frac{\partial \rho}{\partial C} C \quad (6)$$

where ρ_f is the density of freshwater (about 62.43 lb/ft^3). The groundwater flow (eq. 4) and transport (eq. 5) equations are coupled by the specific discharge ($\bar{q}$) and concentration (C) terms. The specific discharge ($\bar{q}$) is expressed by the pressure form of Darcy's law:

$$\bar{q} = \frac{-\kappa}{\mu} \left(\nabla P - pg\ \hat{e}_z \right) \quad (7)$$

where

- κ is the tensor of permeability [L^2],
- μ is the dynamic viscosity [$ML^{-1}T^{-1}$],
- g is the acceleration of gravity [LT^{-2}], and
- $\hat{e}_z$ is a unit vector pointing downward.

Guo and Langevin (2002) reformulated the flow equation (eq. 4) using Darcy's law (eq. 7) to express the specific discharge ($\bar{q}$) in terms of equivalent freshwater head. The resulting flow and transport equations can be iteratively solved by the Variable-Density Flow (VDF) and Integrated Mass Transport (IMT) processes, respectively, of the simulation code SEAWAT–2000 (Langevin and others, 2003). For some groundwater flow simulations, the temporal change of solute concentration may be relatively small and may not appreciably affect the regional spatial distribution of groundwater density. If the objective is the simulation of groundwater levels and not concentrations, as it is in this study, the spatial groundwater density distribution may be considered non-transient in these cases, and the governing equations for variable-density flow and mass transport are de-coupled. The primary objective of this study is to simulate groundwater levels; therefore, the governing equations were de-coupled. Because the iterative solution of the coupled equations is computationally intensive, solution of the variable-density flow equation for a temporally constant-density case using only the VDF process in SEAWAT–2000 saves considerable computation time.

The SEAWAT code used to simulate the variable-density groundwater flow is documented in both Guo and Langevin (2002) and Langevin and others (2003). For this study, the SEAWAT–2000 (Langevin and others, 2003) version of the code was used and is referred to as SEAWAT throughout this report. The specified groundwater density distribution was generated by a separate 108,000-year simulation of Pleistocene freshwater flushing around the Chesapeake Bay impact crater during transient sea-level changes and is described in the appendix.

Spatial Discretization

The finite-difference groundwater model grid was designed to provide good spatial resolution on a regional scale while maintaining acceptable limits on computer execution times. The 24,486-mi^2 area (159 mi by 154 mi) encompassed by the model grid extends in an east-west direction from the Fall Line to the continental shelf and from 31 mi south of the Virginia-North Carolina State line to about 25 mi north of Point Lookout in Maryland (fig. 1). The grid extent is almost twice the area of the Coastal Plain in Virginia (13,000 mi^2), although areas on the continental shelf and in North Carolina have wide column and row spacing, respectively, and therefore did not substantially increase execution times.

The finite-difference model grid is composed of 134 rows, 96 columns, and 60 layers; row numbers increase from north to south, column numbers increase from west to east, and layer numbers increase from the top down. The north-west corner of the grid (row 1 and column 1) is 876,480 ft north and 153,120 ft west of the previously defined original latitude and Lambert central meridian, respectively. The Coastal Plain of Virginia (exclusive of the Eastern Shore) and part of Maryland is discretized with 1-mi^2 grid-cell spacing. The grid spacing along rows (north-south direction) within the southernmost six rows of finite-difference cells in the model, which are south of the Virginia-North Carolina State line, increases through 2, 3, and 5 mi to a maximum of 7 mi. East of the mainland Virginia Beach area, the grid spacing along columns (east-west direction) increases through 2, 3, 5, and 7 mi to a maximum of 10 mi.

Median land-surface altitudes and bathymetric depths for each model cell (1 mi^2 or more) derived from 30-m digital elevation models (DEMs) were used to define the uppermost active layer in a particular row and column. The vertical thickness of the upper 48 layers is uniformly 35 ft. Layers 49–52 are 50 ft thick, and layers 53–60 are 100 ft thick (table 3). The altitude of the base of the lowest model layer is –2,470 ft. This relatively fine vertical discretization was needed to accurately represent the hydrogeologic framework and to simulate the slope of the saltwater transition zones within

Table 3. Model grid-layer thicknesses.

Layer numbers[1]	Cell thickness (feet)
1 – 48	35
49 – 52	50
53 – 60	100

[1]Layers are numbered from the top to the bottom of the model.

individual aquifers. A model cell was simulated as active if the GIS raster representation of a hydrogeologic unit indicated at least 1 ft of thickness at the center of the finite-difference cell. The GIS coverage of basement altitude was used to define the lowermost active layer in a particular row and column.

Internal Flow Package

The numerical representation of a hydrogeologic framework depends on the choice of method for simulating internal flow between finite-difference cells. Three MODFLOW packages exist that can be used to simulate internal flow with SEAWAT. The Block Centered Flow (BCF) and Layer Property Flow (LPF) packages are conceptually identical in their formulation of inter-cell conductance equations; their difference lies in details of model input, with the LPF package facilitating the use of parameters. These packages are well-suited to the approach of associating model layers with hydrogeologic units. The Hydrogeologic-Unit Flow (HUF) package (Anderman and Hill, 2000) is an alternative internal-flow package for formulating the inter-cell conductance equations. Although the horizontal discretization of hydrogeologic units and finite difference cells is identical, the HUF package allows the flexibility of defining the layering and thickness of all hydrogeologic units independently from that of the model finite-difference-grid-cell layers. The HUF package internally calculates storage and inter-cell conductance terms for each cell from the hydraulic-property distributions assigned to individual hydrogeologic units present within that cell. Four considerations favored the use of the HUF package over either the BCF or LPF packages.

1. The complexity of the hydrogeologic framework in the Virginia Coastal Plain rendered the “traditional” approach of associating model finite-difference-cell layers with individual hydrogeologic units impractical. As discussed under the hydrogeologic framework section of the report, no hydrogeologic unit is present throughout the entire groundwater model domain. All 19 units are present in only a portion of the model domain; they may be discontinuous, pinch out laterally, or be incised by river drainages. Some hydrogeologic units contain a “hole” in areas excavated during the Chesapeake Bay bolide impact, which is filled by different hydrogeologic units. Because of the limited spatial extent of the hydrogeologic units, their strict association with individual finite-difference-cell layers was not possible. Approximating that association would have required a very complex finite-difference-cell layering scheme and was deemed impracticable.

2. In the Virginia Coastal Plain, many hydrogeologic units deepen and thicken toward the Atlantic coast and the zone of transition from freshwater to saltwater. Because the greater density of the saltwater affects the direction of groundwater flow, the transition zones are commonly delineated by equal concentration (iso-conc) surfaces that dip landward within individual aquifers. Under natural (steady-state) flow conditions, fresh groundwater discharges upward parallel to iso-conc surfaces. To simulate this variable-density flow effect in the groundwater model, the thicker, seaward portions of individual aquifers had to be represented with multiple layers of finite-difference cells. Using the HUF package conveniently allows improved discretization for numerical accuracy in these areas.

3. The ability to update the groundwater model if and when new hydrogeologic information is obtained was an important design goal. Model features such as observation wells and boundary conditions are referenced to the finite-difference grid and, therefore, require extensive modification if the model grid is modified. Because the extent and thickness of hydrogeologic units as well as their associated hydraulic-property distributions are defined in the HUF package independently from the model grid, they can be updated without changing observation data or boundary specifications. Consequently, the stated design goal is more effectively accomplished with the HUF package than the alternative internal flow packages.

4. Because the hydrogeologic framework (McFarland and Bruce, 2006) was being developed contemporaneously with the groundwater model documented in this report, specification of the hydrogeologic-framework geometry independently from the other model features was crucial to timely completion of the model. During the course of model development, several interim versions of the hydrogeologic framework were used before the final version was incorporated in the model. Because these separate and distinct frameworks could be incorporated and tested without modifying the model grid, the required effort at construction of model input for observation wells or boundary conditions (pumpage, recharge, evapotranspiration, rivers or bay leakage, etc.) was economized.

Temporal Discretization

The 113-year historical transient simulation was time-discretized into 34 stress periods of lengths indicated in table 4. An initial steady-state stress period was used to simulate predevelopment conditions. The time-step length within each transient stress period increased as a geometric progression with ratio 1.4. The number of time steps within each stress period was chosen such that the initial time-step length of each stress period was approximately 33 days. The hydraulic stresses in the second and third stress periods (table 4), which together represent the 30-year interval from 1891 through 1920, are identical; this interval was divided to facilitate calculation of water-level observation times referenced from January 1, 1900. As explained later in the model-calibration section, the initial steady-state stress period was modified to transient to facilitate convergence during parameter-estimation iterations.

Table 4. Time discretization for 113-year historical transient simulation.

Stress period	Year(s) represented	Length in years	Length in days	Time steps in period
1	predevelopment	-	-	1
2	1891–1899	9	3,287	11
3	1900–1920	21	7,670	4
4	1921–1939	19	6,939	13
5	1940–1945	6	2,192	10
6	1946–1952	7	2,557	11
7	1953–1957	5	1,826	10
8	1958–1964	7	2,557	11
9	1965–1967	3	1,095	8
10	1968–1972	5	1,827	10
11	1973–1977	5	1,826	10
12	1978–1981	4	1,461	9
13	1982	1	365	5
14	1983	1	365	5
15	1984	1	366	5
16	1985	1	365	5
17	1986	1	365	5
18	1987	1	365	5
19	1988	1	366	5
20	1989	1	365	5
21	1990	1	365	5
22	1991	1	365	5
23	1992	1	366	5
24	1993	1	365	5
25	1994	1	365	5
26	1995	1	365	5
27	1996	1	366	5
28	1997	1	365	5
29	1998	1	365	5
30	1999	1	365	5
31	2000	1	366	5
32	2001	1	365	5
33	2002	1	365	5
34	2003	1	365	5

Boundary Conditions

Specified Flux Boundaries

The fraction of precipitation resulting in recharge to the water table and groundwater pumpage within the model domain are represented as specified flux boundaries. With two exceptions, no groundwater flow is simulated across the lateral and bottom boundaries of the model domain. The two exceptions where lateral boundary flow is non-zero simulate groundwater underflow: (1) to the north out of the model domain toward Maryland, and (2) from the Piedmont Province (west of the model domain) over the Norfolk Arch (fig. 1).

Transient Areal Recharge

The correlation and similar magnitudes of annual precipitation measured at four stations in the Virginia Coastal Plain (fig. 8) indicate that the spatial variability of annual precipitation is relatively minor and likely less than the spatial variability of either runoff or vadose-zone evapotranspiration. Quantification of the individual magnitudes of either runoff or vadose-zone evapotranspiration or their spatial variability was beyond the scope of this study. Annual precipitation was, therefore, considered spatially homogeneous over the Coastal Plain, but variable in time. Recharge was simulated to be the fraction of this precipitation not lost to the combined magnitude of runoff and vadose-zone evapotranspiration.

Recharge to the water table in the upper hydrogeologic unit (usually the surficial aquifer) was specified for the uppermost active model finite-difference cell using the Recharge (RCH) package of SEAWAT. This recharge flux simulates the fraction of the annual precipitation not lost to runoff or vadose-zone evapotranspiration and includes volumetrically minor amounts of septic-system effluents, return percolation from irrigation, and leakage from water and septic pipelines. Although this specified recharge flux is simulated as spatially homogeneous, it varies in time as a constant fraction of the measured annual Coastal Plain precipitation. This fraction was parameterized for model calibration and found to be correlated with parameters controlling the simulated evapotranspiration flux. Because this fraction could not be uniquely determined through model calibration, it was set to equal 50 percent of the measured annual precipitation. The variation of this simulated flux between stress periods is shown in figure 11. In low-lying areas, most of this recharge simulated within a model time step is lost from the groundwater system as simulated ET within the same model time step.

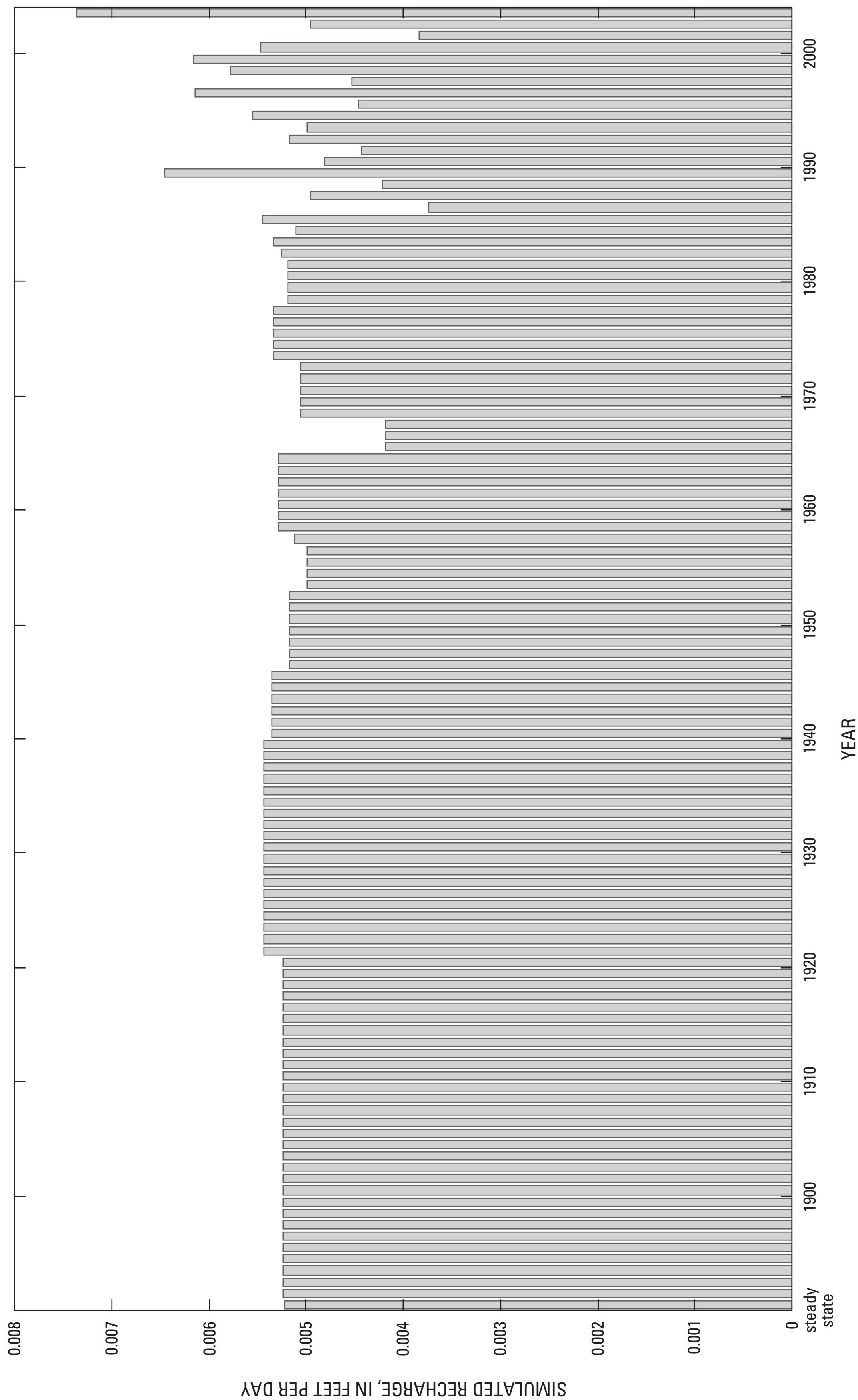

Figure 11. Simulated recharge in the Virginia Coastal Plain by year.

Transient Underflow to Maryland

Groundwater withdrawals from the Aquia aquifer in Maryland have resulted in water-level declines of over 200 ft in part of St. Marys County, MD. This area is included within the model domain, and withdrawals from the Aquia aquifer in that area were specified in the model. Withdrawals from the Upper and Lower Patapsco aquifers in Charles County, MD (which are correlative and laterally contiguous with the Potomac aquifer system in Virginia), have resulted in lower water levels in those aquifers. These withdrawals occur outside of the spatial domain of the Virginia Coastal Plain model (fig. 3) but affect water levels in simulated areas of Virginia and result in northward flow out of Virginia under the Potomac River into Maryland. To simulate declining water levels in Virginia resulting from this flow, a flux boundary was specified from the north side (row 1) of the model domain, from columns 5 to 37, layers 6 to 41, corresponding to the depths of the Potomac aquifer equivalent to the Upper and Lower Patapsco aquifers in Maryland (fig. 12a). This transient specified-flow was simulated with the Flow and Head Boundary (FHB) package (Leake and Lilly, 1997) and increased in a segmented linear fashion from zero before 1950 to a maximum of 8.86×10^5 ft^3/d (6.63 Mgal/d) in 2003.

Constant Underflow from Piedmont

The magnitude of groundwater underflow from pre-Cretaceous bedrock of the Piedmont Province into the Coastal Plain unconsolidated sediments is thought to be volumetrically minor. Under this assumption, the western model boundary was initially designated as no-flow. Analysis of water-level residuals during the course of model calibration suggested a component of inflow through the western boundary of the model. As discussed in the subsequent section entitled Boundary Flux Parameterization, the magnitude of flow through this area was parameterized and estimated in subsequent model calibration runs. In addition to the initial no-flow boundary specification, the hydraulic effects of possible underflow from the Piedmont were evaluated by testing three other specified-flux boundary configurations, each representing different areas of underflow. In the calibrated model, the constant-flux boundary is specified along the west side in the western-most active cell from row 80 to 112 and model layer 7 to 16, corresponding to altitudes from zero to –350 ft (fig. 12b). The total simulated flow through this boundary is 2.16×10^6 ft^3/d (16.2 Mgal/d).

Transient Groundwater Pumpage

Virginia Coastal Plain groundwater withdrawals are for municipal public-supply, industrial, commercial, agricultural, or domestic self-supply uses. Because the locations of municipal and industrial withdrawal wells are known and withdrawals from those wells are reported, these withdrawals can be simulated in space and time by flux assignment to appropriate finite-difference cells and stress periods. In contrast, the location and magnitude of self-supplied domestic groundwater withdrawals are uncertain. Reported and domestic withdrawals were simulated with different packages in SEAWAT and are discussed in the following subsections. Reported values for agricultural withdrawals are included in the withdrawal database and are simulated in the groundwater model. Because not all groundwater withdrawals for agricultural use are reported, not all agricultural withdrawals are simulated in the groundwater model.

Reported Withdrawals

Groundwater withdrawal records were obtained from various sources for different areas and periods of time. In general, specificity with respect to individual wells improves for later simulated time periods. During earlier simulated times, withdrawals from multiple withdrawal wells in a well field may be combined in a single withdrawal record. Because the flux from all wells within the area of a finite-difference cell are simulated as being withdrawn from the center of the cell, this lack of well-specificity for earlier simulated times usually did not introduce any substantial additional numerical inaccuracy.

Site-specific groundwater withdrawal information for the years 1891 through 1981 were adapted from a previous compilation by Harsh and Laczniak (1990). Well-specific annual groundwater withdrawal information for the years from 1982 through 2003 was obtained from the Ground-Water Withdrawal Permitting and the Water Use/Water Supply Planning Programs of the Virginia DEQ (Robin Patton, written commun., 2002, 2003). Historical groundwater withdrawal data for wells in Maryland were obtained from the USGS Water Use Program (Judy Wheeler, written commun., 2005) and the Maryland Geological Survey (D.D. Drummond, written commun., 2005). Historical groundwater withdrawal data for wells in North Carolina were obtained from a compilation for the southern Atlantic Coastal Plain aquifer system (J. Fine, U.S. Geological Survey, written commun., 2005).

The 866 wells for which groundwater withdrawal records exist were simulated with the Multi-Node Well (MNW) package (Halford and Hanson, 2002). The locations of these wells are shown in figure 10. For reported withdrawals from wells with screens that penetrate more than one finite-difference-cell layer, the total reported annual withdrawal from each well is specified, but the layer-by-layer distribution of that flux depends, in part, on the simulated water-level differences between the withdrawal well and each of the screened finite-difference cells. Because of this head-dependency, these reported withdrawals may be considered a head-dependent flux for each layer. Water levels in withdrawal wells may be affected by head losses resulting from turbulent flow near the well or flow through drilling-damaged formation, the gravel pack, or the well screen; these effects were not directly simulated. The hydraulic conductance between simulated withdrawal wells and the finite-difference cells containing the well screen are calculated by the MNW package and

(a)

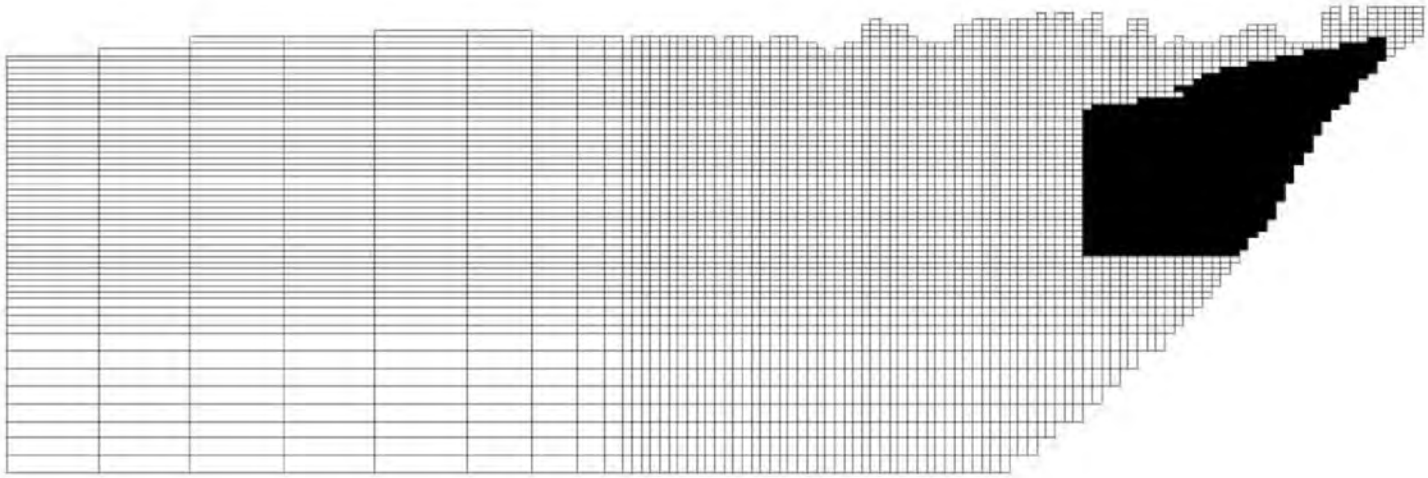

(b)

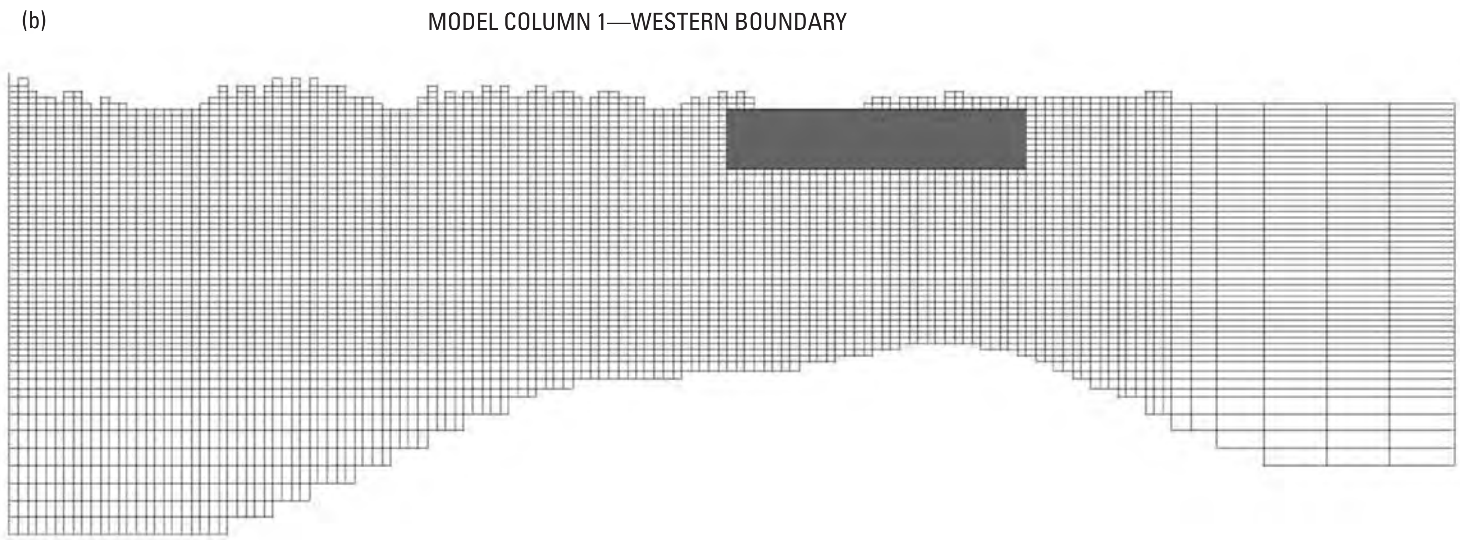

Figure 12. Finite-difference model grid showing cells designated for (a) time-varying specified flux to Maryland in row 1 and (b) constant specified flux from the Piedmont Province in columns 4–20.

depend, in part, on the simulated well radius (r_w) for each well. Because detailed well-construction information was not available for most reported withdrawal wells, the well radius was assumed to be similar for all wells and was estimated to be 0.55 ft during model calibration. Simulated water levels were insensitive to the parameter representing well radius.

Domestic Withdrawals

Unreported self-supplied domestic withdrawals comprise about 25 percent of the groundwater use in the Virginia Coastal Plain. Pope and others (2007) sampled private domestic well-completion records from Virginia Coastal Plain counties and independent cities to estimate the relative magnitudes of domestic groundwater withdrawals from hydrogeologic units within each county or independent city. In order to estimate the horizontal distribution of the magnitude of domestic withdrawals, road-density calculations were used to distribute the total census-block-group populations among the 1-mi^2 model-grid cells within each census-block group. Using a combination of city boundaries and census spatial data on urban areas, grid cells thought to be publicly supplied were excluded to generate a horizontal coverage of model cells thought to be self supplied (fig. 10). Prior to 1950, all domestic-use groundwater was simulated as withdrawals from the surficial aquifer. For simulated times after 1950, the county- or independent-city-specific domestic-flux distribution from Pope and others (2007) was applied to apportion the total estimated domestic flux among the hydrogeologic units present within the area of each model cell. Within each cell area, the appropriate flux for each hydrogeologic unit was specified from the uppermost finite-difference-grid cell containing the hydrogeologic unit. The FHB package (Leake and Lilly, 1997) was used to simulate these domestic groundwater withdrawals and to temporally interpolate the change in flux from every specified finite-difference cell according to changes in decadal population-census data.

Head-Dependent Flux Boundaries

In contrast to the specified-flux boundaries, the simulated flow into or out of the groundwater model through head-dependent-flux boundaries depends on the simulated water level adjacent to the boundary.

Evapotranspiration

Evaporation and transpiration from the water table were simulated with the Evapotranspiration (EVT) package of SEAWAT. Because simulated stress periods were 1 year or longer in length, the maximum possible evapotranspiration flux was simulated to be constant at the potential evapotranspiration rate of 32.4 in/yr (0.0074 ft/d) for Virginia. This simulated maximum flux may occur when the water table is at or above the median land-surface altitude within each finite-difference cell (the specified evapotranspiration surface). The simulated evapotranspiration flux linearly decreases with depth of the simulated water table below this surface and becomes zero at the simulated evapotranspiration extinction depth. This depth, which was simulated to be uniform throughout the model domain, was estimated during model calibration to be 8.5 ft.

Rivers

Reaches of 32 rivers in the Coastal Plain for which the stage is above sea level were simulated with the River (RIV) package of SEAWAT. The total length of these reaches is 792 mi. Reaches of these rivers with stage altitude less than 1 ft were considered tidal and simulated with the General Head Boundary (GHB) package of SEAWAT. Utilizing the best available GIS coverage, the total length of mapped rivers within the model domain is approximately 19,000 mi. Thus, only 4.2 percent of the total river length is explicitly simulated in the model. (Because the larger river segments are simulated, the simulated riverbed seepage area is probably greater than 4.2 percent of the actual riverbed area.) The discrepancy between simulated and actual seepage area available for interaction with the groundwater flow system may be compensated for numerically in two ways: (1) more groundwater discharge to model-represented river segments may be simulated than actually occurs for those segments, partially compensating for flux to river segments that are not represented in the model; and (2) in areas where the water table is sufficiently close to the land surface, discharge to many small streams may be accounted for by increased flux through the EVT package. These issues are discussed further in the water-budget section.

Both the RIV and GHB packages require specification of the hydraulic conductance and water level in the boundary feature being simulated for each model cell. Riverbed leakance (T^{-1}) is the vertical hydraulic conductivity of the riverbed material divided by its thickness (K_z/b). The hydraulic conductance (dimension: [L^2/T]) is the product of the leakance with the area of the boundary feature within the model cell. The water level in the river (river stage), river width, and the bottom altitude of the riverbed sediments were interpolated between river-property control points using the program RIVGRID (Leake and Claar, 1999), which also calculates the length of the river segment within each model cell. The number of control points used for each simulated river depicted in figure 7 are summarized in table 5. Riverbed leakance, which was assumed to be spatially homogeneous, was parameterized and estimated during model calibration to be 1 d^{-1}.

Chesapeake Bay and Ocean Floor Leakage

Surface-water features with water-level altitudes less than 1 ft, such as the Chesapeake Bay, Atlantic Ocean, and river tidal areas were simulated with the GHB package of SEAWAT. To determine the boundary conductance for each model cell,

Table 5. Number of control points for simulated rivers.

River, creek, reservoir, or swamp name	Abbreviation	Number of control points
Appomattox River	appo	10
Assamoosiak Swamp	assa	2
Blackwater River	blac	24
Cat Point Creek	catp	3
Chickahominy River	chic	4
Fontaine Creek	font	2
North Landing River	icwat	3
Kirby's Creek	kirb	2
Marracossic Creek	marr	2
Mattaponi River	matt	5
Meherrin River	mehe	4
Mill Swamp	mill	2
Nansemond River	nans	7
North Anna River	nora	9
Northwest River	norw	2
Nottoway River	nott	8
Piankatank River	pian	2
Piscataway Creek	pisc	3
Poni River	poni	2
Potecasi Creek	pote	2
Rappahannock River	rapp	3
Lake Burnt Mills – Western Branch Reservoir	rivb	7
Seacock Swamp	seac	2
Somerton Creek	some	2
South Anna River	soua	4
Stony Creek	ston	2
Swift Creek	swif	3
Three Creek	thre	2
Totoponomoy Creek	toto	4
Wicomico River	wico	2
James River	jame	10
Rowanty Creek	rowa	5

the leakance parameter, which represents the vertical hydraulic conductivity of the bay or ocean floor material divided by its thickness (K_z/b), was multiplied by the area occupied by these features within each cell. Spatially uniform leakance parameters representing riverbed, bay, or ocean floor materials initially were parameterized separately for estimation. After boundary-leakance-parameter composite-scaled sensitivities indicated that these boundary leakance parameters were not sufficiently sensitive for independent estimation, they were combined into a single parameter representing riverbed, Chesapeake Bay, and ocean-floor materials.

Hydraulic-Property Distribution

Because hydraulic conductivity (K) and specific storage (S_s) depend on the intrinsic permeability and elasticity of the alluvial materials comprising the aquifer system, the spatial distribution of their magnitudes is expected to correlate with the lithologically defined hydrogeologic units. Parameters were, therefore, defined to represent the horizontal conductivity (K_h), vertical conductivity (K_v), and specific storage (S_s) within each hydrogeologic unit. Because the thickness (h) of every aquifer is spatially variable, the transmissivity ($T = K_h h$) and storage coefficient ($S_s h$) of every aquifer varies spatially. Similarly, the thickness (b) of each confining unit and confining zone is spatially variable; consequently, the leakance (K_v/b) of these hydrogeologic units also varies spatially. Where observation data warranted a heterogeneous distribution of horizontal or vertical hydraulic conductivity within a hydrogeologic unit, this complexity was simulated using zonation, horizontal interpolation, or a depth-dependent function.

Horizontal Interpolation of Hydraulic Conductivity

To simulate horizontal heterogeneity of vertical or horizontal hydraulic conductivity within hydrogeologic units, 20 "pilot points" (Doherty, 2003) were placed within the model domain at locations depicted in figure 13. Hydraulic conductivities at these points were parameterized and estimated during model calibration. Hydraulic conductivities between pilot points were calculated by spatial interpolation of the native values of hydraulic conductivity estimated for the pilot points. The spatial interpolation was computed by ordinary kriging with an isotropic exponential variogram.

Depth-Dependence of Potomac Aquifer Horizontal Hydraulic Conductivity

The Potomac is a heterogeneous aquifer in which sharp changes in vertical and horizontal hydraulic conductivity (K_h) occur at interbed boundaries at a scale smaller than can be represented with the model discretization. At the model scale, a change of the average magnitude of K_h with depth may also occur within the Potomac aquifer. This possibility was investigated using the hydraulic-conductivity depth-dependence capability (KDEP) of the HUF package (Anderman and Hill, 2003). The simulated horizontal

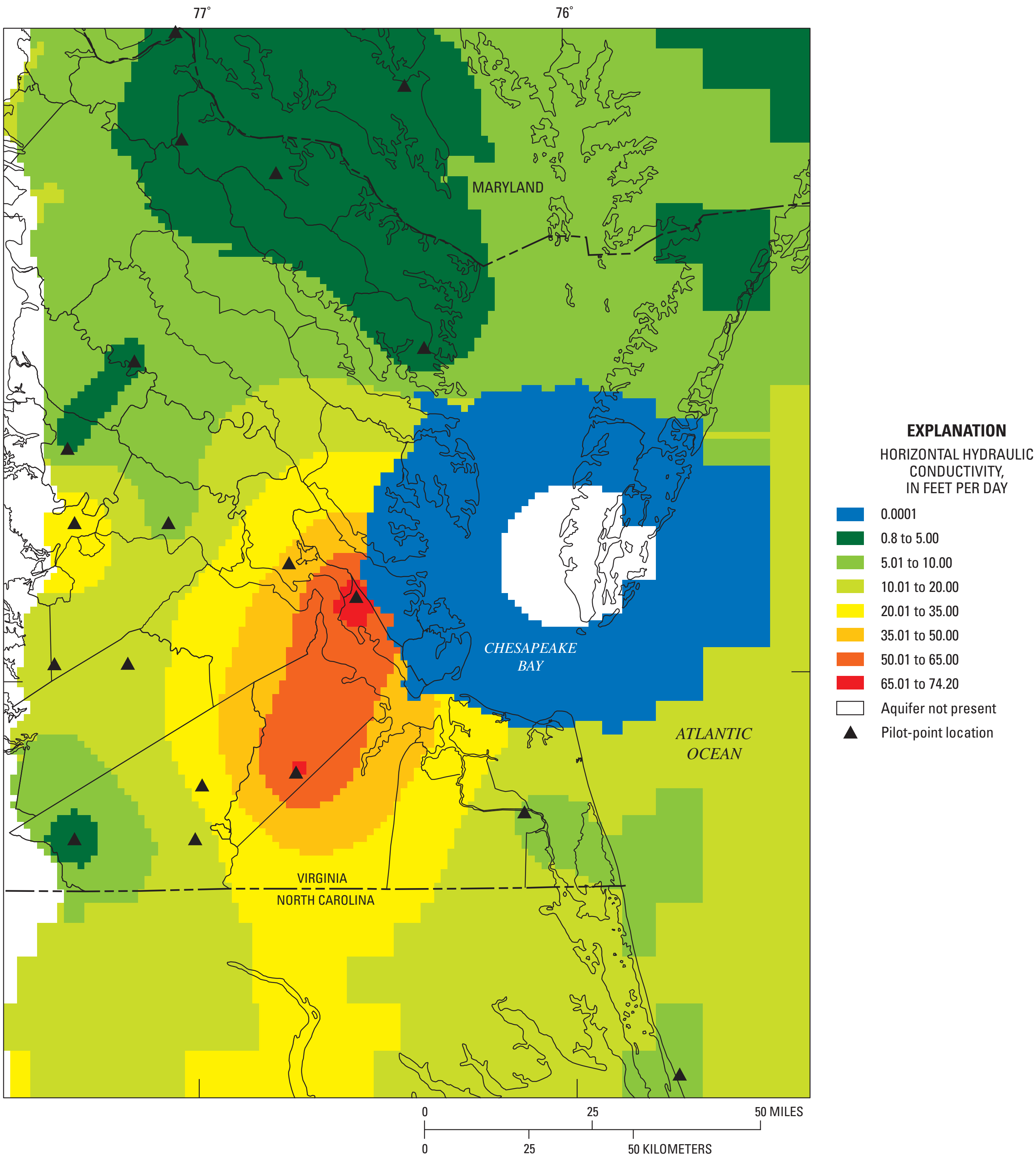

Figure 13. Pilot-point locations and simulated horizontal hydraulic conductivity at the top of the Potomac aquifer of the Virginia Coastal Plain.

hydraulic conductivity (K_h) was calculated for each model cell containing Potomac aquifer material by the exponential equation: ,

$$K_{depth} = K_{surface} 10^{-\lambda d} \tag{8}$$

where

K_{depth} is the horizontal hydraulic conductivity at depth d,

$K_{surface}$ is the horizontal hydraulic conductivity at a reference altitude of 210 ft,

λ is the depth-dependence coefficient, and

d is the depth below the reference altitude of 210 ft.

The depth-dependence coefficient λ, which was parameterized and estimated during model calibration, was initially allowed to be either negative or positive to allow for the possibility of either a general increase or decrease of horizontal hydraulic conductivity with depth. The large composite scaled sensitivity of λ is due, in part, to the large number of Potomac aquifer water-level observations, which were used to estimate its value during the model-calibration regression. The simulated decrease of horizontal hydraulic conductivity with depth for the calibrated value of λ is depicted in figure 14. The highest altitude of the Potomac aquifer (along the Fall Line) is 174 ft, where the magnitude of the horizontal hydraulic conductivity is about 99 percent of the reference depth value (calculated from the horizontal interpolation between pilot points). The magnitude of the horizontal hydraulic conductivity simulated for the Potomac aquifer decreases to about 53 percent of the reference depth value in the bottom finite-difference-cell layer of the model. This decrease may represent either a general increase of sediment compaction with depth or a general change in sediment facies associated with the prograding fluvial-deltaic system that deposited the Potomac Formation.

Model Calibration

The model-calibration goal was to achieve the best fit of simulated to observed water levels (measured at discrete points in space and time) with as few parameters as practical. The parameter-estimation codes UCODE–2005 (Poeter and others, 2005) and PEST (Doherty, 2004) were used to calibrate horizontal and vertical hydraulic conductivity, specific storage, and boundary-flux model parameters to 7,183 historical groundwater level observations in Virginia, Maryland, and North Carolina. Input to UCODE–2005 and PEST is similar, which facilitated utilization of both codes for comparative purposes and maximal advantage of their respective best features. Both PEST and UCODE–2005 utilize non-linear regression to determine an optimal parameter vector $\underline{b}$ that minimizes an objective function $S(\underline{b})$ of the form:

$$S(\underline{b}) = \sum_{i=1}^{7183} w_i \left(h_i - h_i'(\underline{b})\right)^2 \tag{9}$$

where

h_i is observed head,

h'_i is the simulated head, and

w_i is the weight for the observation.

As suggested by Hill (1998), the weights w_i were computed to be proportional to the inverse of the total error variance for each observation. The calculation of observation weights is described further in the subsequent section entitled “weights.”

Although only hydraulic heads were used as observations in the model-calibration regression, groundwater flux and age dates also constrained the calibration. Specification of groundwater withdrawals constrained estimated values of hydraulic conductivity in the confined aquifers, where pumpage and water-level measurements co-exist. The simulated river leakage was compared with discharge fluxes calculated by Richardson (1994b). Backward particle tracking with MODPATH (Pollock, 1994) was utilized to calculate simulated residence times for wells where carbon-14 (C-14)

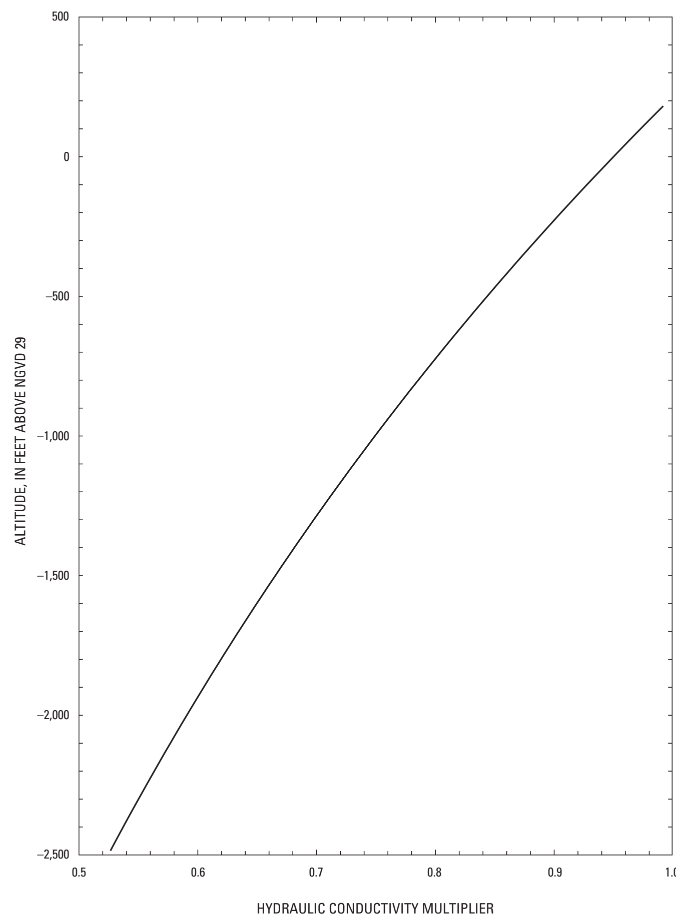

Figure 14. Decrease with depth of the simulated horizontal hydraulic conductivity of the Potomac aquifer of the Virginia Coastal Plain.

groundwater age measurements exist (Nelms and others, 2003). Although river-leakage and C-14 data were not used in the model-calibration regression, similarity of the simulated equivalents to these data supported the general reasonableness of the conceptual flow model and values of simulated hydraulic conductivity.

Calibration Data Set

Within the area encompassed by the groundwater model domain, 497 observation wells in Virginia, Maryland, and North Carolina (fig. 15) were identified from the USGS Groundwater Site Inventory (GWSI). Historical measurements of groundwater levels in the identified wells, together with the associated accuracies of the observation-well location and the water-level measurement techniques, were extracted from GWSI and incorporated into a spreadsheet database. This water-level data set was subsequently modified to obtain a maximum of one measurement per year for each observation well. For wells with multiple observations in any year, the last observation in a calendar year was selected. The number of observation wells and associated water-level observations in each hydrogeologic unit that were used in the calibration process is summarized in table 6. The temporal distribution of water-level observations used in the calibration process is depicted in figure 16.

For the purpose of calibrating the groundwater model, observation wells ideally should have short screen intervals that enable water-level measurement in a single hydrogeologic unit. Water levels measured in wells with long screen intervals spanning multiple hydrogeologic units represent a composite of a potentially vertically varying head distribution of those hydrogeologic units. Comparison of simulated water levels to those observed in multi-aquifer wells is complicated by uncertainty of the influence of the head conditions in the different screened aquifer intervals to the water level in the observation well. The relative influence of the different screened intervals on the water-level measurement depends, in part, on hydraulic conductivity and water-level differences between the different screened hydrogeologic units. Aquifers containing sands or other high-permeability lithologies are expected to transmit fluid-pressure differentials more effectively than confining units composed predominantly of clays or other low-permeability lithologies. Consequently, the water level measured in a well with a screened interval penetrating both aquifer and adjacent confining units is generally biased toward the water level in the more highly permeable aquifer.

To avoid the complications of multi-aquifer water-level observations and improve consistency among water-level observations used for model calibration, the Virginia Coastal Plain observation-well data set was culled to retain water-level observations from wells with screen intervals in a single aquifer. For those observation wells for which screen-interval information exists, the screened intervals of each observation well were compared with the hydrogeologic-unit top altitude from the digital representation of the hydrogeologic framework. Observation wells identified with screened intervals in more than one aquifer were removed from the observation-well data set. Observation wells with screened intervals in more than one hydrogeologic unit were retained if the additional hydrogeologic unit was classified as a confining unit.

The Head-Observation Process (Hill and others, 2000) of SEAWAT interpolates between finite-difference-cell centers to compute simulated equivalents at user-specified observation-well locations. The interpolation can fail for observation-well locations in finite-difference cells adjacent to no-flow boundaries or inactive finite-difference cells. Although SEAWAT continues to execute when this occurs, the correspondence of simulated water levels to observations is corrupted, which creates difficulties for parameter estimation with either UCODE–2005 or PEST. It was, therefore, necessary to remove these observation wells from the water-level observation data set.

Visual inspection of the time series of the observation-well water levels (hydrographs) revealed some problematic observation wells, in which hydrographs were either excessively noisy or contained measurements that were outliers to an overall water-level trend. The alpha-numeric identifier of each of these wells was catalogued according to the type of problem encountered. The problematic observations were either removed from the water-level observation data set or assigned a weight (so as to not unduly influence the parameter-estimation regressions).

After editing, the calibration data set contained a total of 7,183 observations of water levels from 497 observation wells, of which 5,087 observations are from 382 wells in Virginia, 1,826 observations are from 89 wells in Maryland, and 270 observations are from 26 wells in North Carolina.

During final model-calibration regression runs, optimization to the entire water-level data set, which included 1,826 Maryland water-level observations, caused some degradation of model-fit to Virginia observations. An optimal fit to water levels in Virginia was considered more important than accurate simulation of conditions in Maryland, and the final calibration was performed using only the subset of Virginia water-level observations.

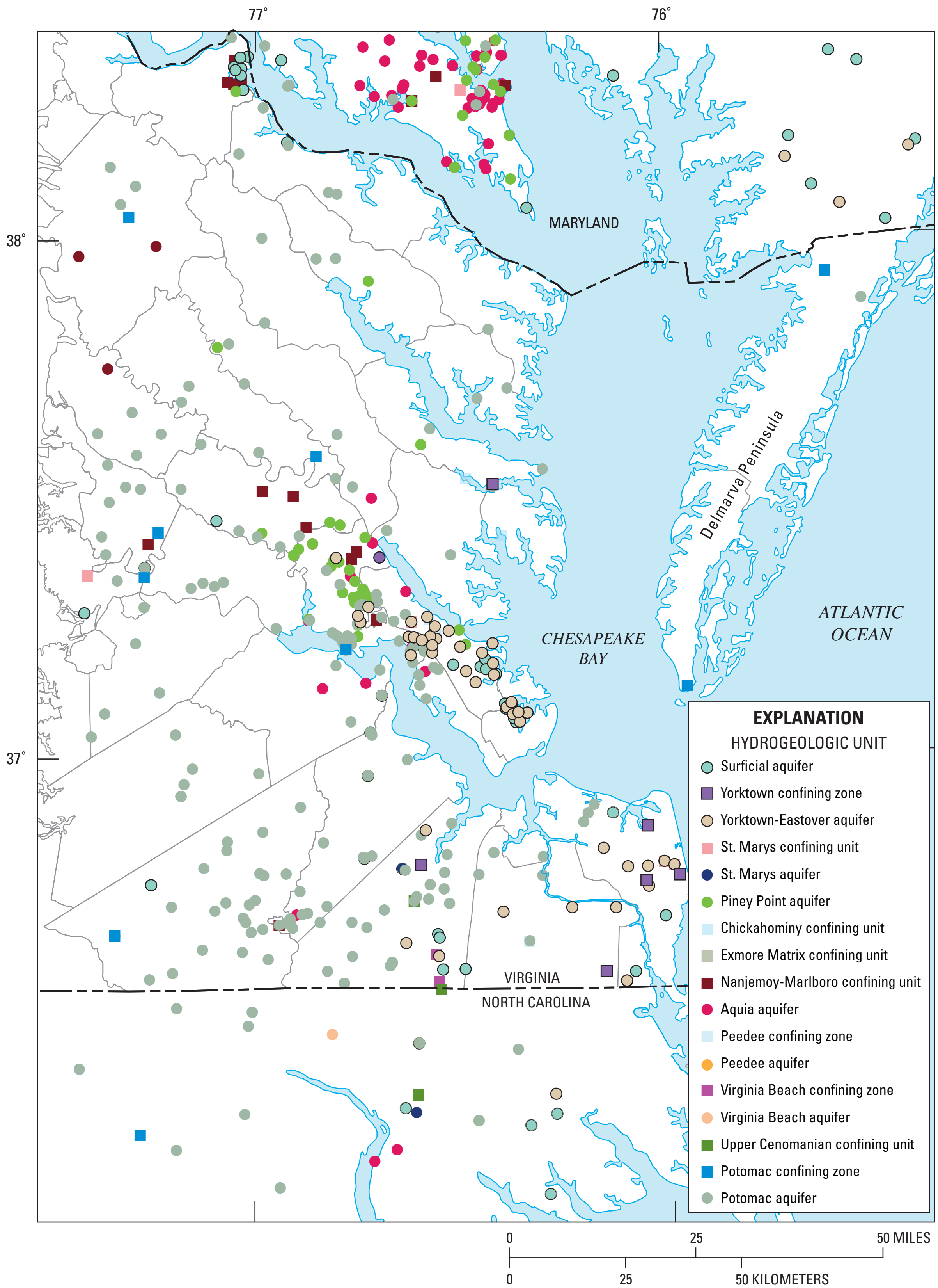

Figure 15. Locations and screened hydrogeologic unit of water-level observation wells in the Virginia Coastal Plain.

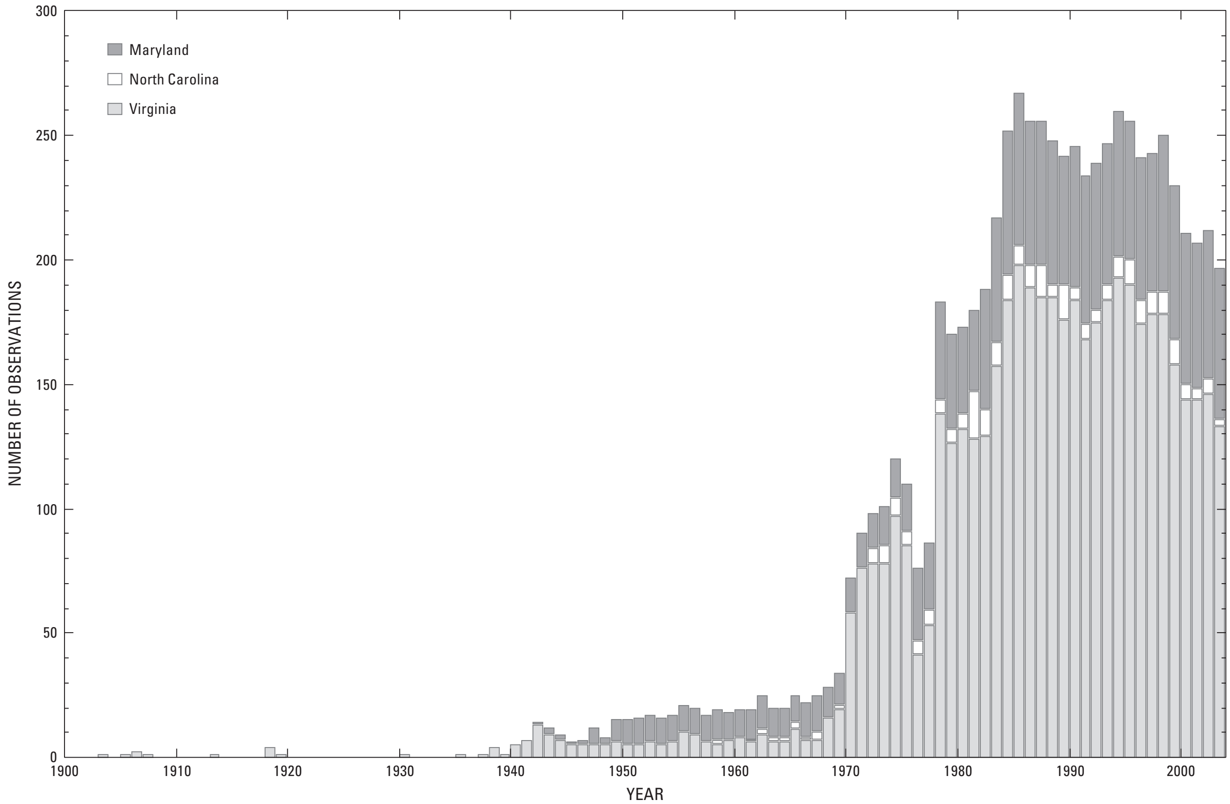

Figure 16. Time distribution and spatial distribution by State of water-level observations used for model calibration.

Table 6. Number of observations and wells primarily associated with each hydrogeologic unit simulated in the Virginia Coastal Plain model.

Hydrogeologic unit[1]	Hydrogeologic unit name	Abbreviation	Wells[2]	Observations[3]
1	Surficial aquifer	SURF	62	873
2	Yorktown confining zone	YTCZ	6	110
3	Yorktown-Eastover aquifer	YEAQ	59	833
4	Saint Marys confining unit	SMCU	5	85
5	Saint Marys aquifer	SMAQ	2	39
6	Calvert confining unit	CACU	0	0
7	Piney Point aquifer	PPAQ	49	523
8	Chickahominy confining unit	CHCU	4	72
9	Exmore Matrix confining unit	XMCU	0	0
10	Exmore Clast confining unit	XCCU	2	28
11	Nanjemoy-Marlboro confining unit	NMCU	17	136
12	Aquia aquifer	AQAQ	63	969
13	Peedee confining zone	PDCZ	1	26
14	Peedee aquifer	PDAQ	1	25
15	Virginia Beach confining zone	VBCZ	2	37
16	Virginia Beach aquifer	VBAQ	1	16
17	Upper Cenomanian confining unit	UCCU	3	53
18	Potomac confining zone	POCZ	8	116
19	Potomac aquifer	POAQ	212	3,242

[1]Units are numbered from the top of the model to the bottom.

[2]Number of observation wells in unit.

[3]Number of water-level measurements used for model calibration.

Water-Level Observation Errors

According to Hill and Tiedeman (2007), "Observation error is error related to any aspect of the observation not accounted for by the model considered, for which the expected value is zero." Quantification of the different sources of error in observations of water levels is necessary to calculate the weights used for model calibration. The sources of these errors are categorized under the following three types:

1. Observation-well location errors:

   a) Altitude error: Water-level measurements typically are referenced to a measuring point on the well head near the land surface. The uncertainty associated with the measuring-point altitude varies among wells depending on the method used to determine the well-head altitudes. Well-head altitudes in Virginia are determined by either a level survey or interpolation between the contours of a topographic map. Altitudes interpolated from topographic maps are considered to be accurate to within one-half of the contour interval of the map. For the 1:24,000 scale USGS topographic maps used in the Coastal Plain, the associated altitude uncertainties are either 2.5 ft or 5 ft.

   b) Horizontal-position error: Because water levels vary spatially, the uncertainty in the location (horizontal position) of an observation well results in further uncertainty in the water-level altitude associated with a specified horizontal location. Coastal Plain observation-well locations were determined either by a survey, such as with the Global Positioning System (GPS) or a theodolite, or by interpolation on a map. The expected accuracies of these methods range from 0.01 second of arc (for some GPS measurements) to 1 minute of arc (for some locations interpolated on a map). For this study, wells for which the position-determination method is unknown are assumed accurate to 1 minute of arc. A typical simulated water-level gradient of $5x10^{-4}$ was used to translate these horizontal-position errors to errors in water-level altitude, which range from insignificant (for GPS measurements) to about 9 ft (for horizontal-position uncertainty of about 1 mi).

2. Water-level measurement errors: Most measurements of Virginia Coastal Plain water levels used for model calibration were made with steel measuring tapes (3,993 measurements). The method of measurement was unknown for 294 reported observations used in the calibration. Other types of measurements and the number of associated observations used in the calibration include graphic recorders (277 measurements), "electric tapes" (249 measurements), "calibrated electric tapes" (215 measurements), manometers (51 measurements), airlines (4 measurements), "pressure gauges" (2 measurements), and "calibrated pressure gauges" (1 measurement), and 1 measurement by a presumably known "other" method. Water levels measured with steel measuring tapes are assumed to be accurate to within 0.05 ft. Water levels measured by unknown methods are assumed to be accurate to within 1 ft. Water levels measured by other methods are assumed to be accurate to within 0.1 ft.

3. Non-simulated transient-stress errors: Some observation wells respond to transient stresses not explicitly simulated in the groundwater model. While it can be argued that these observed responses are not errors in the observation, they are included as such in accordance with the opening definition of this section for the purpose of observation weighting. Examples of these stresses include (a) water-table fluctuations resulting from temporal variations in recharge and(or) evapotranspiration rates, (b) episodic pumping in nearby wells, (c) seasonal or episodic changes in rivers or stream stage, and (d) tides. The amplitude of water-level variation resulting from these stresses was estimated by comparing observed and simulated hydrographs for each observation well. Observed hydrographs were separated into "trend" and "noise" components, corresponding to water-level variations resulting from simulated and non-simulated processes. The amplitude of the interval containing 95 percent of the "noise" component was estimated for each observation hydrograph.

The magnitude of the individual error components for observation-well location and water-level measurements represent one-half of the width of their associated 95-percent confidence intervals. The error-component confidence intervals have a significance level of 5 percent, for which the critical value is 1.96. The component-error variances for each observation well were computed from their confidence intervals and the critical value, which were summed to obtain a total variance associated with each water-level observation.

Weights

In general, the weights (w_i) assigned to water-level observations were calculated as the inverse of the total observation-error variance. The total water-level observation error variance is the sum of the component-error variances described under the sub-heading "Water-Level Observation Errors." Because UCODE–2005 and PEST were used to perform non-linear regressions for parameter estimation, the square root of the weight (square root of the inverse of the total observation error variance) was specified for both program input files to facilitate comparison of objective function values between the two different programs. The magnitudes of observation weights ranged from essentially zero to about 10. Most observations (91.5 percent) had weights between 0.1 and 0.4; and 6.5 percent had weights between 0.4 and 1.1.

Modification of First Stress Period Time-Discretization for Parameter Estimation

Some non-linear effects of head-dependent boundary conditions, particularly the simulation of evapotranspiration, can cause numerical instability resulting in nonconvergence for the initial steady-state solution used to simulate predevelopment conditions. For this model, the convergence problem typically occurred when parameters associated with the boundary condition (such as the ET extinction depth) were adjusted in the regression process used for model calibration. To enable the regression to proceed in these instances, a 100-year transient stress period with no hydraulic stress was substituted for the initial steady-state stress period. This surrogate predevelopment transient stress period consisted of 60 time steps that increased in length in a geometric progression of ratio 1.2, such that the initial time step was approximately 3 hours in length. The storage term in the transient flow equation and small initial time-step length prevented the large head oscillations related to numerical instability and non-convergence for a steady-state solution. The long (100-year) period with no hydraulic stress allowed specified starting water levels sufficient time to adjust to the updated hydraulic-parameter distribution and boundary conditions for each parameter-estimation iteration, and approached steady-state conditions in 100 years. The water-level distribution at the end of this 100-year predevelopment stress period was saved for subsequent use as the starting water-level distribution in later steady-state model solutions computed between regression runs. These steady-state solutions were used to update regression-run starting water-level distributions in order to minimize the possible effect of transient residual starting water levels (calculated from a previous parameter distribution) in low-permeability hydrogeologic units.

Hydraulic Property Parameterization

A parsimonious approach was used for assignment of parameters representing hydraulic conductivity and specific storage in sub-domains of the model. Each hydrogeologic unit was initially assigned a unique parameter representing vertical hydraulic conductivity, horizontal hydraulic conductivity, and specific storage. Computation of the composite scaled sensitivities (CSS) of each of these model parameters identified parameters that could be effectively estimated through non-linear regression. The magnitude of composite scaled sensitivities for these initial parameters was largely dependent on the number of water-level observations within the corresponding hydrogeologic unit. Where possible, parameters with small composite scaled sensitivities were combined in a manner consistent with current knowledge of the hydraulic properties of the corresponding hydrogeologic units. For example, with the exception of the Potomac confining zone, the composite scaled sensitivities of parameters representing horizontal hydraulic conductivity in confining units and zones were low. On the basis of the initial composite scaled sensitivity and lithology of these units, they were subsequently sorted into four groups: (1) the Yorktown confining zone, (2) the Potomac confining zone, (3) the Chickahominy and Exmore confining units, and (4) all other confining units and zones. A single parameter was used to represent the horizontal hydraulic conductivity of each group. In later parameter-estimation runs, the continued small composite scaled sensitivity of the parameter representing horizontal hydraulic conductivity of the Yorktown confining zone suggested further modification of this parameterization scheme, after which it was combined with the parameter representing horizontal hydraulic conductivity of the Yorktown-Eastover aquifer. A similar process of composite scaled sensitivity evaluation and re-parameterization was conducted for those parameters representing vertical hydraulic conductivity in each of the aquifers. With the exception of the Potomac aquifer, all parameters representing vertical hydraulic conductivity in individual aquifers had low composite scaled sensitivities. Following several iterations of re-parameterization and testing, these individual parameters were combined into three groups representing the vertical hydraulic conductivity in (1) the surficial and Yorktown-Eastover aquifers, (2) the Potomac aquifer, and (3) all other aquifers.

For each new parameterization scheme, the model fit was optimized by minimizing the objective function with either UCODE–2005 or PEST. Observation residual maps for each hydrogeologic unit were subsequently generated and inspected to identify (1) large residuals and (2) non-random spatial distribution of the positive and negative weighted residuals. Hydrographs of the observations used in the calibration along with their simulated equivalents were generated and inspected following each parameter-estimation run. Inspection of the hydrographs containing large residuals was useful for diagnosing probable causes of inadequate model fit in some areas. If parameters with large composite scaled sensitivities represented the hydraulic conductivity or specific storage for a hydrogeologic unit in an area of apparent non-random residual distribution, one or more additional parameters were added to represent the hydraulic conductivity or specific storage in that area. The area of influence of the additional parameter was defined either by a refined area zonation or association with an additional pilot point, which effectively modified the spatial interpolation of the hydraulic parameter.

Because aquifer water levels are also affected by leakage through adjacent confining units, the vertical hydraulic conductivity (K_v) of confining units may also affect the pattern of residuals in aquifers. Because water levels within the Piney Point aquifer were sensitive to the vertical hydraulic conductivity of the Calvert confining unit, the spatial variability of vertical hydraulic conductivity within the Calvert confining unit (fig. 17) was simulated with pilot points.

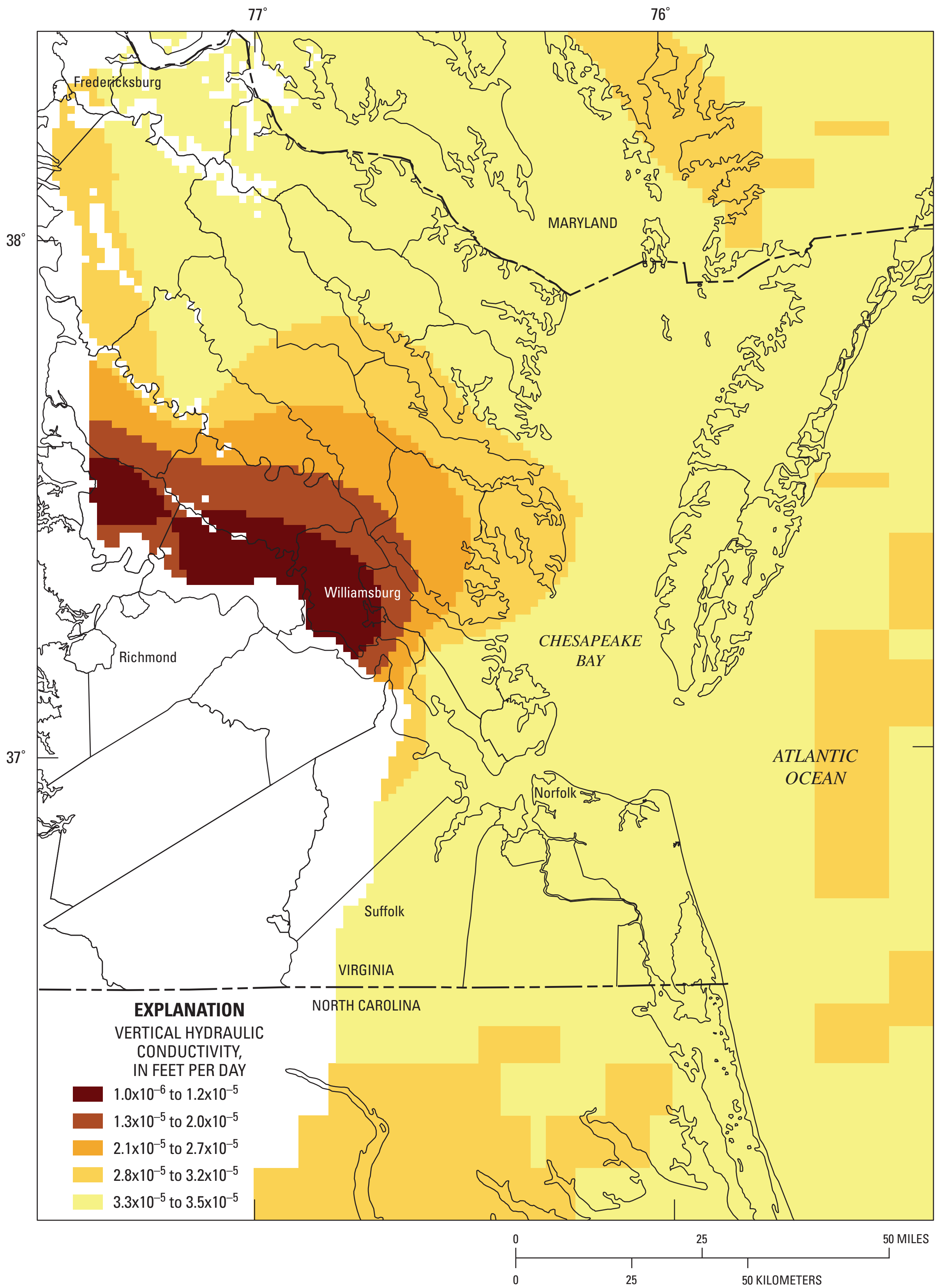

Figure 17. Estimated vertical hydraulic conductivity of the Calvert confining unit of the Virginia Coastal Plain.

Boundary Flux Parameterization

Early in the calibration process, water-level residual maps showed an area around the updip Norfolk Arch (fig. 1) of non-random positive residuals, indicating that observed water levels were greater than simulated water levels. This clustering suggested insufficient groundwater flux to the Potomac aquifer system in that area. Existing boundary-condition specifications (particularly specified river stages) were verified, and various parameterizations of overlying confining units were tested. Two alternative approaches were tested to achieve improvement of the model fit in this area: (1) decrease the horizontal hydraulic conductivity to the west (which increased the hydraulic gradient), or (2) allow some recharge as underflow from the Piedmont groundwater flow system over the Norfolk Arch. Following the first approach, parameter optimization estimated low (1–2 ft/d) hydraulic conductivities in the area. For the second approach, a zone of underflow from the west was defined (fig. 12b) over the Norfolk Arch through which specified flux was parameterized. Sensitivity analysis indicates that water-level observations are sensitive to the parameter representing this flux. Parameter optimization estimated an underflow equivalent to approximately 0.2 percent of precipitation flux over the area of the Piedmont west of the flux boundary. This (underflow) approach was considered more plausible than the alternative (low hydraulic conductivity) approach and was retained for the final model configuration.

Simulated Conditions

The goal of the calibration was to simultaneously meet the following conditions: (1) The non-linear regression converged with a minimum sum-of-squares error (SSE), (2) the regression-determined parameter values were within the range of pre-defined reasonable values, (3) parameters were not excessively correlated, (4) the simulated hydraulic-property distribution within hydrogeologic units was reasonable for the model scale, and (5) positive and negative model residuals were randomly distributed in space and time. The model was considered calibrated when these criteria, which are discussed further in the subsequent section entitled “Calibration Assessment” were met as closely as possible.

Water Levels

The 113-year transient groundwater model simulates the changing distribution of water levels throughout the aquifer system in space and time. Maps of simulated water levels along any altitude or surface of interest within the aquifer system may be generated from model output corresponding to the end of any model-simulated time step. Maps of water levels within hydrogeologic units designated as aquifers are useful for determining directions of flow and assessing aquifer impacts resulting from groundwater development. The maps of simulated water levels in this report illustrate the simulated altitudes of the water table, which are generally in the surficial aquifer and water levels in the middle of the Yorktown-Eastover, St. Marys, Piney Point, Aquia, Peedee, and Virginia Beach aquifers, and at the top of the Potomac aquifer. Because of vertical gradients within the thick, vertically anisotropic Potomac aquifer, maps of water levels differ at various depths within the Potomac aquifer, particularly in areas near large withdrawal wells during transient stress periods. The potentiometric surface at the top of the Potomac aquifer was selected for depiction because conditions at the top of the Potomac aquifer are most likely to be evaluated for groundwater withdrawal-permit applications (Robin Patton, Virginia Department of Environmental Quality, oral commun., 2006). In subsequent sections, simulated water levels corresponding to predevelopment conditions are depicted and discussed for each aquifer, and water levels simulated for the year 2003 are depicted and discussed for the seven aquifers beneath the surficial aquifer. Although simulated water levels within the surficial aquifer are generally similar to those simulated for predevelopment conditions, the drawdown simulated in the surficial aquifer for the drought year 2001 is depicted. The simulated water-level change between predevelopment and 2003 for the Yorktown-Eastover, St. Marys, Piney Point, Aquia, and Potomac aquifers is also depicted as drawdown maps. No substantial regional drawdown within the Peedee and Virginia Beach aquifers was simulated and, therefore, is not depicted for those aquifers.

An estimate of the magnitude of water-level change (drawdown) due to domestic withdrawals within each aquifer was made by assuming model linearity and application of the principal of superposition. Although the model is somewhat non-linear, any error in this calculation from the assumption of model linearity is smaller than that from the uncertainty of domestic withdrawal magnitudes.

Because the model was calibrated to water levels measured at discrete points in space and time, comparison of hydrographs containing the observations used for calibration with their simulated equivalents provides a visual indication of the quality of the model fit in various aquifers and areas of the Coastal Plain. In addition to depicting the quality of the model fit, hydrographs of simulated and observed water levels illustrate the rate of change in water levels at various points in the aquifer system through time. Representative hydrographs of water-level measurements with their simulated equivalents are shown and discussed in subsequent sections for seven of the eight aquifers. Water-level observations for the Virginia Beach aquifer were not available.

Surficial Aquifer

The simulated altitude of the water table in the Virginia Coastal Plain for the steady-state stress period representing predevelopment conditions is shown in figure 18a. Although the water table is generally located within the surficial aquifer, there are some areas where the simulated water table resides within one of the underlying aquifers or confining units. Because of the strong influence of topography, the water-table altitude varies with a higher spatial frequency than the potentiometric surface of any underlying confined aquifer. Simulated evapotranspiration largely controls the depth of the simulated water table, resulting in a water-table surface that is a smoothed and subdued replica of the land-surface altitude specified in the model EVT package. The simulated water-table altitudes depicted in figure 18a suggest that shallow groundwater flows downward away from higher-altitude areas, such as near the Fall Line and the mid-lines of major peninsular interfluves, toward lower altitudes adjacent to simulated rivers. However, most of the water recharged to the surficial aquifer likely discharges to one of the adjacent smaller streams (fig. 7) that were not explicitly simulated. As discussed in the subsequent section entitled “Water Budget,” detailed simulation of surficial-aquifer flow from interfluves to the non-simulated streams is not possible with the resolution of the finite-difference grid of this regional model.

Differences in simulated water-table altitudes between stress periods, including the differences between steady-state and 2003, are predominantly because of simulated differences in recharge between stress periods. Simulated water-table altitudes at the end of the simulation in 2003 are within several feet of the predevelopment water-table altitudes and are, therefore, not depicted in a figure. The below-normal precipitation over the Virginia Coastal Plain during 2001 (fig. 8) was simulated with proportionately smaller recharge, resulting in lower simulated water-table altitudes for 2001. The difference between water-table altitudes simulated for predevelopment conditions and the drought year 2001 is depicted in figure 18b.

The locations of observation wells in the surficial, Yorktown-Eastover, St. Marys, Piney Point, Aquia, and Peedee aquifers for which hydrographs are depicted are shown in figure 19. In the example hydrograph from surficial-aquifer observation well 57D 23 (fig. 20), the simulated water level responds to simulated changes in annual recharge and reasonably mimics observed annual changes in water levels. A superposition analysis indicated that the drawdown resulting from domestic pumpage with a constant recharge rate was less than 1 ft throughout the surficial aquifer.

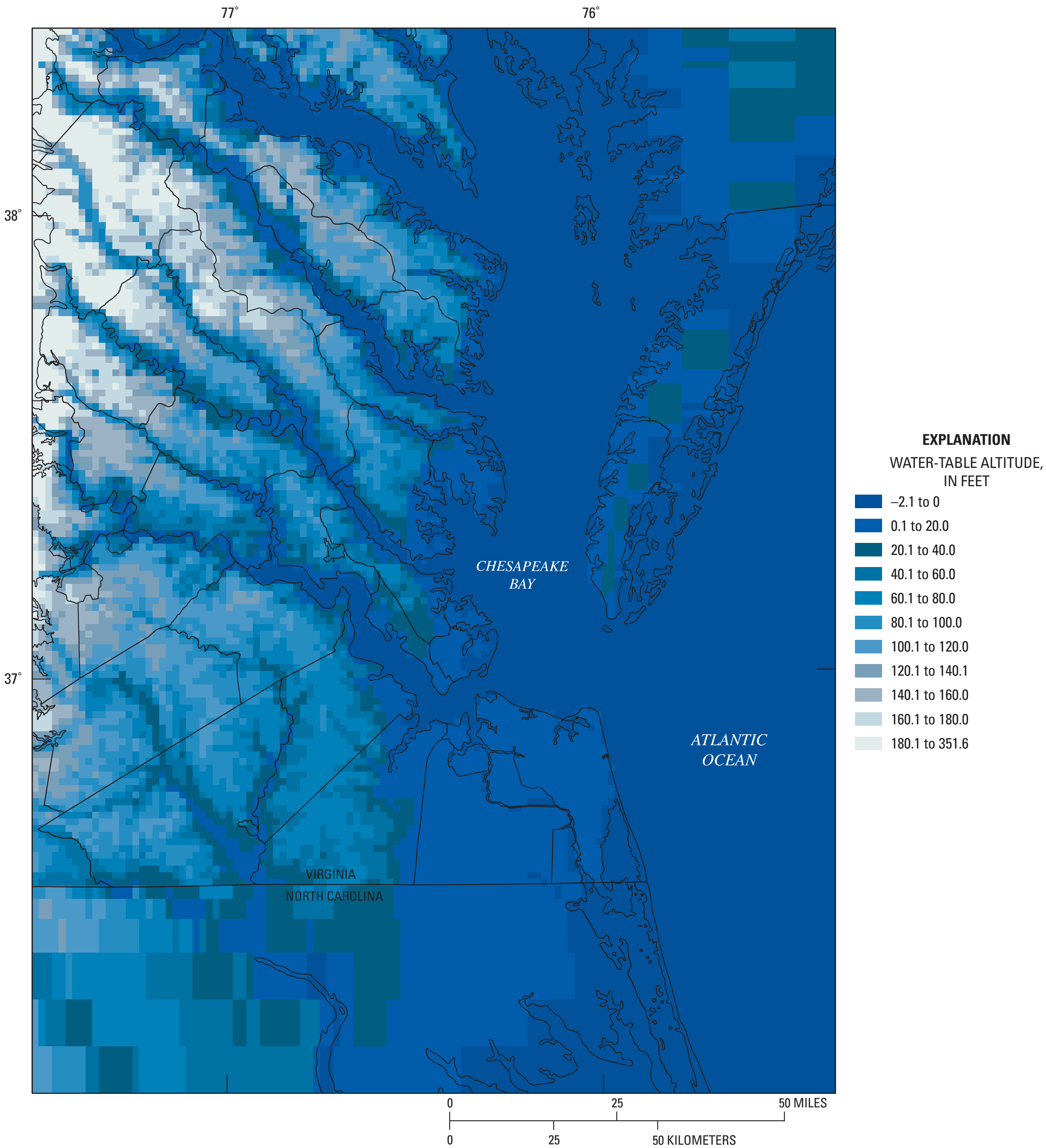

Figure 18a. Simulated predevelopment water table in the Virginia Coastal Plain.

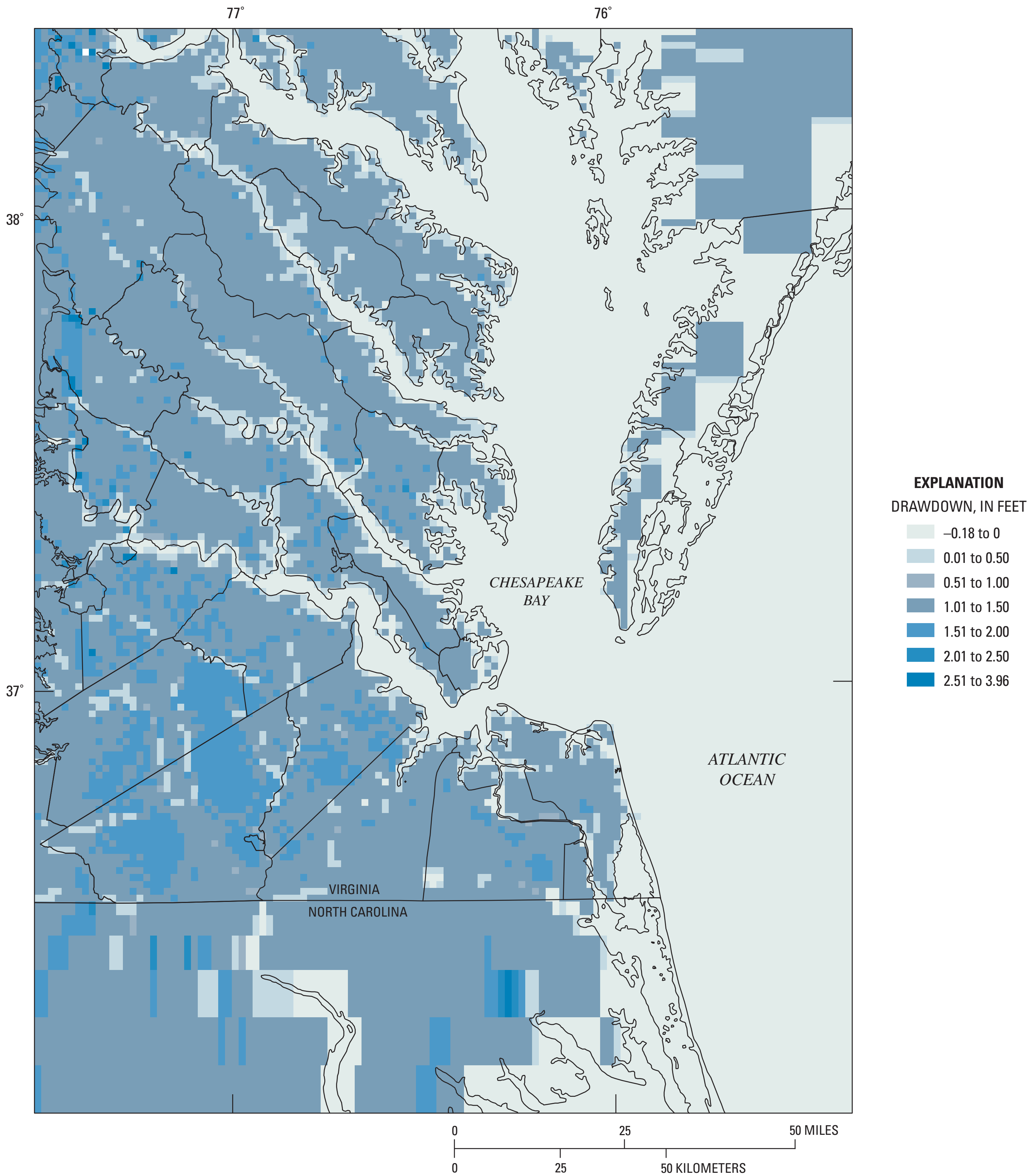

Figure 18b. Simulated water-table drawdown in 2001 in the Virginia Coastal Plain.

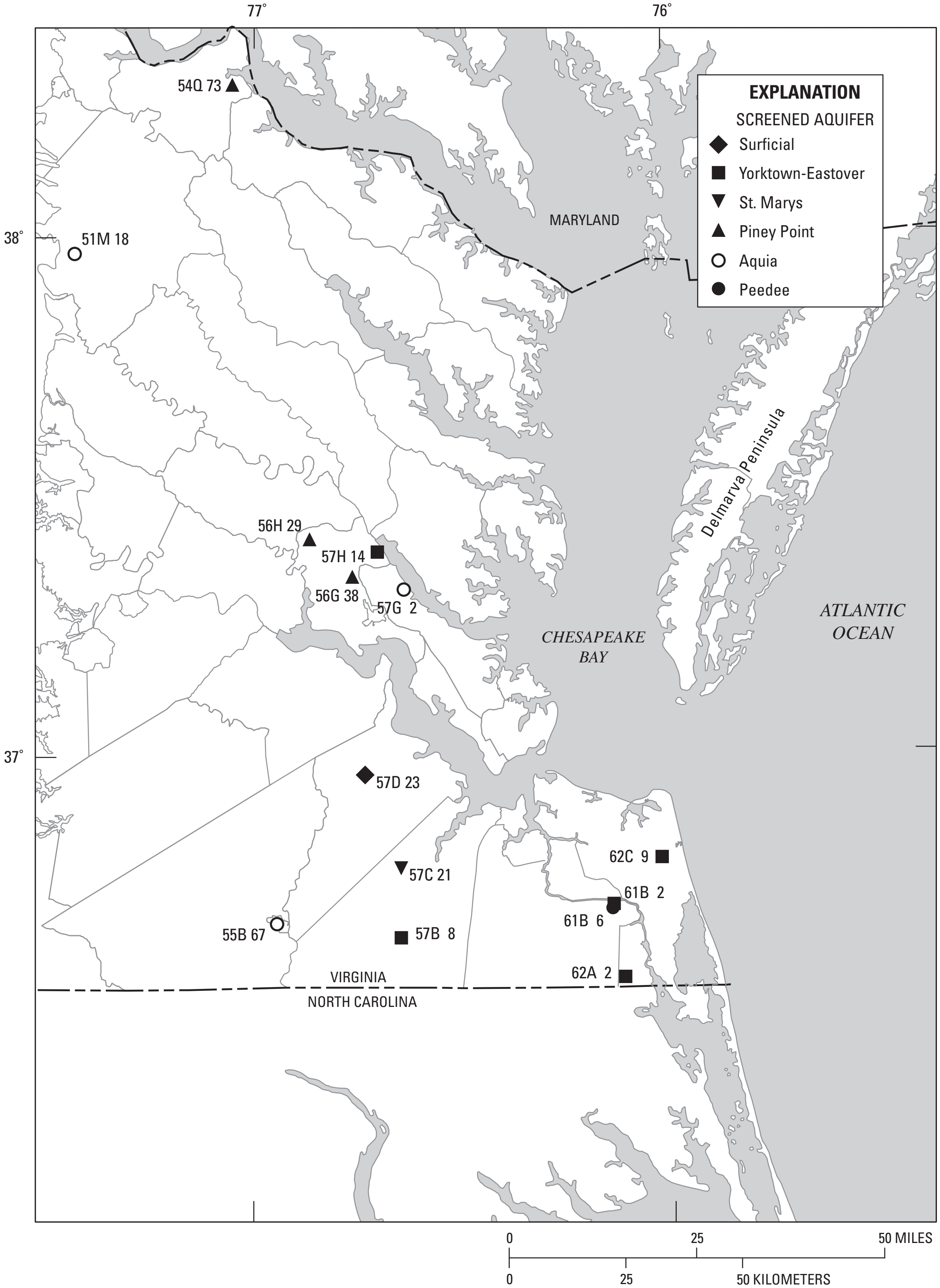

Figure 19. Locations of observation wells screened in the surficial, Yorktown-Eastover, St. Marys, Piney Point, Aquia, and Peedee aquifers for hydrographs depicted in figures 20, 22, 24, 26, 28, and 30.

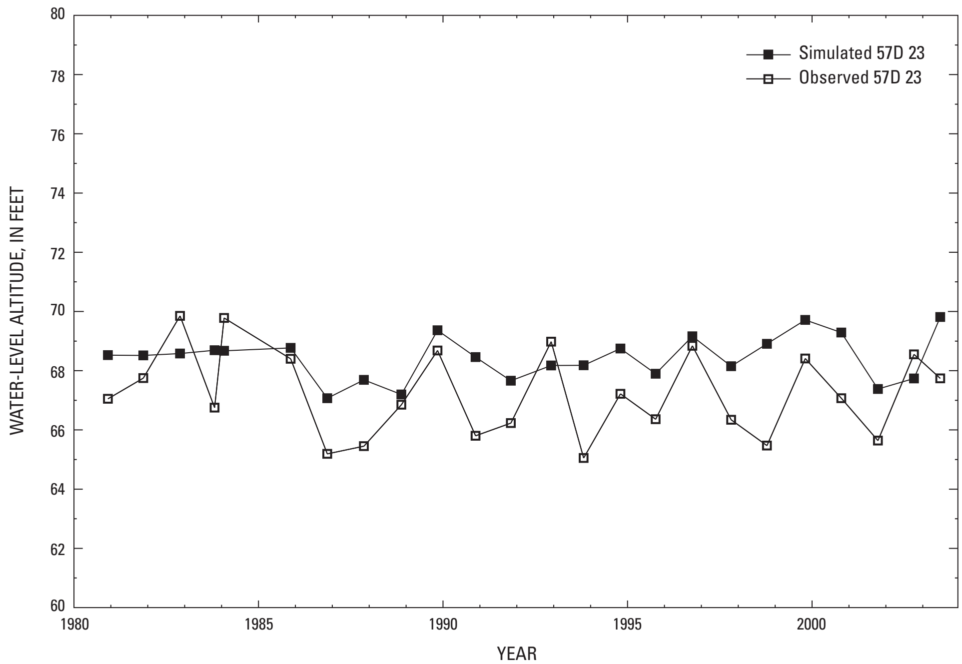

Figure 20. Observed and simulated water levels in the surficial aquifer well 57D 23 in the Virginia Coastal Plain. (Well location is shown in figure 19.)

Yorktown-Eastover Aquifer

The simulated steady-state water levels in the Yorktown-Eastover aquifer (fig. 21a) indicate that predevelopment groundwater in the Yorktown-Eastover aquifer in Virginia flowed away from higher-altitude areas, near the midlines of the Northern Neck, Middle Peninsula, and York-James Peninsula, toward lower-altitude discharge areas, including major rivers and the Chesapeake Bay. The simulated water levels in the Yorktown-Eastover aquifer for 2003 (fig. 21b) suggest that regional groundwater flow during 2003 was similar to that simulated for predevelopment conditions. The drawdown of groundwater levels in the Yorktown-Eastover aquifer, derived by subtracting simulated 2003 water levels from predevelopment water levels, is shown in figure 21c. The drawdown under low-altitude areas, such as major rivers and the Chesapeake Bay, typically is less than 1 ft and likely results from decreased groundwater discharge through the Yorktown-Eastover aquifer due to groundwater withdrawals from the regional aquifer system. Simulated water-level drawdowns under land areas, resulting from localized groundwater withdrawals from the Yorktown-Eastover aquifer, generally are less than 2 ft, with a maximum of 2.77 ft in the southeastern part of the city of Chesapeake. Large land areas with up to 1 ft of simulated groundwater-level recovery, result from transient recharge greater than the long-term average value simulated during the steady-state stress period.

Wells 57H 14, 61B 2, 62A 2, 62C 9, and 57B 8 are screened in the Yorktown-Eastover aquifer at various locations in the Coastal Plain (fig. 19). The hydrograph in figure 22 depicts water levels measured in these wells along with their corresponding simulated values.

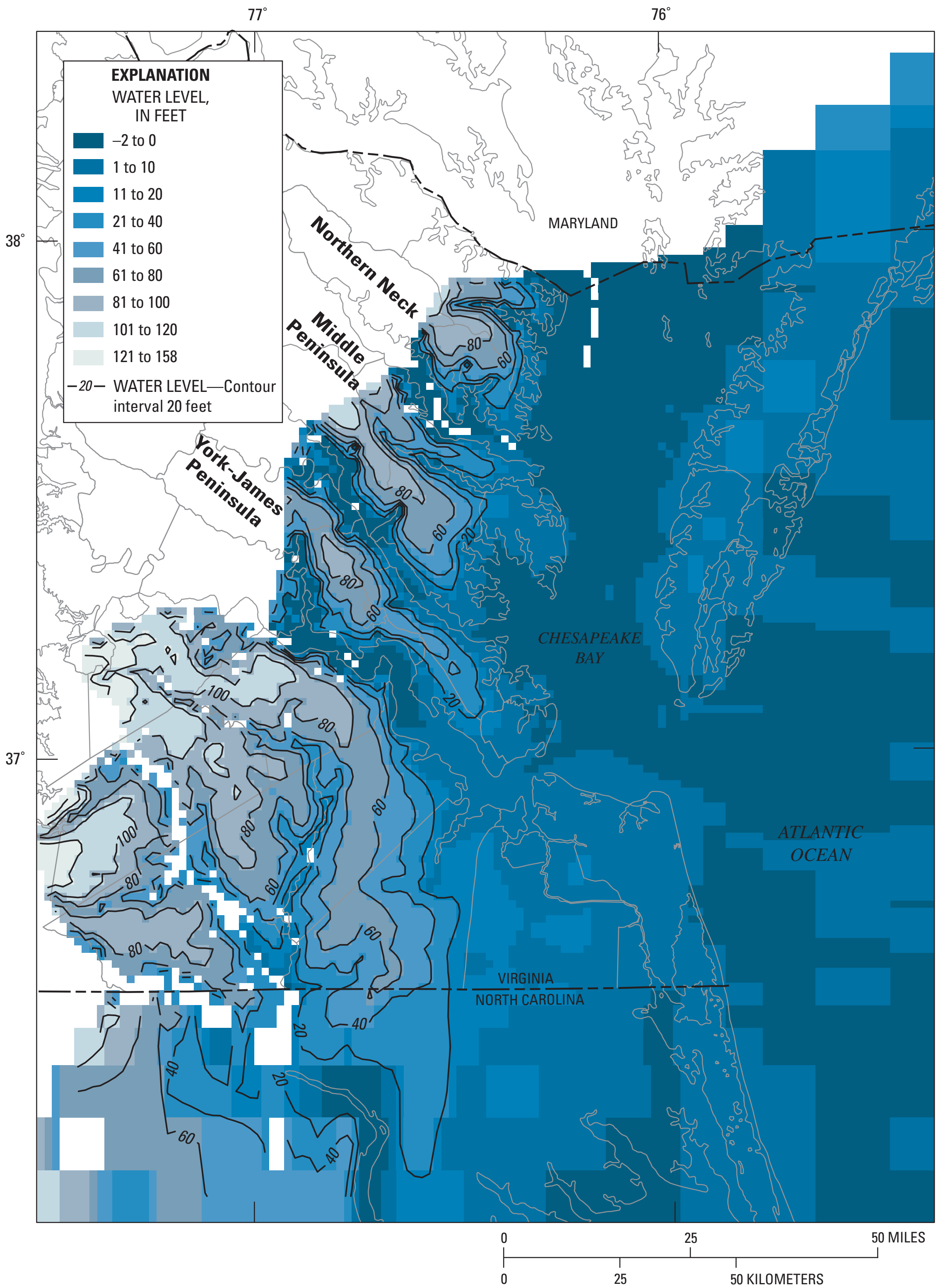

Figure 21a. Simulated predevelopment water levels in the Yorktown-Eastover aquifer of the Virginia Coastal Plain.

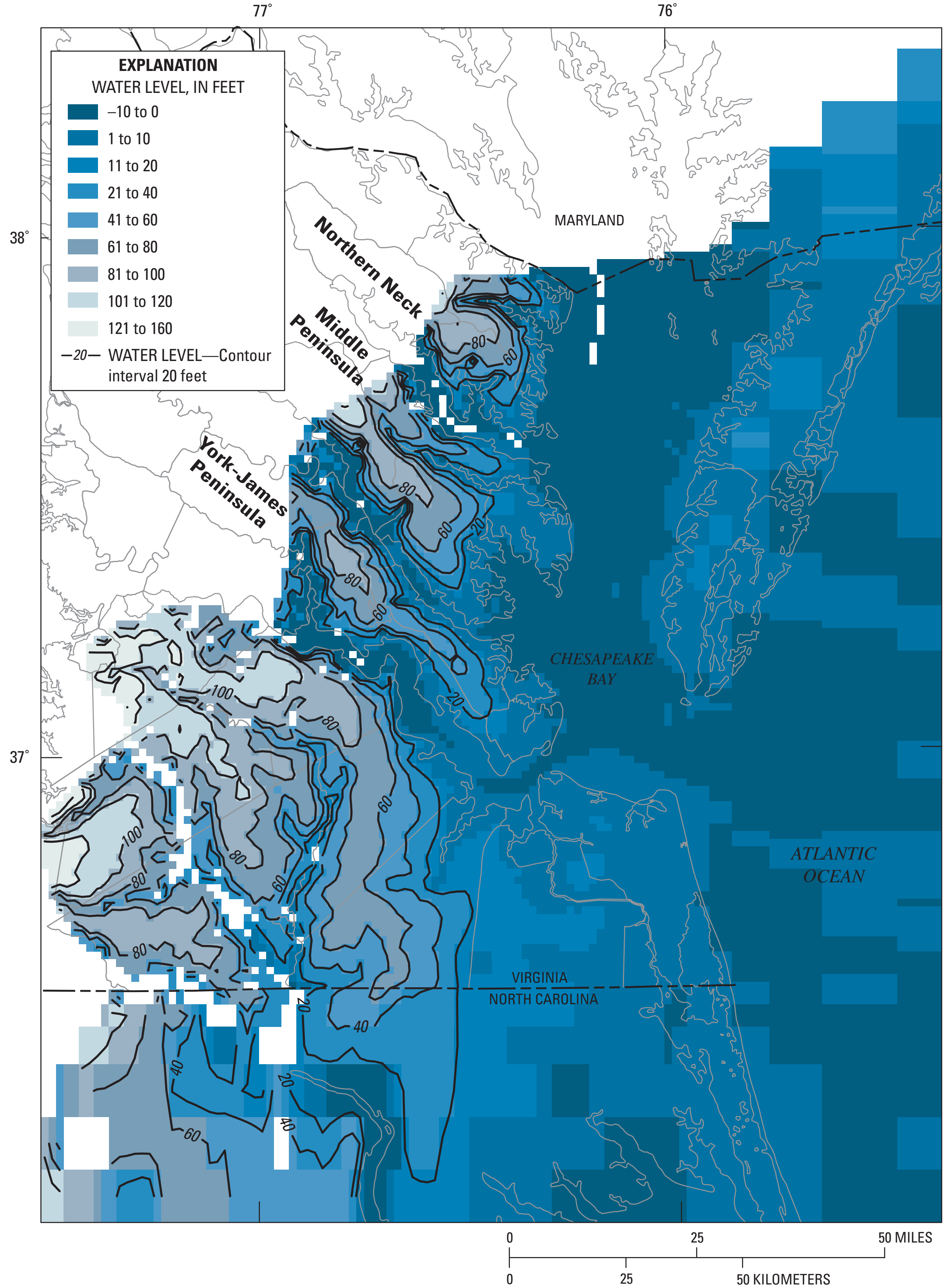

Figure 21b. Simulated 2003 water levels in the Yorktown-Eastover aquifer of the Virginia Coastal Plain.

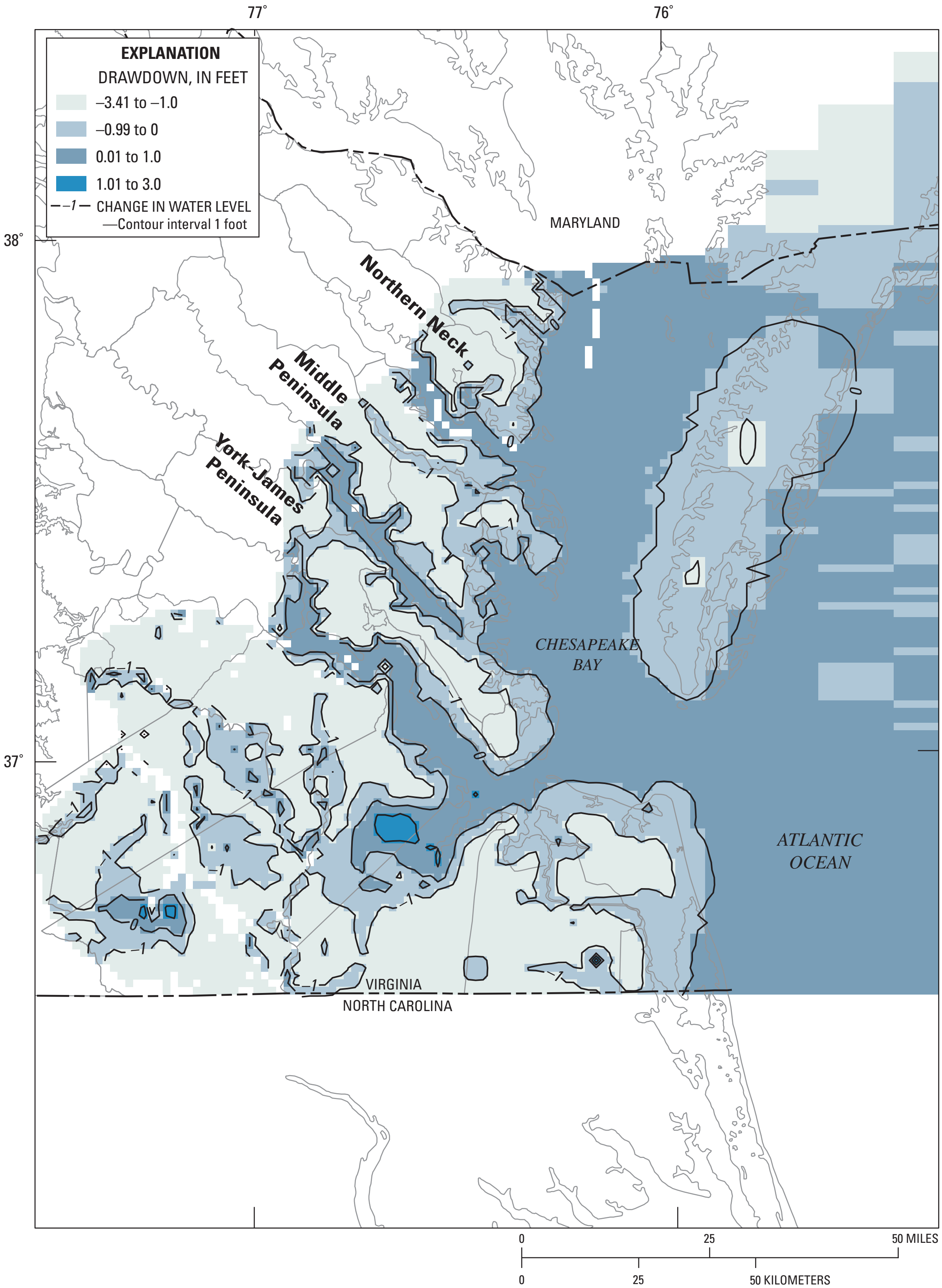

Figure 21c. Simulated drawdown from predevelopment to 2003 in the Yorktown-Eastover aquifer of the Virginia Coastal Plain.

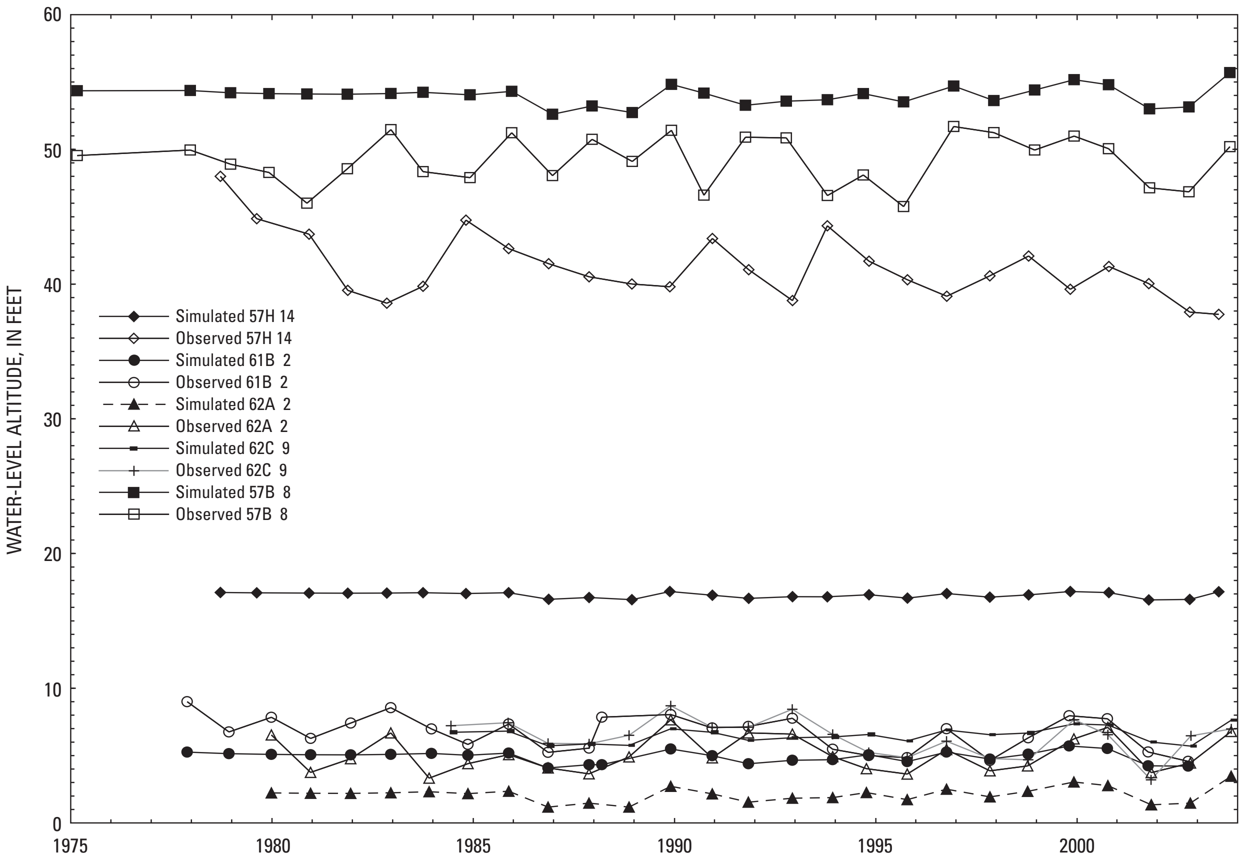

Figure 22. Observed and simulated water levels in wells 57H 14, 61B 2, 62A 2, 62C 9, and 57B 8 in the Yorktown-Eastover aquifer of the Virginia Coastal Plain. (Well locations are shown in figure 19.)

St. Marys Aquifer

In southern Virginia, the St. Marys aquifer is present as a north-south trending sand layer approximately 50 ft thick between the underlying Calvert confining unit and the overlying St. Marys confining unit. Predevelopment water levels in the St. Marys aquifer simulated by the steady-state stress period are depicted in figure 23a. The simulated predevelopment water-level contours suggest that groundwater flowed generally from west to east through the St. Marys aquifer in Virginia and south into North Carolina. Water levels simulated in the St. Marys aquifer for 2003 (fig. 23b) are lower, but suggest flow directions similar to those simulated for predevelopment time. The simulated water-level drawdown from predevelopment through 2003 exceeds 40 ft near the northern terminus of the St. Mary's aquifer in southern Virginia (fig. 23c).

The St. Marys aquifer, (along with the Peedee aquifer), is one of the least-utilized aquifers in southern Virginia; the relatively small quantity of withdrawn groundwater (table 2) is used for private water supplies in the city of Suffolk. In comparison with other developed Coastal Plain aquifers, the St. Marys aquifer in southern Virginia has relatively limited area and low transmissivity (fig. 45b, p. 89), which may account for the disproportionately large simulated drawdown resulting from the relatively modest groundwater withdrawals from the St. Marys aquifer. A superposition analysis indicates that simulated domestic withdrawals account for up to 3 ft of the drawdown in the St. Marys aquifer in southern Virginia.

The location of a water-level observation well (57C 21) that is screened in the St. Marys aquifer in southern Virginia is depicted in figure 19. Figure 24 depicts water levels measured in this well, along with the corresponding simulated values.

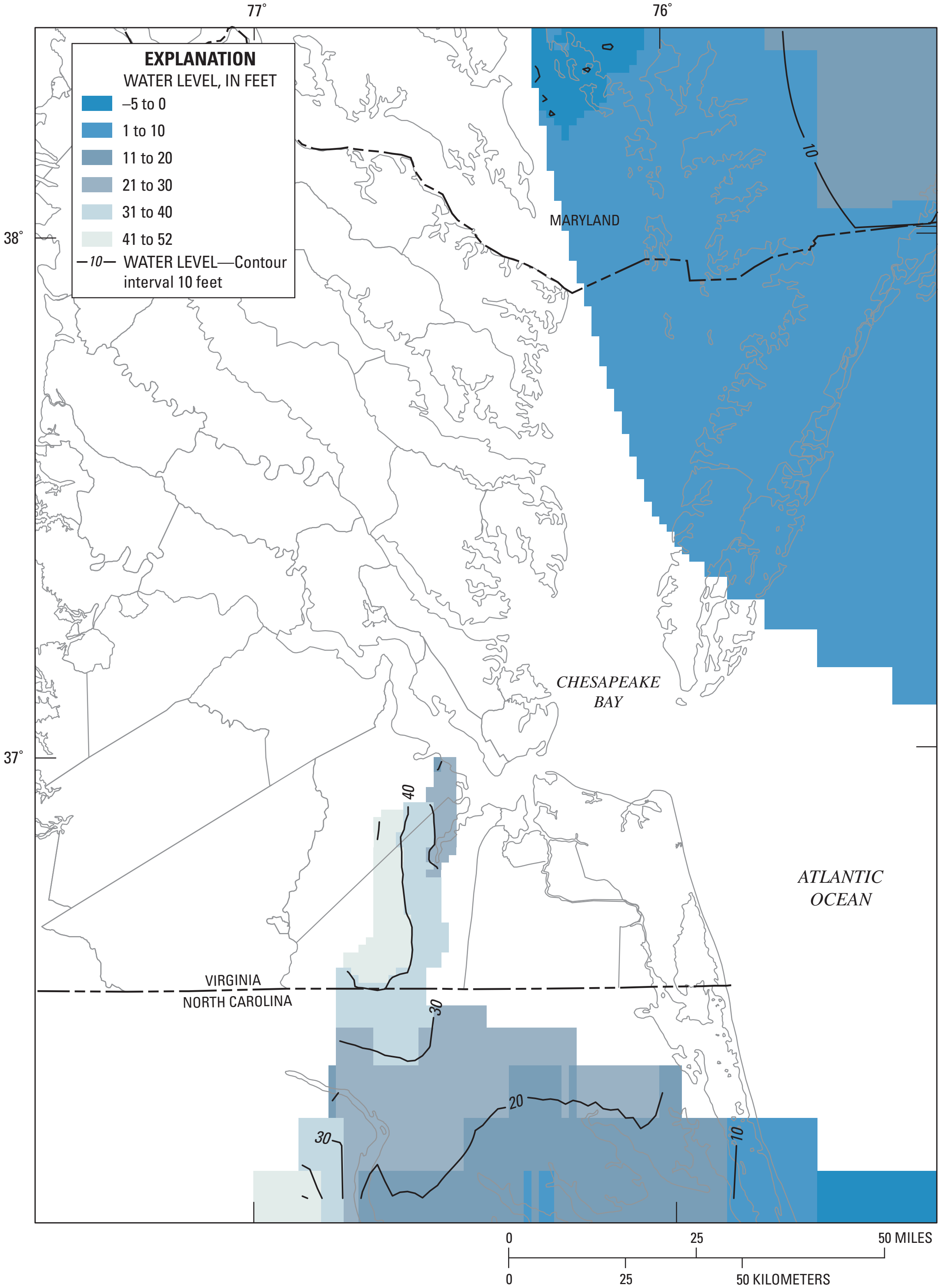

Figure 23a. Simulated predevelopment water levels in the St. Marys aquifer of the Virginia Coastal Plain.

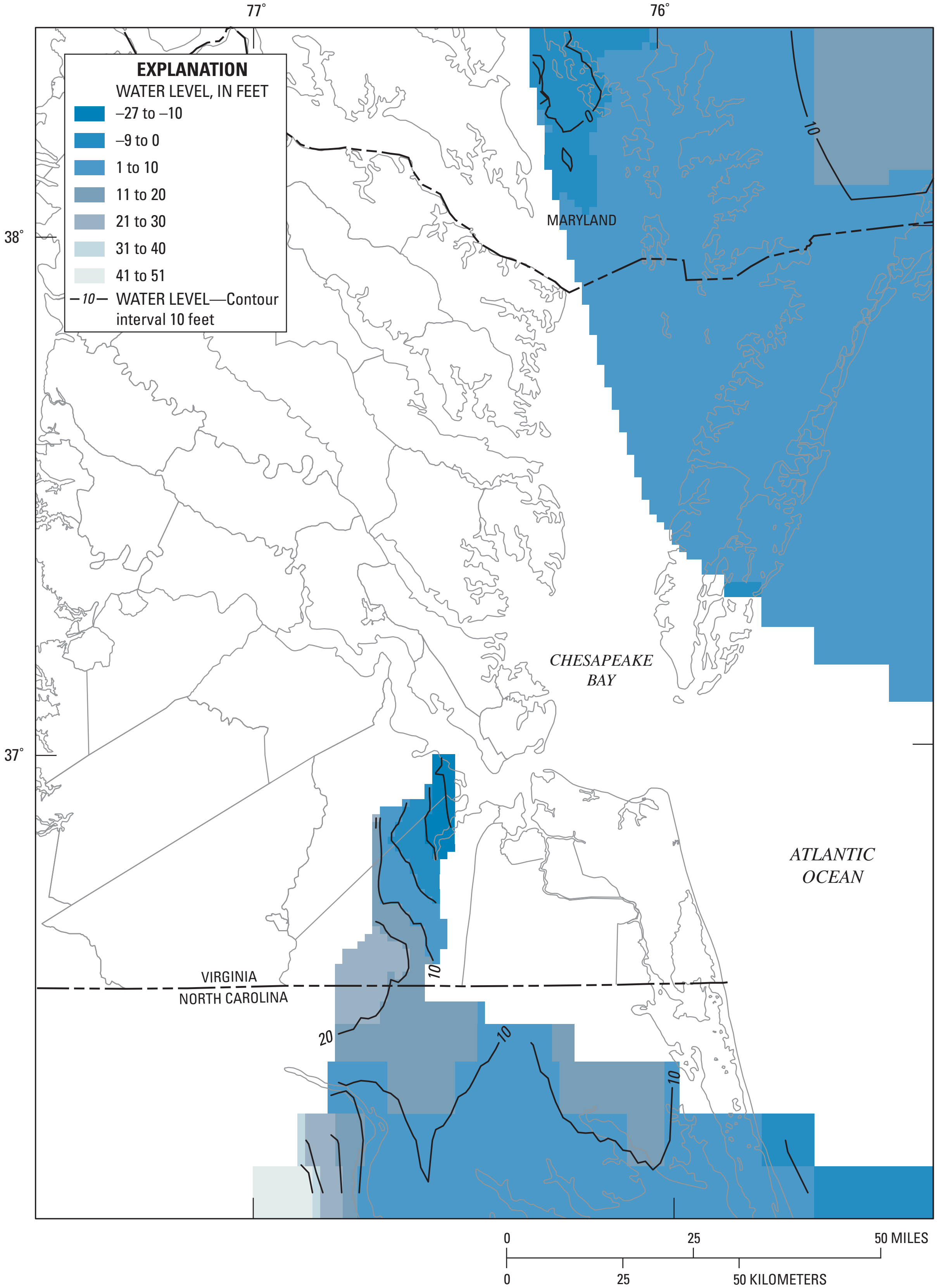

Figure 23b. Simulated 2003 water levels in the St. Marys aquifer of the Virginia Coastal Plain.

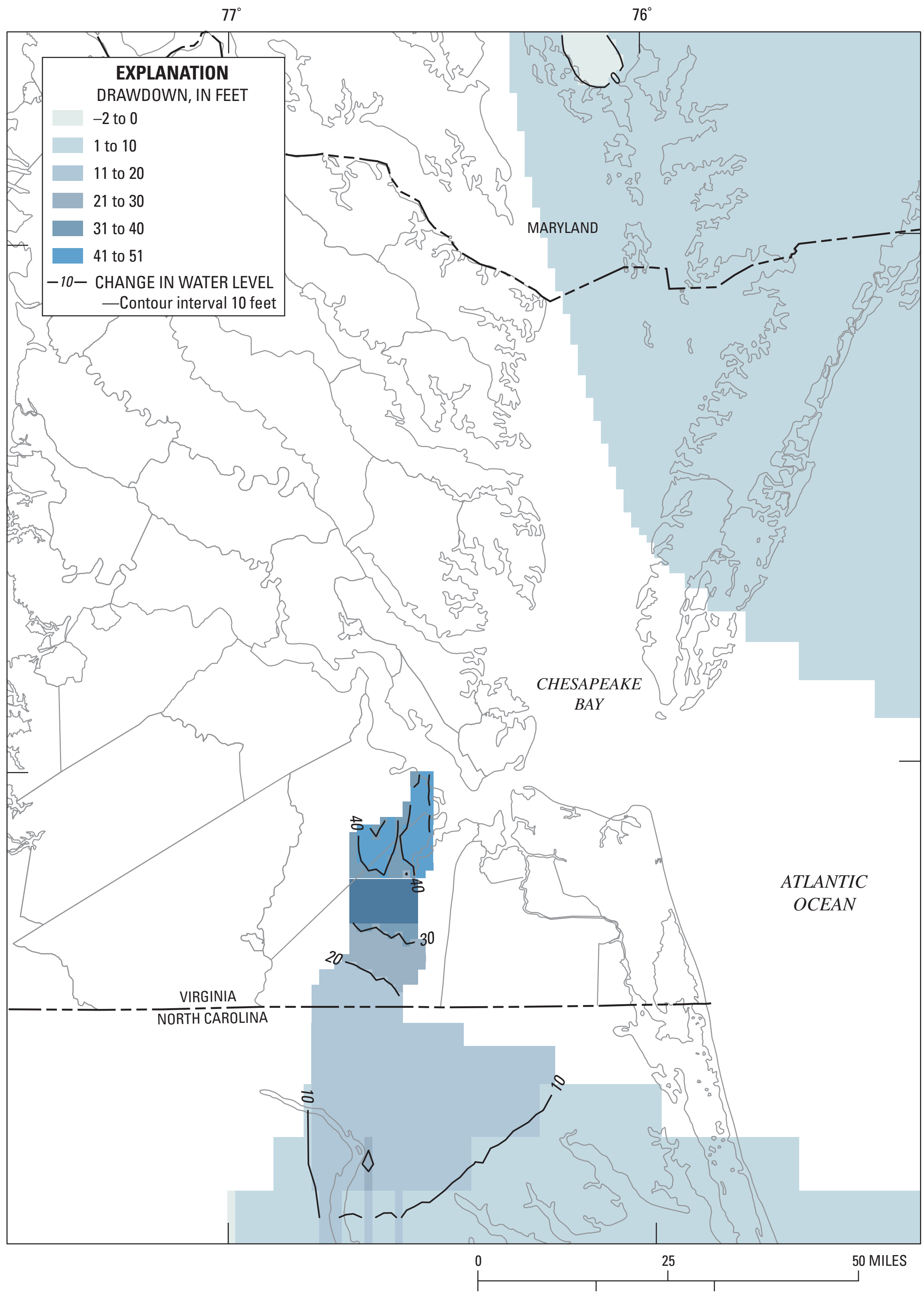

Figure 23c. Simulated drawdown from predevelopment to 2003 in the St. Marys aquifer of the Virginia Coastal Plain.

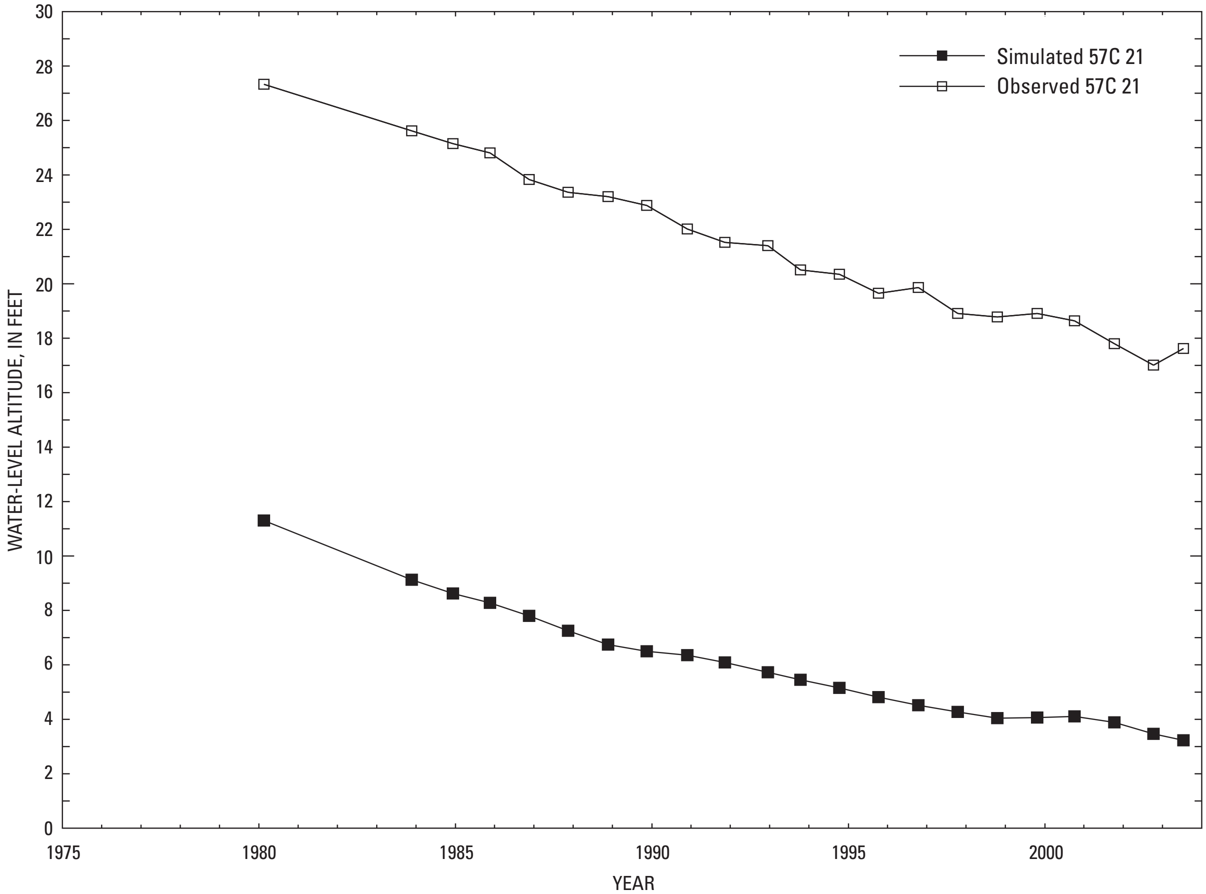

Figure 24. Observed and simulated water levels in well 57C 21 in the St. Marys aquifer of the Virginia Coastal Plain. (Well location is shown in figure 19.)

Piney Point Aquifer

Although the Piney Point aquifer is regionally extensive beneath the Coastal Plain, it is relatively thin south of the James River, with correspondingly low transmissivity. The simulated potentiometric surface of the Piney Point aquifer during the steady-state stress period is shown in figure 25a. Predevelopment groundwater flowed from western up-dip areas toward the east and southeast, to discharge through the overlying Calvert confining unit near the Atlantic Coast. By the year 2003, concentrated groundwater withdrawals resulted in several cones of depression (fig. 25b) that altered flow directions in the Piney Point aquifer in the vicinity of the Middle and York-James Peninsulas. The maximum simulated drawdown in the Piney Point aquifer near Williamsburg is 127 ft (fig. 25c). A superposition analysis indicates that simulated domestic withdrawals may account for approximately 10 ft of drawdown in the Piney Point aquifer near Williamsburg, and from 7 to 9 ft across the eastern portions of the Middle Peninsula and Northern Neck.

A hydrograph for observation wells 54Q 73, 56G 38, and 56H 29 in the Piney Point aquifer is depicted in figure 26. Except for a few observations near Williamsburg, the fit of simulated to observed water levels in Piney Point observation wells is good. Simulated water levels in the Piney Point aquifer with less-than-optimal fit to observed water levels near Williamsburg were sensitive to magnitudes of vertical hydraulic conductivity of the adjacent Calvert and Nanjemoy-Marlboro confining units. Although further refinement of the simulated spatial variation of the Calvert confining unit vertical hydraulic conductivity could improve the model fit for some observation wells, such an adjustment was limited during model calibration because of uncertainty in the magnitudes of domestic withdrawals in the Williamsburg area. An informal polling of domestic well drillers (Scott Bruce, Virginia Department of Environmental Quality, oral commun., 2006) suggested that actual domestic withdrawals from the Piney Point aquifer in the Williamsburg area could be substantially greater than the simulated fluxes, which were based on the analysis of Pope and others (2007). Superposition analysis of drawdown rates resulting from the specified domestic withdrawals suggested that under-representation of the domestic-withdrawal flux may also account for the magnitude of differences between water levels simulated and observed in some Piney Point observation wells.

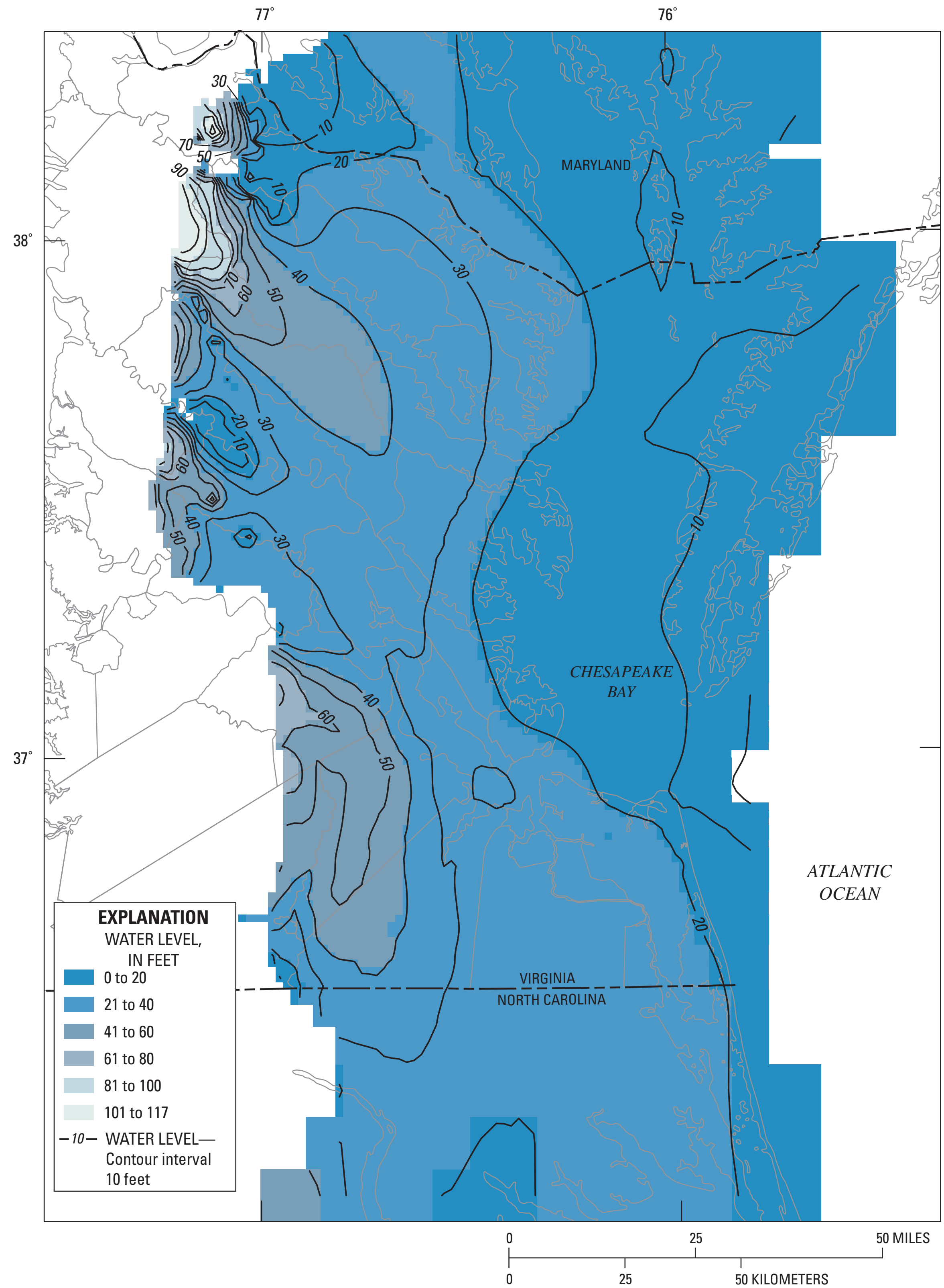

Figure 25a. Simulated predevelopment water levels in the Piney Point aquifer of the Virginia Coastal Plain.

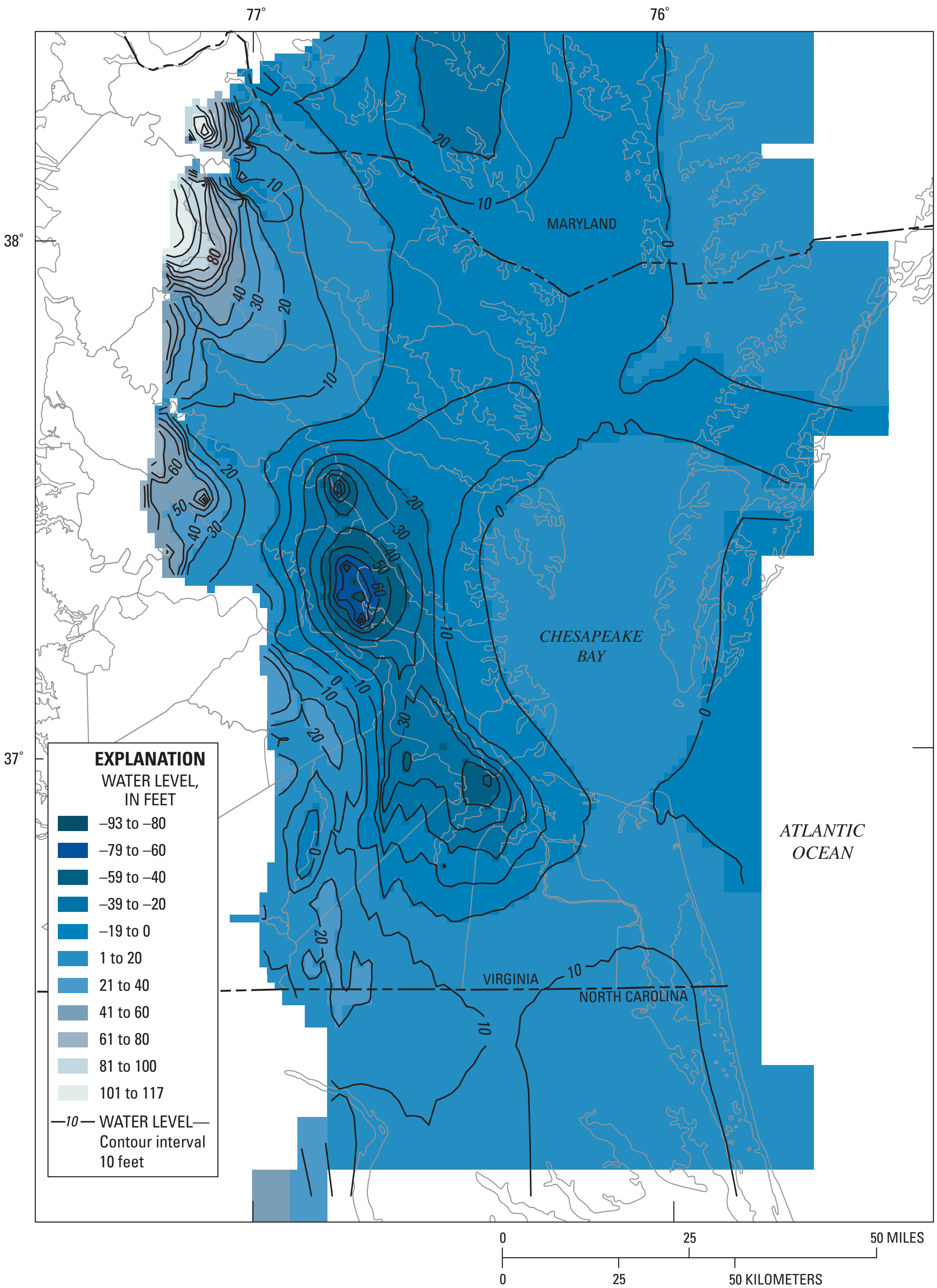

Figure 25b. Simulated 2003 water levels in the Piney Point aquifer of the Virginia Coastal Plain.

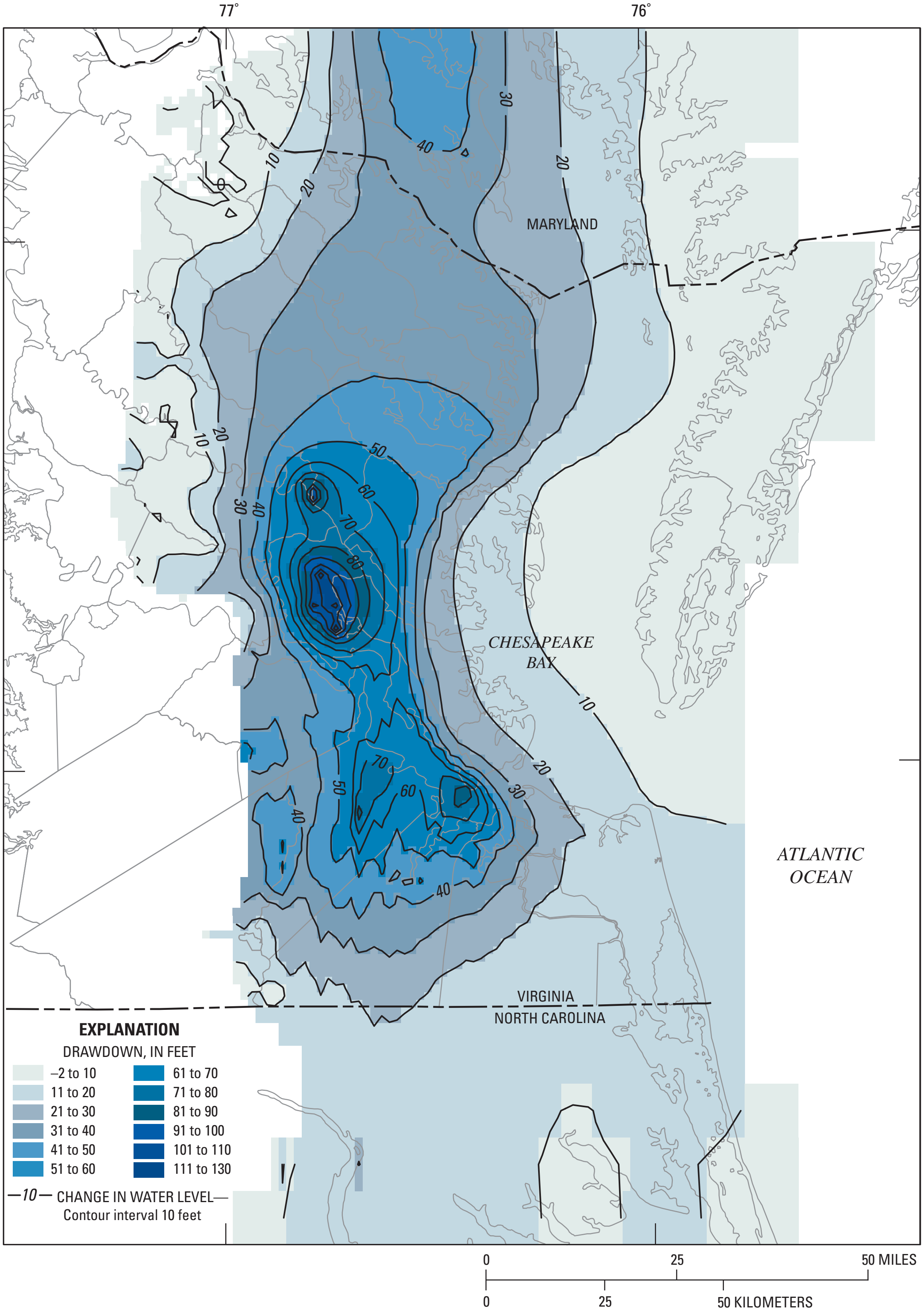

Figure 25c. Simulated drawdown from predevelopment to 2003 in the Piney Point aquifer of the Virginia Coastal Plain.

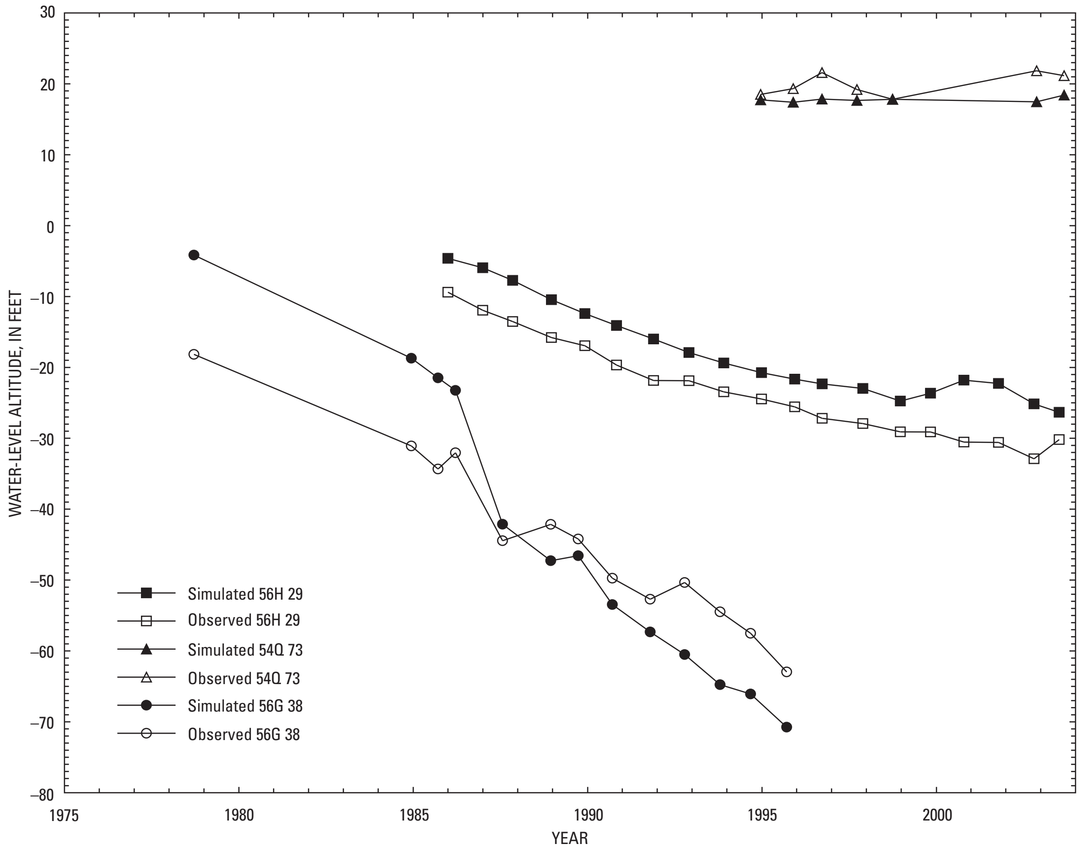

Figure 26. Observed and simulated water levels in wells 56H 29, 54Q 73, and 56G 38 in the Piney Point aquifer of the Virginia Coastal Plain. (Well locations are shown in figure 19.)

Aquia Aquifer

The predevelopment groundwater flow within the Aquia aquifer, as inferred from contours of simulated steady-state water levels (fig. 27a), originated from western up-dip areas and flowed toward the east, where it bifurcated around the low-permeability hydrogeologic units filling the Chesapeake Bay impact crater. The steady-state flow to the northeast and southeast around the Chesapeake Bay impact crater discharged through adjacent hydrogeologic units, primarily the Nanjemoy-Marlboro confining unit. By 2003, groundwater withdrawals had produced a broad area of lower water levels west of the Chesapeake Bay impact crater (fig. 27b). The maximum water-level drawdown simulated in the Aquia aquifer just west of the Chesapeake Bay impact crater is about 135 ft (fig. 27c).

Simulated groundwater withdrawals from the Aquia aquifer in Maryland have produced a well-defined drawdown bowl centered near longitude –76.4 ° in southern Maryland (fig. 27c). A groundwater divide near latitude 38 ° separates groundwater in the Aquia aquifer that flows from northern Virginia into Maryland from groundwater in the remainder of Virginia that flows generally toward the broad area of lower water levels west of the Chesapeake Bay impact crater.

Water-level measurements from Aquia observation wells 51M 18, 57G 2, and 55B 67 (fig. 28) are well-simulated in trend, although the water levels simulated for some observation wells are consistently greater than observed water-level altitudes by up to approximately 15 ft.

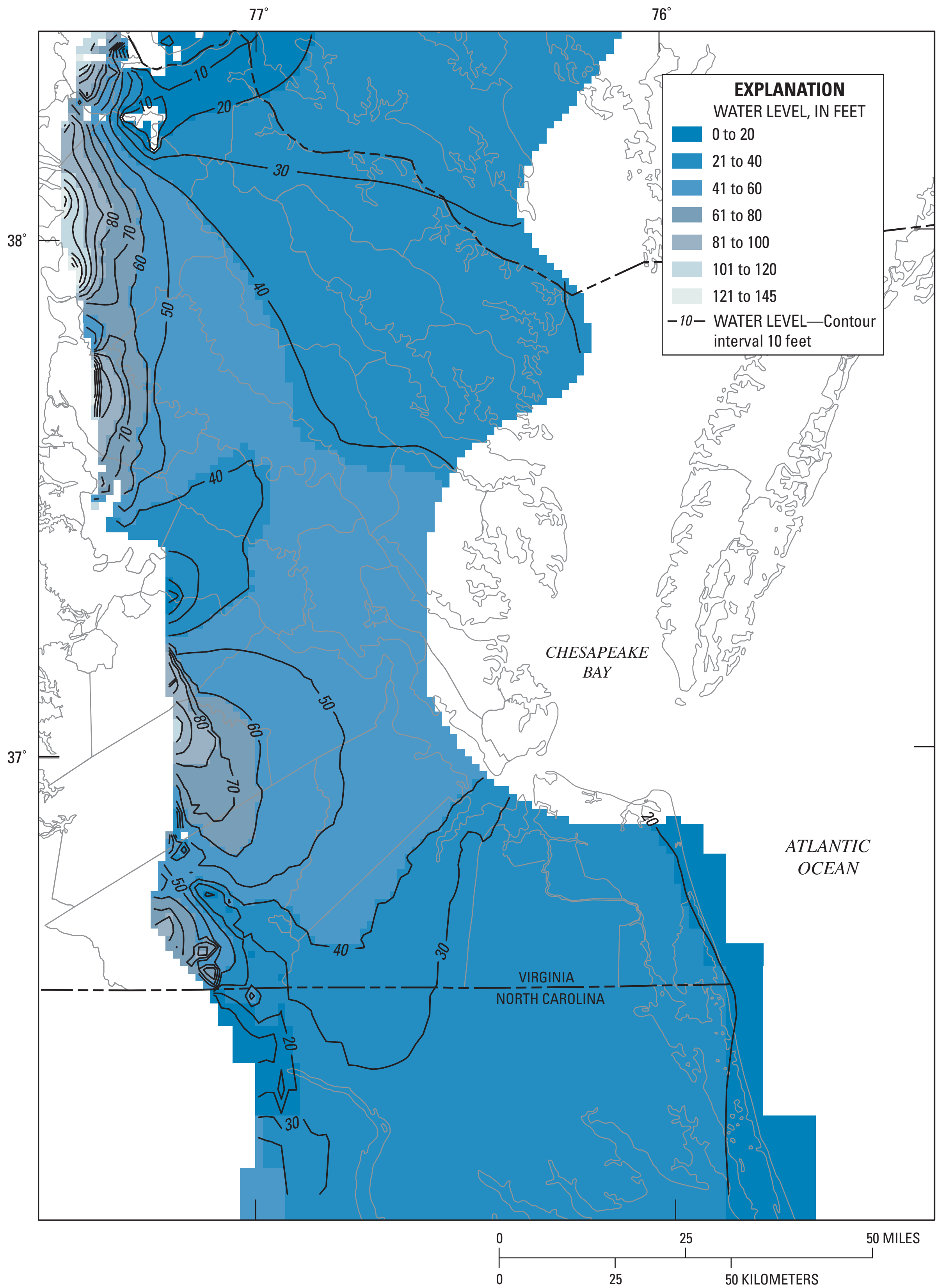

Figure 27a. Simulated predevelopment water levels in the Aquia aquifer of the Virginia Coastal Plain.

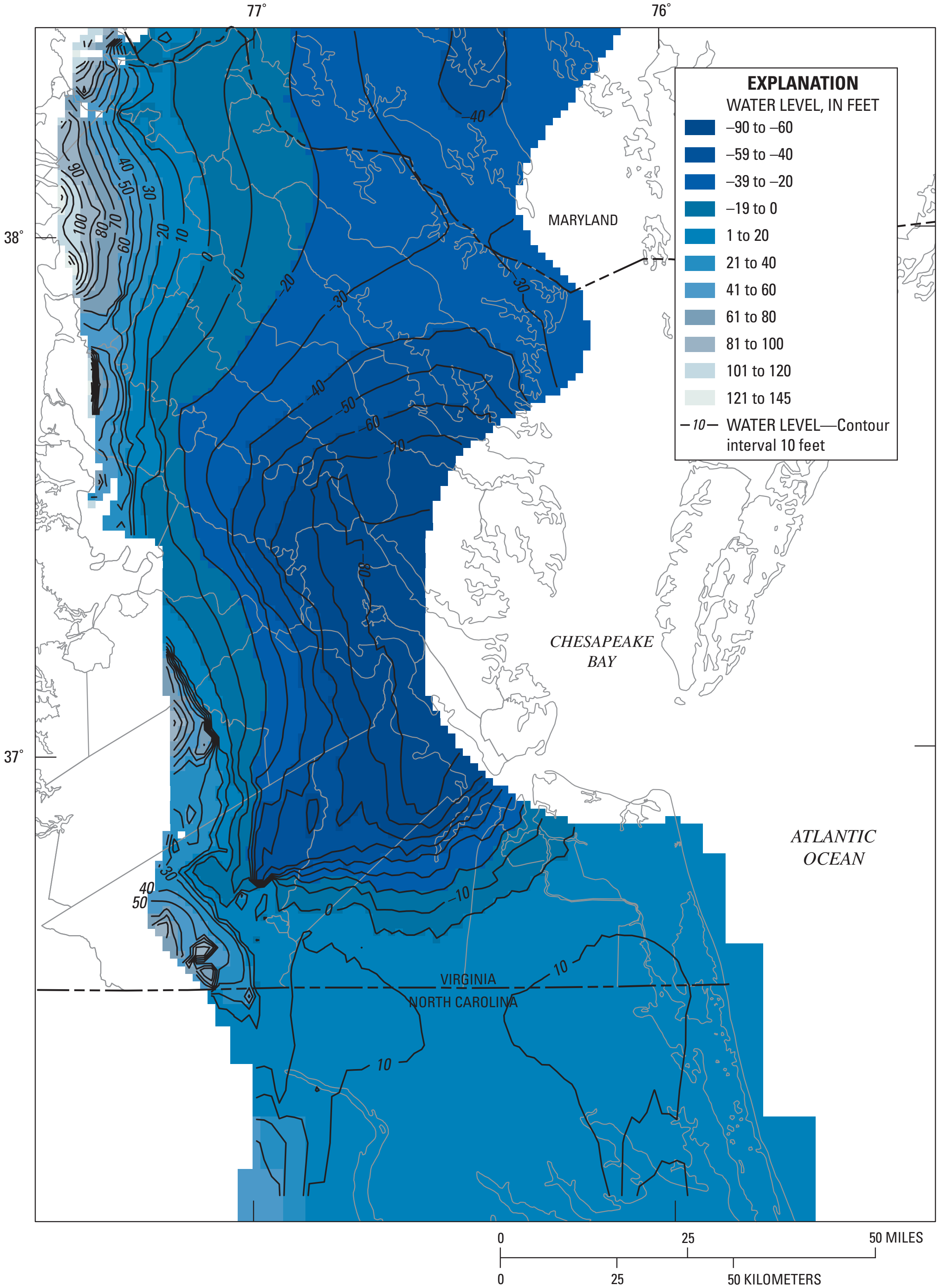

Figure 27b. Simulated 2003 water levels in the Aquia aquifer of the Virginia Coastal Plain.

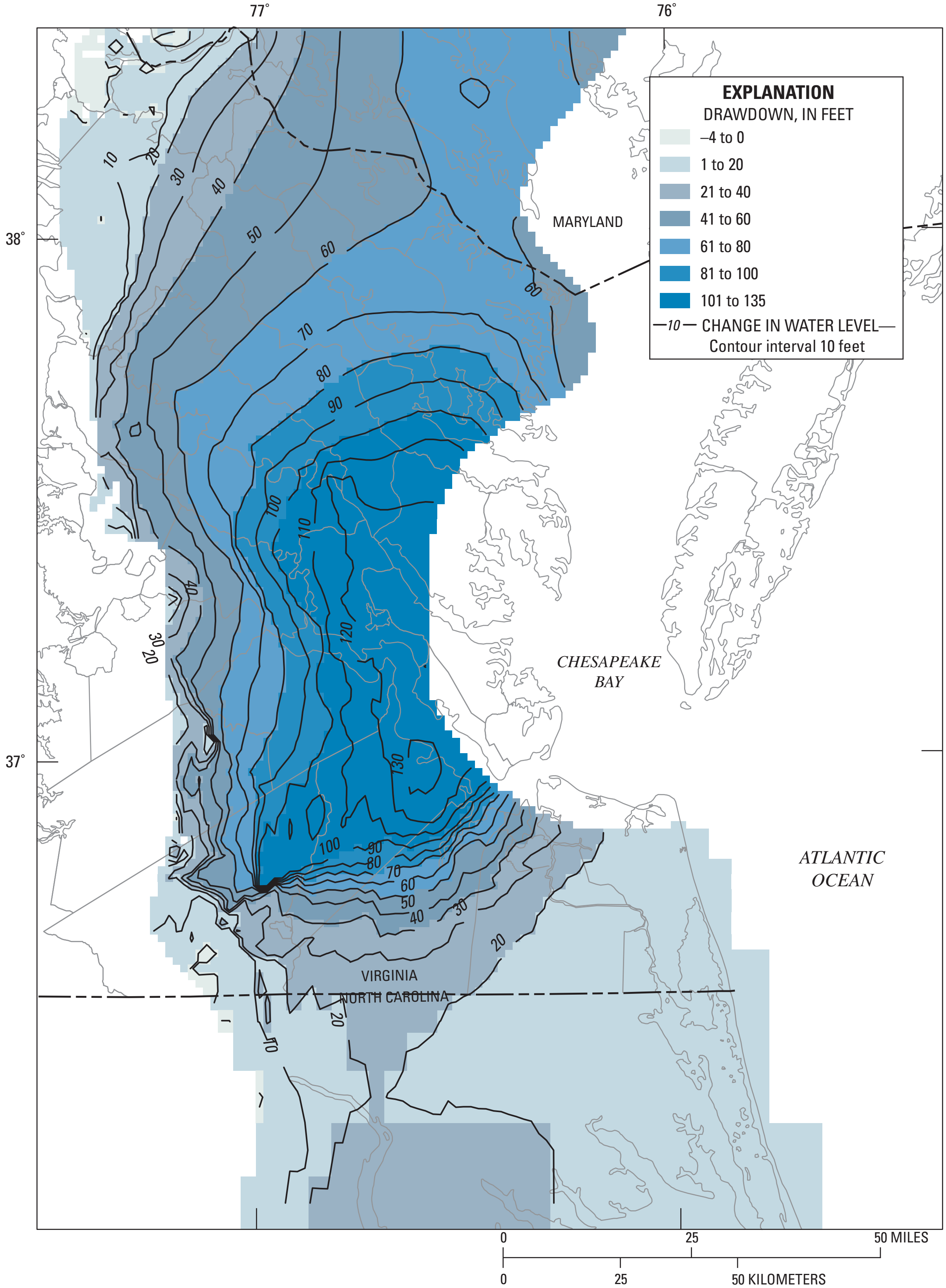

Figure 27c. Simulated drawdown from predevelopment to 2003 in the Aquia aquifer of the Virginia Coastal Plain.

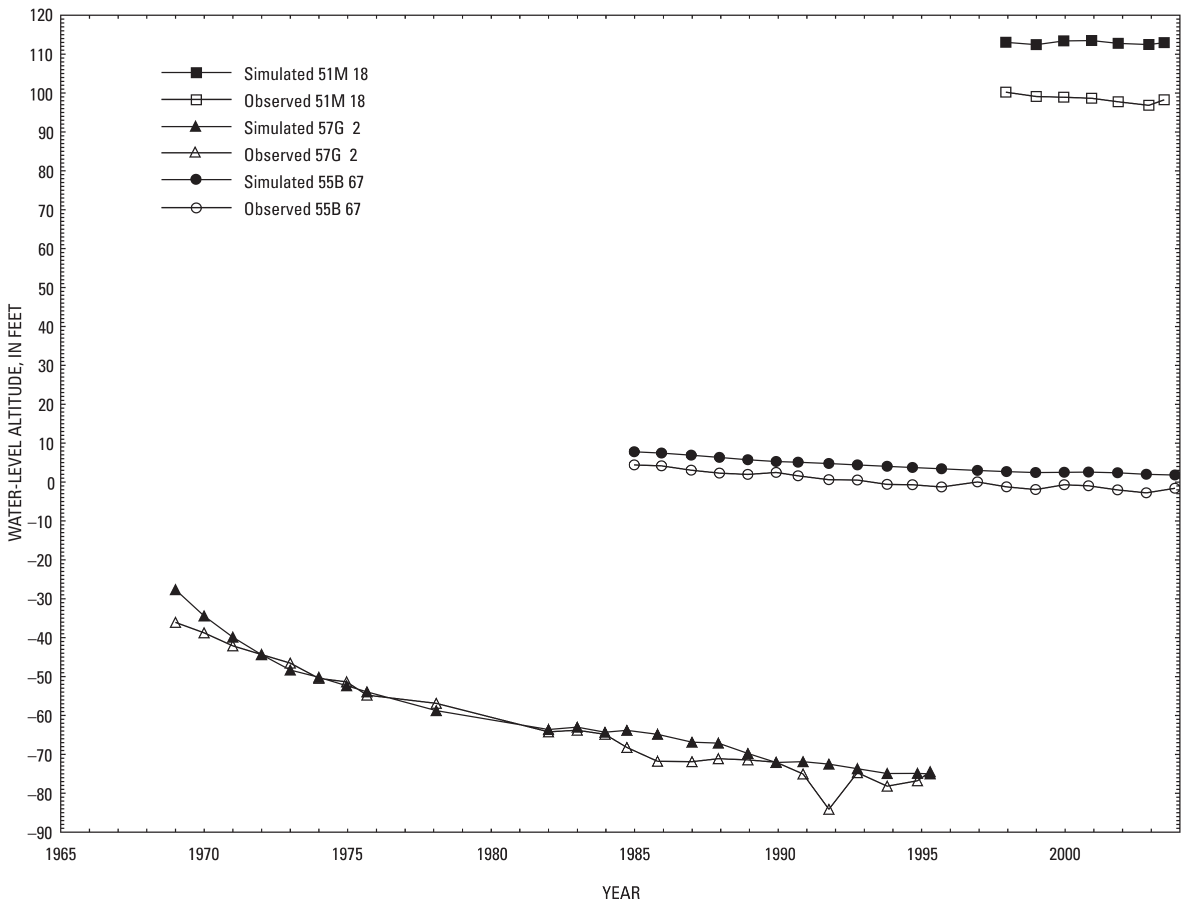

Figure 28. Observed and simulated water levels in wells 51M 18, 57G 2, and 55B 67 in the Aquia aquifer of the Virginia Coastal Plain. (Well locations are shown in figure 19.)

Peedee Aquifer

The Peedee aquifer is present in a limited area in southeast Virginia and extends to the south into North Carolina (figs. 29a, b). Contours of simulated water levels in the Peedee aquifer for the steady-state stress period (fig. 29a) indicate that predevelopment groundwater flowed from west to east through the Peedee aquifer. Lower water-level altitudes simulated for 2003 (fig. 29b) suggest that water levels have declined throughout the aquifer. The relation between simulated water levels and water levels measured in the Peedee aquifer observation well 61B 6 indicates that the model is accurately simulating actual water-level conditions in this aquifer (fig. 30). Because groundwater withdrawals from the Peedee aquifer have not been reported and unreported domestic withdrawals are considered not to occur (Pope and others, 2007), no groundwater withdrawals from the Peedee aquifer were specified in the groundwater model. The simulated water-level decline in the Peedee aquifer, therefore, likely results from flow to hydraulically connected aquifers in North Carolina.

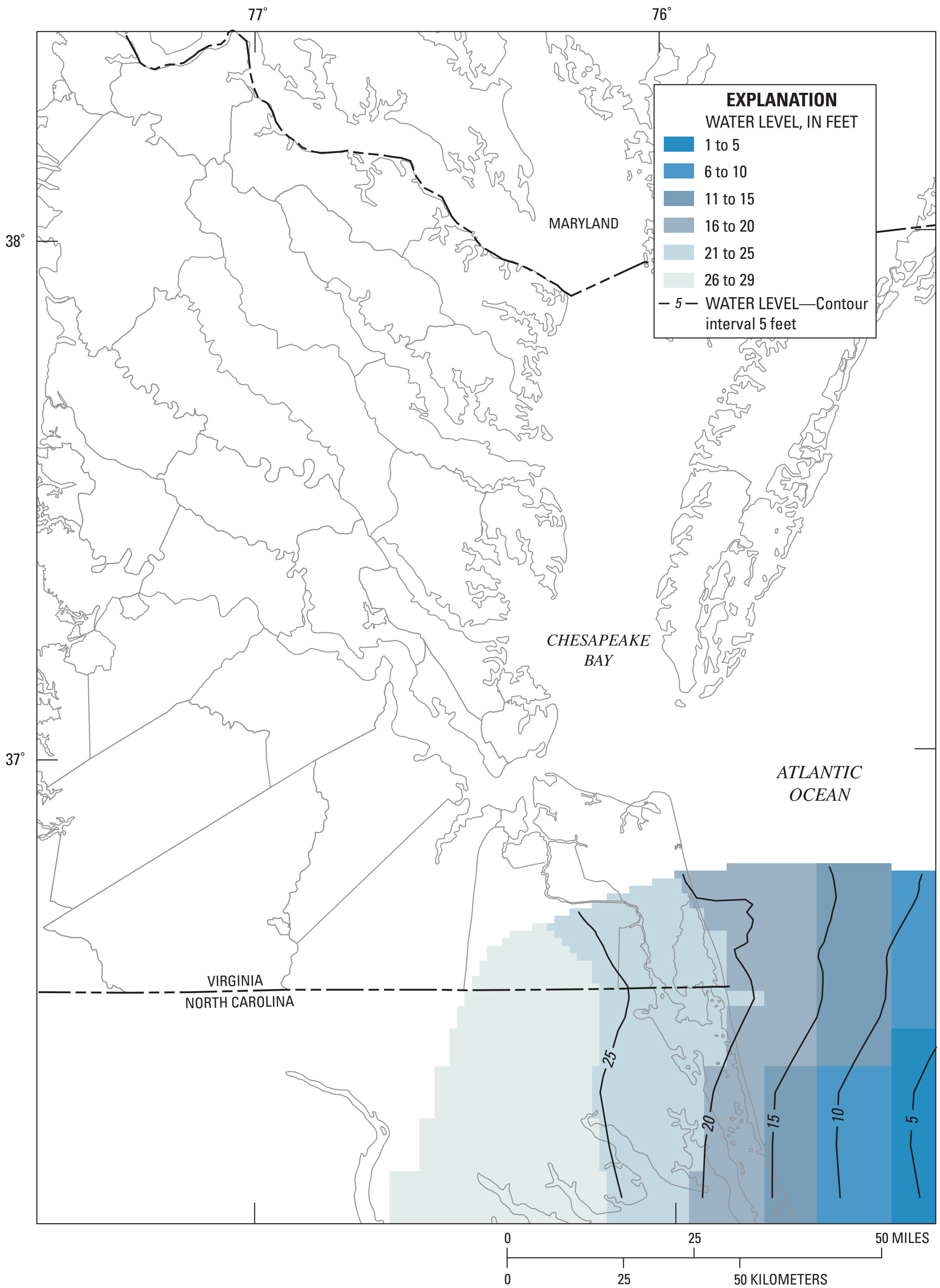

Figure 29a. Simulated predevelopment water levels in the Peedee aquifer of the Virginia Coastal Plain.

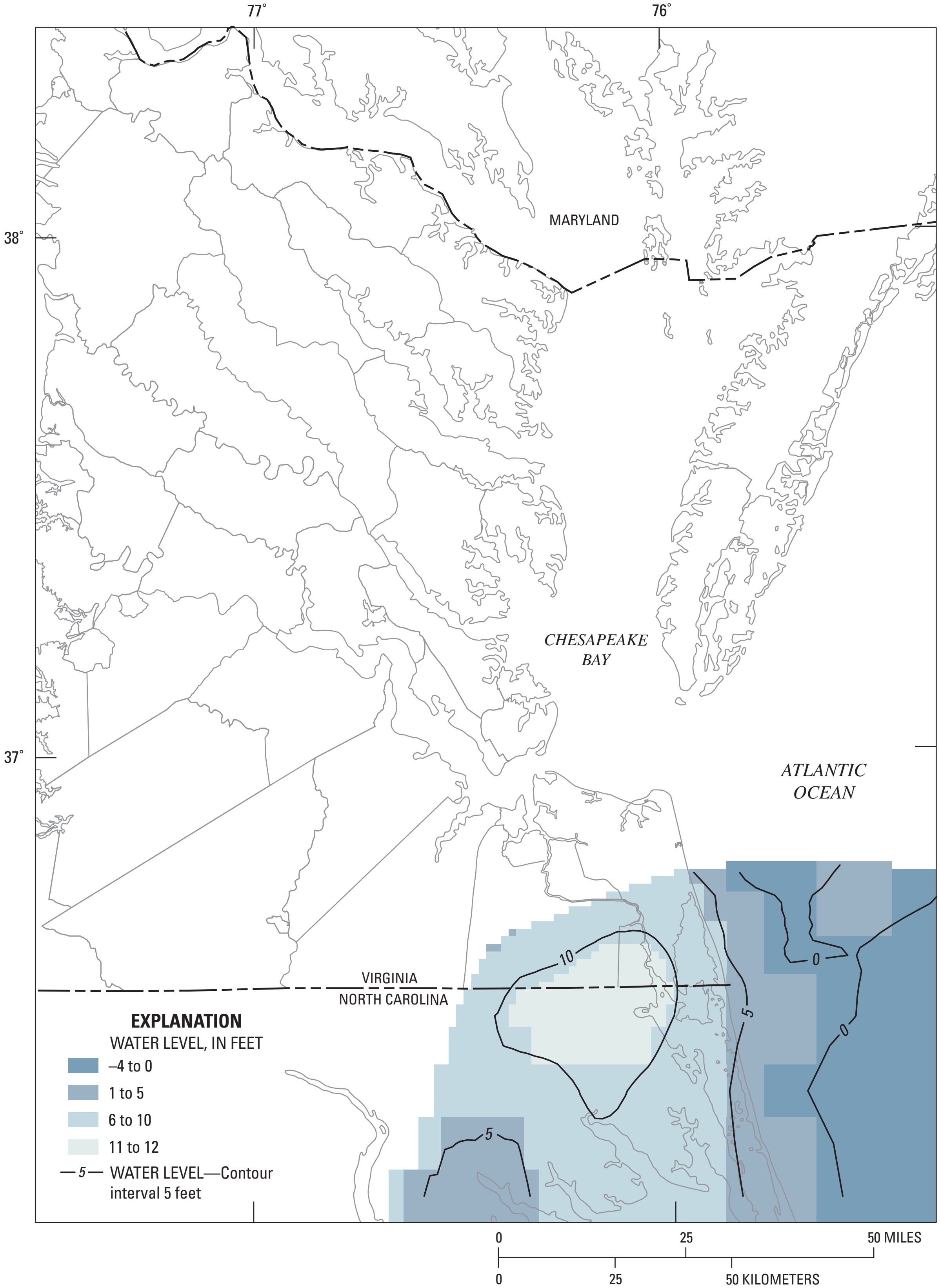

Figure 29b. Simulated 2003 water levels in the Peedee aquifer of the Virginia Coastal Plain.

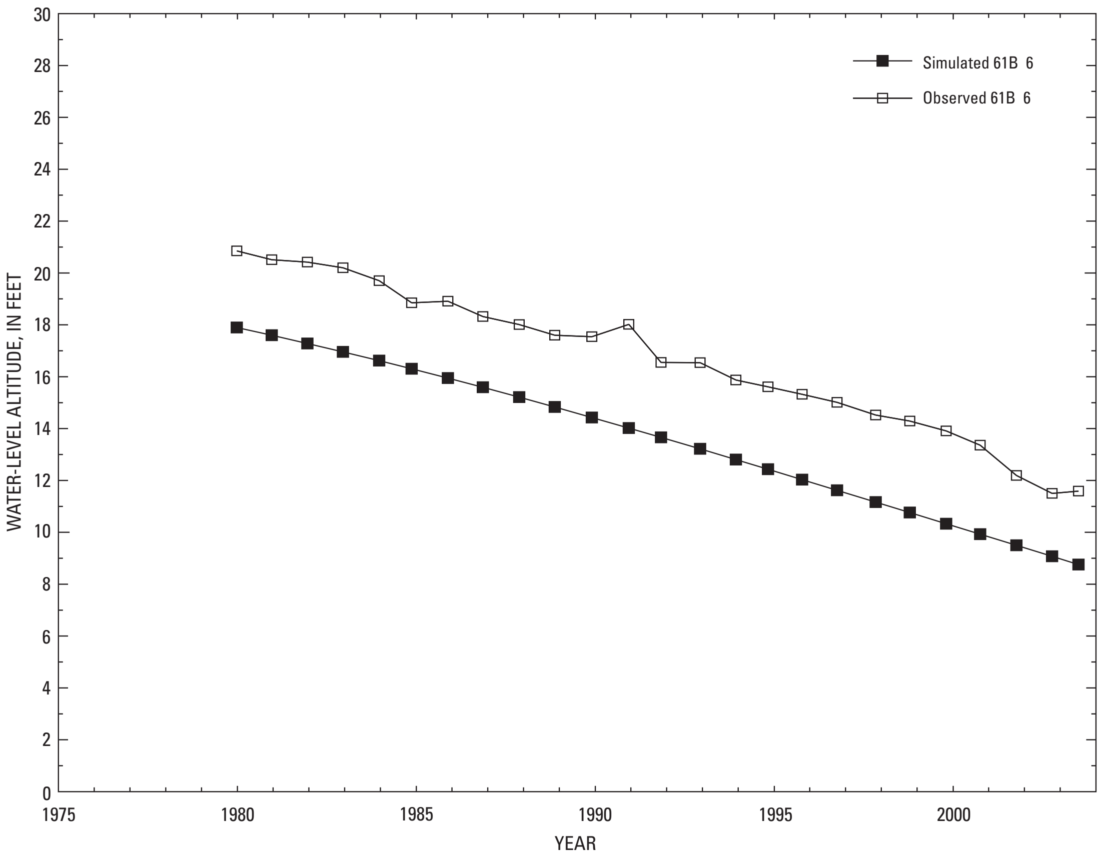

Figure 30. Observed and simulated water levels in well 61B 6 in the Peedee aquifer of the Virginia Coastal Plain. (Well location is shown in figure 19.)

Virginia Beach Aquifer

The Virginia Beach aquifer is present in southeast Virginia, where it extends offshore beneath the continental shelf and into North Carolina (figs. 31a, b). Contours of the simulated water levels in the Virginia Beach aquifer for the steady-state stress period (fig. 31a) indicate that predevelopment groundwater flowed from western up-dip areas through the Virginia Beach aquifer toward the east. Reported and self-supplied withdrawals from the Virginia Beach aquifer in southeast Virginia caused simulated water levels to decline by the end of 2003, resulting in a relatively flat simulated potentiometric surface in the down-dip area of the aquifer (fig. 31b). Because water-level measurements from observation wells screened in the Virginia Beach aquifer were not available for model calibration or evaluation, the accuracy of these simulated water levels is unknown. A superposition analysis indicates that simulated domestic withdrawals may account for approximately 1 ft of drawdown in the Virginia Beach aquifer.

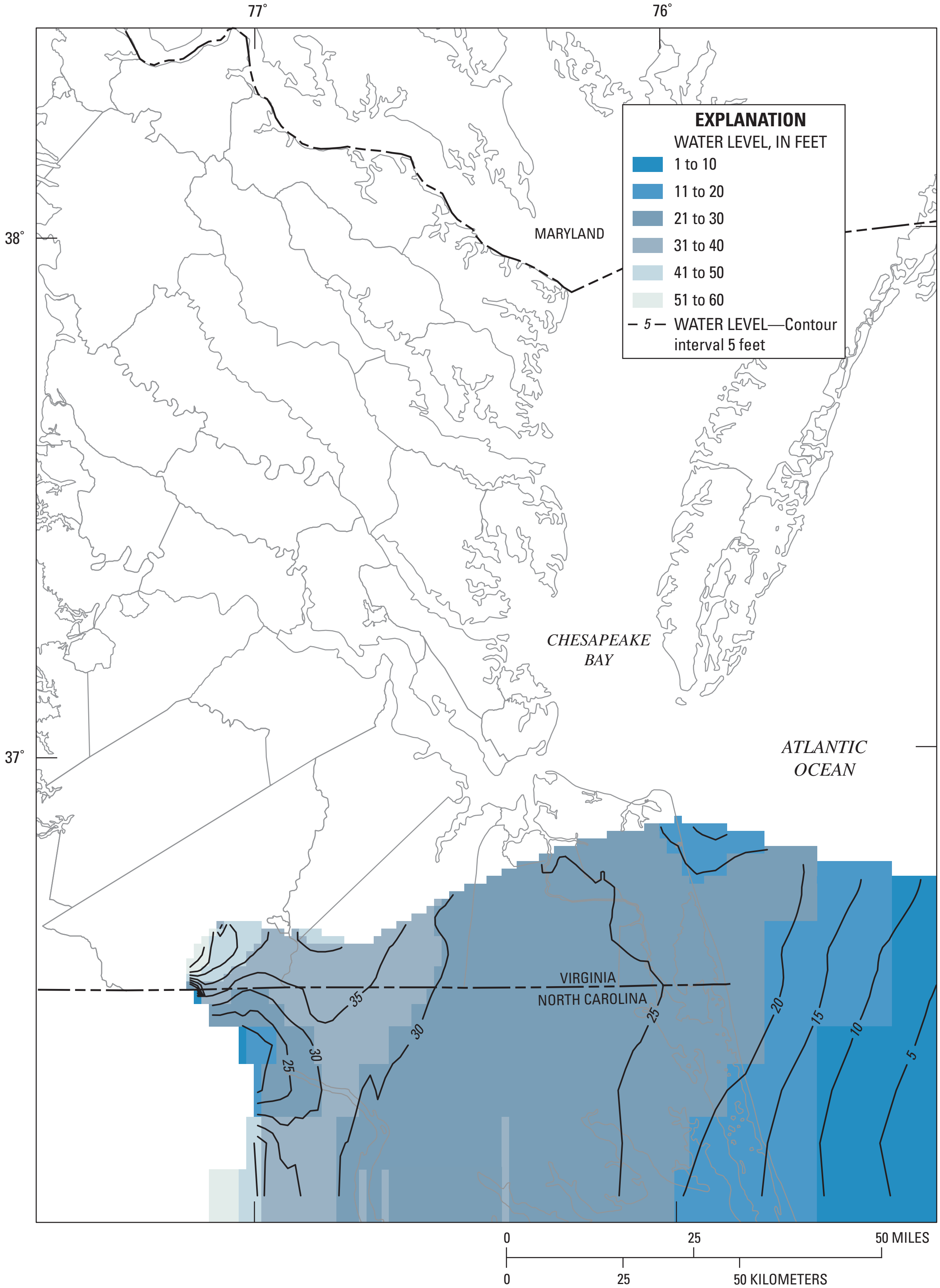

Figure 31a. Simulated predevelopment water levels in the Virginia Beach aquifer of the Virginia Coastal Plain.

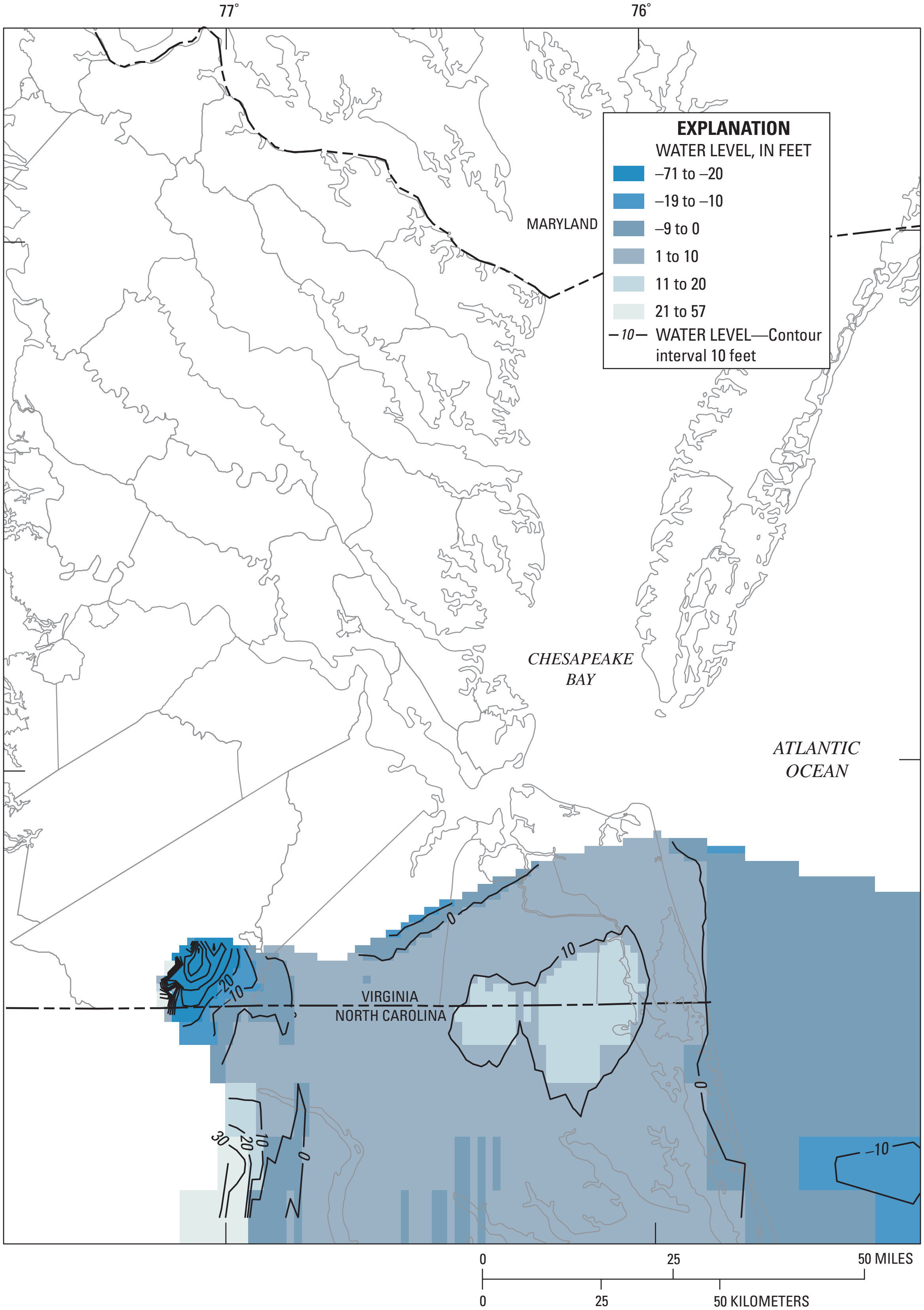

Figure 31b. Simulated 2003 water levels in the Virginia Beach aquifer of the Virginia Coastal Plain.

Potomac Aquifer

The top of the Potomac aquifer is at a shallow depth near the Fall Line, where it has good hydraulic connection through the surficial aquifer to the water table and probably receives groundwater recharge (fig. 4a–d). The contours of simulated predevelopment water levels at the top of the Potomac aquifer (fig. 32a) suggest that groundwater-flow directions were influenced by the proximity of sea level along the James River near the Fall Line. Water-level contours east of the Fall Line in the northern and southern Coastal Plain indicate generally easterly-directed groundwater flow, which bifurcated to flow northeasterly and southeasterly around the Chesapeake Bay impact crater. Between these areas, east of Richmond near latitude 37.3°N, predevelopment groundwater flow from the north and south converged and discharged to the James River. Immediately northeast, within a broad area of relatively small water-level gradient, a groundwater divide near 37.4°N, –76.6°W separated this area of convergent flow from the area that flowed toward the north side of the Chesapeake Bay impact crater. Concentric contours near 37°N, –76.85°W (fig. 32a) delineate where the Potomac aquifer is near the land surface and proximal to the Nottoway River, which consequently largely controls water levels simulated at the top of the Potomac aquifer in that area.

Industrial and municipal groundwater withdrawals, which began to increase during the 1940s, have resulted in substantial decline of water levels in the Potomac aquifer and the formation of two major "cones of depression" in Virginia centered near Franklin and West Point (fig. 32b). At the end of the simulation in December 2003, the maximum drawdown simulated at the top of the Potomac aquifer was 235 ft near Franklin and 232 ft near West Point (fig. 32c). Regional groundwater-flow directions within the Potomac aquifer have changed substantially from their predevelopment pattern as a result of these declines. Groundwater within the Potomac aquifer generally flows toward one of the major withdrawal centers at either Franklin or West Point, although it may be intercepted by one of many Potomac wells elsewhere in the Coastal Plain. The water-level gradients near the Atlantic coast have reversed from their predevelopment direction, which has increased the potential for landward transport of saltwater toward production wells. As of 2006, consistent trends of increased chloride concentration have not been observed in wells, however.

Substantial groundwater withdrawals from the Potapsco aquifer in Maryland, which correlates by age, depth, and lithology with the Potomac aquifer in Virginia, have generated an area of substantial drawdown north of the model domain near longitude –77° in Maryland. Because these withdrawals cannot be explicitly simulated within the model domain, their effect on groundwater flow out of northern Virginia was simulated with a specified-flux boundary, which was discussed in the preceding section entitled "Transient Underflow to Maryland." This flux has caused simulated groundwater flow in northern Virginia to be redirected under the Potomac River and north toward the Potapsco-withdrawal area in southern Maryland.

Observed water levels from 37 Potomac aquifer observation wells (fig. 33) are shown with their simulated equivalents (figs. 34–39) at various locations throughout the Virginia Coastal Plain. In general, simulated water levels agree within several feet of observed water levels in the Potomac aquifer, with few differences in excess of 10 ft. One exception is observation well 58F 1 (fig. 37), located in James City County southeast of Williamsburg (fig. 33). Four observations beginning in 1998 are more than 10 ft lower than their simulated equivalents, and the observed water level in year 2002 is 41 ft lower than its simulated equivalent. These discrepancies may be because of unreported groundwater withdrawals that were not simulated in the model. Simulated equivalents to water levels in well 52J 34 (fig. 36), located in eastern Henrico County, are increasingly higher than the rising water levels observed after 1997. The observed rising water levels are likely because of decreased groundwater withdrawals in this area. Although a relatively low horizontal hydraulic conductivity (on the order of 10 ft/d) in this area yields a good overall fit to observed water levels, lithologies (such as a channel-fill facies) with higher horizontal hydraulic conductivity may be present locally and influence the observation-well response.

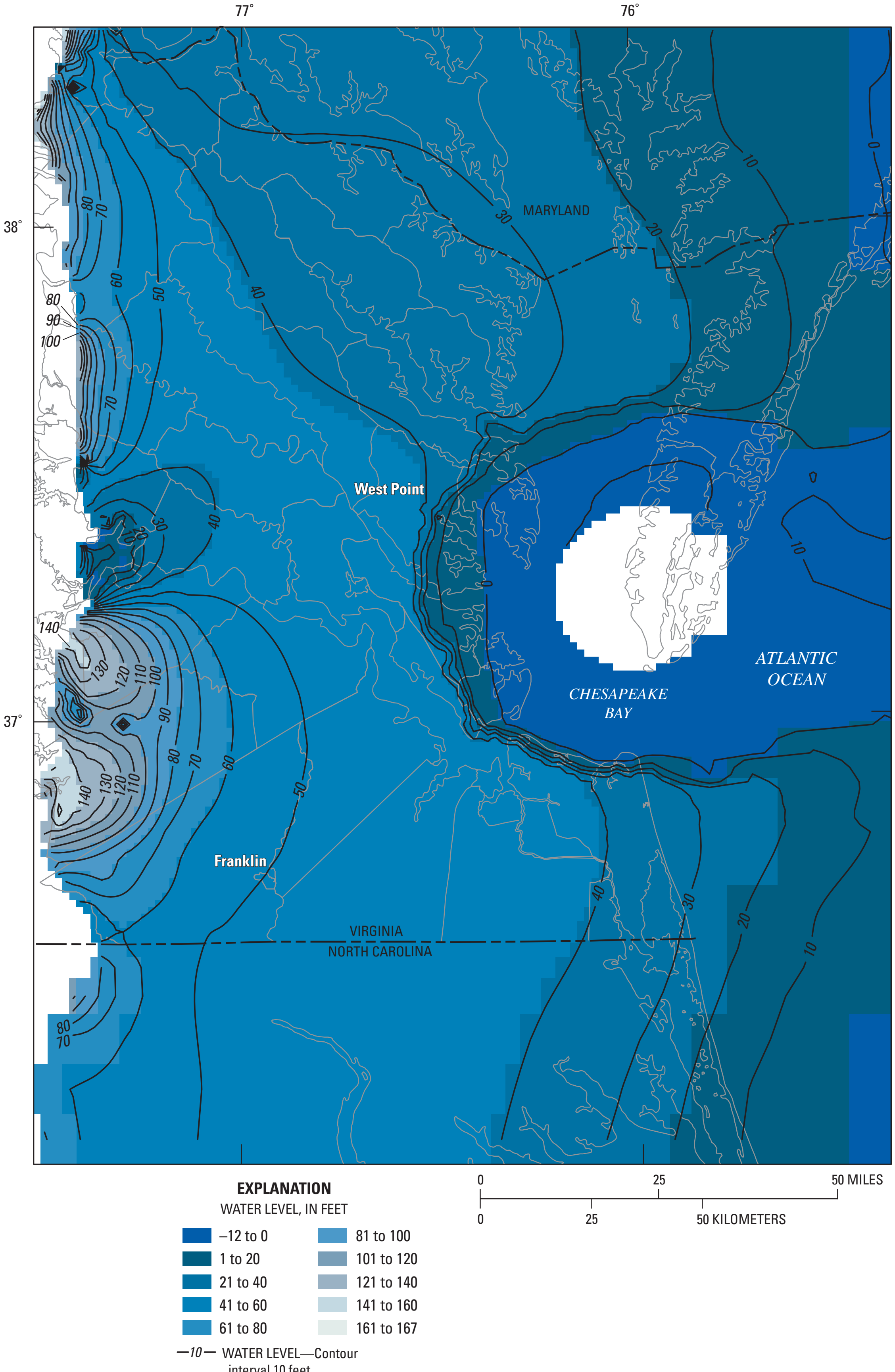

Figure 32a. Simulated predevelopment water levels in the Potomac aquifer of the Virginia Coastal Plain.

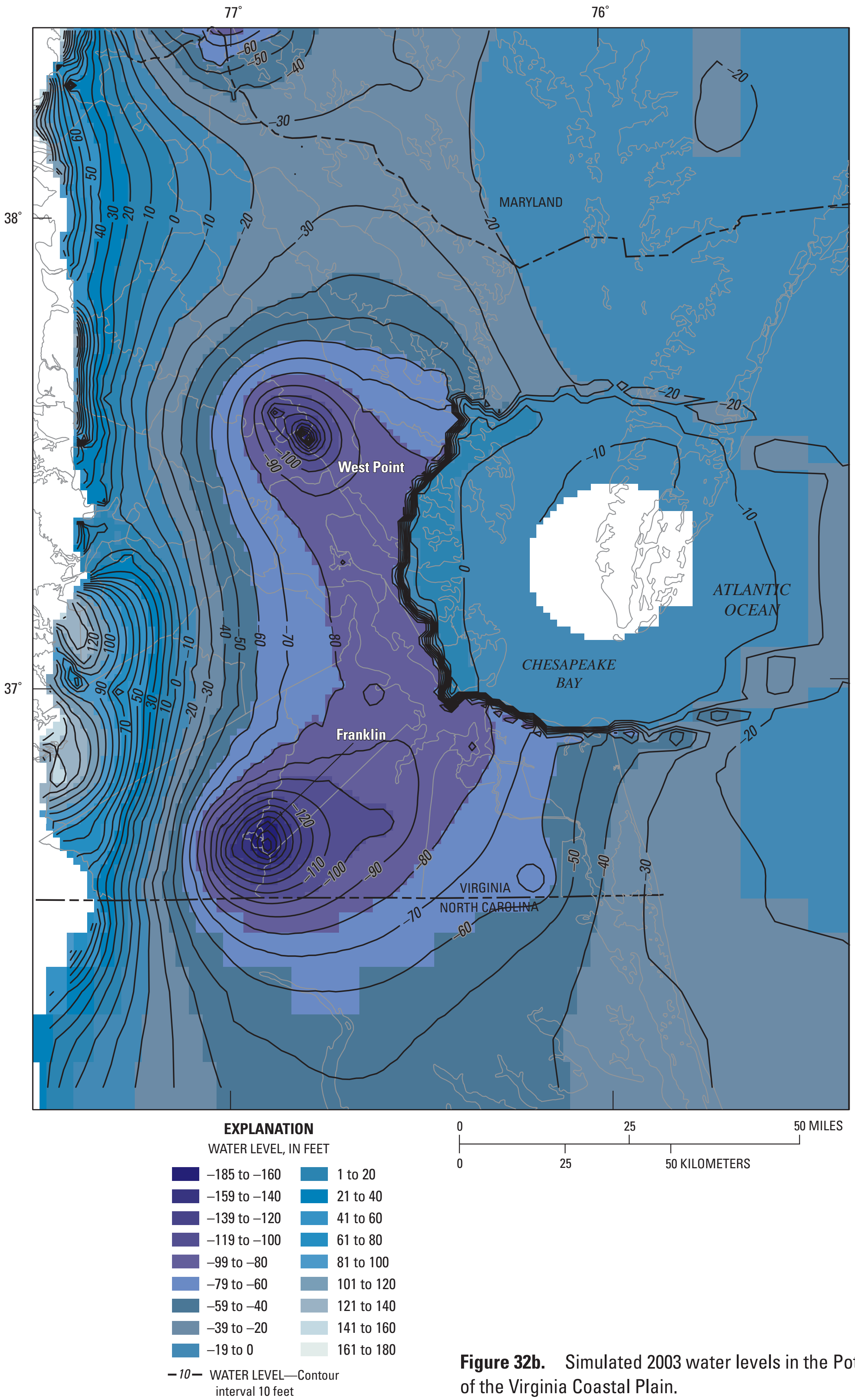

Figure 32b. Simulated 2003 water levels in the Potomac aquifer of the Virginia Coastal Plain.

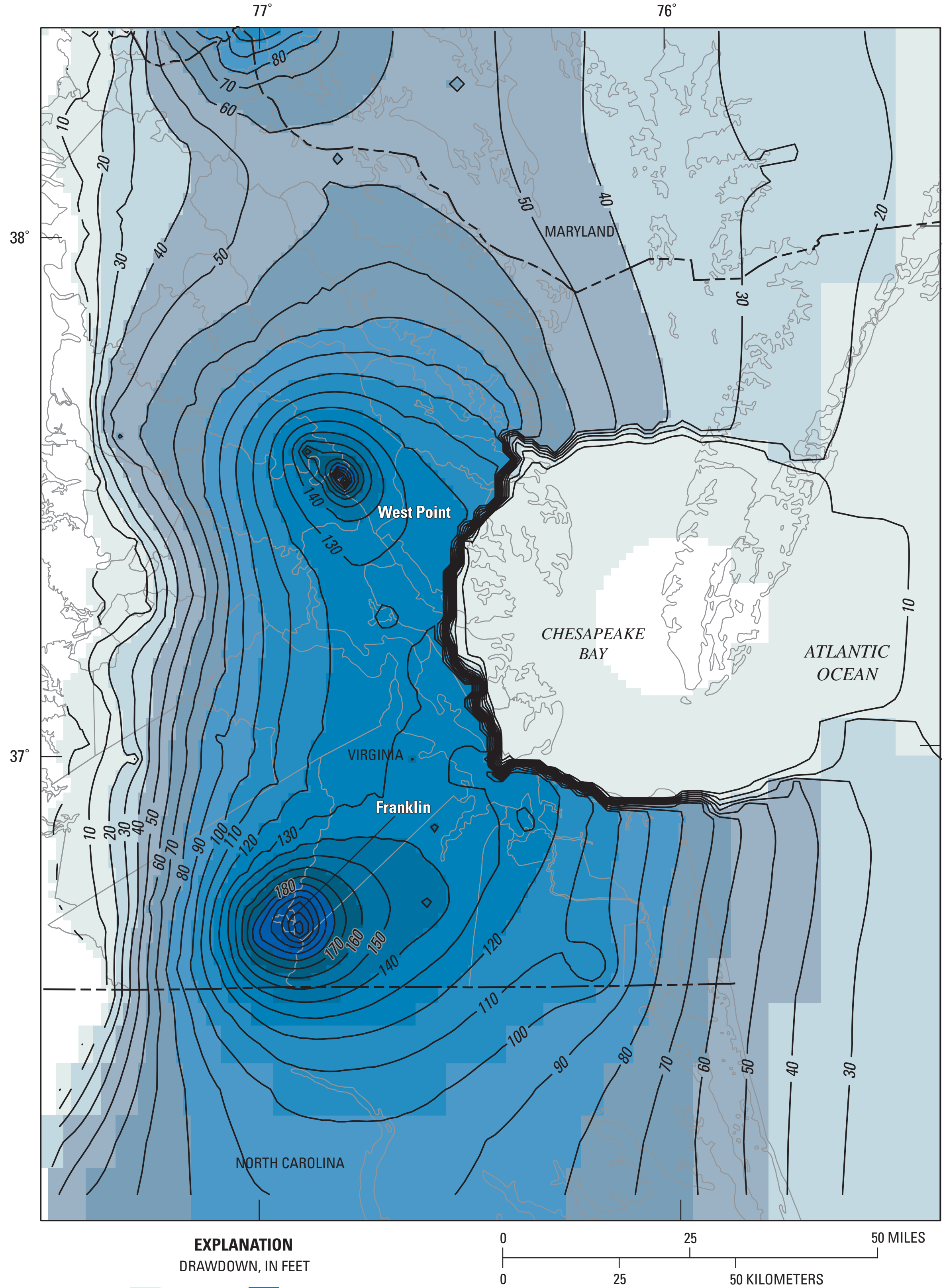

EXPLANATION

DRAWDOWN, IN FEET

- –2 to 20
- 21 to 40
- 41 to 60
- 61 to 80
- 81 to 100
- 101 to 120
- 121 to 140
- 141 to 160
- 161 to 180
- 181 to 200
- 201 to 240

— *10* — CHANGE IN WATER LEVEL—Contour interval 10 feet

Figure 32c. Simulated drawdown from predevelopment to 2003 in the Potomac aquifer of the Virginia Coastal Plain.

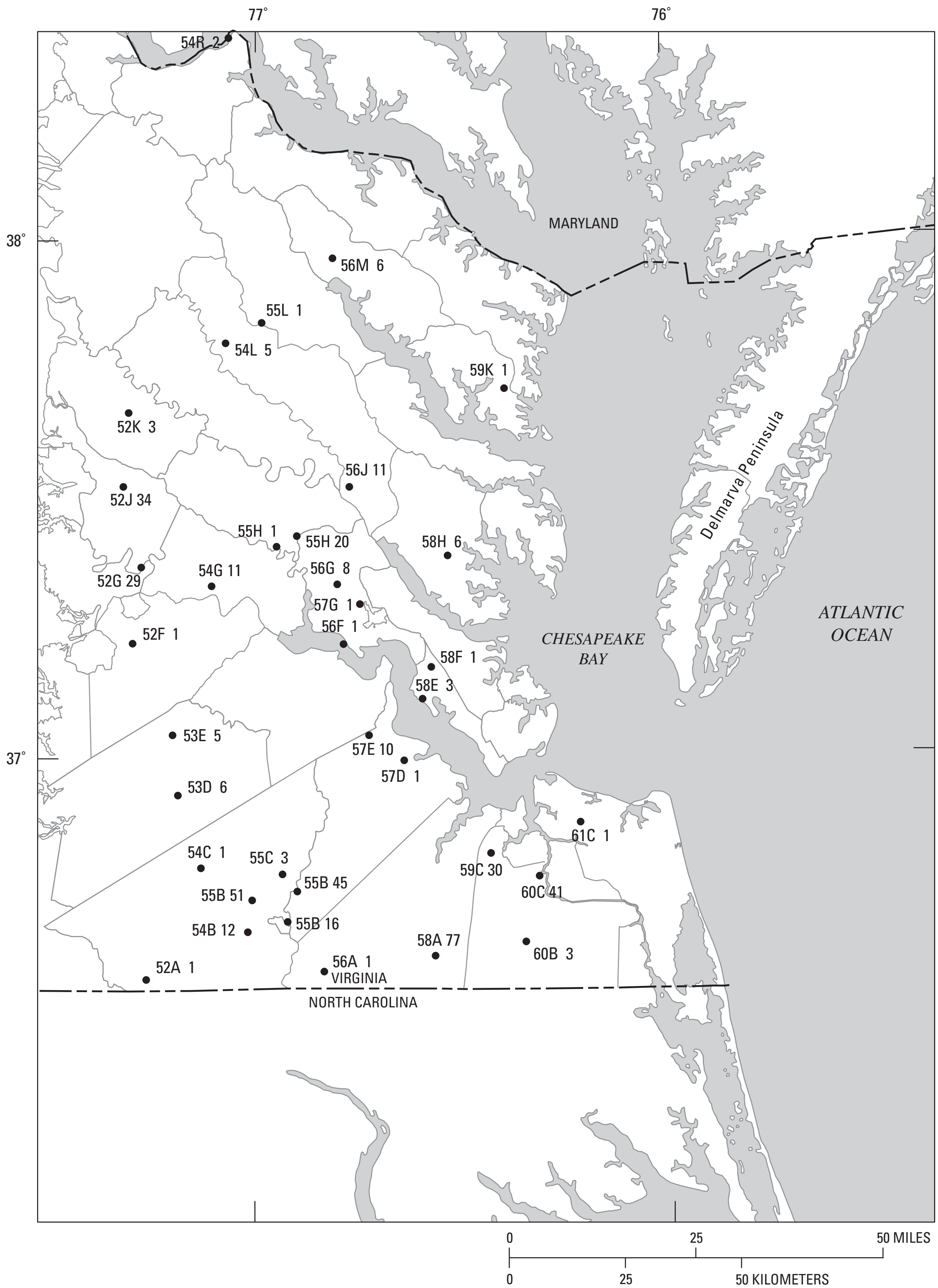

Figure 33. Locations of observation wells screened in the Potomac aquifer for hydrographs depicted in figures 34–39.

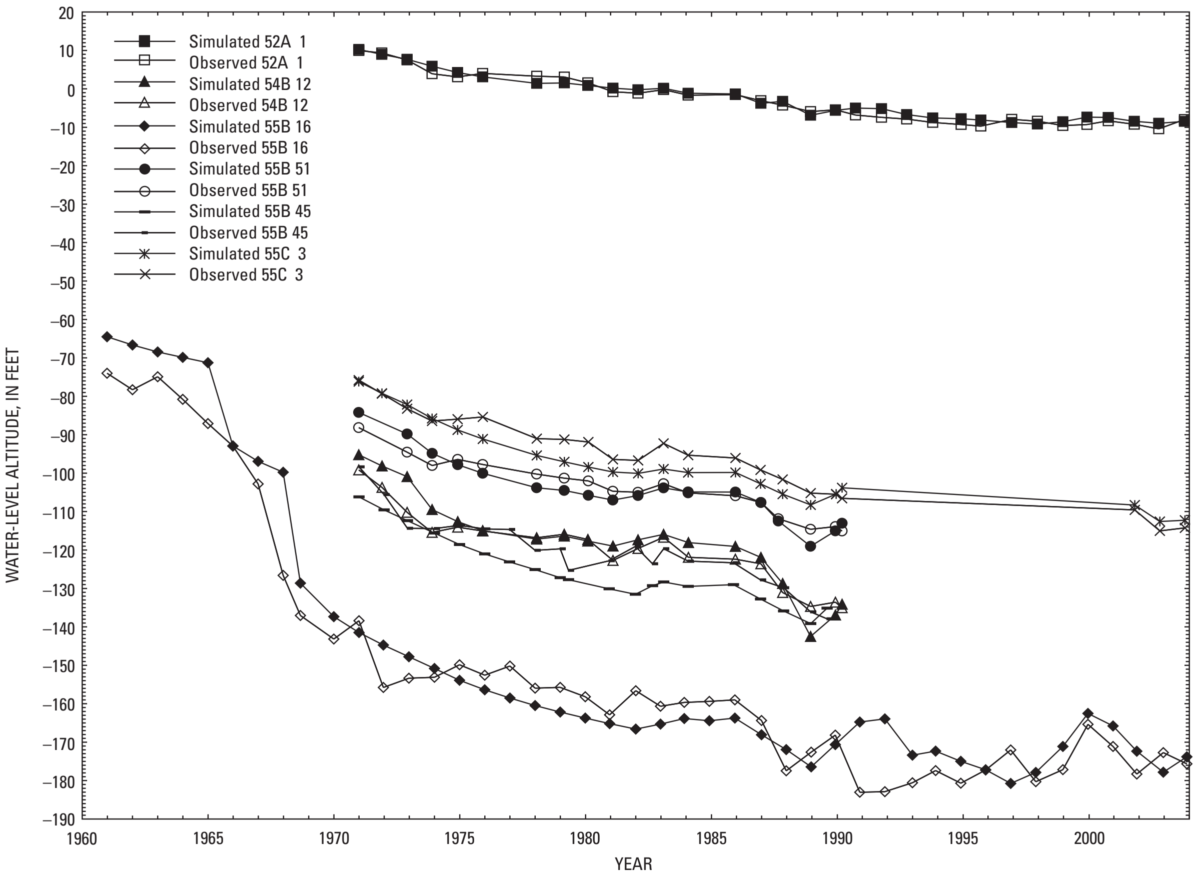

Figure 34. Observed and simulated water levels of selected wells screened in the Potomac aquifer in the southwest model area. (Locations of wells are shown in figure 33.)

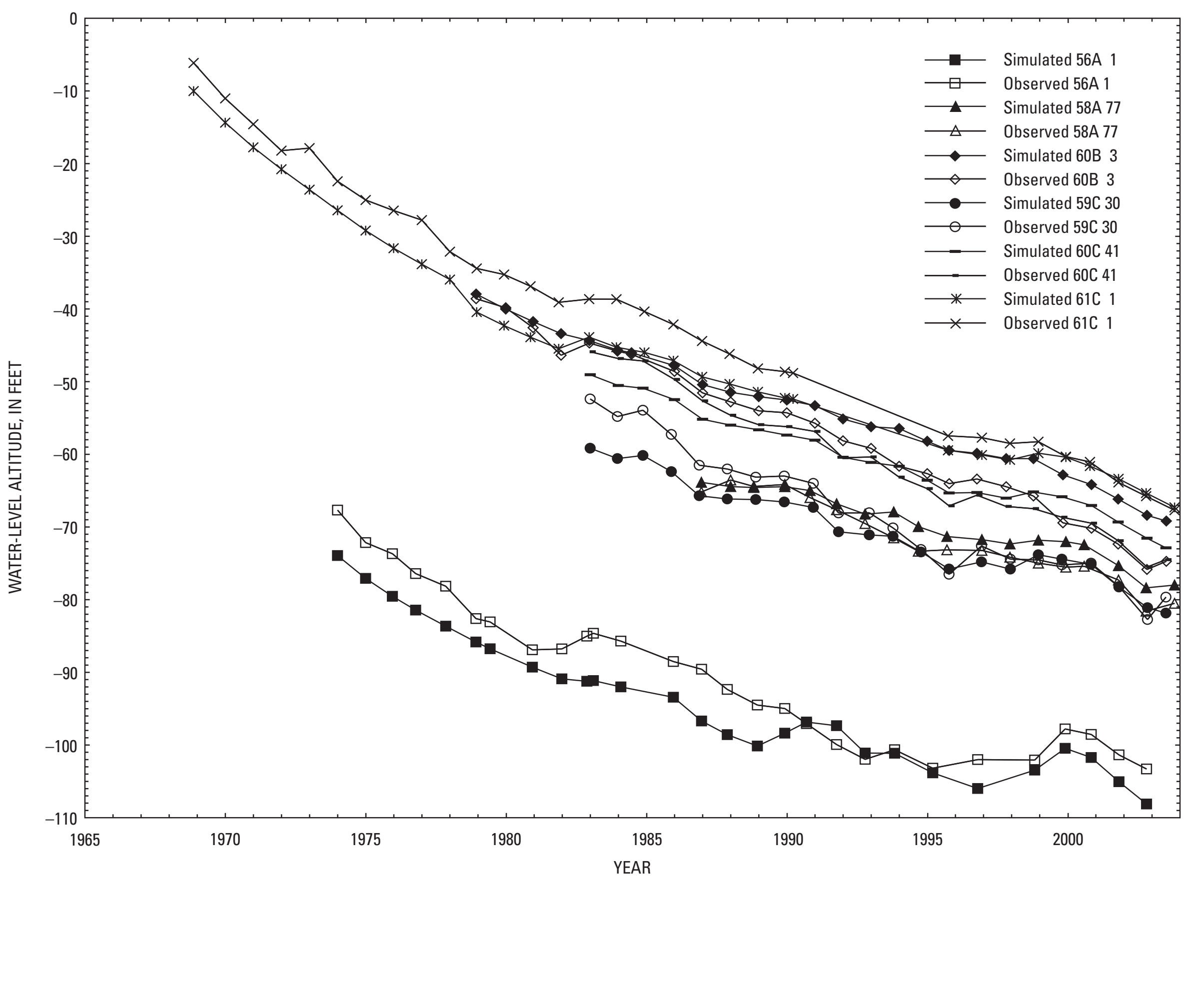

Figure 35. Observed and simulated water levels of selected wells screened in the Potomac aquifer in the southeast model area. (Locations of wells are shown in figure 33.)

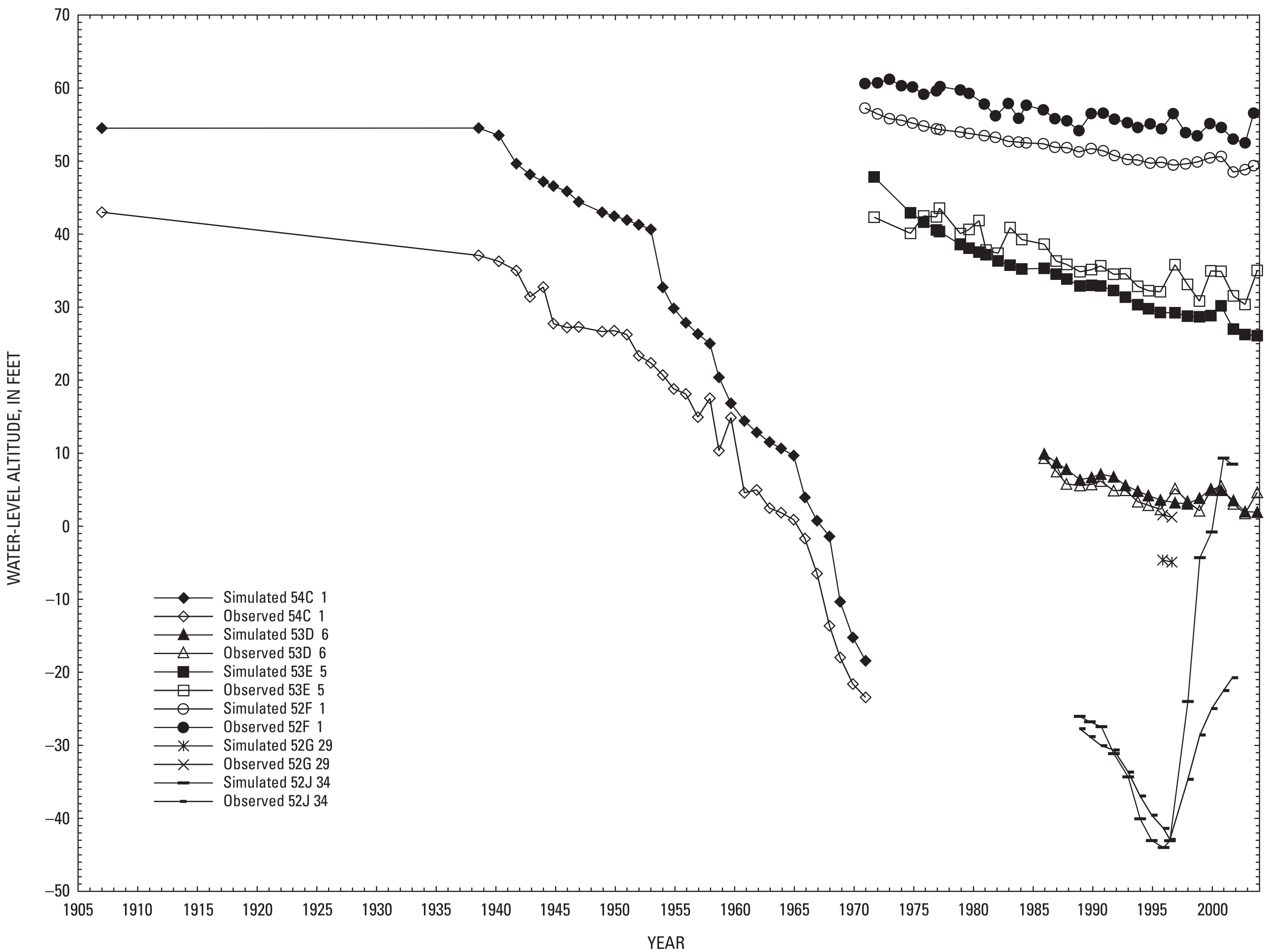

Figure 36. Observed and simulated water levels of selected wells screened in the Potomac aquifer in the western model area. (Locations of wells are shown in figure 33.)

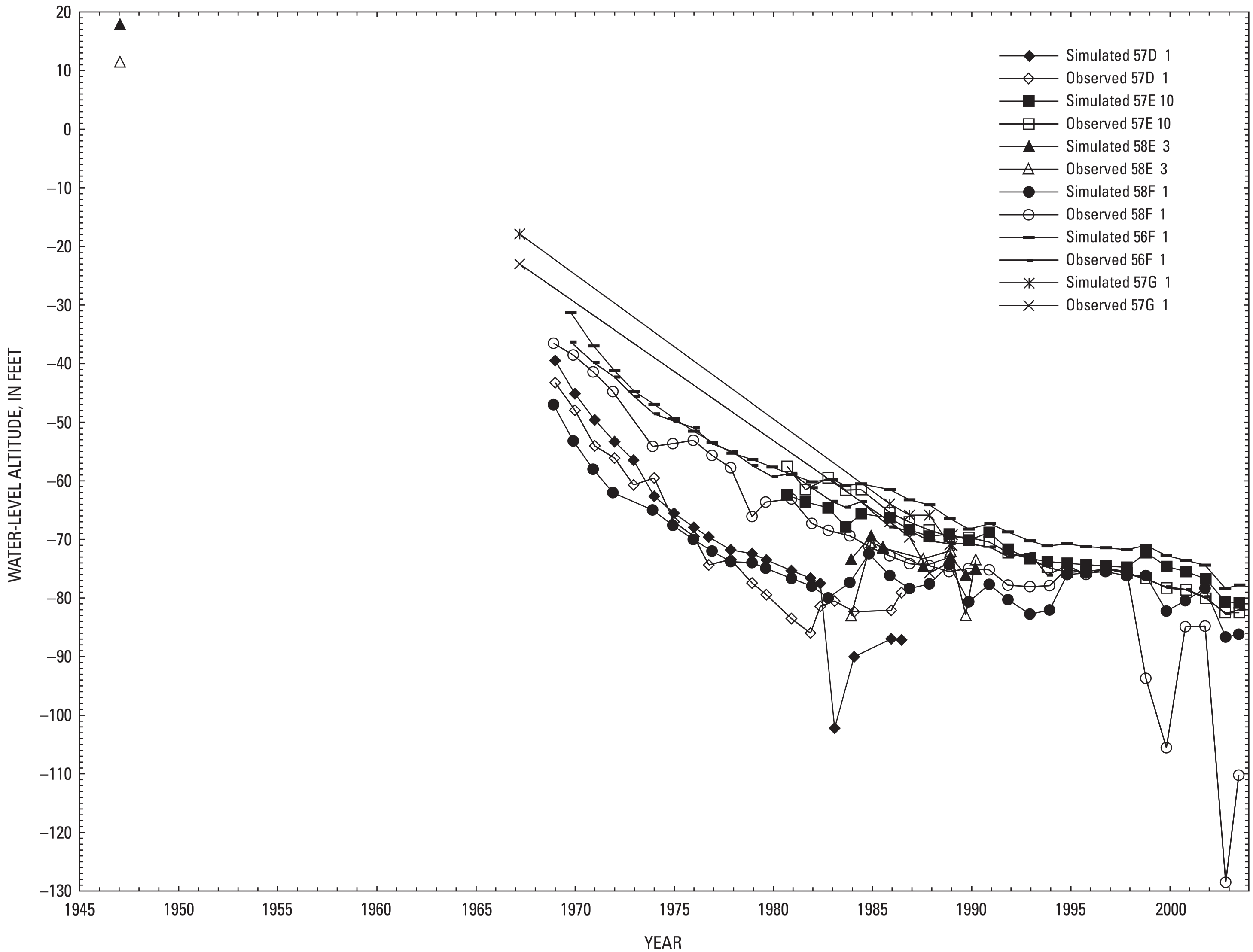

Figure 37. Observed and simulated water levels of selected wells screened in the Potomac aquifer in the eastern model area. (Locations of wells are shown in figure 33.)

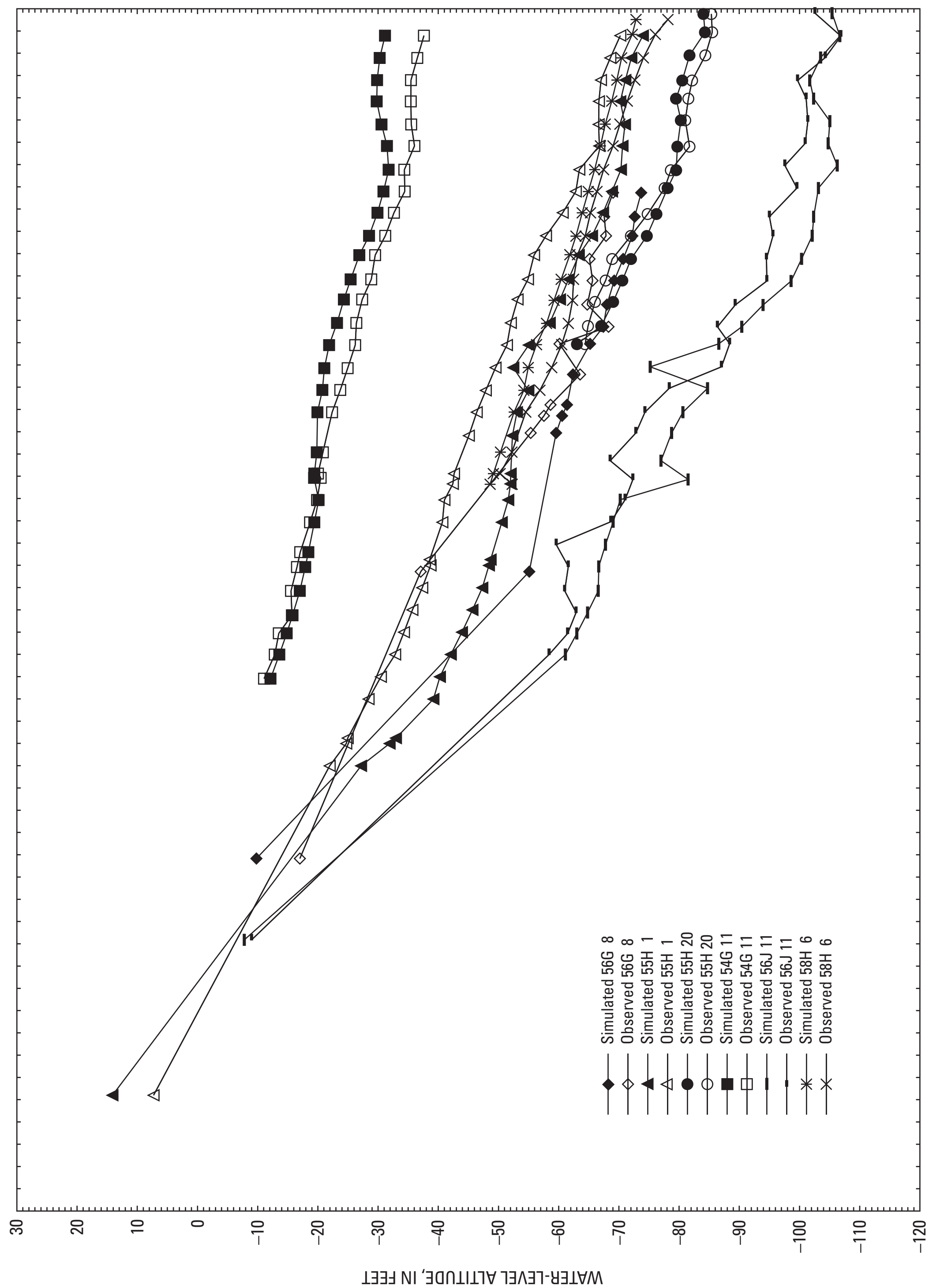

Figure 38. Observed and simulated water levels of selected wells screened in the Potomac aquifer in the central model area. (Locations of wells are shown in figure 33.)

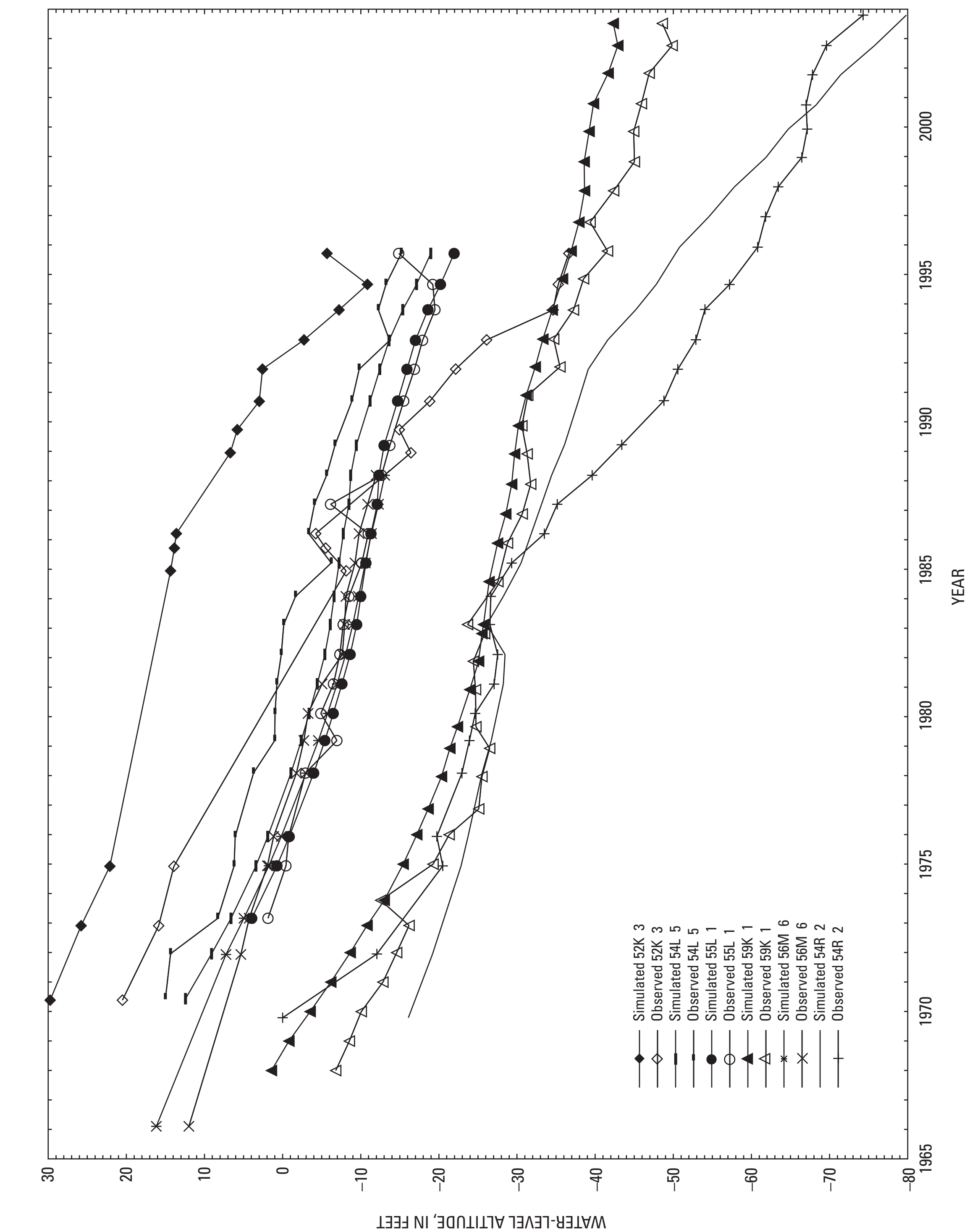

Figure 39. Observed and simulated water levels of selected wells screened in the Potomac aquifer in the northern model area. (Locations of wells are shown in figure 33.)

Water Budget

Recharge and evapotranspiration are large compared to other steady-state budget components and the pumpage and storage components that appear in the transient stress periods. Predevelopment water-budget components for the model domain (table 7) are discussed in the following section on the steady-state water budget. Water-budget components for the portion of the model in Virginia (table 8) were calculated with the program ZONEBUDGET (Harbaugh, 1990) for the steady-state and two transient stress periods.

Table 7. Steady-state water-budget components for model domain.

Component	Volume (cubic feet per day)	Volume (million gallons per day)	Percent of total
Inflows			
Recharge to water table	1.47 x10^{9}	11,013	97.17
Simulated rivers above sea level	3.85 x10^{7}	288	2.54
Tidal rivers	2.30 x10^{6}	17	.15
Underflow from Piedmont	2.16 x10^{6}	16	.14
TOTALS	1.51 x10^{9}	11,334	100.00
Outflows			
Evapotranspiration and non-simulated streams	1.34 x10^{9}	10,048	88.66
Simulated rivers above sea level	1.27 x10^{8}	953	8.40
Tidal rivers, Chesapeake Bay, ocean	4.45 x10^{7}	333	2.94
TOTALS	1.51 x10^{9}	11,334	100.00

Table 8. Steady-state and transient water-budget components for Virginia sub-domain.

Component	Predevelopment volume (million gallons per day)	2001 volume (million gallons per day)	2003 volume (million gallons per day)
Inflows			
Recharge to water table	7,636	5,617	10,770
Net from storage	0	817	–1,157
Underflow from Piedmont	16	16	16
Underflow from North Carolina	2	23	23
TOTALS	7,654	6,473	9,652
Outflows			
Evapotranspiration and non-simulated streams	6,891	5,725	8,650
Net leakage to rivers	492	389	617
Net leakage to tidewaters and bay	269	236	266
Underflow to Maryland	2	3	3
Reported pumpage	0	94	89
Domestic pumpage	0	26	27
TOTALS	7,654	6,473	9,652

Steady-State Water Budget

Components of the groundwater budget for simulated predevelopment (steady-state) conditions are summarized in table 7. For the initial (steady-state) model stress period, the specified annual recharge flux to the water table (22.95 in.) is equivalent to 50 percent of the average Coastal Plain precipitation. The 50 percent of precipitation that does not enter the groundwater model is considered overland runoff and evapotranspiration from the vadose zone. Relatively small quantities of recharge are simulated as underflow from the Piedmont Province to the west and seepage from rivers. Of the simulated recharged groundwater, a substantial fraction is lost as evapotranspiration from the water table and seepage to small streams, both of which are accounted for by the outflow flux simulated with the EVT package. As discussed in the section on rivers, only 4.2 percent of the total length of mapped rivers in the Virginia Coastal Plain is explicitly represented with the RIV package. Because seepage to the remaining rivers, which exist in every finite-difference cell, is not explicitly simulated, some of this seepage flux is effectively compensated for by increased simulated flux through the EVT package. Although the relative magnitude of these two components simulated with the EVT package is uncertain, approximately 35 percent of the simulated evapotranspiration flux (about 7.1 in.) probably occurs as seepage to the small streams shown in figure 7. Under that assumption, 75 percent of the total base flow (9.8 in.) discharges to non-simulated small streams. In reality, these streams drain into the larger rivers, the seepage to which is explicitly simulated in the model. Although their combined length is 24 times that of the major rivers explicitly represented in the model, this flux is only 3.7 times greater than the explicitly simulated river flux. The flux per unit length to non-simulated streams is 15 percent of the flux per unit length to explicitly represented rivers, which is consistent with their smaller stream widths and associated seepage areas.

Transient Water Budget

As the magnitude of simulated recharge increases or decreases between stress periods during the transient simulation, the simulated evapotranspiration changes in response to the different head in the uppermost active model layer. Variations in recharge and ET result in smaller changes in storage and flow through head-dependent boundaries, which also respond to changes in specified pumpage.

To illustrate budget differences between the steady-state and transient stress periods, budget components from the Virginia model sub-domain have been summarized in table 8. Although both inflows and outflows occur from storage and head-dependent boundaries, the net volume for these components was computed in order to simplify table 8. The simulated recharge rate during the steady-state stress period was specified equal to 50 percent of the average historical Coastal Plain precipitation (fig. 11). In contrast, recharge specified for transient stress periods representing 2001 and 2003 were below and above the annual average, respectively. Extensive groundwater development resulted in lower water levels in southern Virginia by 2001, which also caused increased groundwater underflow from North Carolina toward the areas of drawdown in southern Virginia. Similarly, groundwater development in Maryland had increased the underflow of groundwater from Virginia into Maryland. (Flow leaving the model domain was not included as simulated underflow from Virginia to Maryland in table 8.) In comparison to the predevelopment conditions, by 2001 groundwater pumpage had caused withdrawals from storage and decreased net outflows to rivers and the Chesapeake Bay.

Following several years of drought conditions, 2003 was an unusually “wet” year in Virginia. Specified recharge to the surficial aquifer increased water levels in the surficial aquifer, and water-level declines in underlying aquifers generally decreased as well. The resulting addition to storage in the groundwater system is represented by the negative value in the “from storage” component of the 2003 Virginia water budget (table 8). In comparison to the predevelopment and 2001 rates, the relative abundance of simulated water in the shallow aquifer system in 2003 resulted in more evapotranspiration and outflows to rivers, and outflow rates to tidewater bodies (including the Chesapeake Bay) close to predevelopment rates.

Calibration Assessment

If the weights of the water-level observations accurately represent observation error and the model correctly represents the relevant hydrologic processes influencing the simulated equivalents to the observations, the distribution of weighted residuals should be random in space and time. Parameter values should not be strongly correlated if they are to be independently estimated. The final estimated parameter values should be within the range of expected reasonable values, or their confidence intervals should overlap with the range of expected reasonable values.

During the course of model calibration, many configurations of the model were tested with various parameterization schemes. For each of these model realizations, the optimal parameter values were estimated by minimization of the objective function with either PEST or UCODE–2005. Following each parameter-estimation run, the magnitude and distribution of residuals (observed minus simulated water levels) and estimated parameter values were evaluated to identify possible model error or bias. Model bias is a form of model error that may appear in the spatial or temporal pattern of residuals. Areas with patterns or magnitudes of residuals suggestive of model bias were identified for alternative parameter schemes or other possible approaches of improving model fit. The criteria used for these evaluations are reviewed in the following sections as they apply to the calibrated model.

Residual Plots

The model fit of simulated to observed water levels over the entire range of groundwater levels measured in the Virginia Coastal Plain is illustrated in figure 40a. The outlying group with observed water-level altitudes between 80 and 110 ft, which are greater than their simulated equivalents, are from three Potomac aquifer observation wells. Two of these observation wells (52P 10 and 52N 1), which are close to mapped faults in Caroline County, are anomalous compared with other nearby Potomac observation wells, which have simulated and observed water levels in close agreement. Water levels observed in the third well (52H 17), located about 1.5 mi northeast of the James River in eastern Henrico County, are anomalously high and may represent perched conditions. These observations were assigned a large variance (low weight), so as not to influence aquifer-system parameter estimates.

The relation between weighted simulated and weighted observed water levels (fig. 40b) is a preferred indicator of model error because the expected error variance has been accounted for by the observation weights. Weighted residuals are calculated as the difference between weighted observed and weighted simulated water levels. Trends resulting from model bias are more easily detected when weighted residuals versus weighted simulated water levels are graphed as in figure 41. Ideally, the residual distribution should appear randomly distributed about the horizontal line with ordinate = 0. The weighted residuals in figure 41 do not appear entirely random. A pattern that appears non-random occurs for positive weighted residuals with weighted simulated equivalents near zero. These residuals correspond to observations in cells where the water level is controlled by head-dependent flux boundaries representing tidal river areas or the Chesapeake Bay. Several similar vertical clusters of weighted residuals along abscissa values greater than zero are likely because of the control of river boundaries on the simulated water levels

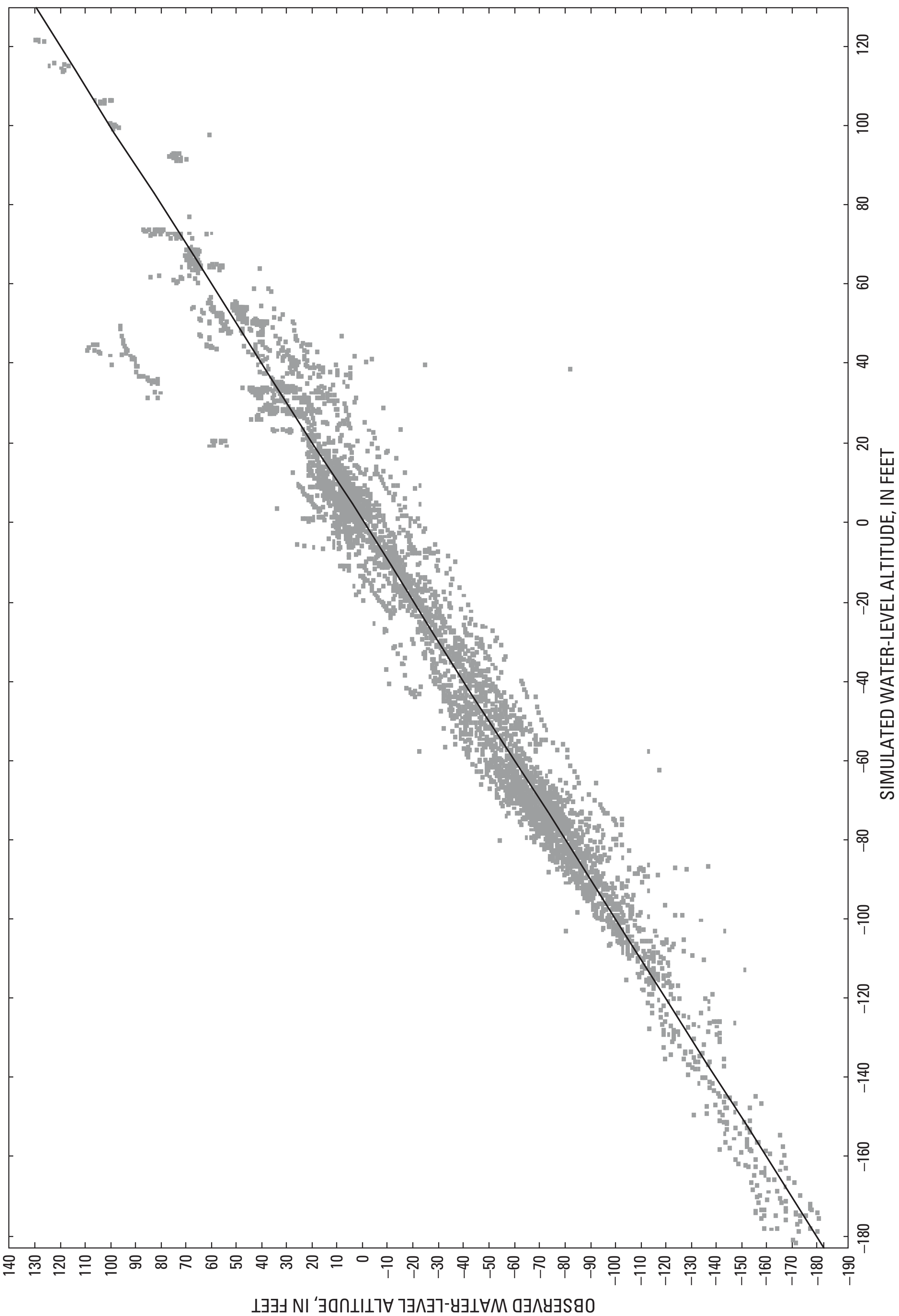

Figure 40a. Relation between observed and simulated water levels in the Virginia Coastal Plain.

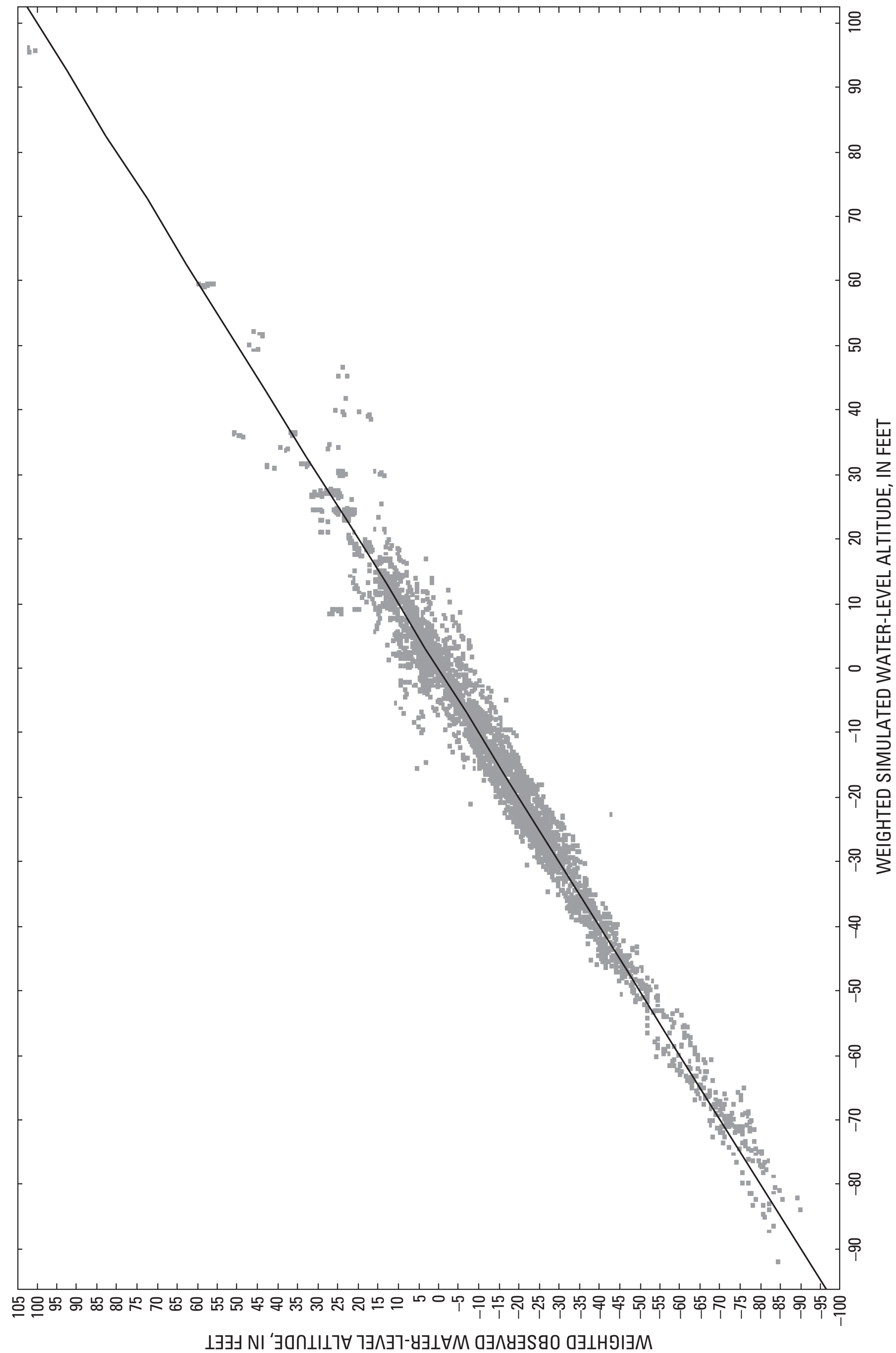

Figure 40b. Relation between weighted observed water levels and weighted simulated water levels in the Virginia Coastal Plain.

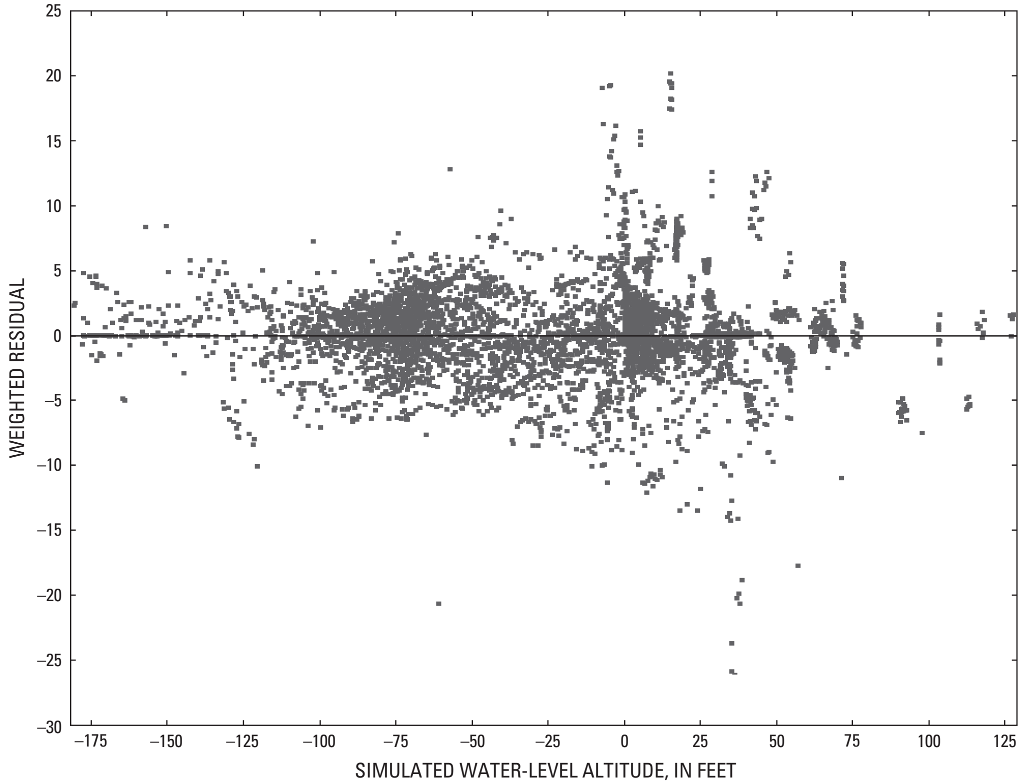

Figure 41. Relation between weighted residuals and simulated water levels in the Virginia Coastal Plain.

in cells containing observation wells. In these cases, residuals result from topographically influenced observed water levels not being accurately simulated at the regional model scale.

Weighted Residual Maps

If the weights of the water-level observations adequately represent observation error and the model sufficiently represents the relevant hydrologic processes influencing the simulated equivalents to the observations, the residual distribution should be random in space. Ideally, positive and negative weighted residuals should be approximately equal in number and appear randomly distributed. In a transient model, many water-level observations from each observation well may be used for model calibration. The observation with the maximum weighted residual from each observation well was selected to generate maps of weighted residuals. To depict the spatial distribution of model error within each aquifer (fig. 42a–f), the weighted residuals were sorted according to the aquifer screened by each corresponding observation well.

Because the residual (observed minus simulated water level) is weighted by the inverse of the error variance associated with each measurement, the magnitudes of weighted residuals differ from the raw residual magnitudes. For an observation with a large measurement-error variance (representing large uncertainty in well altitude or water-level measurement), the corresponding small regression weight may result in a weighted residual less than the difference between the measured water level and its simulated equivalent. Conversely, an accurate water-level measurement in a surveyed well can have a weighted residual greater than the difference between the measured water level and its simulated equivalent. For example, well 52G 29 on the map of Potomac weighted residuals (fig. 42f) appears to be among the largest positive weighted residuals, yet the actual differences between measured and simulated water levels in this well are only about 4 ft (fig. 36). The average (root mean square error) of the 5,087 weighted residuals for Virginia water-level observations is 3.6 ft.

Positive maximum weighted residuals outnumber negative maximum weighted residuals in the surficial aquifer (fig. 42a). This suggests that either (1) model error affects simulated water-table altitudes, or (2) a bias in the sampling of water-table altitudes by surficial-aquifer observation wells. Simulated water-table altitudes are calculated for the center of each finite-difference cell and are interpolated between the centers of the finite-difference cells to calculate the simulated equivalent to the water-table observation. Because of the strong influence of simulated evapotranspiration on the simulated water-table altitude within each finite-difference cell, the specified evapotranspiration-surface altitude for each cell largely controls the simulated water-table altitude. The evapotranspiration-surface altitude for each model cell was specified to be equal to the median altitude within each finite-difference cell determined from digital elevation model

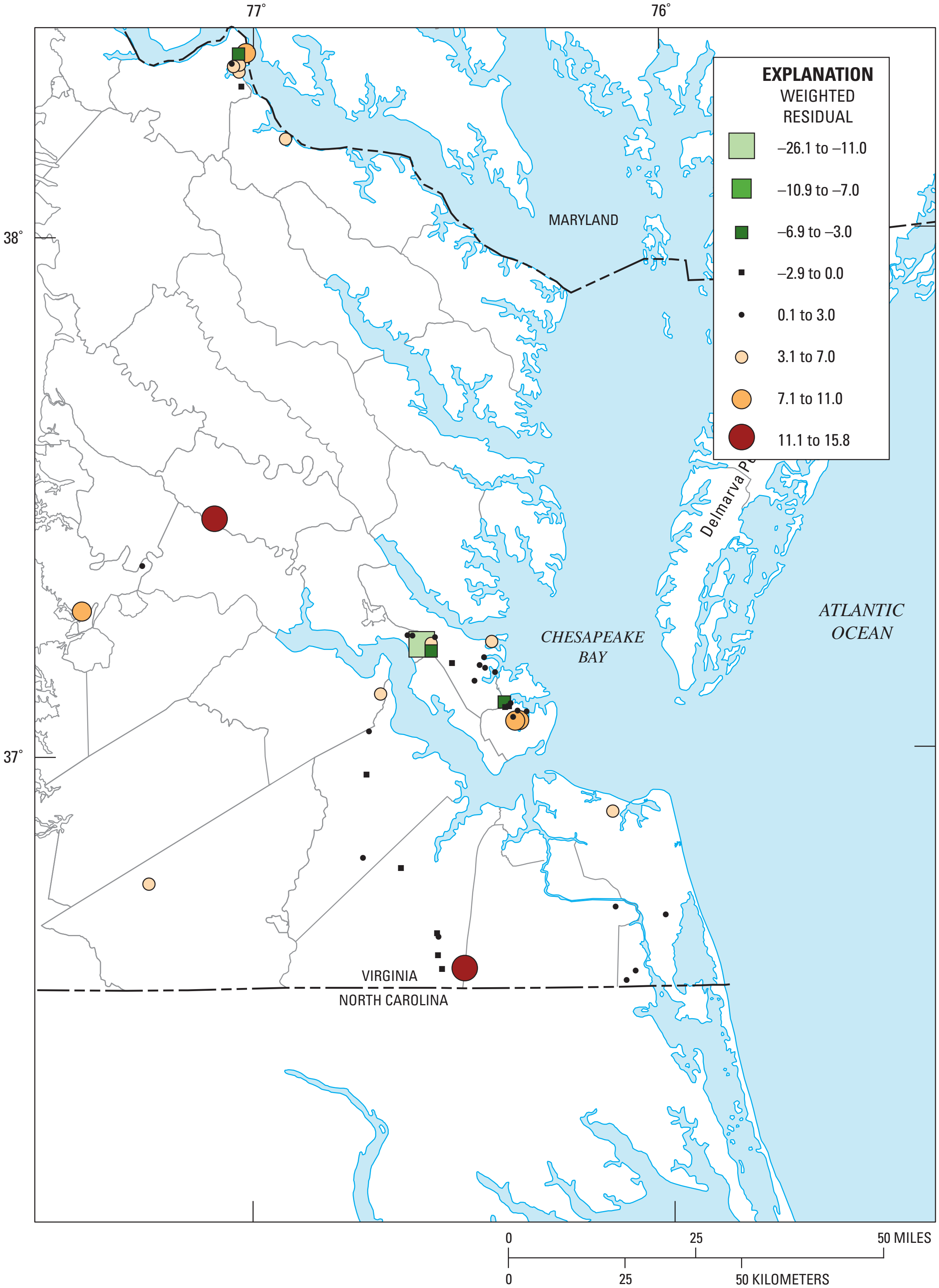

Figure 42a. Maximum residual magnitudes for observation wells screened in the surficial aquifer of the Virginia Coastal Plain.

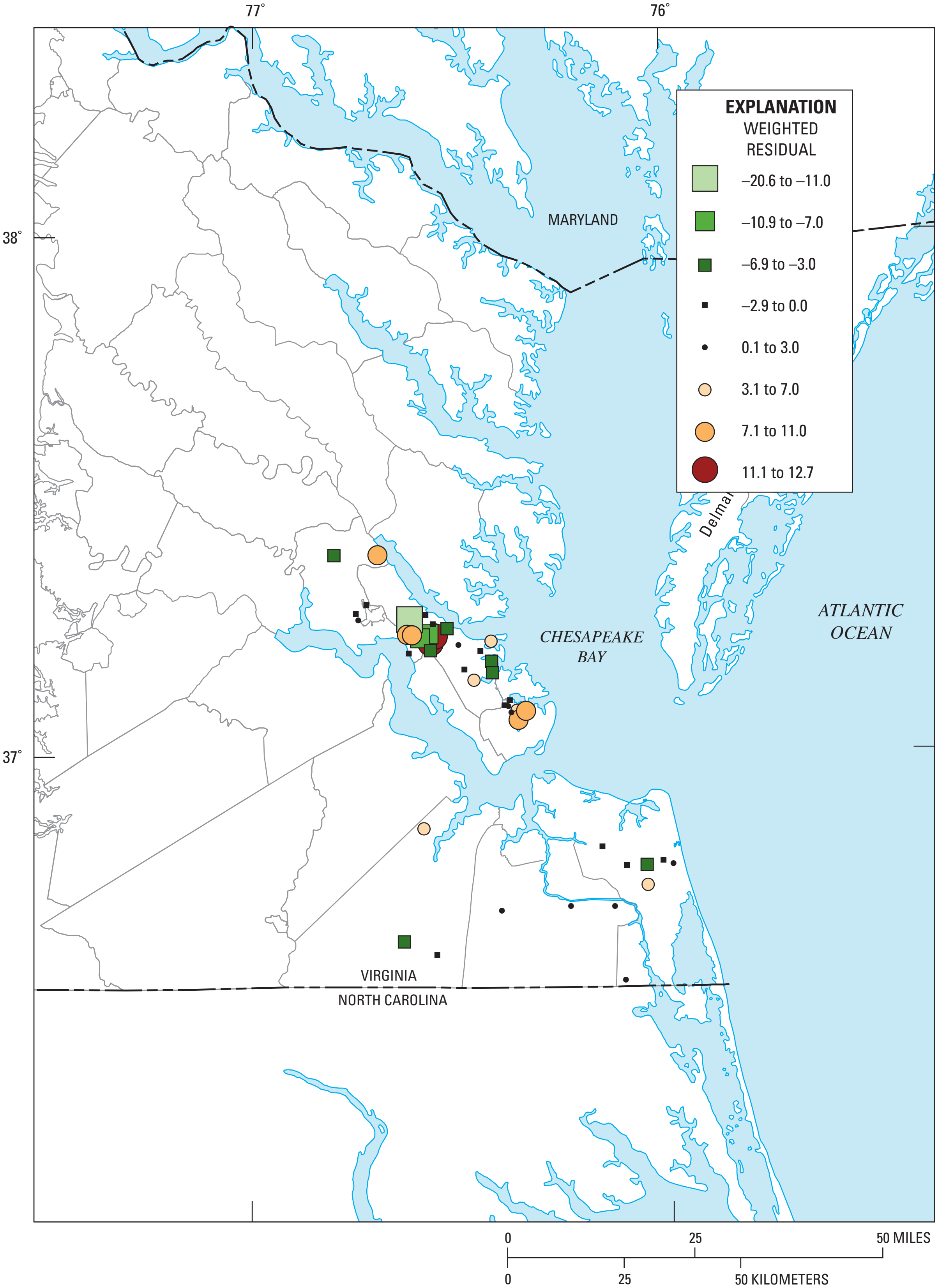

Figure 42b. Maximum residual magnitudes for observation wells screened in the Yorktown-Eastover aquifer of the Virginia Coastal Plain.

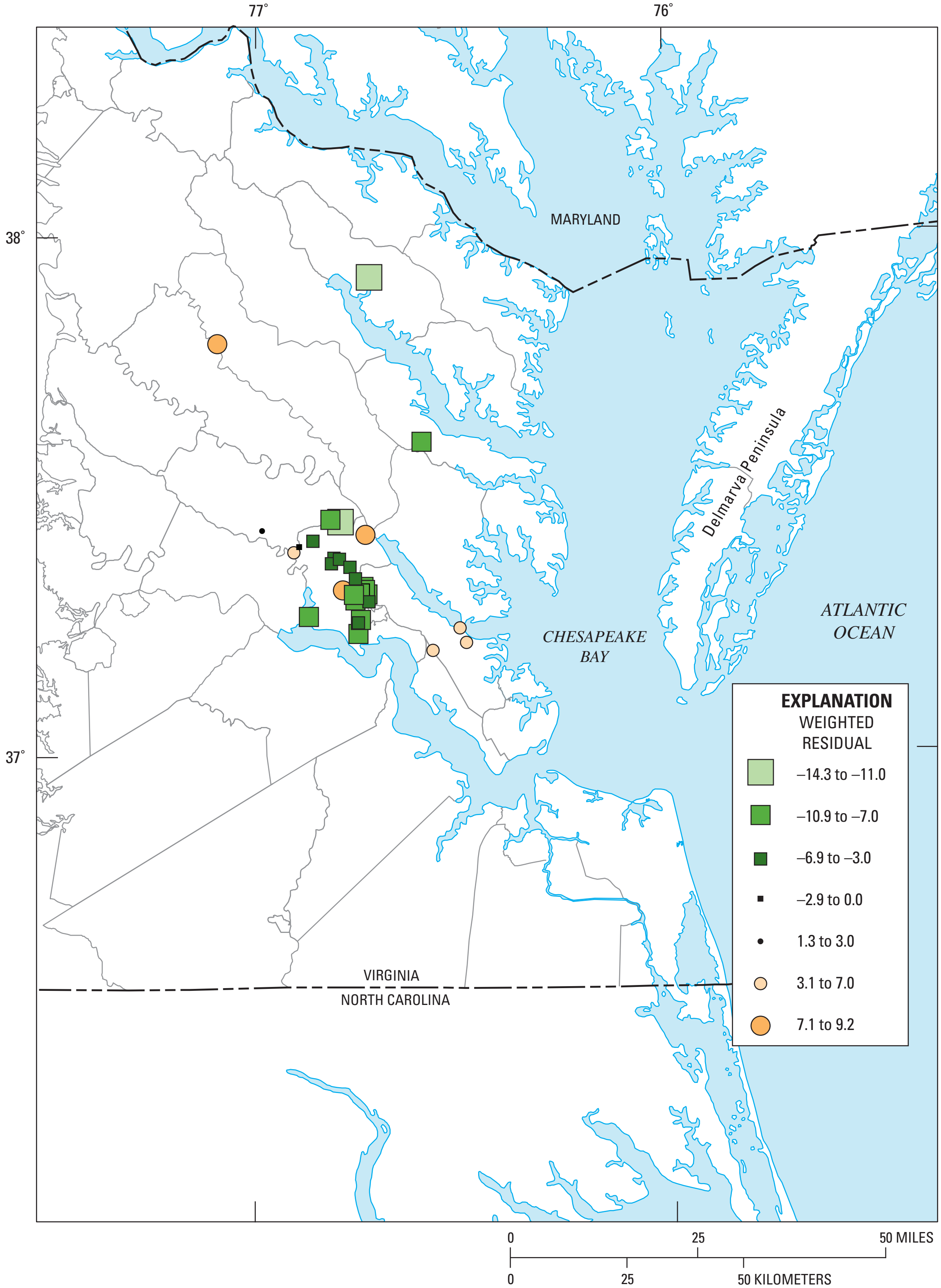

Figure 42c. Maximum residual magnitudes for observation wells screened in the Piney Point aquifer of the Virginia Coastal Plain.

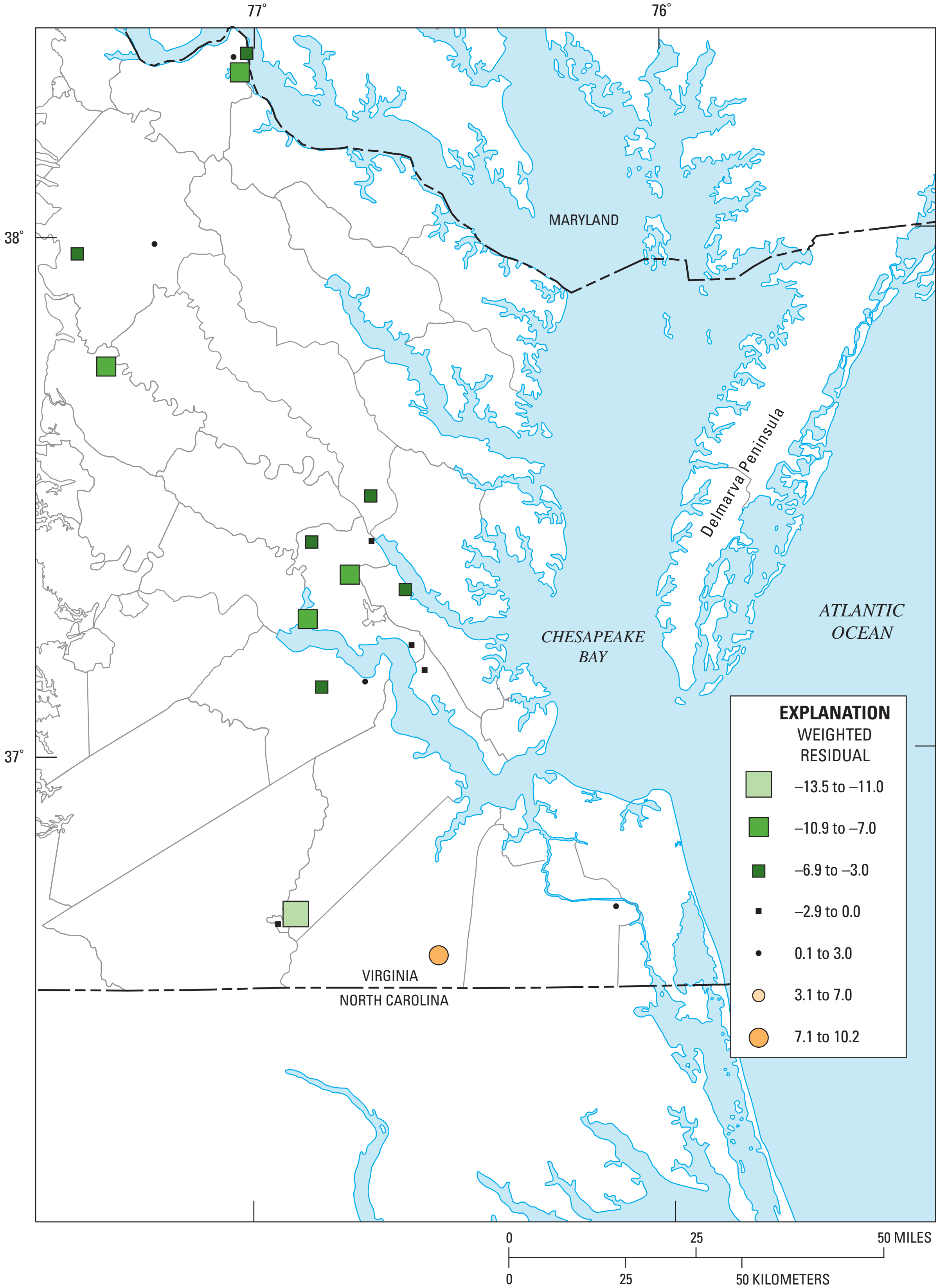

Figure 42d. Maximum residual magnitudes for observation wells screened in the Aquia aquifer of the Virginia Coastal Plain.

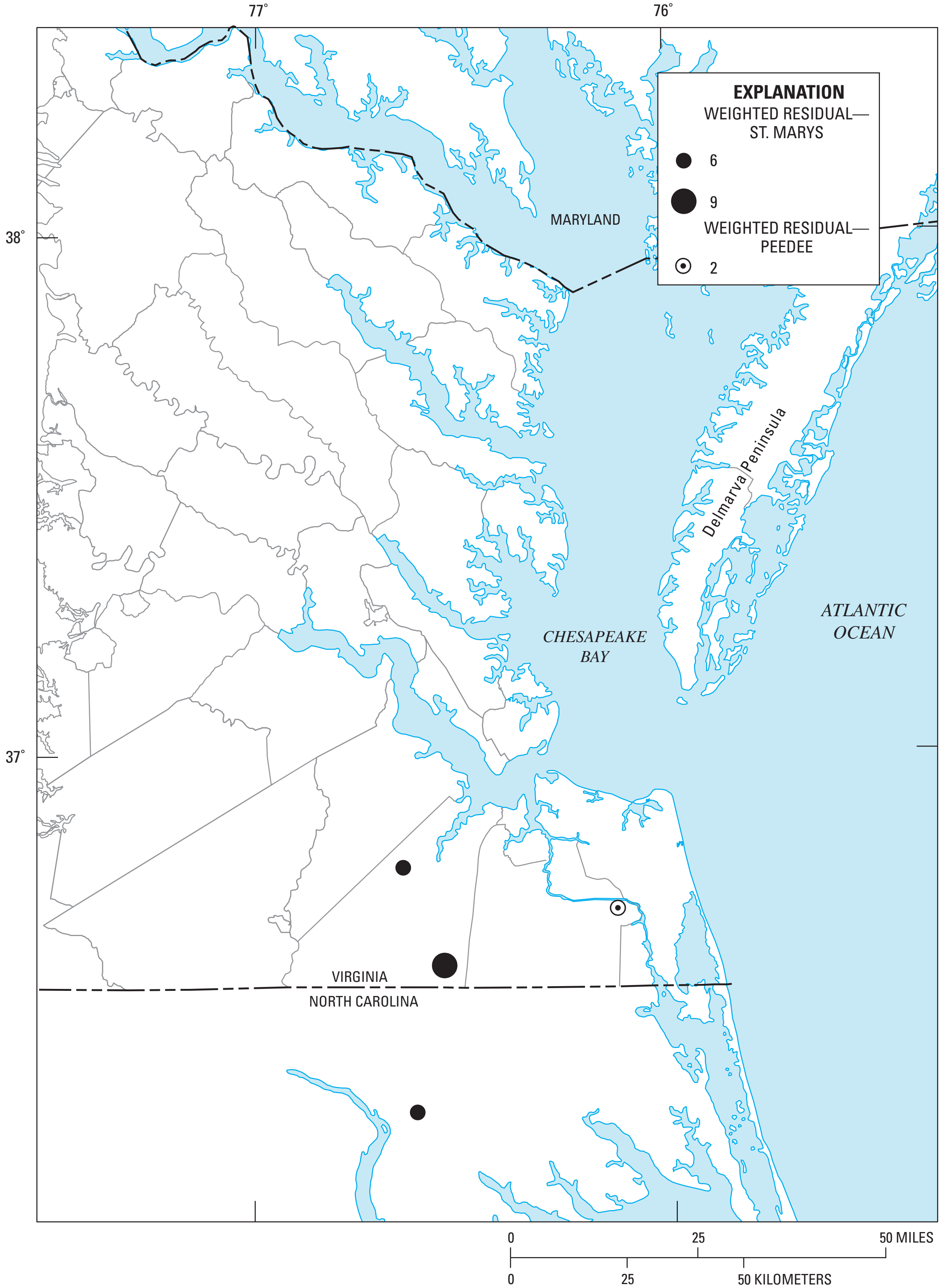

Figure 42e. Maximum residual magnitudes for observation wells screened in the Peedee and St. Marys aquifers of the Virginia Coastal Plain.

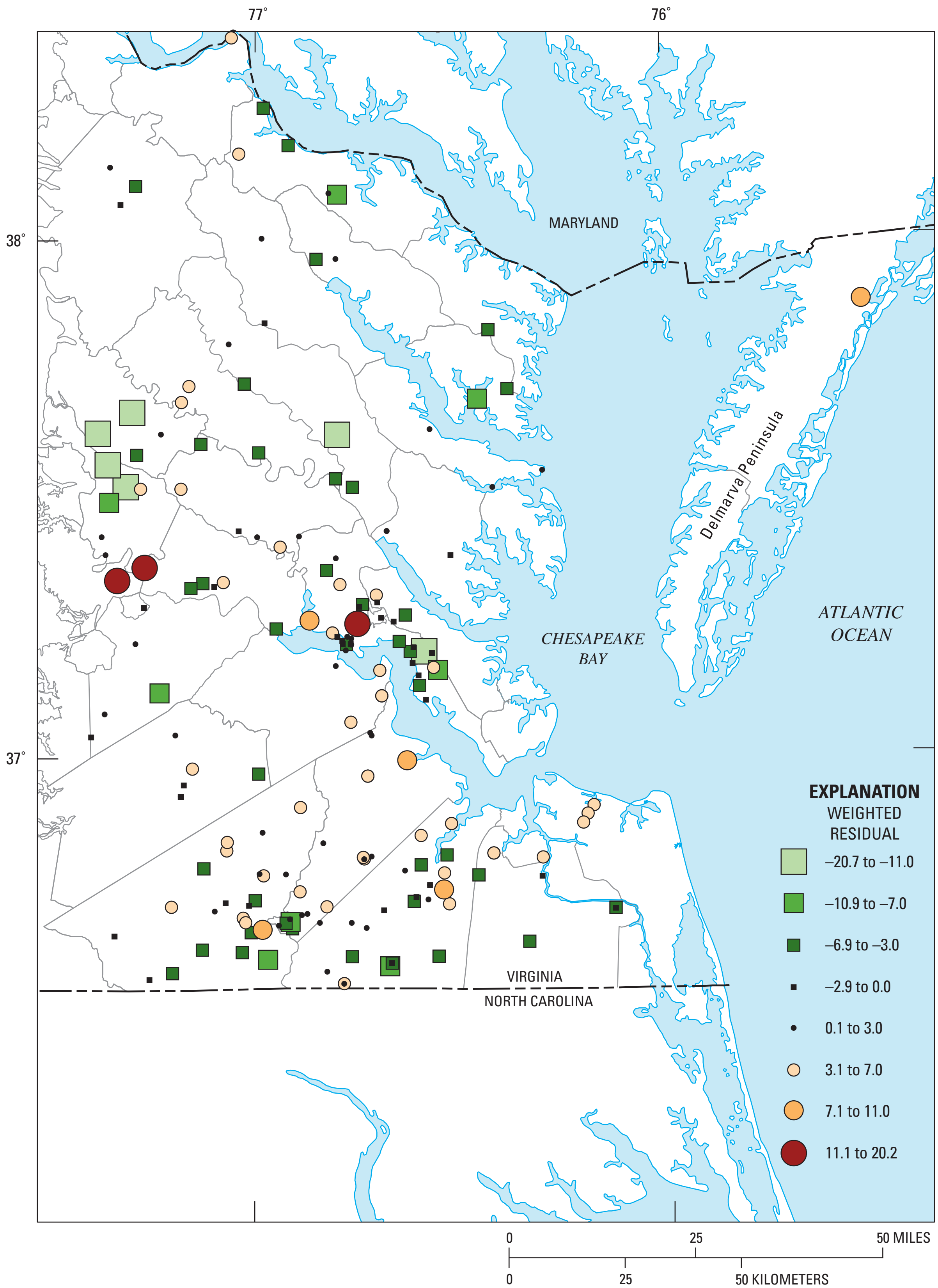

Figure 42f. Maximum residual magnitudes for observation wells screened in the Potomac aquifer of the Virginia Coastal Plain.

(DEM) data. Analysis of DEM data for the Virginia Coastal Plain indicates that the range of altitudes within each model cell is of a similar order to the range of residual magnitudes. Comparison of observation well-head altitudes with their corresponding median cell altitudes indicates that 67 percent of observation wells used for model calibration have well-head altitudes greater than the median altitude in the cell, 29 percent have well-head altitudes less than the median altitude in the cell, and 4 percent have well-head altitudes equal to the median altitude in the cell. In general, observation-well altitudes are greater than the median land-surface altitudes calculated for the 1-mi^2 model grid cells, indicating that wells tend to be located on higher-altitude areas. Because water-table altitudes correlate with topographic altitude, there is probably a positive bias in the sampling of water-table altitudes by surficial-aquifer observation wells. If such a bias exists, a larger number of positive residuals than negative residuals would be expected for the surficial aquifer. Although unequal in number, the positive and negative residuals appear to have random spatial distribution, suggesting the residual-sign inequality more likely results from observation-sampling bias than model error.

The spatial distribution of positive and negative maximum weighted residuals within the Yorktown-Eastover aquifer (fig. 42b) appears to be random, indicating it is not affected by substantial systematic model error.

A clustering of negative maximum weighted residuals within the Piney Point aquifer near Williamsburg (fig. 42c) indicates that the spatial distribution of positive and negative maximum weighted residuals is not random and that simulated water levels are affected by some model error. As discussed in the preceding section on simulated conditions within the Piney Point aquifer, the cause of this model error is uncertain but may be either insufficient simulated domestic-withdrawal flux or inaccurate simulated confining-unit leakance in the area of the clustered negative residuals.

A prevalence of negative weighted residuals within the Aquia aquifer indicates that the spatial distribution of positive and negative maximum weighted residuals is not random (fig. 42d). Hydrographs of simulated and observed Aquia water levels show that simulated water levels in some observation wells are greater than observed water levels by up to approximately 15 ft. A complex distribution of Aquia horizontal hydraulic conductivity with 5 parameters associated with 20 pilot points did not substantially improve the fit of simulated to observed water levels during model calibration using regression. It is possible that localized inaccuracy of spatial leakance through either the Nanjemoy-Marlboro confining unit or Potomac confining zone may contribute to the over-prediction of water levels in some of the Aquia observation wells, but that hypothesis was not tested during model calibration.

The number of observation wells was insufficient to evaluate the spatial distribution of residuals for the Peedee, Virginia Beach, or St. Marys aquifers. Residuals from observation wells in the Peedee and St. Marys aquifers are depicted in figure 42e to show observation-well locations.

Frequent analysis of the spatial distribution of Potomac aquifer weighted residuals during model calibration was necessary to evaluate different configurations of pilot points or zones, each with their associated parameters, which were used to specify horizontal variations of hydraulic conductivity. The spatial clustering of positive and negative maximum weighted residuals within the Potomac aquifer (fig. 42f) indicates that this residual distribution for the calibrated model is not entirely random.

Parameter Correlation

The parameter correlation coefficients computed by UCODE–2005 are useful for designing parameterization schemes, as well as determining which parameters may be effectively estimated by the parameter-estimation regression process. Examination of the parameter correlation coefficients following each regression during model calibration occasionally suggested modifications to the parameterization scheme. Several parameter pairs in the final model version have large correlation coefficients (table 9). The “recharge” parameter, which represents the fraction of precipitation that infiltrates to the water table, is completely correlated with the “et_max_rate” parameter, which represents the maximum evapotranspiration flux from the water table. This correlation indicates that it is not possible to estimate the magnitude of either parameter by regression. Recharge was also somewhat correlated with the parameter representing the evapotranspiration extinction depth. The regression was sensitive to the ratio of “recharge” and “et_max_rate”; final values were obtained for “et_max_rate” by regression after fixing the “recharge” parameter and the evapotranspiration extinction depth at reasonable values.

The parameter “kdepth1,” which is used to simulate the change with depth of Potomac aquifer horizontal hydraulic conductivity, is correlated with the parameter “k_islewight,”

Table 9. Parameter pairs with absolute correlation coefficients greater than 0.8.

[et_max_rate, maximum evapotranspiration flux; recharge, specified recharge flux; k_islewight, horizontal hydraulic conductivity at pilot point in Isle of Wight County; kdepth1, λ in exponent in equation 8; k_potom_cz, horizontal hydraulic conductivity of Potomac confining zone; k_megabloc, horizontal hydraulic conductivity of Potomac aquifer within Chesapeake Bay impact crater; k_kinggeorg, horizontal hydraulic conductivity at pilot point in King George County; mdflow, specified flux out of model row 1]

Parameter pair		Correlation coefficient
et_max_rate	recharge	1.00
k_islewight	kdepth1	0.95
k_potom_cz	k_megabloc	–0.94
k_kinggeorg	mdflow	0.86

representing Potomac aquifer horizontal hydraulic conductivity at a pilot point in Isle of Wight County.

The parameter “k_kinggeorg,” representing Potomac aquifer horizontal hydraulic conductivity at a pilot point in model row 1 and in King George County, is correlated with the parameter “mdflow,” which represents the magnitude of groundwater flux out of the model domain in this area toward Maryland.

The parameter “k_potom_cz,” which represents horizontal hydraulic conductivity within the Potomac confining zone, is inversely correlated with the parameter “k_megabloc,” which represents horizontal hydraulic conductivity of the Potomac aquifer within the Chesapeake Bay impact crater. (The composite scaled sensitivities of “k_megabloc” indicates it is not a sensitive parameter; this apparent inverse correlation may be a numerical artifact.) Regression runs with UCODE–2005 and PEST were made with sub-sets of the total model-parameter set. Possible difficulties estimating unique values for parameters in pairs with correlation coefficients between 0.8 and 0.95 (considered “somewhat correlated” parameters) were avoided by including members of the correlated pairs in separate parameter-estimation runs.

Parameter Sensitivities

The composite scaled sensitivity reflects the total amount of information provided by the water-level observations for the estimation of one model parameter (Hill and Tiedeman, 2007). The composite scaled sensitivities for estimated parameters were computed by UCODE–2005 and are displayed graphically in figure 43. In general, parameters with composite scaled sensitivities greater than about 1 can be well-estimated and have correspondingly smaller 95-percent confidence intervals. Parameters with composite scaled sensitivities smaller than about 1 may be more difficult to estimate and(or) have larger 95-percent confidence intervals.

Estimated Parameters

The model-parameter values estimated by non-linear regression are shown with their respective reasonable-value ranges and individual linear 95-percent confidence intervals in figure 44. The confidence intervals were computed by assuming that the model is linear, true observation errors are

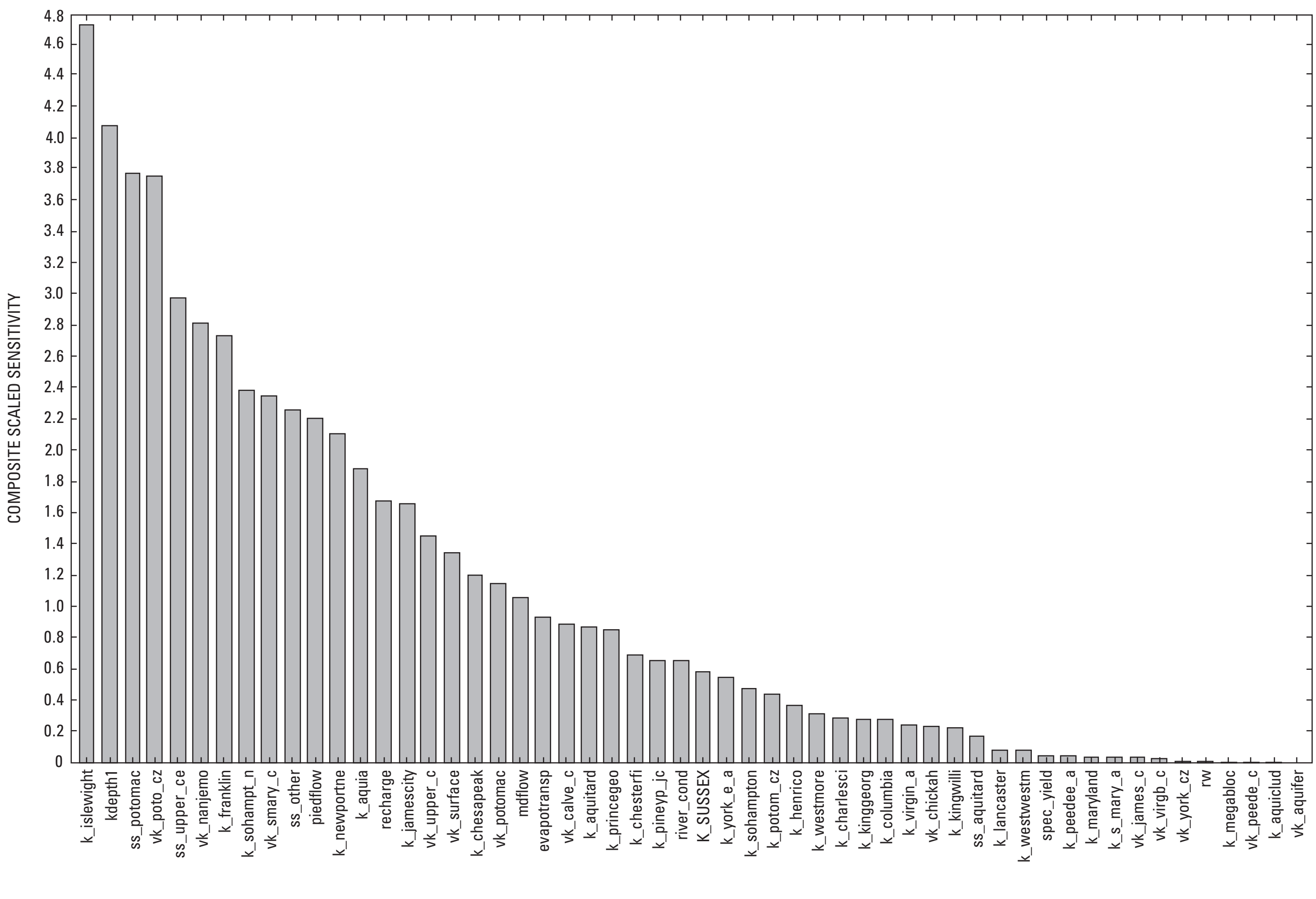

Figure 43. Composite scaled sensitivities for model parameters. (Parameter definitions are on p. x.)

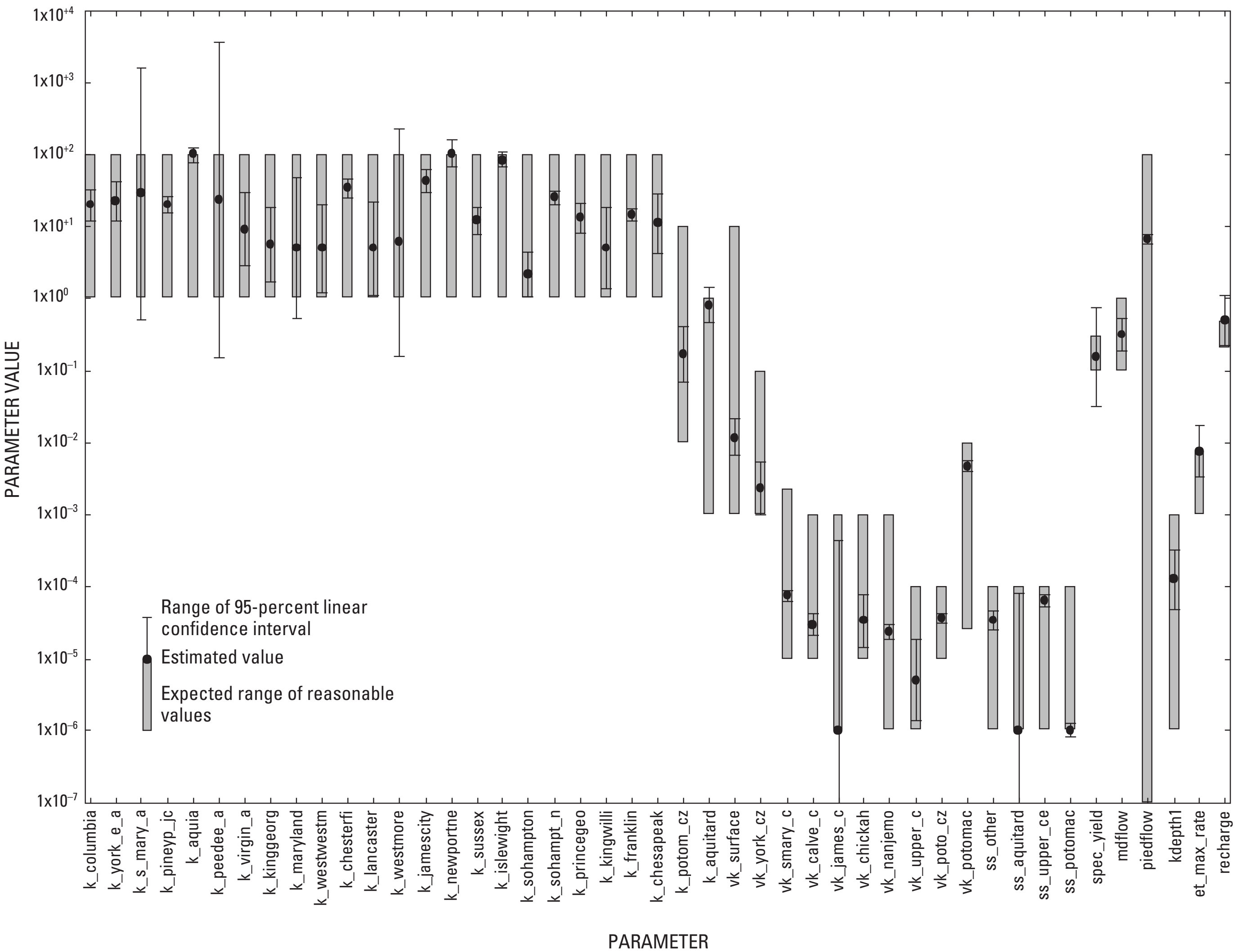

Figure 44. Estimated values, confidence intervals, and reasonable ranges for parameters representing horizontal hydraulic conductivity, vertical hydraulic conductivity, specific storage, and other fluxes. (Parameter definitions are on p. x.)

random, and weighted true errors are independent. Because the groundwater model is non-linear, the depicted intervals are not entirely accurate. Calculation of the more accurate non-linear confidence intervals (Vecchia and Cooley, 1987) requires months of computer execution time, which was prohibitive to this project. Despite their inherent inaccuracy, the depicted confidence intervals are somewhat useful indicators of the relative confidence of the estimated parameter values.

All estimated parameter values fall within their respective ranges of reasonable values for hydraulic properties or model parameters of their type. Horizontal hydraulic conductivity (K_h, designated by the prefix ‘k’ in fig. 44) values are larger than values for vertical hydraulic conductivity (prefix: ‘vk’), specific storage (prefix: ‘ss’), and other parameters; parameters representing K_h in hydrogeologic units and at different pilot-point locations are shown on the left side of figure 44. With the exception of parameters representing horizontal hydraulic conductivity in the St. Marys and Peedee aquifers, where few observations exist, and at a pilot-point location in Westmoreland county (representing K_h in the Potomac aquifer), the computed 95-percent confidence intervals for these parameters are also within a range of reasonable values for horizontal hydraulic conductivity of these hydrogeologic units.

The magnitudes of parameter values for specific yield, Piedmont and Maryland specified fluxes, evapotranspiration and recharge rates, and the decrease of horizontal hydraulic conductivity with depth in the Potomac aquifer, while not meaningful compared to each other, are also shown with respect to their confidence intervals and reasonable ranges on the right side of figure 44. With the exception of the parameter representing simulated well radii, which is insensitive, limits of the 95-percent confidence intervals for each parameter are within an order of magnitude of their corresponding estimated parameter values.

Parameters representing the vertical hydraulic conductivities of aquifers and the Peedee and Virginia Beach confining units have both very small composite scaled sensitivities and large linear confidence intervals and were not well-estimated by the model-calibration regression. The parameters representing horizontal hydraulic conductivity in the Chickahominy and Exmore confining units and the horizontal hydraulic conductivity in the structurally disrupted “mega block” zone of the Potomac aquifer similarly had very small composite scaled sensitivities and large linear confidence intervals and also were not well-estimated by the model-calibration regression.

Aquifer and Confining-Unit Spatial Variability

Because the thickness (b) of every aquifer is spatially variable, the transmissivity ($T = K_h b$) and storage coefficient ($S_s b$) of every aquifer varies spatially. Similarly, the thickness of each confining unit and confining zone is spatially variable; consequently, the leakance (K_v /b) of these hydrogeologic units also varies spatially. Maps of model-calculated transmissivity for each aquifer are presented in figures 45a–f. Maps of model-calculated leakance for each confining unit are presented in figures 46a–k. Maps of aquifer transmissivity may be useful for visualizing differences in the relative potential productivity of the thinner confined aquifers above the Potomac aquifer system. These maps are also useful for visualizing the extent and variations in thickness of each hydrogeologic unit.

Model Limitations

The model was designed to simulate regional groundwater flow and water levels in the confined aquifers of the Virginia Coastal Plain. For most of the study area, water-table altitudes and horizontal flow directions within the surficial aquifer are affected by topographic variations and streams that cannot be adequately simulated with the 1-mi^2 finite-difference-cell size used for the model. Therefore, the model may not be suitable, for example, to study site-specific groundwater contamination problems in the surficial aquifer.

The groundwater model discretization, which employs 1-mi^2 finite-difference cells, is most appropriate for evaluating the drawdown of withdrawal wells at distances greater than approximately 1 mi from those wells. Because specified withdrawals are simulated from the center of each finite-difference cell, the simulated withdrawal may be horizontally displaced up to 3,733 ft from the actual location of the withdrawal well. A Cooper-Jacob (1946) approximation of water-level drawdown resulting from a withdrawal of 0.1 Mgal/d (3,000,000 gal per month) from an aquifer with values of transmissivity T = 10,000 ft^2/d and storage S = 0.0001, which are typical of those estimated from Potomac aquifer tests (table 1), is 0.7 ft at a distance of 1 mi after 1 year. The similar drawdown approximation for the withdrawal of 0.01 Mgal/d (300,000 gal per month) is less than 0.1 ft at 1 mi after 1 year. Drawdown resulting from well withdrawals between 0.01 and 0.1 Mgal/d may be of concern within a mile or two from a pumping well. Because the finite-difference approximation is less accurate at this scale, it may be more effective to employ a local-scale model or analytical solution when evaluating drawdown at this range.

Because the minimum stress-period length of the model is 1 year, seasonal variations of groundwater levels are not simulated. However, it would be possible to simulate future seasonal variations by modifying the temporal discretization and specifying appropriate fluxes in the model stress packages.

Although the change of groundwater density resulting from spatial variation of solute concentration is simulated, the model is not currently capable of accurately simulating or predicting temporal changes of solute concentration resulting from saltwater intrusion. A useful transport model of areas of potential seawater intrusion will likely require finer horizontal discretization and a computationally intensive solution algorithm, such as Total-Variation-Diminishing (Zheng and Wang, 1999) that minimizes the effects of numerical dispersion and oscillation on simulated solute concentrations.

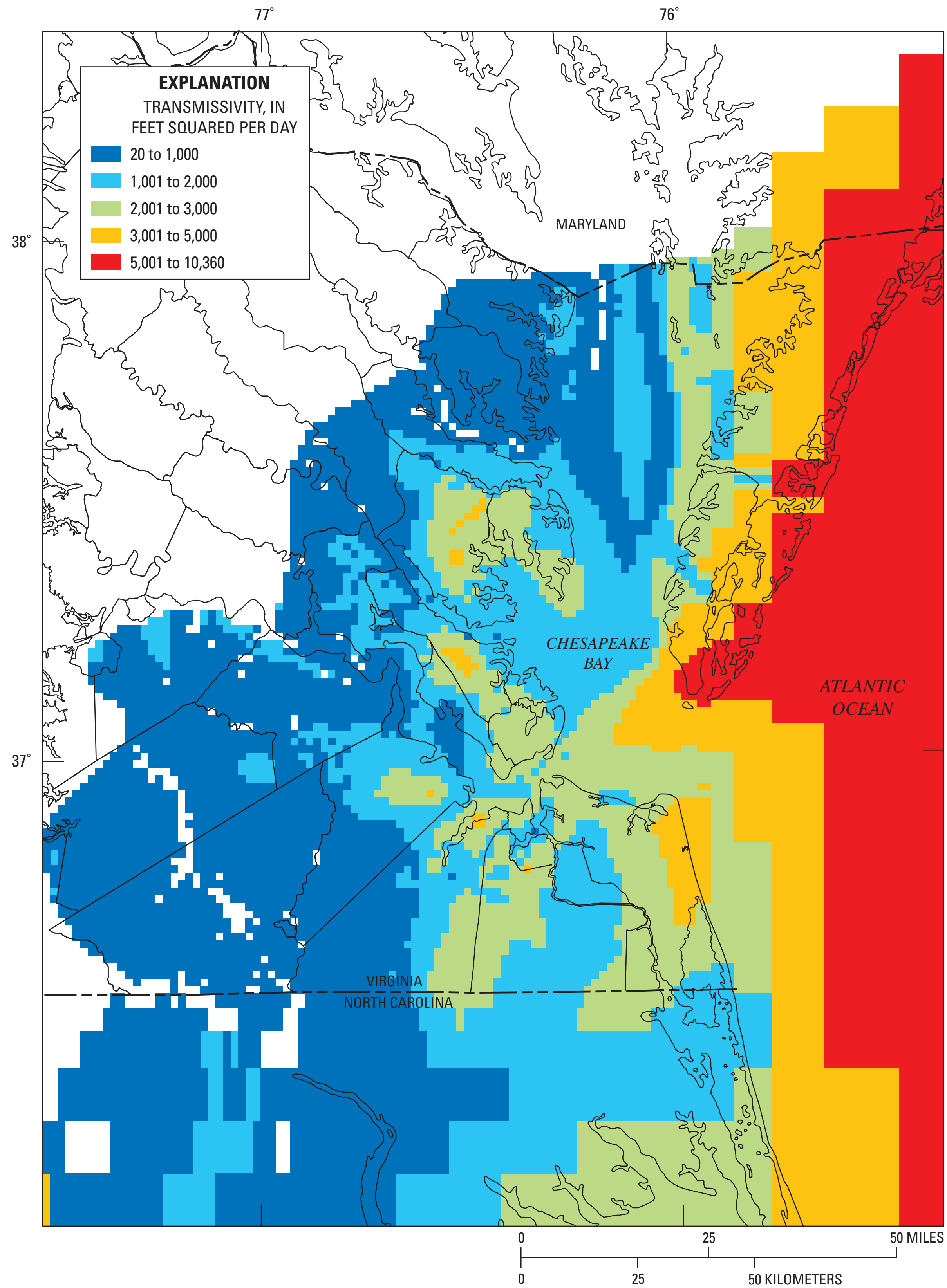

Figure 45a. Estimated transmissivity of the Yorktown-Eastover aquifer of the Virginia Coastal Plain.

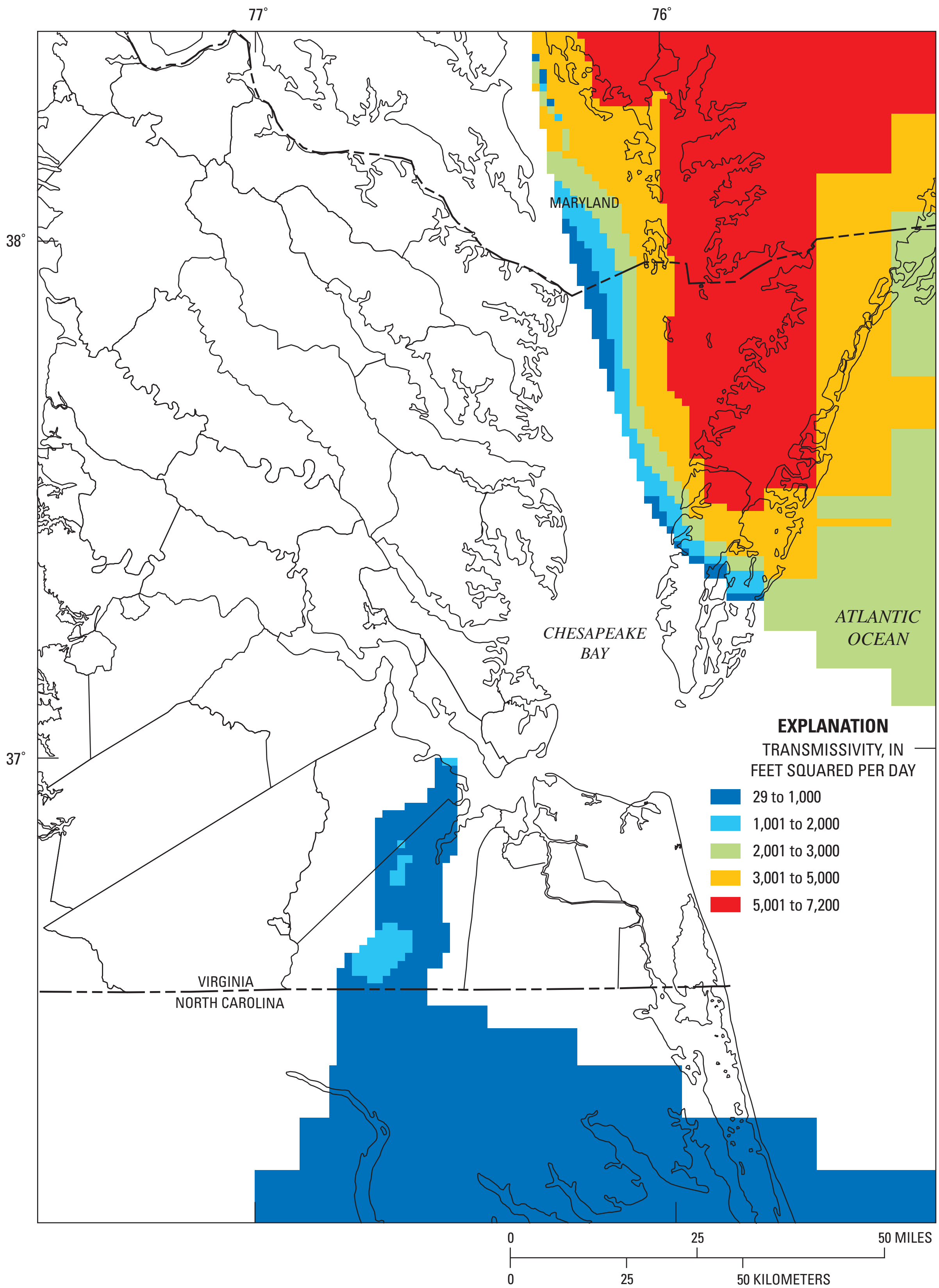

Figure 45b. Estimated transmissivity of the St. Marys aquifer of the Virginia Coastal Plain.

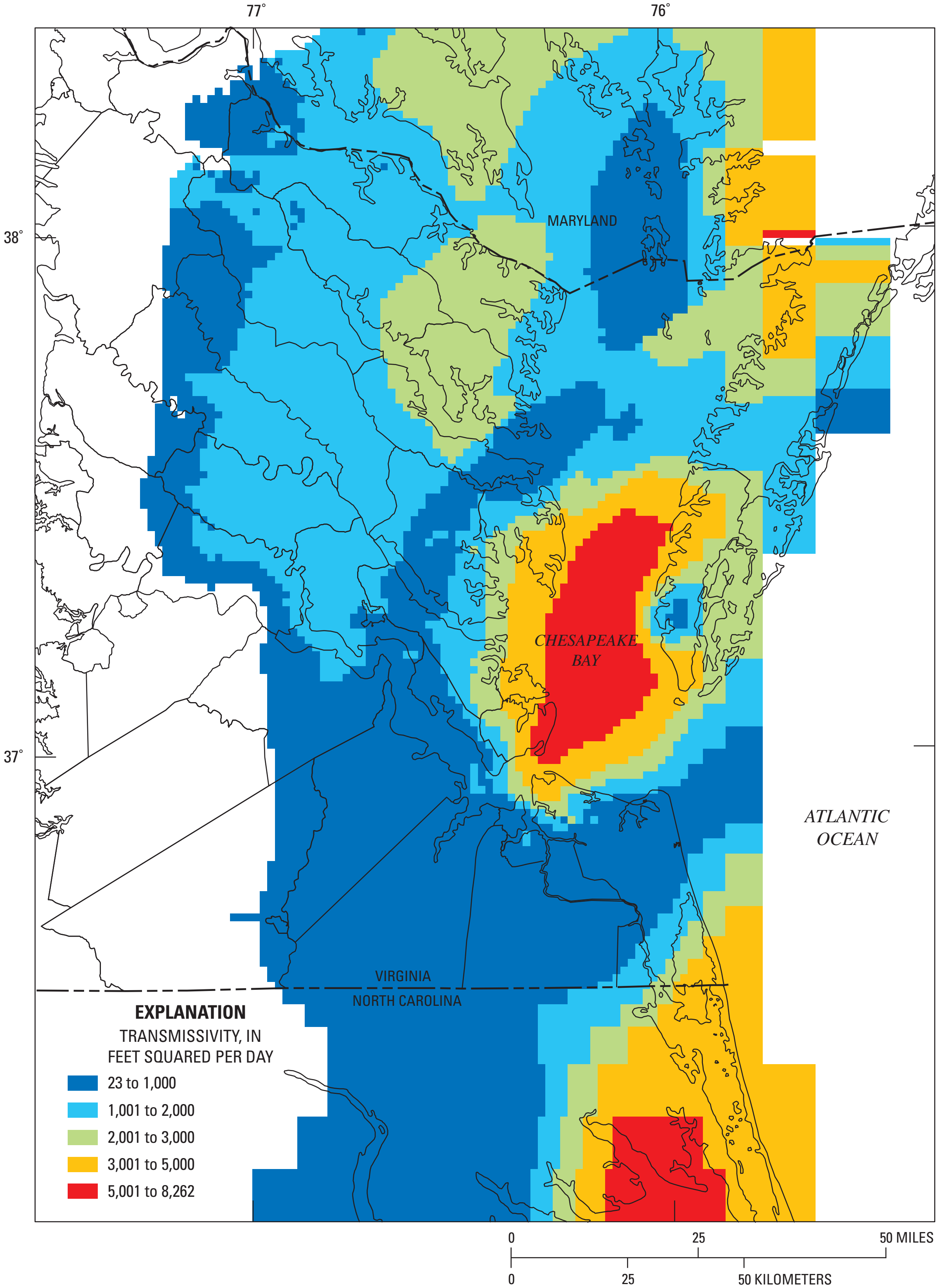

Figure 45c. Estimated transmissivity of the Piney Point aquifer of the Virginia Coastal Plain.

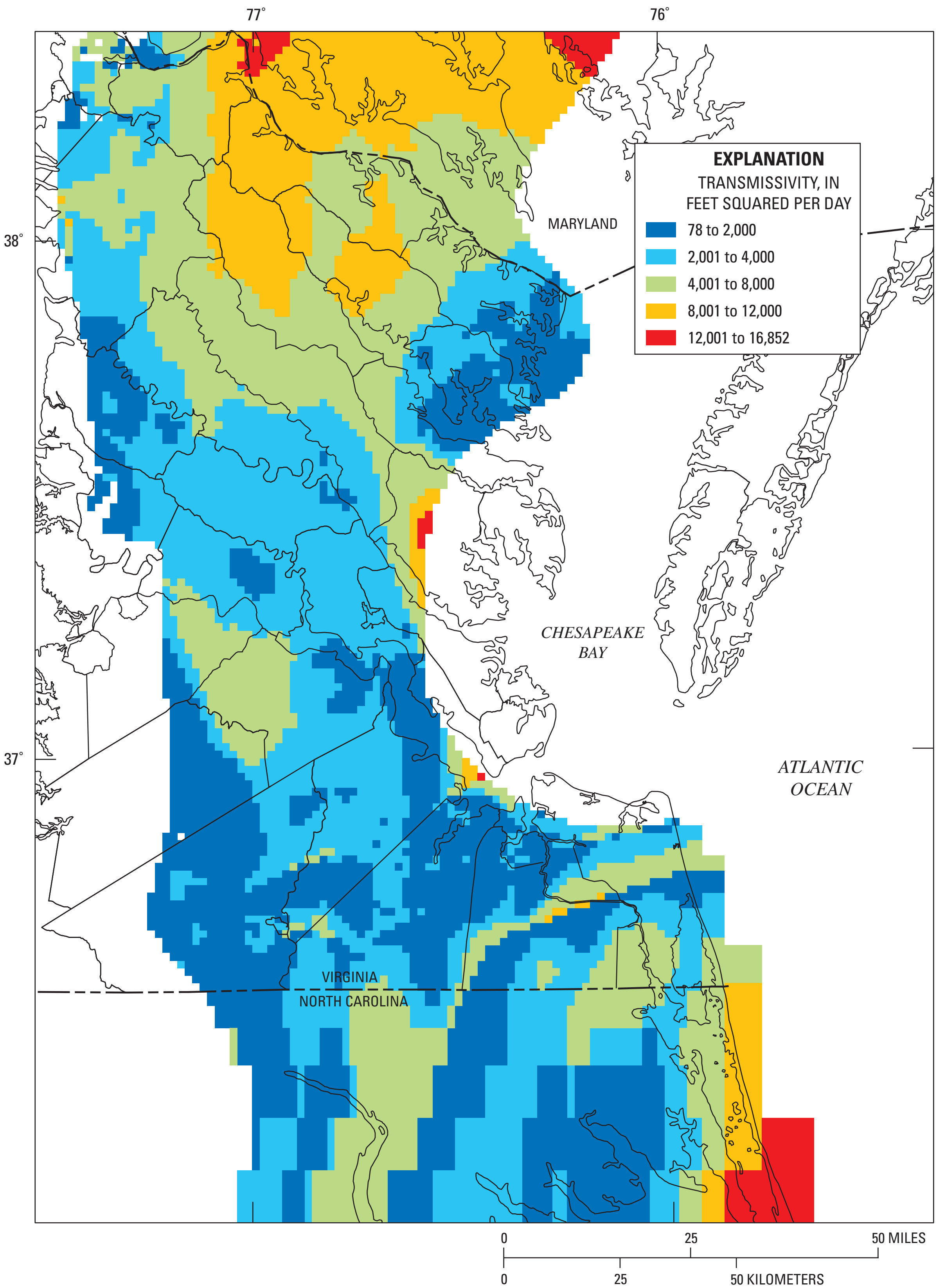

Figure 45d. Estimated transmissivity of the Aquia aquifer of the Virginia Coastal Plain.

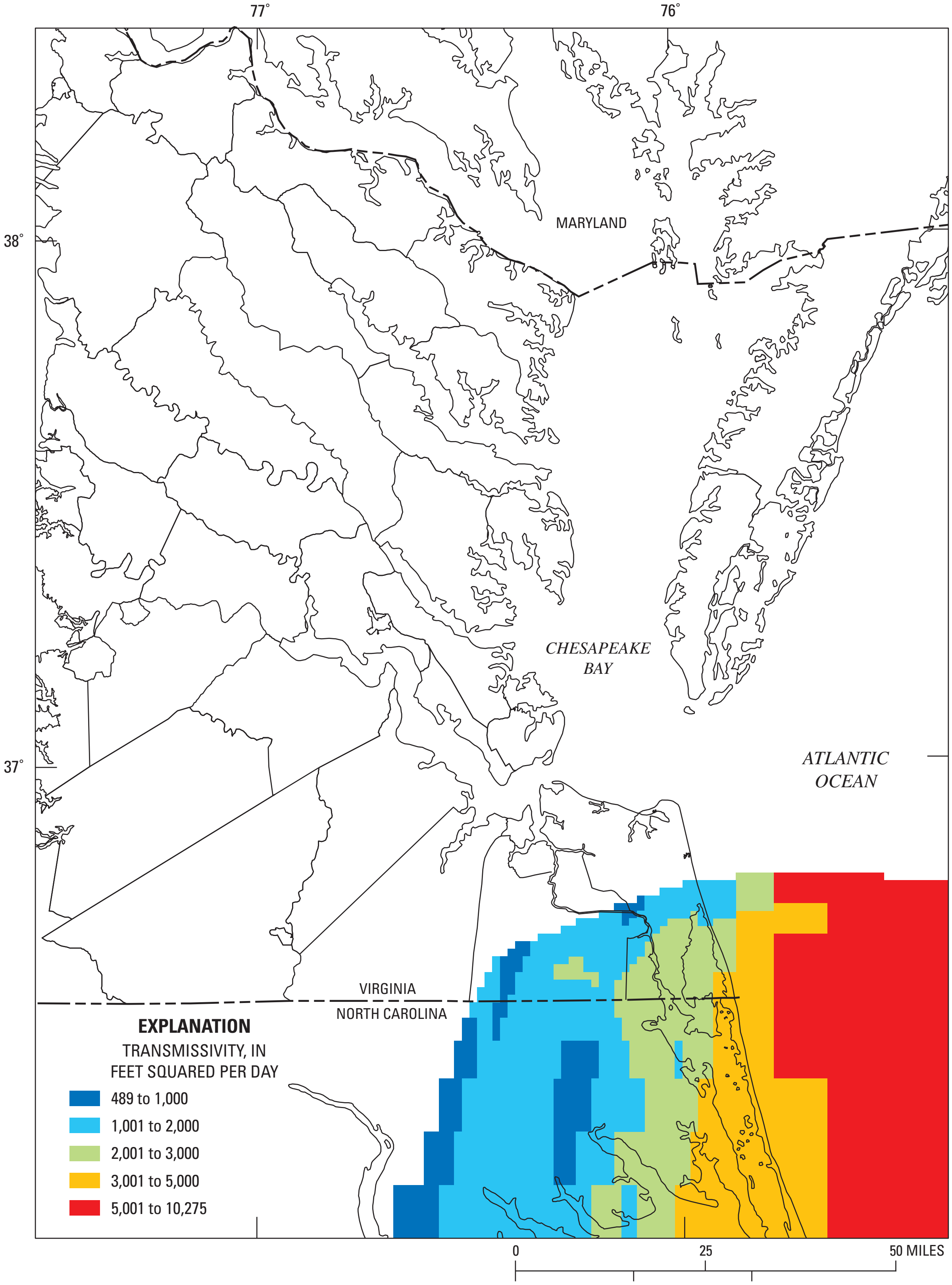

Figure 45e. Estimated transmissivity of the Peedee aquifer of the Virginia Coastal Plain.

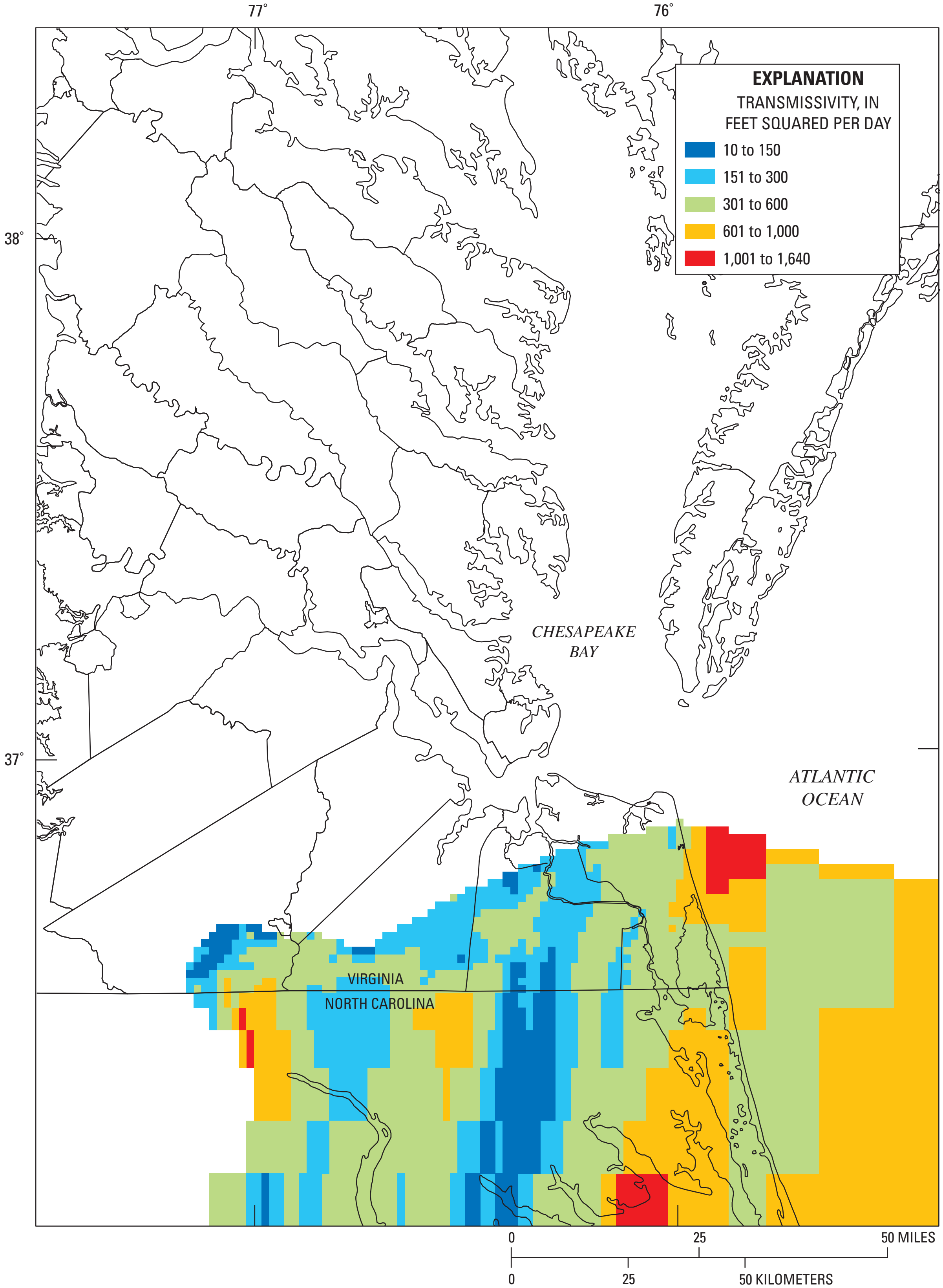

Figure 45f. Estimated transmissivity of the Virginia Beach aquifer of the Virginia Coastal Plain.

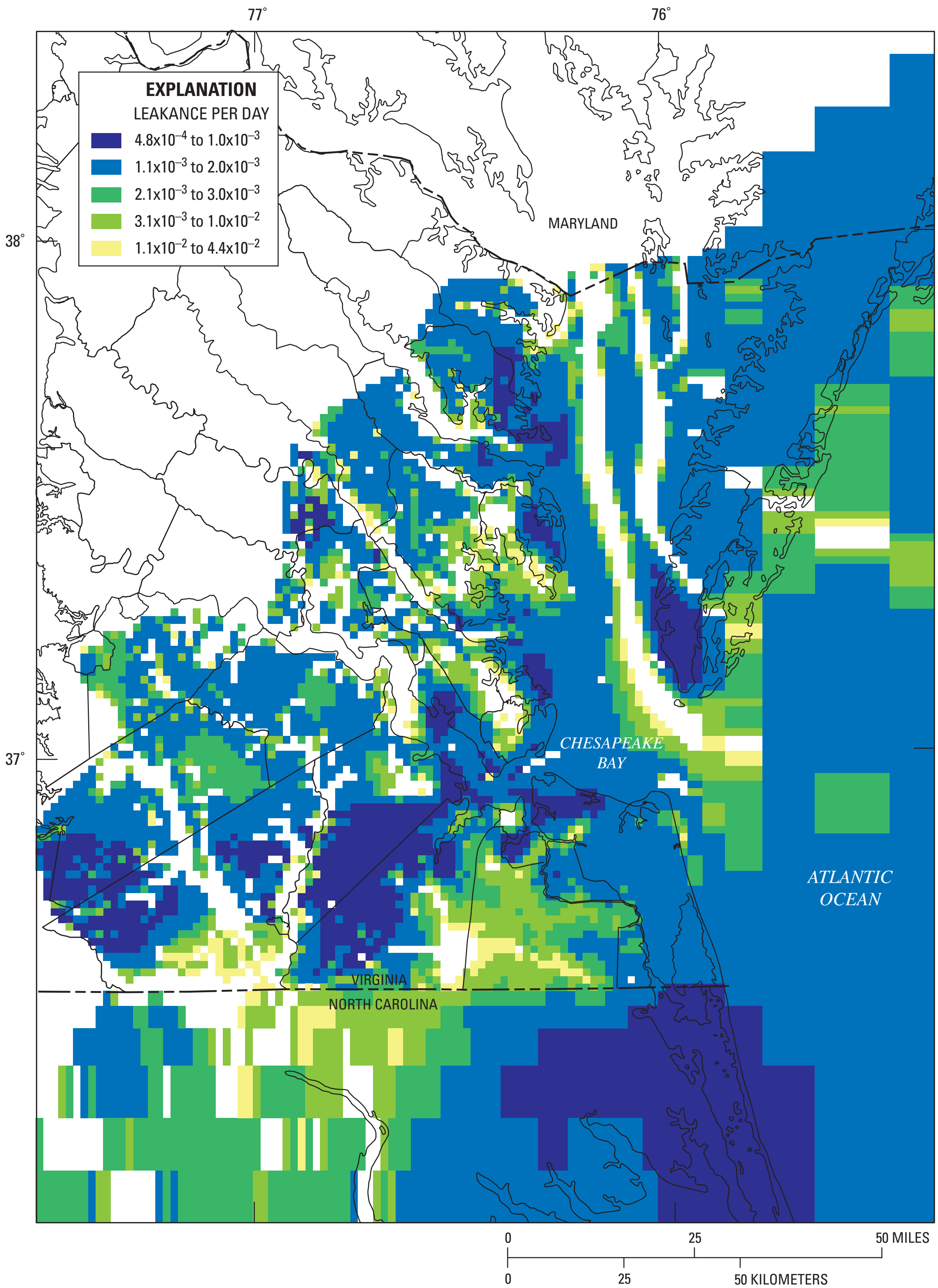

Figure 46a. Estimated leakance of the Yorktown confining zone of the Virginia Coastal Plain.

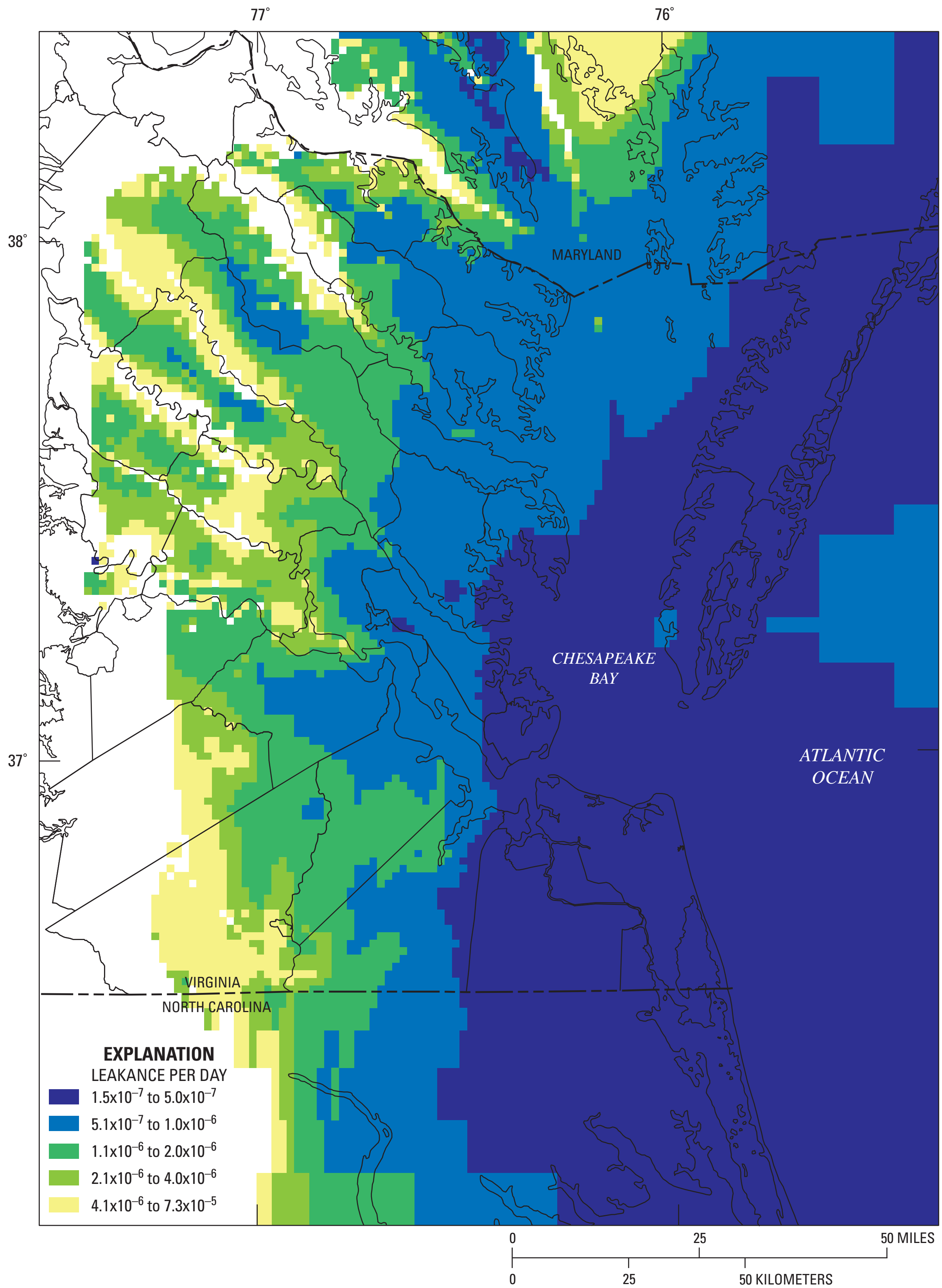

Figure 46b. Estimated leakance of the St. Marys confining unit of the Virginia Coastal Plain.

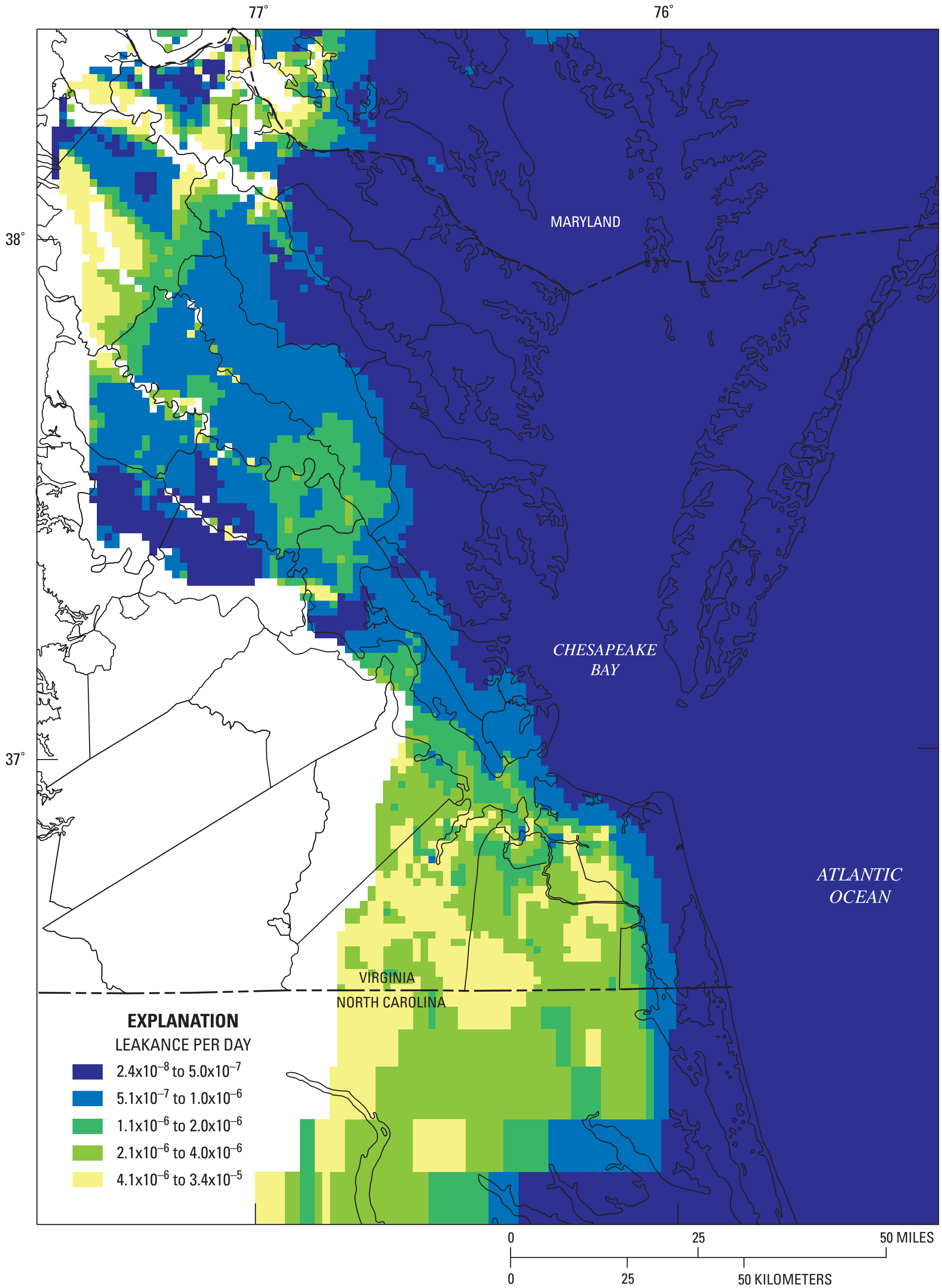

Figure 46c. Estimated leakance of the Calvert confining unit of the Virginia Coastal Plain.

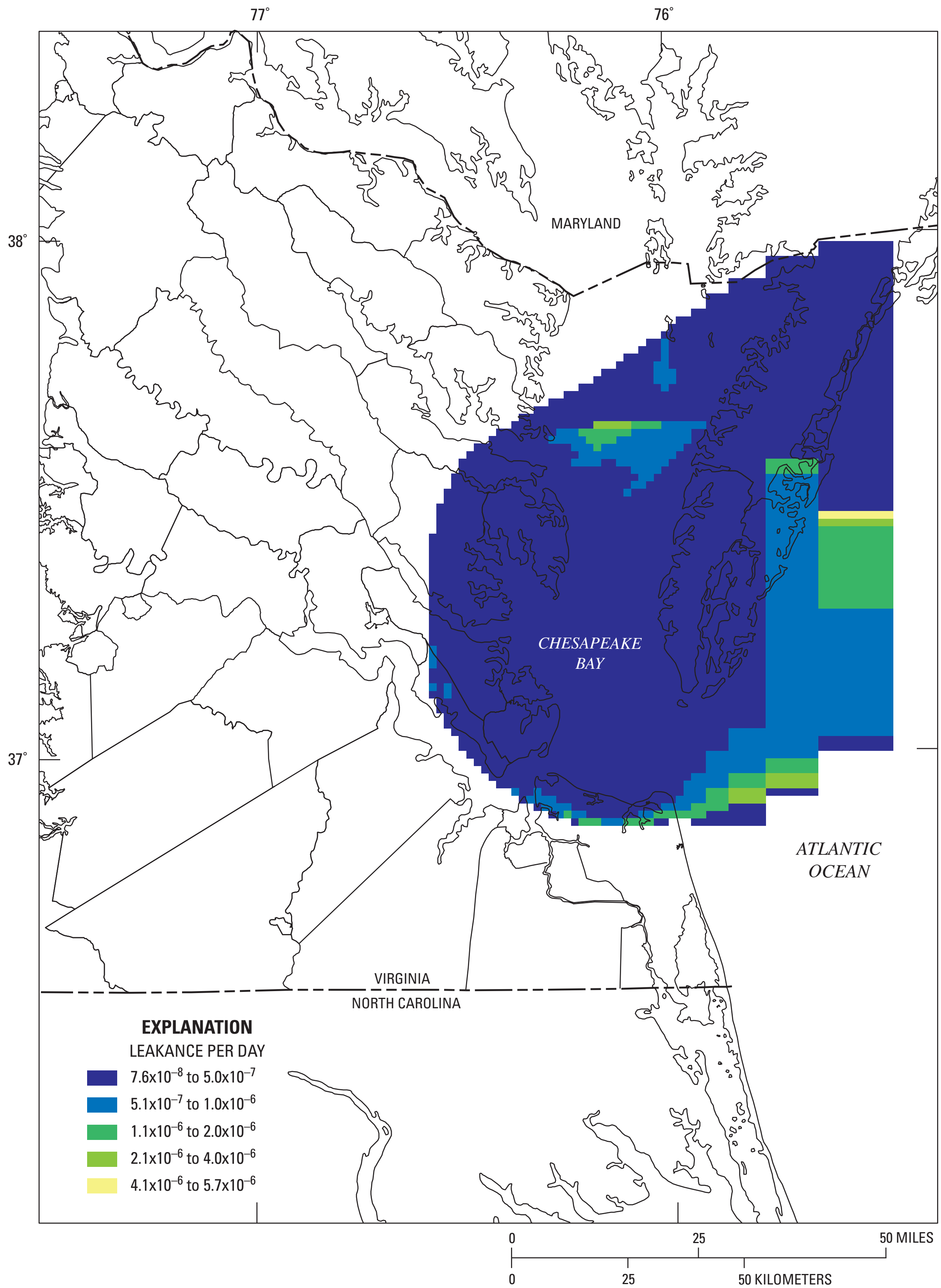

Figure 46d. Estimated leakance of the Chickahominy confining unit of the Virginia Coastal Plain.

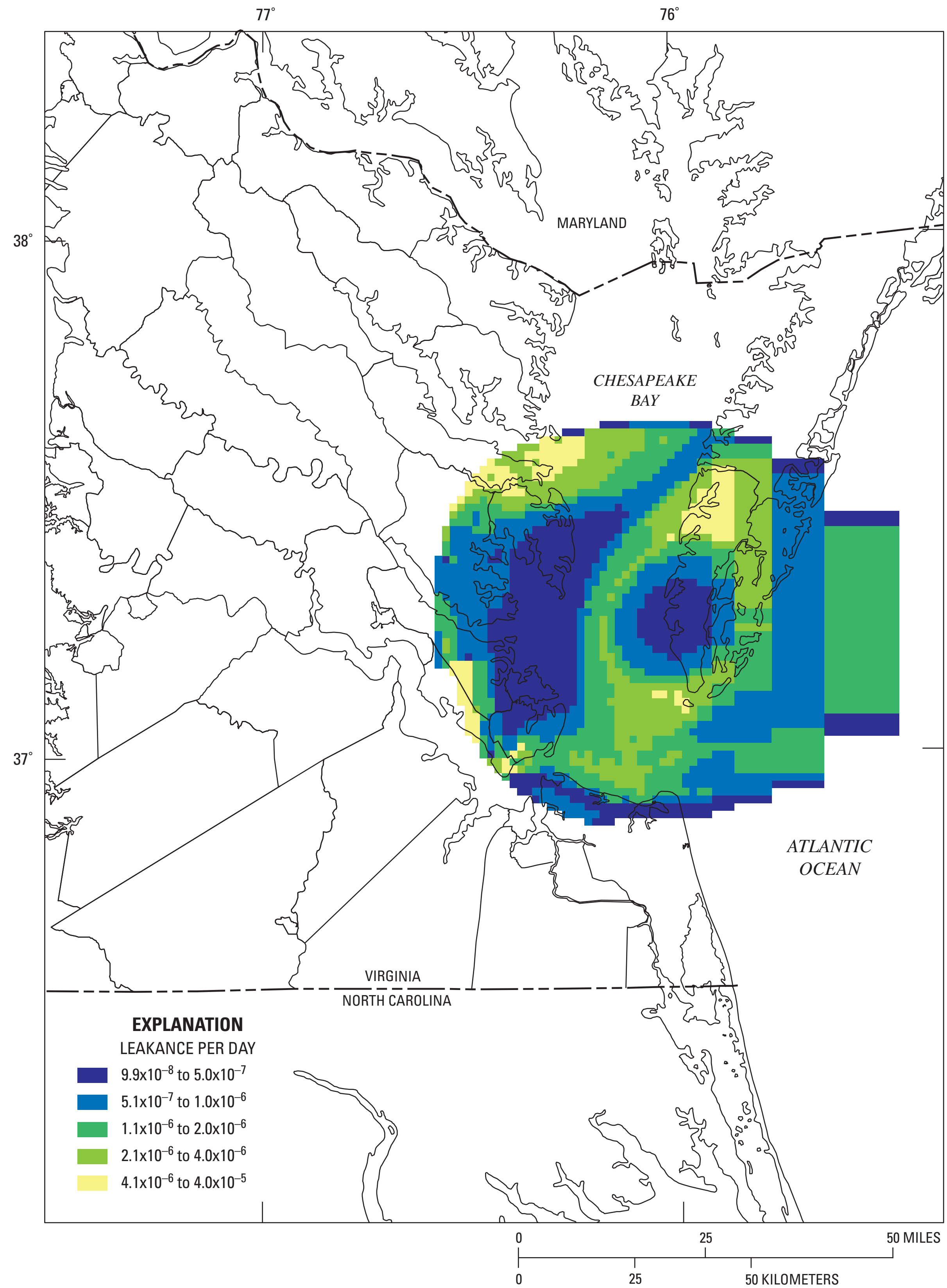

Figure 46e. Estimated leakance of the Exmore matrix confining unit of the Virginia Coastal Plain.

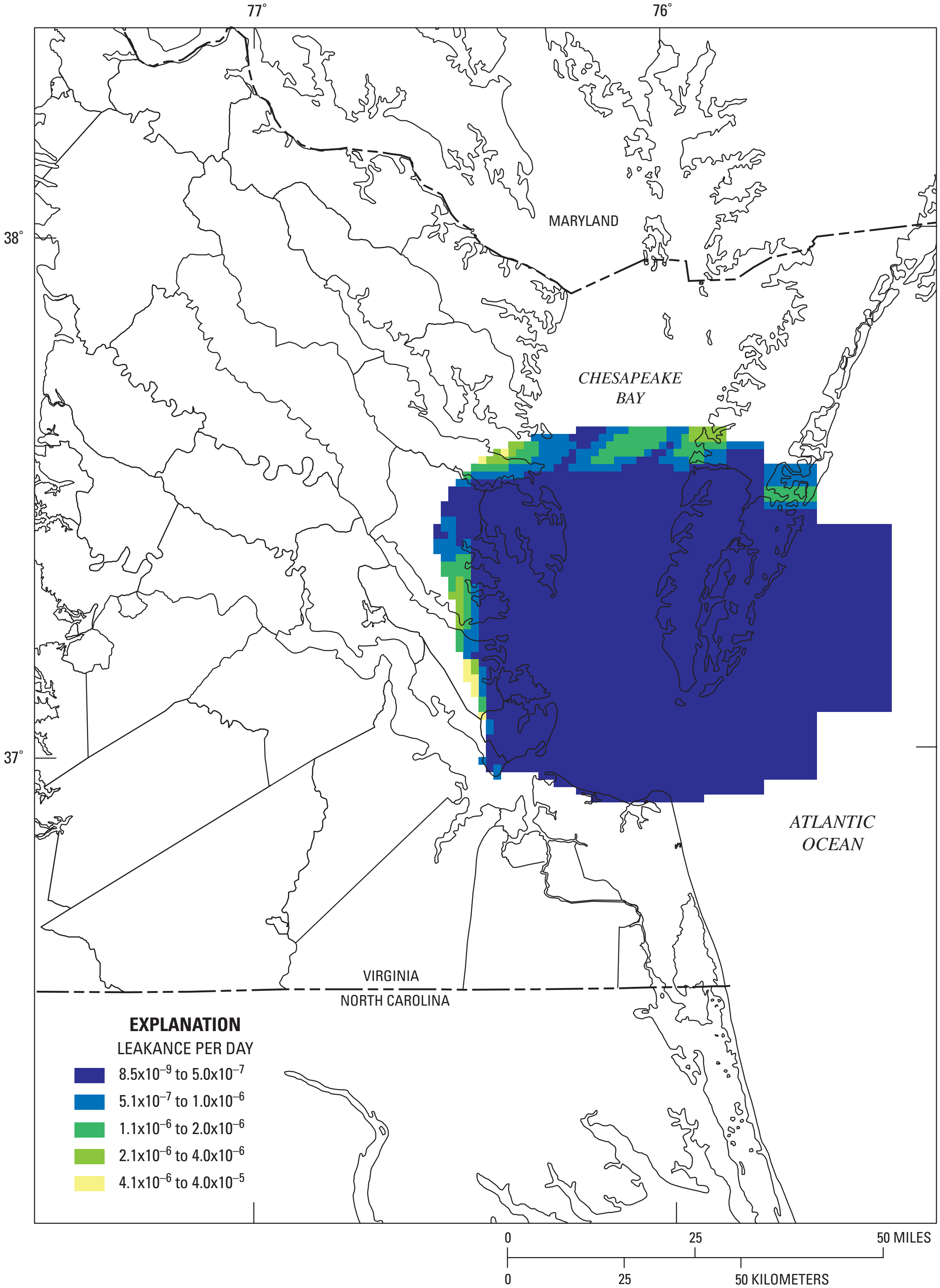

Figure 46f. Estimated leakance of the Exmore clast confining unit of the Virginia Coastal Plain.

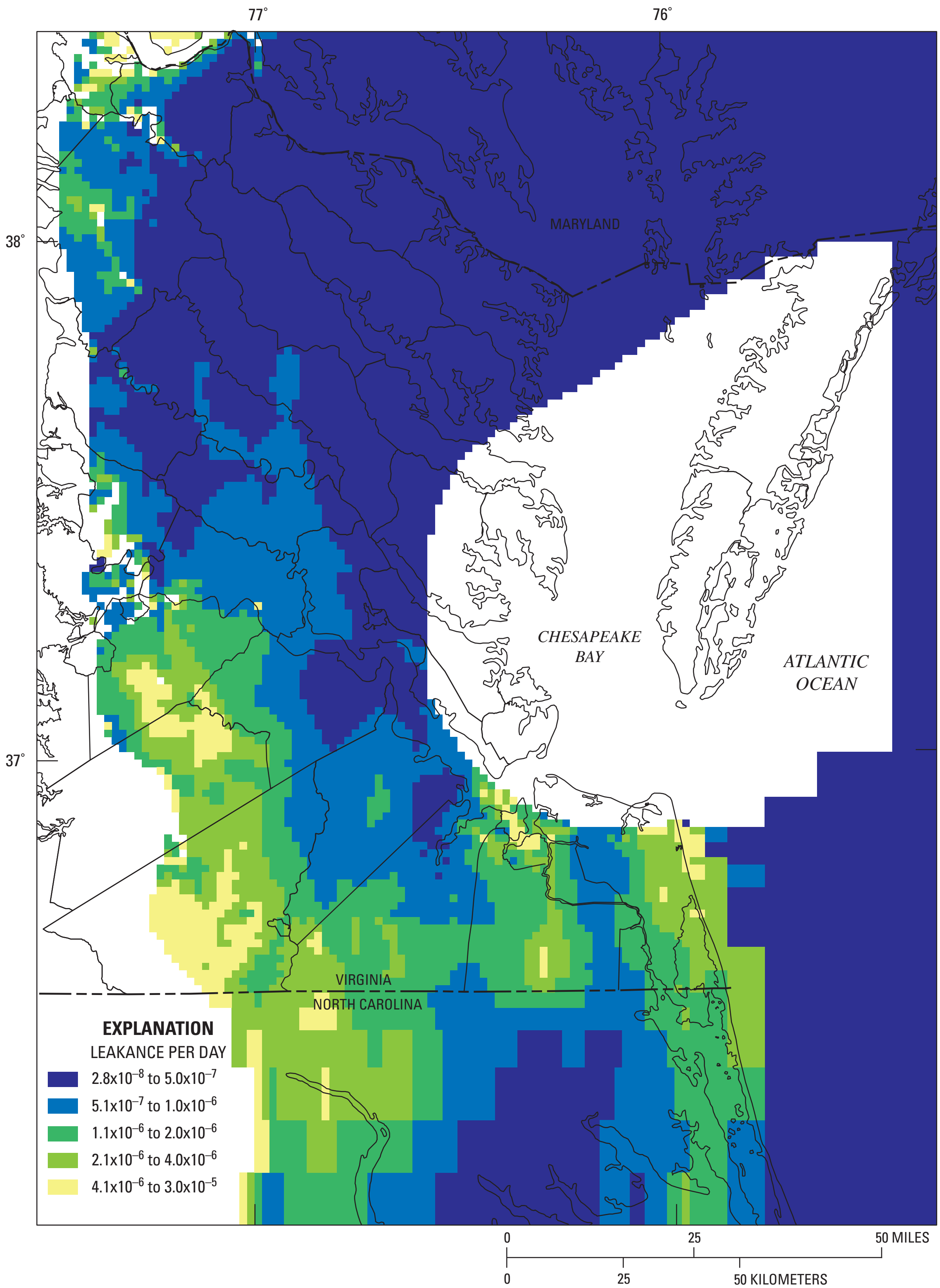

Figure 46g. Estimated leakance of the Nanjemoy-Marlboro confining unit of the Virginia Coastal Plain.

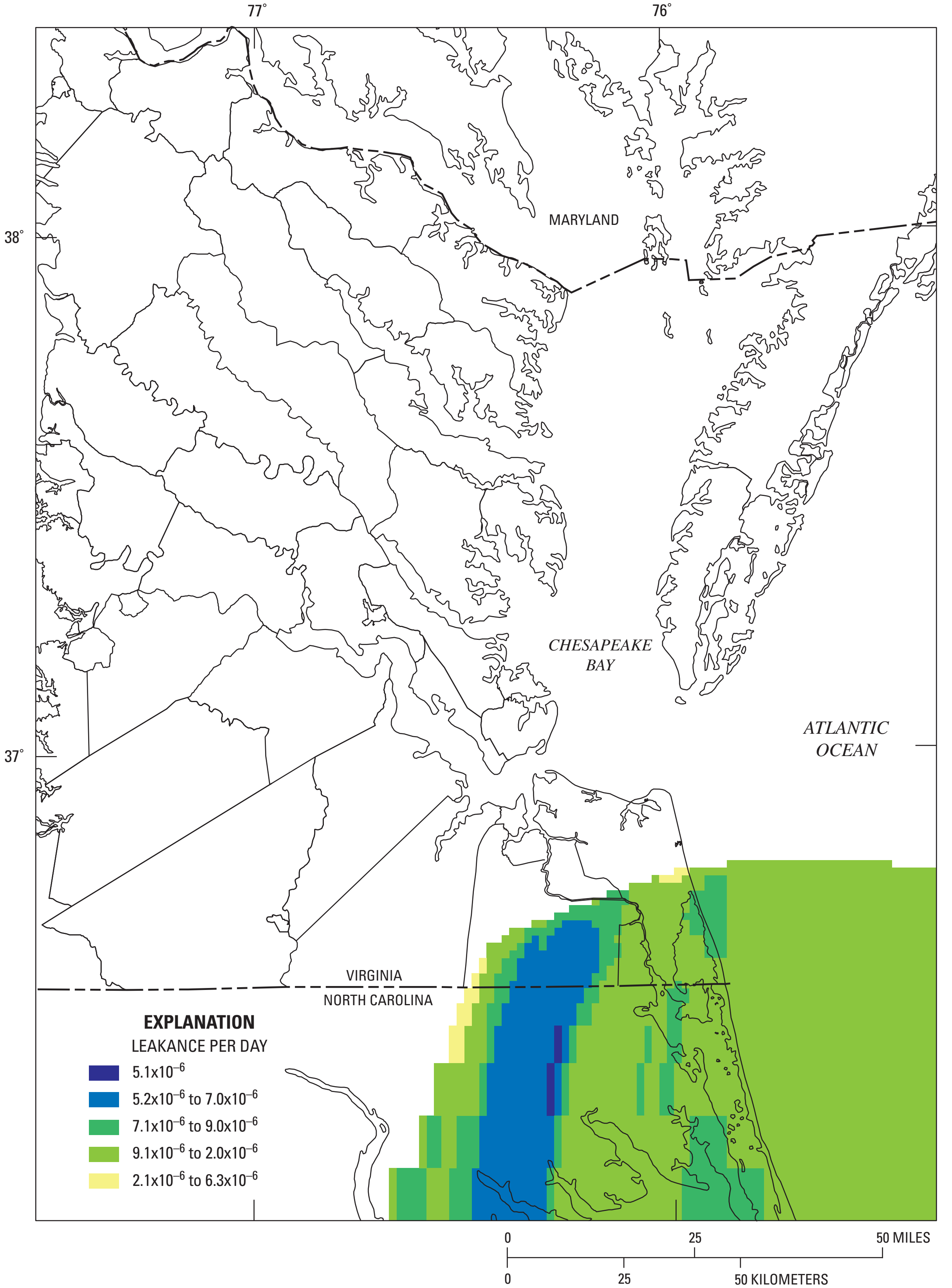

Figure 46h. Estimated leakance of the Peedee confining zone of the Virginia Coastal Plain.

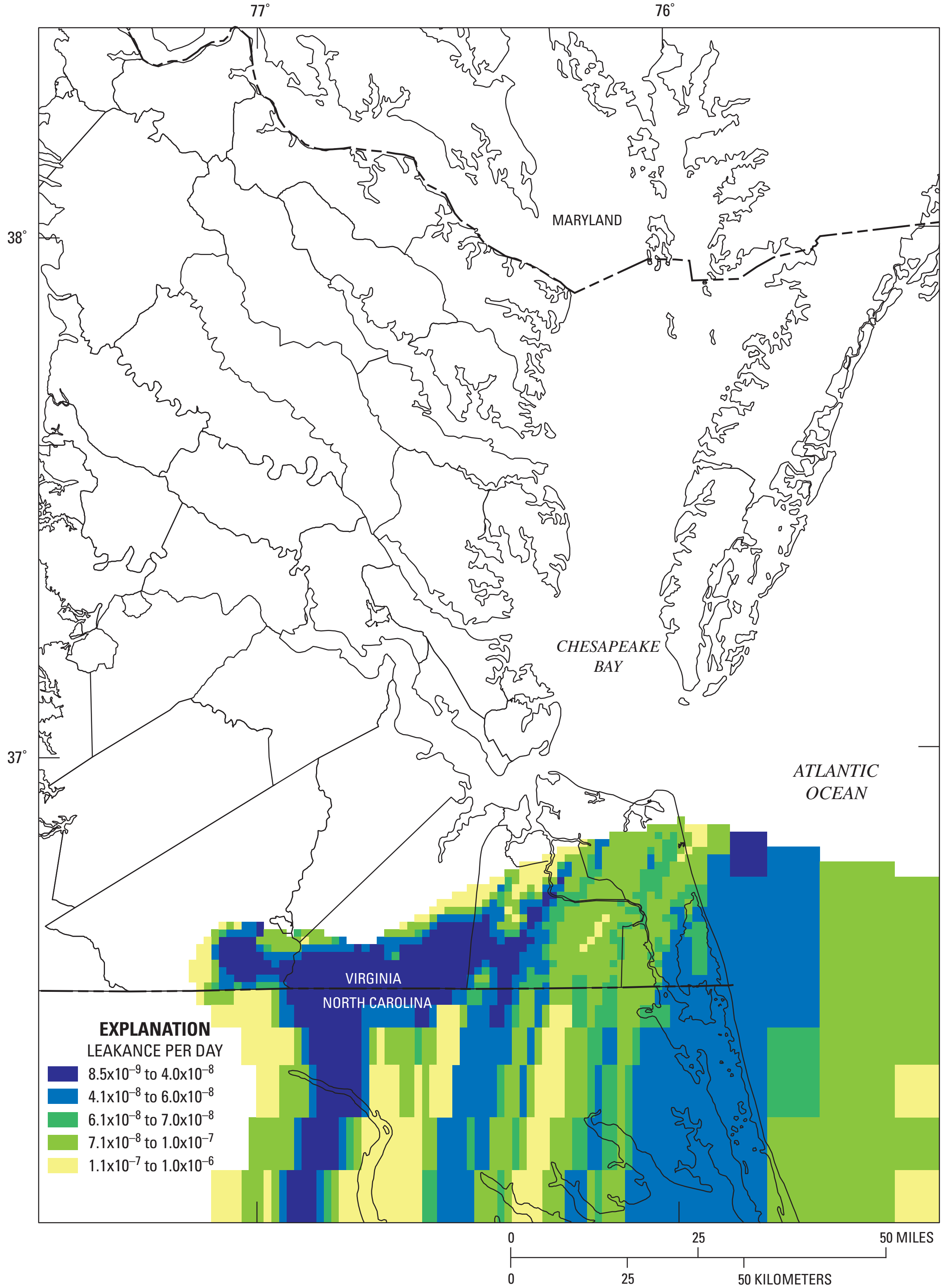

Figure 46i. Estimated leakance of the Virginia Beach confining zone of the Virginia Coastal Plain.

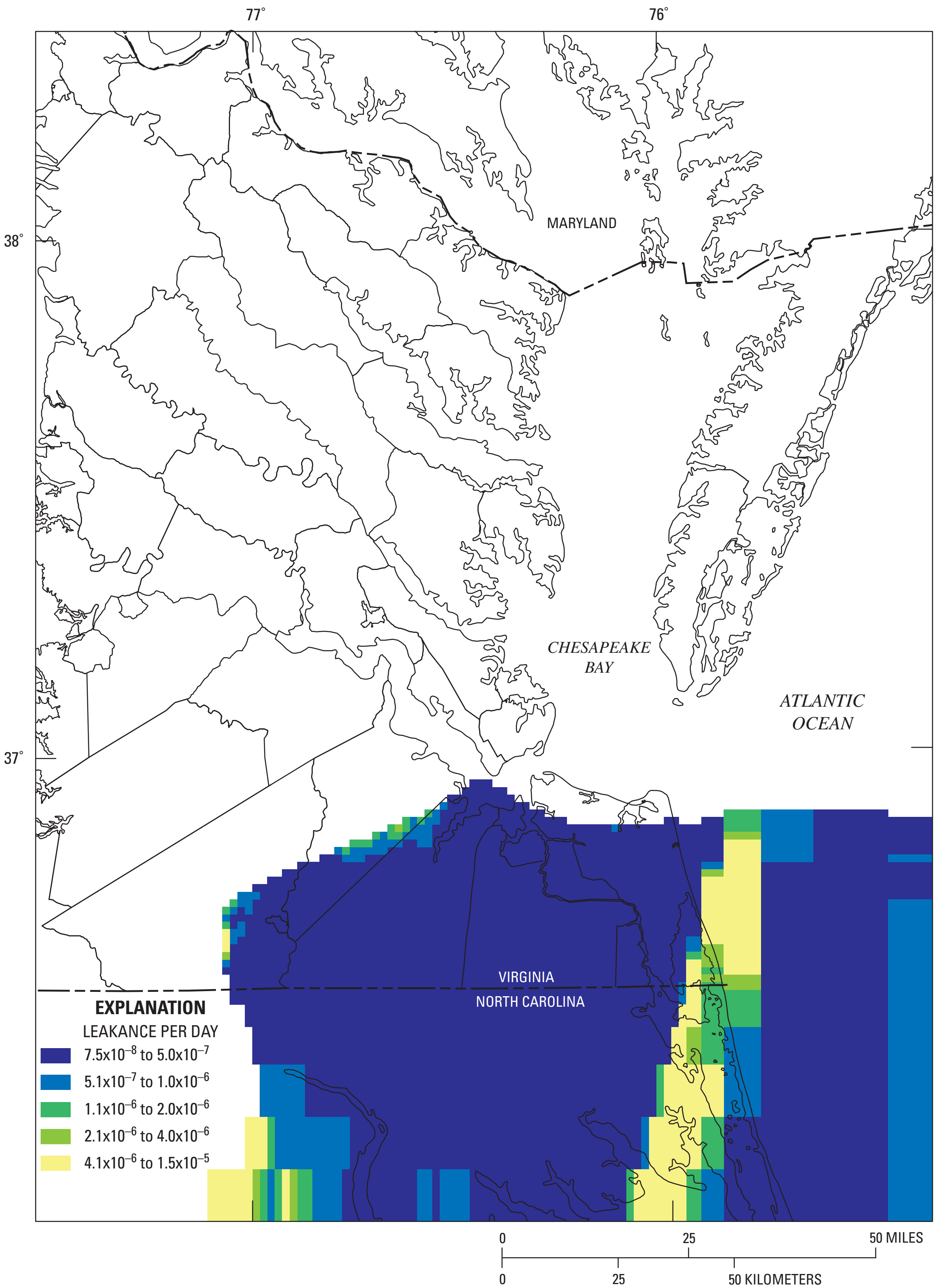

Figure 46j. Estimated leakance of the Upper Cenomanian confining unit of the Virginia Coastal Plain.

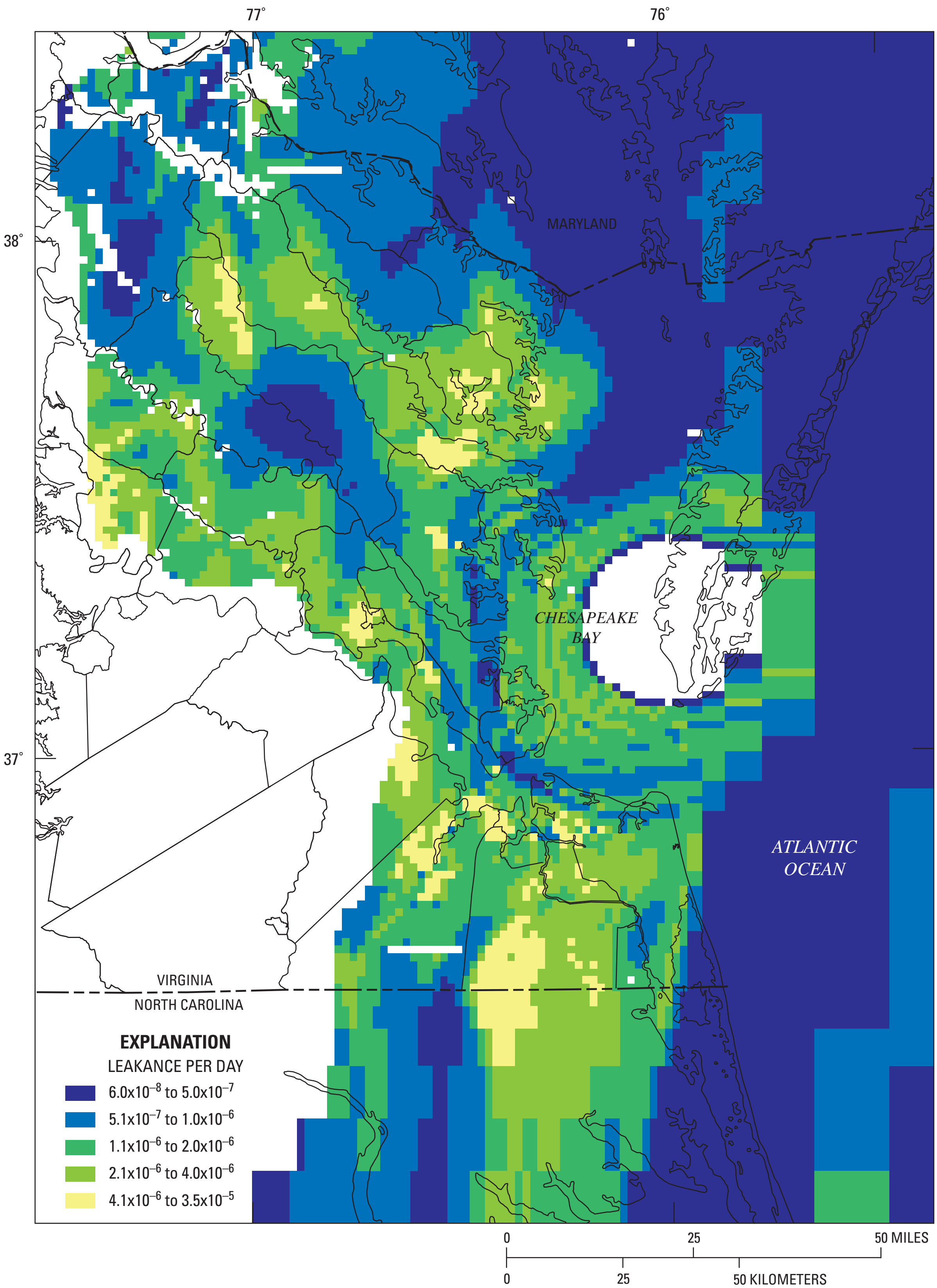

Figure 46k. Estimated leakance of the Potomac confining zone of the Virginia Coastal Plain.

Because the transient release of water stored in low-permeability confining units is simulated, the drawdown resulting from simulated pumping stresses may change substantially through time before reaching steady state. Model testing indicates that several decades may be required for the aquifer system to equilibrate, or approximate steady-state conditions, after an appreciable change in pumping conditions. One procedure sometimes used for assessing future groundwater levels for management purposes is to include all pumping stresses in a steady-state simulation. Such an evaluation of the "eventual water levels" does not consider the timing of influence of hydraulic boundaries and may, therefore, over- and under-predict water levels at different locations through time. A more accurate evaluation of probable future aquifer-system responses to proposed pumping should be attainable from transient simulations of water levels at different future times.

Summary

Groundwater withdrawals have lowered water levels in Virginia Coastal Plain aquifers and have resulted in drawdown in the Potomac aquifer exceeding 200 ft in some areas. The discovery of the buried impact crater beneath the Chesapeake Bay is the most dramatic of several changes in the conceptualization of the Virginia Coastal Plain hydrogeologic framework that affects the simulation of groundwater flow. In order to issue groundwater withdrawal permits, State water-management authorities need an improved groundwater model capable of predicting aquifer-system responses to proposed groundwater withdrawals. In response to this need, a transient, three-dimensional variable-density groundwater flow model of the Virginia Coastal Plain aquifer system was developed and calibrated.

The model simulates historical water levels and groundwater drawdown resulting from development since 1890. The 113-year historical transient simulation was time-discretized into 34 stress periods of various lengths. The spatial scale of the model is appropriate for assessing the regional water-level responses of the confined aquifers of the Coastal Plain. Because groundwater flow in the unconfined surficial aquifer is influenced by topography and streams that cannot be represented at the regional model scale, local horizontal groundwater flow through the surficial aquifer is not intended to be accurately simulated. However, vertical flow through the surficial aquifer from and to the water table in areas of groundwater recharge and discharge is simulated and allows transmission of groundwater to and from underlying confined aquifers. Representation of recharge, evapotranspiration, and interaction with surface-water features, such as major rivers, lakes, the Chesapeake Bay, and the Atlantic Ocean, enable simulation of shallow flow-system details that influence centers of recharge to and discharge from the deeper confined flow system. The increased groundwater density associated with the transition from fresh to salty groundwater near the Atlantic Ocean affects regional groundwater flow and was simulated with the VDF Process of SEAWAT. The specified groundwater density distribution was generated by a separate 108,000-year simulation of Pleistocene freshwater flushing around the Chesapeake Bay impact crater during transient sea-level changes, which is described in the appendix.

Specified-flux boundaries simulate increasing groundwater underflow out of the model domain into Maryland and a small amount of recharge underflow from the Piedmont Physiographic Province over the Norfolk Arch. Historically reported municipal, industrial, commercial, and public-supply groundwater withdrawals accounted for approximately 75 percent of total Coastal Plain groundwater withdrawals in the year 2000, the locations of which are known and were specified in the transient model. The remaining fraction of the total Coastal Plain groundwater withdrawals are unreported self-supplied domestic withdrawals, the locations of which are uncertain but were spatially estimated and allocated to individual aquifers.

The groundwater flow model was calibrated to 7,183 historic water-level observations from 497 observation wells with the parameter-estimation codes UCODE–2005 and PEST. Most water-level observations were from the Potomac aquifer system, which consequently enabled a more detailed estimation of the spatial distribution of hydraulic parameters than was possible for other hydrogeologic units. The zone-boundary approach was used to distribute hydraulic parameters according to known hydrogeologic boundaries and geologic features, such as the extent of the Chesapeake Bay impact crater. Spatial interpolation of horizontal hydraulic conductivity within the Potomac aquifer and vertical hydraulic conductivity within the Calvert confining unit was facilitated with the use of pilot points. The average (RMSE) of 5,087 weighted water-level residuals in Virginia is 3.6 ft, indicating a good fit of simulated to observed water levels and that the model is a good representation of the physical groundwater flow system. Magnitudes and distributions of water-level residuals indicate that, while not entirely absent, model bias is not problematic.

The simulated water-table altitude in the Virginia Coastal Plain varies with a higher spatial frequency than the potentiometric surface of any underlying confined aquifer. The simulated evapotranspiration flux largely controls the simulated water-table altitude, resulting in a water-table surface that is a smoothed and subdued replica of the land-surface altitude represented in the model EVT package. It is unlikely that the surficial aquifer conducts shallow groundwater flow horizontally for distances substantially greater than 1 mi because of the numerous rivers or non-simulated streams available for discharge.

Simulated contours of water levels in the Yorktown-Eastover aquifer indicate that predevelopment and current directions of groundwater flow are away from the higher-altitude areas in southern Virginia and near the midlines of the Northern Neck, Middle Peninsula, and York-James Peninsula toward discharge areas in lower altitude areas, including major rivers and the Chesapeake Bay.

Simulated steady-state water-level contours suggest that predevelopment groundwater flowed from west to east through the St. Marys aquifer. Water levels simulated in the St. Marys aquifer for 2003 are up to 40 ft lower than those simulated for predevelopment time, but suggest similar flow directions.

Simulated predevelopment groundwater flow in the Piney Point aquifer is from western up-dip areas toward the east and southeast, where it discharges through the overlying Calvert confining unit near the Atlantic coast. By 2003, groundwater withdrawals had formed several cones of depression, with a simulated maximum drawdown of 127 ft. Groundwater flow within the Piney Point aquifer is directed toward these drawdown cones in the vicinity of the Middle and York-James Peninsulas.

The simulated steady-state groundwater flow within the Aquia aquifer originated from western up-dip areas and flowed toward the east, where flow paths split around low-permeability hydrogeologic units within the Chesapeake Bay impact crater. By 2003, groundwater withdrawals had produced a broad area of lower water levels west of the Chesapeake Bay impact crater, where the maximum groundwater level drawdown was 135 ft. Substantial simulated groundwater withdrawals from the Aquia aquifer in southern Maryland have produced a well-defined cone of depression there.

Contours of the simulated steady-state water levels in the Peedee aquifer indicate that predevelopment groundwater flowed from west to east through the aquifer. Observed water levels and the simulated potentiometric surface for 2003 indicate that water levels have declined in the western area of the Peedee aquifer, possibly because of flow to hydraulically connected aquifers in North Carolina.

Contours of the simulated steady-state water levels in the Virginia Beach aquifer indicate that predevelopment groundwater flowed from western up-dip areas through the Virginia Beach aquifer toward the east. Reported and self-supplied withdrawals from the Virginia Beach aquifer in southeast Virginia have caused simulated water levels to decline, resulting in a relatively flat simulated potentiometric surface at the end of 2003. Simulated conditions in the Virginia Beach aquifer are poorly constrained because of the lack of observation wells.

Simulated steady-state water levels at the top of the Potomac aquifer indicate a complex pattern of predevelopment groundwater flow that was influenced by the proximity of sea level along the James River near the Fall Line. Simulated water-level contours east of the Fall Line in the northern and southern Coastal Plain indicate west to east paths of groundwater flow, which became northeasterly and southeasterly where flow bifurcated on either side of the Chesapeake Bay impact crater. Between these areas and east of Richmond, groundwater flow from the north and south converged to flow west and discharge to the James River.

Industrial and municipal groundwater withdrawals, which began to increase during the 1940s, have resulted in a substantial decline of water levels in the Potomac aquifer and in the formation of two major cones of depression in Virginia centered near Franklin and West Point. The maximum simulated drawdown near the top of the Potomac aquifer was 235 ft near Franklin and 232 ft near West Point by the year 2003. As a result of these declines, regional groundwater flow velocities within the Potomac aquifer have changed substantially from their predevelopment state and generally are directed toward either of the major withdrawal centers at Franklin or West Point. The water-level gradients near the Atlantic coast have reversed from their predevelopment direction, which has increased the potential for landward transport of salty water toward production wells.

Acknowledgments

Discussions with Robin Patton, Beverly Quinlan, T. Scott Bruce, and Terry D. Wagner of the Virginia DEQ, and Scott Emry and Whitney Katchmark of HRPDC provided useful guidance for this study. Additional discussions with and assistance from Leonard Orzol, Mary Hill, Eileen Poeter, Steffen Mehl, Richard Yager, Christian Langevin, Randall McFarland, Ward Sanford, and other USGS colleagues are greatly appreciated. A substantial portion of this study was supported by the USGS Office of Groundwater (OGW) through the Groundwater Resources Program. The authors thank the OGW for its support of the study.

References Cited

Anderman, E.R., and Hill, M.C., 2000, MODFLOW–2000, The U.S. Geological Survey modular ground-water model—Documentation of the Hydrogeologic-Unit Flow (HUF) package: U.S. Geological Survey Open-File Report 00–342, 89 p.

Anderman, E.R., and Hill, M.C., 2003, MODFLOW–2000, the U.S. Geological Survey modular ground-water model—Three additions to the Hydrogeologic-Unit Flow (HUF) Package—Alternative storage for the uppermost active cells, flows in hydrogeologic units, and the hydraulic-conductivity depth-dependence (KDEP) capability: U.S. Geological Survey Open-File Report 03–347, 36 p.

Canadell, J., Jackson, R.B., Ehleringer, J.R., Mooney, H.A., Sala, O.E., and Schulze, E.D., 1996, Maximum rooting depth of vegetation types at the global scale: Oecologia, v. 108, p. 583–595.

Cederstrom, D.J., 1943, Chloride in groundwater in the coastal plain in southeastern Virginia: Virginia Geological Survey Bulletin 58, 36 p. 4 pl.

Cederstrom, D.J., 1945, Geology and ground-water resources of the Coastal Plain in southeastern Virginia: Virginia Geological Survey Bulletin 63, 384 p.

Cederstrom, D.J., 1957, Geology and ground-water resources of the York-James Peninsula, Virginia: U.S. Geological Survey Water-Supply Paper 1361, 237 p.

Cederstrom, D.J., 1969, Geology and ground-water resources of the Middle Peninsula, Virginia: U.S. Geological Survey Open-File Report 69–37, 231 p.

Cooper, H.H., and Jacob, C.E., 1946, A generalized graphical method for evaluating formation constants and summarizing well field history: American Geophysical Union Trans., v. 27, p. 526–534.

Daniel, C.C., III, 1989, Statistical analysis relating well yield to construction practices and siting of wells in the Piedmont and Blue Ridge Provinces of North Carolina: U.S. Geological Survey Water-Supply Paper 2341–A, 27 p.

Doherty, John, 2003, Ground water model calibration using pilot points and regularization: Ground Water, v. 41, no. 2, p. 170–177.

Doherty, John, 2004, PEST model-independent parameter estimation (5th ed.): Corinda, Australia, Watermark Numerical Computing, 336 p.

Domenico, P.A., and Mifflin, M.D., 1965, Water from low-permeability sediments and land subsidence: Water Resources Research, v. 1, no. 4, p. 563–576.

Domenico, P.A., and Schwartz, F.W., 1990, Physical and chemical hydrogeology: New York, John Wiley & Sons, 824 p.

Epstein, V.J., 1987, Hydrologic and geologic factors affecting land subsidence near Eloy, Arizona: U.S. Geological Survey Water-Resources Investigations Report 87–4143, 28 p.

Gardner, W.R., and Fireman, M., 1958, Laboratory studies of evaporation from soil columns in the presence of a water table: Soil Science, v. 85, p. 244–249.

Guo, W., and Langevin, C.D., 2002, User's guide to SEAWAT; a computer program for simulation of three-dimensional variable-density ground-water flow: U.S. Geological Survey Techniques of Water-Resources Investigations 6–A7, 77 p.

Halford, K.J., and Hanson, R.T., 2002, User guide to the drawdown-limited, multi-node well (MNW) package for the U.S. Geological Survey's modular three-dimensional finite-difference ground-water flow model, versions MODFLOW–96 and MODFLOW–2000: U.S. Geological Survey Open-File Report 02–293, 33 p.

Harbaugh, A.W., 1990, A computer program for calculating subregional water budgets using results from the U.S. Geological Survey modular three-dimensional finite-difference ground-water flow model: U.S. Geological Survey Open-File Report 90–392, 24 p.

Harbaugh, A.W., Banta, E.R., Hill, M.C., and McDonald, M.G., 2000, MODFLOW–2000, the U.S. Geological Survey modular ground-water model—User guide to modularization concepts and the ground-water flow process: U.S. Geological Survey Open-File Report 00–92, 121 p.

Harsh, J.F., and Laczniak, R.J., 1990, Conceptualization and analysis of ground-water flow system in the Coastal Plain of Virginia and adjacent parts of Maryland and North Carolina: U.S. Geological Survey Professional Paper 1404–F, 100 p.

Helm, D.C., 1974, Evaluation of stress-dependent aquitard parameters by simulation of observed compaction from known stress history: Berkeley, University of California, Ph.D. dissertation, 175 p.

Heywood, C.E., 1995, Investigation of aquifer-system compaction in the Hueco Basin, El Paso, Texas, USA, *in* Proceedings of the Fifth International Symposium on Land Subsidence: The Hague, IAHS Publication no. 234, p. 35–45.

Heywood, C.E., 1998, Piezometric—Extensometric estimations of specific storage in the Albuquerque Basin, New Mexico, *in* Borchers, J.W., ed., Land subsidence case studies and current research; Proceedings of the Dr. Joseph F. Poland symposium on land subsidence, Association of Engineering Geologists Special Publication No. 8, Belmont, Calif., Star Publishing Company, p. 435–440.

Hill, M.C., 1998, Methods and guidelines for effective model calibration: U.S. Geological Survey Water-Resources Investigations Report 98–4005, 90 p.

Hill, M.C., Banta, E.R., Harbaugh, A.W., and Anderman, E.R., 2000, MODFLOW–2000, The U.S. Geological Survey modular ground-water model—User guide to the observation, sensitivity, and parameter-estimation processes and three post-processing programs: U.S. Geological Survey Open-File Report 00–0184, 209 p.

Hill, M.C., and Tiedeman, C.R., 2007, Effective groundwater model calibration—with analysis of data, sensitivities, predictions, and uncertainty: Hoboken, NJ, John Wiley & Sons, 455 p.

Ireland, R.L., Poland, J.F., and Riley, F.S., 1984, Land subsidence in the San Joaquin Valley, California, as of 1980: U.S. Geological Survey Professional Paper 437–I, 105 p., 1 pl.

Johnson, A.I., 1967, Specific yield—Compilation of specific yields for various materials: U.S. Geological Survey Water-Supply Paper 1662–D, 74 p.

Kernodle, J.M., and Philip, R.D., 1988, Using a geographic information system to develop a ground-water flow model: American Water Resources Association Monograph, series no. 14, p. 191–202.

Langevin, C.D., Shoemaker, W.B., and Guo, W., 2003, MODFLOW–2000, The U.S. Geological Survey modular groundwater model—Documentation of the SEAWAT–2000 version with the variable-density flow process (VDF), and the integrated MT3DMS transport process (IMT): U.S. Geological Survey Open-File Report 03–426, 43 p.

Larsen, C.E., and Clark, I., 2003, Scale in sea level studies *in* Book of Abstracts, Coastal Sediments ‘03, Crossing Disciplinary Boundaries: Fifth International Symposium on Coastal Engineering and Science of Coastal Sediment Processes, May 18–23, 2003, Clearwater, FL, p. 432–433.

Leake, S.A., and Claar, D.V., 1999, Procedures and computer programs for telescopic mesh refinement using MODFLOW: U.S. Geological Survey Open-File Report 99–238, 53 p.

Leake, S.A., and Lilly, M.R., 1997, Documentation of a computer program (FHB1) for assignment of transient specified-flow and specified-head boundaries in applications of the Modular Finite-Difference Ground-Water Flow Model (MODFLOW): U.S. Geological Survey Open-File Report 97–571, 56 p.

Leahy, P.P., and Martin, M., 1993, Geohydrology and simulation of ground-water flow in the northern Atlantic Coastal Plain aquifer system: U.S. Geological Survey Professional Paper 1404–K, 81 p.

McDonald, M.G., and Harbaugh, A.W., 1988, A modular three-dimensional finite-difference ground-water flow model: U.S. Geological Survey Techniques of Water-Resources Investigations, book 6, chap. A1, 586 p.

McFarland, E.R., 1998, Design, revisions, and considerations for continued use of a ground-water-flow model of the Coastal Plain aquifer system in Virginia: U.S. Geological Survey Water-Resources Investigations Report 98–4085, 49 p.

McFarland, E.R., and Bruce, T.S., 2005, Distribution, origin, and resource-management implications of ground-water salinity along the western margin of the Chesapeake Bay impact structure in eastern Virginia, *in* Horton, J.W., Jr., Powars, D.S., and Gohn, G.S., eds., Studies of the Chesapeake Bay impact structure—The USGS–NASA Langely corehole, Hampton, Virginia, and related coreholes and geophysical surveys: U.S. Geological Survey Professional Paper 1688, chap. K, 32 p.

McFarland, E.R., and Bruce, T.S., 2006, The Virginia Coastal Plain hydrogeologic framework: U.S. Geological Survey Professional Paper 1731, 118 p. 25 pls.

Meisler, H., 1989, The occurrence and geochemistry of salty ground water in the northern Atlantic Coastal Plain: U.S. Geological Survey Professional Paper 1404–D, 51 p.

Meisler, H., Leahy, P.P., and Knobel, L.L., 1984, Effect of eustatic sea-level changes on saltwater-freshwater in the Northern Atlantic Coastal Plain: U.S. Geological Survey Water-Supply Paper 2255, 28 p.

Meng, A.A., III, and Harsh, J.F., 1988, Hydrogeologic framework of the Virginia Coastal Plain: U.S. Geological Survey Professional Paper 1404–C, 82 p.

National Climate Data Center, 2002, accessed March 20, 2009, at http://www.ncdc.noaa.gov/oa/ncdc.html

Nelms, D.L., Harlow, G.E., Plummer, N., and Busenberg, E., 2003, Aquifer susceptibility in Virginia, 1998–2000: U.S. Geological Survey Water-Resources Investigations Report 03–4278, 58 p.

Orzol, L.L., 1997, User’s guide for MODTOOLS—Computer programs for translating data of MODFLOW and MODPATH into geographic information system files: U.S. Geological Survey Open-File Report 97–240, 86 p.

Peltier, R.W., 1994, Ice age paleotopography: Science, v. 265, p. 195–201.

Poag, C.W., 1999, Chesapeake invader—Discovering America’s giant meteorite crater: Princeton, NJ, Princeton University Press, 183 p.

Poag, W.C., Powars, D.S., Poppe, L.J., and Mixon, R.B., 1994, Meteoroid mayhem in Ole Virginny—Source of the North American tektite strewn field: Geology, v. 22, p. 691–694.

Poeter, E.P., Hill, M.C., and Banta, E.R., 2005, UCODE_2005 and six other computer codes for universal sensitivity analysis, calibration, and uncertainty evaluation: U.S. Geological Survey Techniques and Methods, book 6, chap. 11, 283 p.

Pollock, D.W., 1994, Users guide for MODPATH/MODPATH-PLOT, version 3: A particle tracking post-processing package for MODFLOW, the U.S. Geological Survey finite-difference ground-water flow model: U.S. Geological Survey Open-File Report 94–464, 249 p.

Pope, J.P., and Burbey, T., 2004, Multiple-aquifer characterization from single borehole extensometer records: Groundwater, v. 42, no. 1, p. 45–58.

Pope, J.P., McFarland, E.R., and Banks, R.B., 2007, Private domestic-well characteristics and the distribution of domestic withdrawals among aquifers in the Virginia Coastal Plain: U.S. Geological Survey Scientific Investigations Report 2007–5250, 47 p., http://pubs.usgs.gov/sir/2007/5250/

Powars, D.S., 2000, The effects of the Chesapeake Bay impact crater on the geologic framework and the correlation of hydrogeologic units of Southeastern Virginia, south of the James River: U.S. Geological Survey Professional Paper 1622, 53 p., 1 pl.

Powars, D.S., and Bruce, T.S., 1999, The effects of the Chesapeake Bay impact crater on the geological framework and correlation of hydrogeologic units of the lower York-James Peninsula, Virginia: U.S. Geological Survey Professional Paper 1612, 82 p., 9 pls.

Powell, J.D., and Abe, J.M., 1985, Availability and quality of ground water in the Piedmont province of Virginia: U.S. Geological Survey Water-Resources Investigations Report 85–4235, 32 p.

Quinlan, B.J., 2004, Virginia Coastal Plain model 2002 withdrawals simulation, reported use: Virginia Department of Environmental Quality, Water Resources Division, Office of Ground-Water Withdrawal Permitting, 37 p.

Quinlan, B.J., 2005, Virginia Coastal Plain model 2004 withdrawals simulation: Virginia Department of Environmental Quality, Water Resources Division, Office of Ground-Water Withdrawal Permitting, 43 p.

Richardson, D.L., 1994a, Hydrogeology and analysis of the ground-water flow system of the Eastern Shore, Virginia: U.S. Geological Survey Water-Supply Paper 2401, 82 p., 1 pl.

Richardson, D.L., 1994b, Ground-water discharge from the Coastal Plain of Virginia: U.S. Geological Survey Water-Resources Investigation Report 93–4191, 15 p.

Riley, F.S., 1998, Mechanics of aquifer systems—The scientific legacy of Joseph F. Poland, *in* Borchers, J.W., ed., Land subsidence case studies and current research, Proceedings of the Dr. Joseph F. Poland symposium on land subsidence: Belmont, CA, Star Publishing Company, Association of Engineering Geologists Special Publication No. 8, p. 13–27.

Rutledge, A.T., 1993, Computer programs for describing the recession of ground-water discharge and for estimating mean ground-water recharge and discharge from streamflow records: U.S. Geological Survey Water-Resources Investigation Report 93–4121, 45 p.

Sanford, S., 1913, The underground water resources of the Coastal Plain province of Virginia: Virginia Geological Survey Bulletin No. 5, 361 p.

Sanford, W.E., Pope, J.P., and Nelms, D.L., 2009, Simulation of ground-water level and salinity changes in the Eastern Shore, Virginia: U.S. Geological Survey Scientific Investigations Report 2009–5006, 125 p.

Thornthwaite, C.W., 1948, An approach toward a rational classification of climate: Geographic Review, v. 38, p. 55–94.

University of Virginia Climatology Office, 2007; accessed on March 6, 2008, at http://climate.virginia.edu/

U.S. Geological Survey, 2002, National Water-Use Information Program 2000 data for counties; accessed in May 2002 at http://water.usgs.gov/watuse/

Vecchia A.V., and Cooley, R.L., 1987, Simultaneous confidence and prediction intervals for nonlinear regression models with application to a groundwater flow model: Water Resources Research, v. 22, no. 2, p. 95–108.

Wright, J., 2006, Virginia Coastal Plain model 2005 withdrawals simulation: Virginia Department of Environmental Quality, Water Resources Division, Office of Ground-Water Withdrawal Permitting, 50 p.

Zheng, C., and Wang, P., 1999, MT3DMS—A modular three-dimensional multispecies transport model for simulation of advection, dispersion, and chemical reactions of contaminants in groundwater systems—Documentation and user's guide: U.S. Army Corps of Engineers, U.S. Army Engineer Research and Development Center, Strategic Environmental Research and Development Program, 221 p.

Appendix

Transient Saltwater-Transport Simulation

A three-dimensional digital representation of the Virginia Coastal Plain groundwater density distribution is needed for SEAWAT to realistically simulate regional groundwater flow near the saltwater transition zone. A preliminary simulation of Coastal Plain saltwater transport generated a saltwater distribution in reasonable agreement with observed concentration data and supported the "differential flushing" hypothesis for the persistence of saltwater within the Chesapeake Bay impact crater (Heywood, 2003). A possible alternative approach for generating a representative density distribution is extrapolation of observed concentration data, which is sparse in Virginia and preferentially samples low-concentration areas in relatively high-permeability hydrogeologic units. The modeling approach described in this appendix was considered superior because it facilitated generation of a three-dimensional density distribution consistent with the geometry of aquifers and confining units in the hydrogeologic framework. The model described in this section employs different boundary conditions than are employed for the model described in the main report. To avoid confusion, the 108,000-year saltwater-transport model described in this appendix is termed the "glacial model," whereas the term "historical model" refers to the 113-year transient model described in the main report body.

The objective of the glacial model was to generate a reasonable approximation of the present saltwater transition zone, across which groundwater density increases by about 2.5 percent. The late Pleistocene through Holocene epochs are simulated in the glacial model, during which multiple ice ages caused sea-level transgressions and regressions across the continental shelf and current Coastal Plain of Virginia (fig. A1). This history of late Quaternary sea-level change has influenced the configuration of the resulting (present day) saltwater transition zone. During Pleistocene glacial periods, when sea level was as much as 300 ft below its current level, the average hydraulic gradient through Coastal Plain hydrogeologic units was three to four times greater than present, and local gradients near the present day Atlantic coast were substantially greater. These gradients enabled enhanced flushing of meteoric groundwater through relatively hydraulically conductive hydrogeologic units. Saltwater was retained in areas of low regional horizontal hydraulic conductivity, such as the crater-filling clast- and matrix-supported Exmore confining units (Exmore Tsunami Breccia). In the glacial simulation described in this appendix, recharged freshwater displaced and mixed with saltwater to form a freshwater-saltwater transition zone that migrates toward a position of hydrodynamic equilibrium.

A subsidiary use of the glacial model was for simulation of the fraction of Carbon-14 (^{14}C) in the dissolved carbon in Coastal Plain groundwater. Groundwater age dates can be used as a surrogate for flow data, such as streamflow gains and losses, in constraining values of groundwater flux (and hence recharge and hydraulic conductivities) through the aquifer system. Simulations of ^{14}C ages using particle tracking with the steady-state stress period of the historical Coastal Plain model were unsatisfactory, in part, because the simulated hydraulic gradients were not representative of the probable Coastal Plain hydraulic gradients during the Pleistocene ice ages, during which older-observed waters were transported from their recharge areas. Apparent groundwater ages calculated from Coastal Plain ^{14}C observations generally increase from west to east and with depth and range from about 9,000 to 40,000 radiocarbon years (Nelms and others, 2003). The time scale of the glacial model was sufficiently long to simulate the effect of sea-level changes on hydraulic gradients and consequent transport velocities. Dissolved ^{14}C concentrations were simulated by specifying the ^{14}C radioactive-decay rate in the MT3DMS (Zheng and Wang, 1999) Chemical Reaction Package in SEAWAT–2000. Because the constituent lithologies of Virginia Coastal Plain hydrogeologic units are predominantly siliciclastic, with negligible carbonate rocks, the effects of carbon-exchange reactions in the aquifers and confining units were not simulated. The simulated ^{14}C concentration distribution (expressed as Percent-Modern-Carbon) is in general agreement with ^{14}C observations (considering the probable range of effective porosity and other uncertainties) and served to validate the conceptual flow model and the simulated recharge (within an order of magnitude).

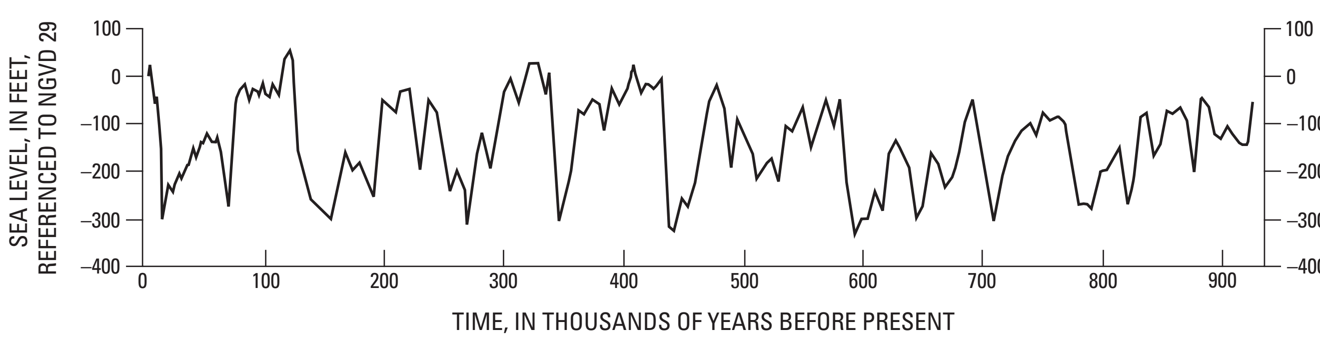

Figure A1. Sea levels during the Pleistocene and Holocene epochs (modified from Zellmer, 1979).

Boundary Condition Modifications

The model domain, hydrogeologic framework, and associated hydraulic properties of the glacial model described in this appendix are identical to those of the historical model. The purpose of the glacial model required changing the top-surface boundary conditions of the standard model to simulate changes in sea level. The head-dependent flux boundaries at the top surface of the historical model used to simulate recharge, evapotranspiration, and seepage to and from rivers, the Chesapeake Bay, and the Atlantic Ocean floor were replaced by time-varying specified-head boundaries, which were simulated with the FHB package (Leake and Lilly, 1997). Specified-head boundaries on the continental shelf and slope represented lowered sea levels at various times during the late-Pleistocene simulation. The water level in the top-most-active finite-difference cell at each row-column location was specified as the greater of either the cell-surface altitude or the Pleistocene sea level. Cell-surface altitudes were referenced to NGVD 29 and are negative for cells under the Chesapeake Bay or Atlantic Ocean. The FHB package internally interpolated sea levels between the specified levels (table A1) at times selected to represent the Pleistocene sea-level history depicted in figure A1.

Table A1. Specified Pleistocene-Epoch sea levels.

Simulation time (years)	Sea level (feet NGVD 29)	Time before present (years)
0	–30	108,000
28,000	–30	80,000
38,000	–270	70,000
48,000	–130	60,000
63,000	–300	45,000
94,000	–300	14,000
101,000	–30	7,000
108,000	0	0

The solute concentrations at specified-head boundaries were specified to simulate appropriate recharge concentrations. Recharge through areas with top-surface altitudes above the simulated sea level (table A1) was specified at the freshwater concentration; boundary concentrations at areas below the simulated sea level were specified at the seawater concentration.

Initial Conditions

Solute initial conditions were specified homogeneously at seawater concentration. This simple initial condition represents the salinity distribution that might have existed following a marine transgression similar to that which occurred during the Pliocene epoch. The extent of saltwater inundation into Coastal Plain sediments resulting from the Pleistocene marine transgression during the Eemian-Sangamon interglacial era (130,000–115,000 years before present) is uncertain and may not have been as extensive as during the Pliocene epoch. Because simulated saltwater is transported from shallow and western Coastal Plain sediments after several thousand years, the specified homogeneous initial condition does not substantially alter the final simulated configuration of the saltwater transition zone.

Simulation of Mass Transport

Values of aquifer-system properties required for variable-density flow and mass transport simulation are summarized in table A2. To facilitate model calibration to different salinity indicators, the groundwater-solute concentration C was normalized to the concentration for a seawater density ρ_s. The groundwater density was calculated from the equation of state where $\partial\rho/\partial C = 1.56$ lb/ft^3 for the normalized solute concentration C. Numerical dispersion of simulated concentrations may generate unrealistic densities; such effects were controlled by limiting calculated groundwater densities to range between the values corresponding to freshwater and seawater concentrations (table A2). Neither chemical reactions nor sorption were simulated because the major solute species comprising seawater are not considered to react or adsorb on the porous media.

The governing equations for variable-density groundwater flow and mass transport (see Numerical Method section of main report) were explicitly coupled and iteratively solved (with a one time step lag) by the Variable-Density Flow (VDF) and Integrated Mass Transport (IMT) processes of SEAWAT–2000 (Langevin and others, 2003).

The mass-transport equation was solved with implicit finite differences using upstream weighting and a Courant number of 1. Upstream weighting was computationally

Table A2. Values used for transport simulation.

[ft, feet; ft^2/d, feet squared per day; lb/ft^3, pound per cubic foot]

Symbol	Parameter name	Value
α_L	longitudinal dispersivity	100 ft
α_{TH}	transverse horizontal dispersivity	10 ft
α_{TV}	transverse vertical dispersivity	1 ft
D_m	molecular diffusion coefficient	10^{-3} ft^2/d
ρ_f	freshwater density	62.43 lb/ft^3
ρ_s	seawater density	63.99 lb/ft^3
θ	effective porosity	.2
C_0	initial solute concentration	1
C_r	recharge concentration	0

efficient (simulations ran in 1 to 2 days) but introduced numerical dispersion. Other solution techniques less susceptible to numerical dispersion were tested but required unacceptably long computer-execution times.

The simulated groundwater densities in the vicinity of the saltwater transition zone are depicted in plan and cross-section views in figures A2 and A3, respectively. Although they were not used in the formal estimation of model parameters

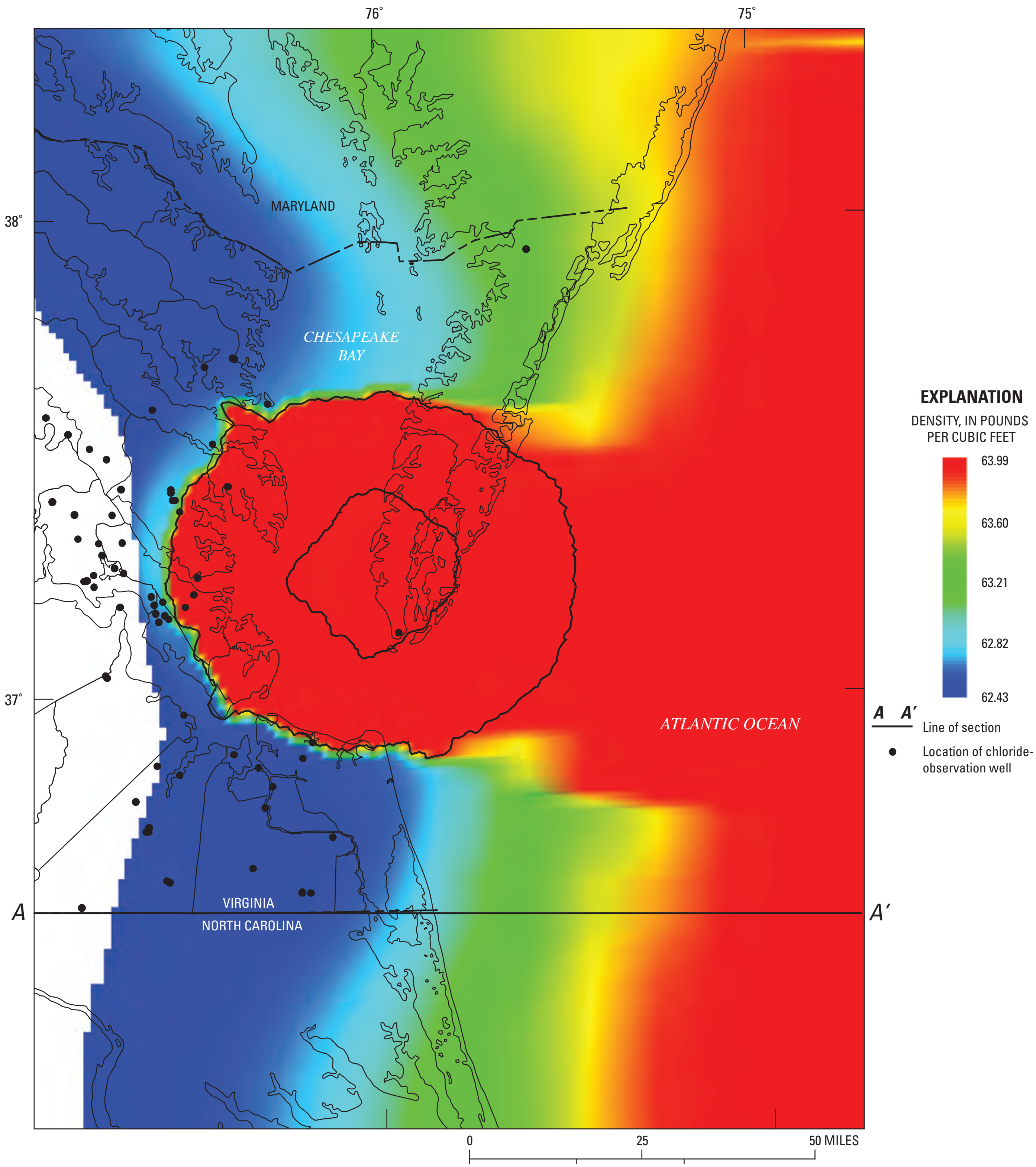

Figure A2. Simulated water density near the saltwater transition zone of the Virginia Coastal Plain.

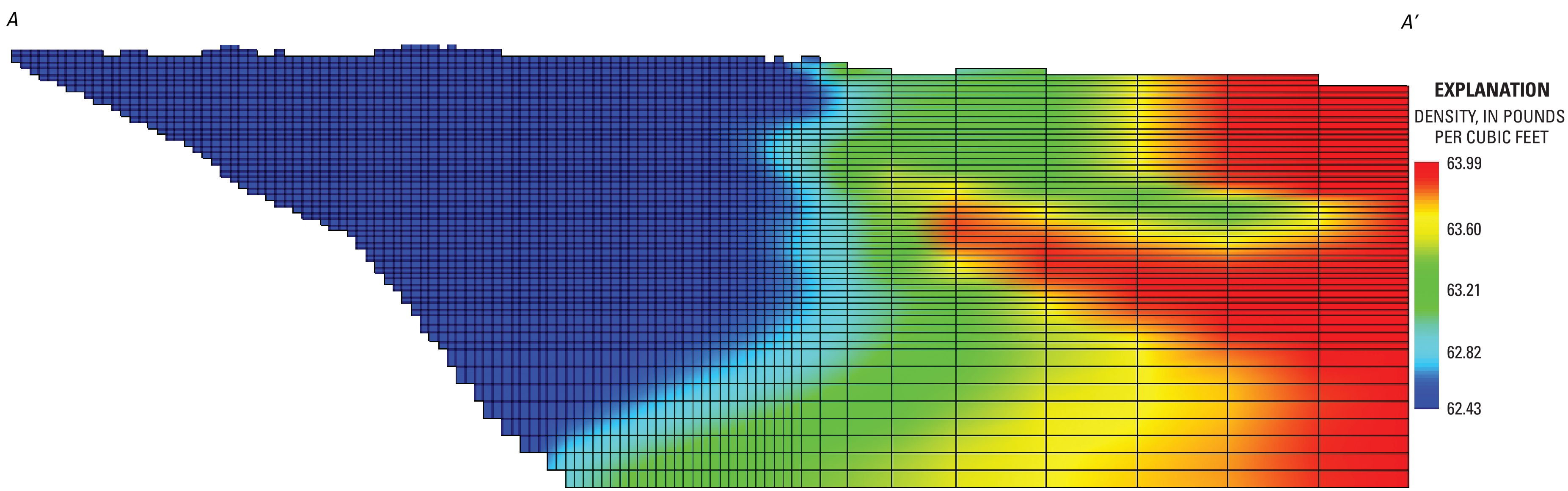

Figure A3. Simulated water density near the saltwater transition zone of the Virginia Coastal Plain. (Location of cross section shown in figure A2.)

described in the main report body, 117 chloride-concentration observations helped to constrain the modern salinity distribution calculated for the end of the 108,000-year simulation described in this appendix. The relation between observed normalized chloride concentrations and simulated equivalents is shown in figure A4. In general, the simulated concentrations agree reasonably well with observed concentrations near the transition zone in deeper parts of the aquifer system. However, shallow wells with observed chloride concentrations up to about 13 percent that of seawater are simulated as essentially fresh and appear along the x-axis in figure A4. Because configuration of the simulated saltwater transition zone within the deeper aquifers, particularly the Potomac, was considered the more important influence on regional groundwater flow, the less accurate fit to observed salinities in other areas is acceptable for the purpose of this simulation.

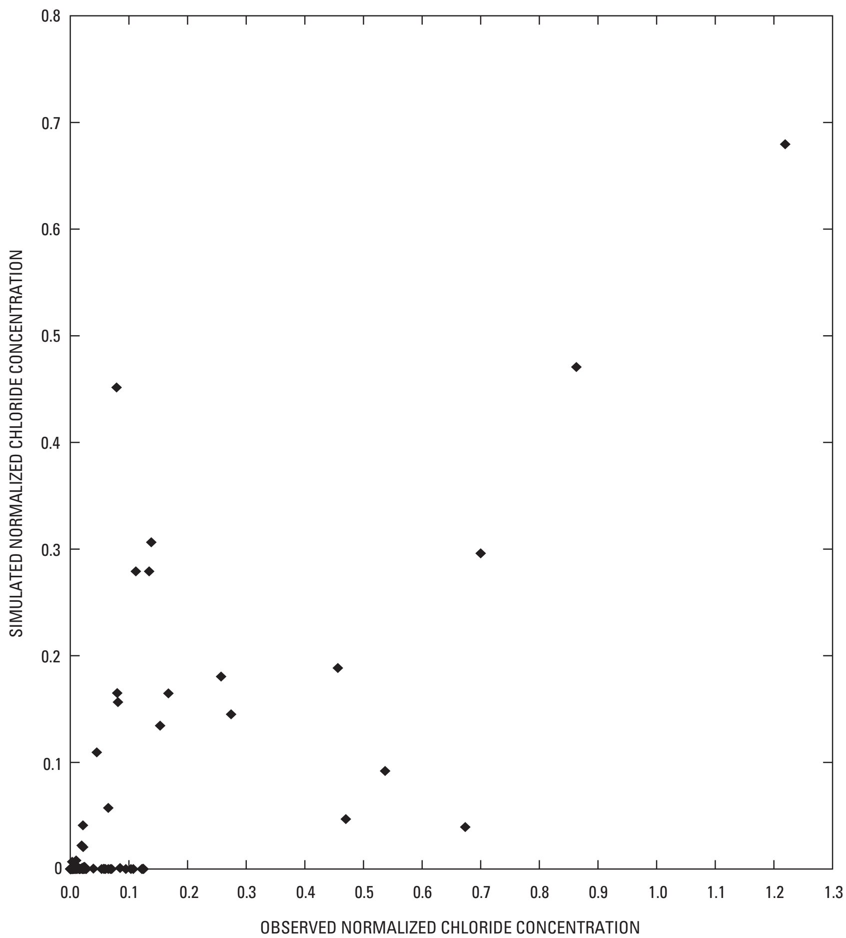

Figure A4. Relation between simulated and observed normalized chloride concentrations.

Appendix References Cited

Heywood, C.E., 2003, Influence of the Chesapeake Bay impact structure on ground-water flow and salinity in the Atlantic Coastal Plain aquifer system of Virginia, in MODFLOW and More 2003—Understanding through modeling: Proceedings of the 5th International Conference of the International Ground Water Modeling Center, Golden, CO, Colorado School of Mines, p. 871–875.

Langevin, C.D., Shoemaker, W.B., and Guo, W., 2003, MODFLOW–2000, The U.S. Geological Survey modular ground-water model—Documentation of the SEAWAT–2000 version with the variable-density flow process (VDF), and the integrated MT3DMS transport process (IMT): U.S. Geological Survey Open-File Report 03–426, 43 p.

Leake, S.A., and Lilly, M.R., 1997, Documentation of a computer program (FHB1) for assignment of transient specified-flow and specified-head boundaries in applications of the Modular Finite-Difference Ground-Water Flow Model (MODFLOW): U.S. Geological Survey Open-File Report 97–571, 56 p.

Nelms, D.L., Harlow, G.E., Plummer, N., and Busenberg, E., 2003, Aquifer susceptibility in Virginia, 1998–2000: U.S. Geological Survey Water-Resources Investigations Report 03–4278, 58 p.

Zellmer, L.R., 1979, Development and application of a Pleistocene sea level curve to the Coastal Plain of southeastern Virginia: Williamsburg, Virginia, College of William and Mary, School of Marine Science, M.S. thesis, 85 p.

Zheng, C., and Wang, P., 1999, MT3DMS—A modular three-dimensional multispecies transport model for simulation of advection, dispersion, and chemical reactions of contaminants in groundwater systems—Documentation and user's guide: U.S. Army Corps of Engineers, U.S. Army Engineer Research and Development Center, Strategic Environmental Research and Development Program, 221 p.

Prepared by:
USGS Publishing Network
Raleigh Publishing Service Center
3916 Sunset Ridge Road
Raleigh, NC 27607

For additional information regarding this publication, contact:
Director
USGS Virginia Water Science Center
1730 East Parham Road
Richmond, VA 23228
phone: 804–261–2600
email: dc_va@usgs.gov

Or visit the Virginia Water Science Center Web site at:
http://va.water.usgs.gov

This publication is available online at http://pubs.usgs.gov/sir/2009/5039/.

Heywood and Pope—**Simulation of Groundwater Flow in the Coastal Plain Aquifer System of Virginia**—Scientific Investigations Report 2009–5039

ISBN 978-1-4113-2418-3

Printed on recycled paper